Microbial Biostabilization in fine Sediments

vorgelegt von Dr. rer. nat. Sabine Ulrike Gerbersdorf

Institut für Wasser- und Umweltsystemmodellierung
Lehrstuhl für Wasserbau
und Wassermengenwirtschaft
2022

CONTENT

Deutsche Zusammenfassung 1
Summary 11
List of Figures 12
List of Tables 17

I. Introduction 19
I.1. Life in confined Spaces: Biofilm 19
I.2. Hazards and Services of “Microbial Cities” 21
I.3. Biostabilization: an important Ecosystem Function 23
I.4. Status Quo in Biostabilization Research 24
I.4.1. Attachment and Settlement of biostabilizing Biofilm 24
I.4.2. Growth Requirements of the maturing Biofilm 29
I.4.3. Species Composition - internal Competition and external Forcing 35
I.4.4. The EPS Matrix - Key to Functionality? 41
I.5. Topics of this Habilitation Thesis 49

II. Material and Methods 54
II.1. Substratum, Biofilm Growth and Sampling 54
II.2. Chemical Analyses 54
II.2.1. EPS Extraction and Determination 54
II.3. Biological Analyses 56
II.3.1. Chlorophyll a and Pheophytin 56
II.3.2. Diatom Community 57
II.3.3. Bacterial Cell Numbers 58
II.3.4. Bacterial Community 59
II.3.5. Bacterial Division Rate 63
II.4. Determination of Adhesion and Sediment Stability 64
II.4.1. Cohesive Strength Meter (CSM) 64
II.4.2. Magnetic Particle Induction (MagPI) 65
II.4.3. Erosion Measurements in the SETEG Flume 67
II.5. Statistics 68

III. The Biostabilization Potential of natural benthic bacterial Assemblages from an Estuary 69
III.1. Abstract 69
III.2. Background 69
III.3. Experimental Settings 72
III.3.1. Bacterial Cultures 72
III.3.2. Experimental Set-up 73
III.3.3. Sampling 73
III.4. Results 74
III.4.1. The Stability and Cohesion of the Substratum 74
III.4.2. Bacterial EPS (Extracellular Polymeric Substances) 76
III.4.3. Bacterial Cell Numbers 81
III.4.4. Bacterial Composition: Phylogenetic Analysis by FISH 81
III.4.5. Relations between Bacterial Cell Numbers, EPS and Sediment Stability 82
III.5. Discussion 84
III.5.1. Bacterial Stabilization Potential 84
III.5.2. The Effect of Nutrient Addition for bacterial Biostabilization 86

III.5.3. The Effect of Nutrient Addition on the bacterial Community 87
III.5.4. The potential Role of Proteins for Adhesion 88
III.6. Conclusions 90

IV. Synergistic Effects by mixed versus single Taxa Biofilm Communities for Biostabilization 92
IV.1. Abstract 92
IV.2. Background 93
IV.3. Experimental Settings 94
IV.3.1. Bacterial Cultures 94
IV.3.2. Diatom Cultures 95
IV.3.3. Experimental Set-up 96
IV.3.4. Sampling 96
IV.4. Results 97
IV.4.1. Microphytobenthos Composition 97
IV.4.2. Bacterial Assemblages 98
IV.4.3. Microbial Biomass, Cell Numbers and Growth Rate 99
IV.4.4. Changes in EPS Components 101
IV.4.5. The Stability of the Substratum 103
IV.4.6. Relation between Biological Variables and Surface Adhesion and Stability 105
IV.5. Discussion 107
IV.5.1. Biostabilization by microbial Assemblages from estuarine Sediments 107
IV.5.2. The individual and combined engineering Capability of microbial Assemblages 107
IV.5.3. The EPS Matrix - Key to Substratum Stabilization? 111
IV.6. Conclusions 113

V. The Significance and Seasonality of Biostabilization in Freshwaters 114
V.1. Abstract 114
V.2. Background 115
V.3. Experimental Settings 117
V.3.1. Mesocosm: six straight Flumes with own Circuit 117
V.3.2. Control of Temperature, Light Intensity and Hydrodynamics 118
V.3.3. Biofilm Cultivation 120
V.3.4. Experiments and Sampling 121
V.4. Results 124
V.4.1. Water Chemistry 124
V.4.2. Inter- and intra-flume Comparison in Experiment I 124
V.4.3. The Biofilm EPS Matrix and microbial Biomass over Time 125
V.4.4. Biofilm Adhesiveness, Substratum Stability, mechanical Failure Types 126
V.4.5. Seasonal Aspects and Interactions of Biofilm Features 130
V.4.6. Microbial Community: Heterotrophic Bacteria 131
V.4.7. Microbial Community: Diatoms 133
V.5. Discussion 137
V.5.1. The Suitability of the new Mesocosm for Biofilm Studies 137
V.5.2. Significance of Biostabilization in Freshwaters 138
V.5.3. Seasonal Effects upon Biostabilization 139
V.5.4. Driving Factors for Biofilm Growth and Biostabilization 140
V.5.5. The mechanical Process of Erosion for biostabilized Sediments 146
V.6. Conclusions 147

VI. The Effect of Light and Fluid Dynamics on microbial Biostabilization in Freshwaters 149
VI.1. Abstract 149
VI.2. Background 150
VI.3. Experimental Settings 152
VI.4. Results 153
VI.4.1. Overview on the Effects of Light and Hydrodynamic Treatments 153
VI.4.2. Temporal Biofilm Development 153
VI.4.3. Microbial Parameters: algal Biomass, bacterial Cell Numbers, EPS 157
VI.4.4. Bacterial Community 159
VI.4.5. Diatom Community 162
VI.4.6. Biofilm Adhesiveness 166
VI.4.7. Biofilm Stability 167
VI.5. Discussion 169
VI.5.1. Illumination Intensity and Nutrients 170
VI.5.2. The Impact of the Hydrodynamic Regime 173
VI.5.3. Possible Key Players for Biostabilization 175
VI.6. Conclusions 178

VII. Magnetic Particle Induction - MagPI: A promising Tool to determine Adhesive Capacity of Biofilm on the Mesoscale 180
VII.1. Abstract 180
VII.2. Background 181
VII.2.1. Biofilm, their Adhesive Capacity and how to address it 181
VII.2.2. Measuring Procedure by MagPI 183
VII.2.3. The Thresholds for Determination of Adhesion Levels 185
VII.2.4. Ferromagnetic Particles on Substratum 186
VII.2.5. Physics of magnetic Particles in a magnetic Field 186
VII.2.6. Open Questions and Objectives 188
VII.3. Material and Methods 190
VII.3.1. Configuration of MagPI Electromagnets 190
VII.3.2. Electrical Equipment 190
VII.3.3. Positioning of MagPI 190
VII.3.4. Magnetic Field generated by a Solenoid with magnetic Core 191
VII.3.5. Quantification of magnetic Field 192
VII.3.6. Ferromagnetic Particles 193
VII.3.7. Superconducting Quantum Interference Device (SQUID) 193
VII.3.8. Substratum used 194
VII.4. Results and Discussion 194
VII.4.1. Design of the Electromagnet 194
VII.4.2. Roles of magnetic Field and Gradient of magnetic Field 199
VII.4.3. Characteristics of the magnetic Particles 201
VII.5.Conclusions 205
Bibliograph 207

DEUTSCHE ZUSAMMENFASSUNG

Die Dynamik der Feinsedimente in Flüssen, Seen und Küstengebieten ist ökologisch, ökonomisch und auch human-gesundheitlich von eminenter Bedeutung. Es ist daher nicht erstaunlich, dass große Anstrengungen unternommen worden sind, die Mobilität von Feinsedimenten und der oft assoziierten Schadstoffe besser zu verstehen und vor allem zu prognostizieren. In den letzten Jahrzehnten zeigte sich aber immer mehr, dass dies nur bedingt gelingt. Grund dafür sind die Mikroorganismen, die sich bevorzugt an Feinsedimente anheften, und dort einen sogenannten Biofilm bilden. Dieser Biofilm besteht aus heterotrophen Bakterien, eukaryotischen Mikroalgen, Protisten sowie einer selbstproduzierten Matrix aus extrazellulären polymeren Substanzen (EPS). Mittels seiner Adhäsionskraft beeinflusst der Biofilm sowohl die Erosionsstabilität von Feinsedimenten als auch deren Transport, Deposition sowie Konsolidierung und damit den gesamten sogenannten ETDC Zyklus. Daher gewann man über die letzten Jahrzehnte zunehmend die Erkenntnis, dass diese biologisch-chemischen Vorgänge in den Sedimentwissenschaften berücksichtigt werden müssen. Mit den Begriffen „Ökohydraulik oder Ökogeomorphologie“ sollte die Notwendigkeit multidisziplinärer Forschung unterstrichen werden. Entsprechend stiegen in den letzten Jahren die Anzahl der Publikationen auf dem Gebiet der Biostabilisierung, die bald als wichtige Ökosystemfunktion erkannt wurde.

Diese Habilitationsschrift präsentiert die Beiträge der Antragstellerin und ihres Teams zu diesem innovativen Forschungsgebiet. Nach der allgemeinen Einführung (Kapitel I.) und dem Material- und Methodenteil (Kapitel II.) werden die folgenden Themen in fünf Kapiteln (III. – VII.) behandelt:

(1) Das Stabilisierungspotential heterotropher bakterieller Gemeinschaften in Feinsedimenten aus dem Ästuarbereich

(2) Synergieeffekte von Biofilmen mit gemischter Biozönose gegenüber Biofilmen mit jeweils nur einem Taxon (Bakterien, Kieselalgen) in Bezug zur Biostabilisierung

(3) Die Bedeutung und Saisonalität der mikrobiellen Biostabilisierung von Feinsedimenten in Süßgewässern

(4) Der Einfluss von Licht und Hydrodynamik auf die Biostabilisierung in Feinsedimenten in lotischen Gewässern

(5) Die Weiterführung eines innovativen Geräts: Magnetic Particle Induction (MagPI) zur Bestimmung der adhäsiven Kapazität von Biofilmen

(1) Die Organismen im Biofilm gelten als "Ökosystemingenieure", da sie die Verfügbarkeit von Ressourcen für andere Arten modulieren, indem sie Veränderungen in der Struktur, Funktion und Biodiversität aquatischer Ökosysteme bewirken (Boogert *et al.*, 2006). Es wurde lange vermutet, dass es hauptsächlich Mikroalgen (Mikrophytobenthos) sind, die durch ihre selbstproduzierten EPS-Zucker die Feinsedimente stabilisieren. Folglich konzentrierte sich die Forschung auf die gut sichtbaren mikrobiellen Matten in der Gezeitenzone (z.B. Smith & Underwood, 2000) sowie auf die Aufklärung der Struktur und Zusammensetzung ihrer EPS-Zucker, welche an den Wanderungen und der Anheftung der Mikroalgen beteiligt sind (z.B. Wustman *et al.*, 1997; Bahulikar & Kroth, 2008). In diesen Untersuchungen wurden die heterotrophen Bakterien und ihre mögliche Rolle in der Biostabilisierung weitgehend unbeachtet gelassen, obwohl auch diese in der Lage sind, signifikante Mengen an EPS zu produzieren, wie aus der Medizin, der Biotechnologie und der Abwasserreinigung bekannt ist (Morton *et al.*, 1998; Flemming & Wingender, 2001a; Liu & Fang, 2003).

Darüber hinaus sind heterotrophe Bakterien - horizontal wie vertikal - in Feinsedimenten ubiquitär verbreitet. Die von Bakterien ausgeschiedenen polymeren Substanzen bestehen zu einem Großteil aus hydrophoben Proteinen mit negativ-geladenen funktionellen Gruppen, welche als extrazelluläre Enzyme fungieren, aber durchaus auch eine strukturelle Rolle innehaben. Im Zusammenspiel mit Polysacchariden konnte eine Erhöhung der Festigkeit dieser EPS-Komplexe beobachtet werden (Pennisi, 2002; Zeng *et al.*, 2015a), aber mögliche Effekte auf die Sedimentstabilisierung durch Biofilme waren bis dato unbekannt.

Im Kapitel III. konnte zum ersten Mal das hohe Stabilisierungspotential benthischer heterotropher Bakteriengemeinschaften aufgezeigt werden. Dazu wurden Bakterien aus den Sedimentschichten im Gezeitenbereich des Eden Ästuars (Schottland, GB) isoliert und ihr Aufwuchs als Biofilm auf künstlichem Substrat (hier inerte, nicht-kohäsive Glasperlen von 150µm Durchmesser) mit und ohne Nährstoffzugabe über einige Wochen verfolgt. Die über die Zeit zunehmende Stabilität des Substrates wurde mittels CSM (Cohesive Strength Meter) gemessen und war signifikant höher als in der Kontrolle ohne bakteriellen Biofilm. Die Nährstoffzugabe resultierte im Vergleich zu den Kulturen ohne Nährstoffe in einer erhöhten Stabilisierungsleistung (x3.6 gegenüber x1.8). Erhöhte Stabilitäten des Substrates korrelierten sowohl mit den bakteriellen Zellzahlen (R^2=0.75/0.78), als auch mit den EPS-Proteinen (R^2=0.96/0.53) (jeweils für die Kulturen mit/ohne Nährstoffzugabe), aber nicht mit den EPS-Zuckern. Damit wies diese Studie zum einen die Adhäsionseigenschaften bakterieller EPS-Proteine nach, die für die Biostabilisierung bedeutender sind als bisher angenommen. Zum anderen wurde gezeigt, dass die Biostabilisierung bakterieller Lebensgemeinschaften stark von den abiotischen Bedingungen, u.a. der Nährstoffverfügbarkeit, abhängt. Die

Veröffentlichung von Gerbersdorf et al. in FEMS (Federation of European Microbiological Societies) Microbiological Letters (2008b) ging in dieses Kapitel ein.

(2) Mit diesen Erkenntnissen über die Bedeutung heterotropher Bakterien für die Sedimentstabilität erschienen frühere Ergebnisse zum Stabilisierungspotenzial von Mikroalgen in einem neuen Licht, denn die bislang untersuchten natürlichen Mikroalgenmatten beherbergen immer hohe Abundanzen an Bakterien. Um die Einzelleistung der verschiedenen Taxa (Prokaryonten/heterotrophe Bakterien versus Eukaryonten/Mikroalgen) besser beurteilen zu können, sollten diese separat sowie in Kombination untersucht werden. Frühere Studien gaben Hinweise auf eine vorteilhafte Koexistenz oder Symbiose zwischen heterotrophen Bakterien und Mikroalgen im Biofilm, was vor allem durch Nährstoffrecycling begründet zu sein schien (Schäfer *et al.*, 2002; Grossart & Simon, 2007). Andere Untersuchungen wiesen jedoch eine gegenseitige Unterdrückung nach, sowohl durch bakterizide als auch durch algizide Ausscheidungen (Mu *et al.*, 2007; Ribalet *et al.*, 2008). Das Kapitel IV. adressiert diese Bakterien - Mikroalgen – Wechselwirkungen im Hinblick auf mögliche Effekte für die Bildung der Biofilm-Matrix und der daraus resultierenden Substratstabilisierung.
Hierzu wurden Bakterien und Mikroalgen aus den oberen Sedimentschichten des Eden Ästuars isoliert und ihr Aufwuchs als Biofilm auf Glasperlen (150µm Durchmesser) als Substrat sowohl getrennt als auch kombiniert über einige Wochen untersucht. Mittels MagPI und CSM sind die Adhäsion als auch die Stabilität der Biofilmoberfläche regelmäßig gemessen worden. Die individuelle Stabilisierungsleistung der heterotrophen bakteriellen Populationen war teilweise doppelt so hoch wie in den axenischen (=bakterienfreien) Kieselalgenkulturen. Die aus autotrophen und heterotrophen Organismen bestehenden Biofilme resultierten in der höchsten

Biostabilisierung, welche im Mittel 7.5fach (MagPI) und 9.5fach (CSM) höher war als in den Kontrollen. Obwohl die Daten damit nicht auf synergistische (=mehr als additive) Effekte in der gemischten Biofilmgemeinschaft hindeuteten, zeigten sie doch die Signifikanz der einzelnen Taxa für die Biostabilisierung und die höchste Effektivität in deren Zusammenspiel. Die Erklärung wird in der EPS-Matrix gesehen, deren Quantität als auch Qualität für die hier bewertete Funktionalität wichtig waren. Die gewonnenen Erkenntnisse über die Leistungen der beteiligten „Keyplayer“ und die unterschiedlichen Funktionen der EPS-Matrix (für Mobilität oder Anheftung) sind entscheidend für das konzeptionelle Verständnis der mikrobiellen Biostabilisierung. Dieses Kapitel basiert primär auf der Veröffentlichung von Lubarsky et al. in PLoS ONE (2010).

(3) Das Biostabilisierungspotential von Biofilmen in Feinsedimenten ist nicht nur im Hinblick auf Küstenerosion oder Sedimenttransport im Gezeitenbereich bedeutsam, sondern auch in den Fließgewässern. Deposition und Erosion von Feinsedimenten spielen sowohl in der Erhaltung der Wasserstraßen, als auch in der Freisetzung von assoziierten Schadstoffen bei erhöhtem Abfluss (z.B. bei einem Hochwasserereignis) eine ökonomisch und ökologisch wichtige Rolle. Lange wurde jedoch angenommen, dass die mikrobielle Verklebung von Sedimenten nur in marinen Habitaten aufgrund der dort bei diesem Bindungsprozess hilfreichen hohen Ionenkonzentrationen signifikant sein würde (Spears *et al.*, 2008). Dabei wurden im Süßwasser beeindruckend hohe EPS-Konzentrationen gemessen (Hirst *et al.*, 2003; Cyr & Morton, 2006).
Im Kapitel V. wurde das Potenzial der Biostabilisierung in Feinsedimenten zum ersten Mal im Süßwasser unter Berücksichtigung saisonaler Effekte untersucht. Obwohl die großen Schwankungen biologischer Prozesse und die Veränderungen der mikrobiellen Gemeinschaft im Biofilm (Lyautey *et al.*, 2005; Power *et al.*, 2008) über das Jahr hinweg

bekannt sind, lässt sich doch über die Auswirkungen auf die Biostabilisierung nur spekulieren. Um diese Funktionalität adäquat zu adressieren, wurde ein Mesokosmos konzipiert, der die Vorteile von Feldmessungen (Relevanz unter natürlichen Verhältnissen) mit Laborexperimenten (kontrollierbare reproduzierbare Bedingungen) kombiniert, und dabei sowohl Ingenieurwissen als auch naturwissenschaftliche Erkenntnisse berücksichtigt. Der Mesokosmos besteht aus sechs autarken Fließrinnen, in welchen 200L Flusswasser zirkulieren können, aus dem sich letztendlich die Biofilme rekrutieren. Diese quasi-natürlichen Biofilme wuchsen in der jeweiligen Testsektion auf Glasperlen (150µm Durchmesser) und unter jeweils variierenden Bedingungen von Lichtquantität und Fließgeschwindigkeit. In einem ersten Großexperiment konnte nachgewiesen werden, dass der neu entwickelte Mesokosmos ein repräsentatives Wachstum von Biofilmen, sowohl in den verschiedenen Bereichen einer Fließrinne als auch in den jeweiligen sechs Fließrinnen ermöglicht – eine wichtige Voraussetzung für zukünftige manipulative Experimente. In weiteren fünf Experimenten wurde dann die signifikant hohe Biostabilisierungsleistung der Biofilme im Süßwasser bestätigt. Die höchsten Adhäsionswerte (mittels MagPI) sowie die höchsten Sedimentstabilitäten (mittels „Strömungskanal zur Ermittlung der tiefenabhängigen Erosionsstabilität von Gewässersedimenten“ SETEG Rinne) wurden jeweils im Frühjahr gemessen und waren im Durchschnitt 8-10-mal bzw. 3-5-mal höher als im Sommer bzw. im Herbst. Die höchsten Bindungskapazitäten gingen mit den höchsten EPS-Werten im Frühjahr einher, und es zeigte sich erneut die Bedeutung der EPS-Proteine für die beobachtete Stabilisierungsleistung. In Bezug auf die mikrobielle Gemeinschaft wurde jedoch deutlich, dass nicht die Biomasse allein entscheidend war, sondern vielmehr die Artenzusammensetzung und die Lebensweise (mobil oder sessil) der dominierenden Arten. Die mikrobielle Gemeinschaft und die ökologisch diversen Ansprüche der

einzelnen Arten spiegelten sich auch in mechanisch deutlich unterschiedlichen Biofilmen wieder, welche im Vergleich zu abiotischen Sedimenten völlig neue Erosionsmuster aufwiesen. Doch nicht nur das tiefere Verständnis dieser Strukturen und mechanischen Eigenschaften der mikrobiell veränderten Sedimente ist für die Implementierung in Erosionsgleichungen und Sedimenttransportmodelle wichtig, auch die Erkenntnisse zur Bedeutung und Saisonalität von Biostabilisierung im Süßwasser sind ein großer Fortschritt. Die in diesem Kapitel dargelegten Inhalte wurden in Environmental Sciences Europe ESEU (Schmidt *et al.*, 2015), Freshwater Biology (Schmidt *et al.*, 2016) und im International Journal of Sediment Research (Thom *et al.*, 2015) publiziert.

(4) Umweltbedingungen beeinflussen sowohl die Biofilmstruktur (Blenkinsopp & Lock, 1994) als auch die Stoffwechselwege (Romani *et al.*, 2004; Marcarelli *et al.*, 2009; Kendrick & Huryn, 2015) und die Diversität der beteiligten Mikroorganismen (Lawrence *et al.*, 2004; Wagner *et al.*, 2015). Obschon das Wissen um die Interaktionen zwischen abiotischen Parametern und Mikroorganismen wächst, ist wenig bis gar nichts darüber bekannt wie die Funktionalität von Biofilmen beeinflusst wird. Licht ist einer der treibenden Parameter für die Biostabilisierung, da die photosynthetische Aktivität, die EPS-Produktion und die Mobilität der Mikroalgen stark von den Lichtbedingungen abhängen (Smith & Underwood, 2000; Orvain *et al.*, 2003). Zuviel Licht kann aber die konsolidierten Sedimentstrukturen durch die Entwicklung von Sauerstoffblasen aufbrechen, während die Stabilisierungsleistung im Dunkeln auch von heterotrophen Bakterien übernommen werden kann (siehe Kapitel III. und IV.). Auswirkungen der Hydrodynamik auf das Biofilmwachstum umfassen die Balance zwischen erhöhter Stoffaustauschrate (z.B. molekularer Diffusion von Nährstoffen in den Biofilm) und

möglicher Ablösung (z.B. durch Förderung der Biofilm-Erosion) (Characklis & Cooksey, 1983; Nikora, 2010); doch potentielle Effekte auf die Biostabilisierungsleistung sind nicht bekannt. Kapitel VI. beschreibt diese neue Verbindung zwischen der Funktionalität der in den Fließrinnen aufgewachsenen Biofilme und den jeweils variierenden Randbedingungen Licht und Hydrodynamik. Während Adhäsion (MagPI) und Sedimentstabilität (SETEG) mit zunehmender Lichtintensität signifikant anstiegen, verzögerte sich das heterotrophe Bakterienwachstum im Dunkeln, vermutlich aufgrund der begrenzten Nährstoffversorgung im oligotrophen Flusswasser. Höhere Abflüsse und daraus resultierende höhere Sohlschubspannungen führten zu einer deutlich verzögerten Entwicklung des Biofilms mit signifikanten Auswirkungen auf die Biostabilisierung. Dabei konnten sowohl die Lebensweise der detektierten Arten (mobil oder sessil) sowie Veränderungen in der Diversität, Dynamik von Artenverschiebungen, funktionellen Organisation und im Spezialisierungsgrad des Biofilms eindeutig mit der induzierten Bindungskraft in Verbindung gebracht werden. Neben den neuen grundlegenden Einsichten in die Wechselwirkungen zwischen Randbedingungen und Biofilmen (sei es in der natürlichen Umwelt oder im vom Menschen operativ betriebenen System wie beispielswiese in einem Reservoir) wurde damit die Bedeutung der mikrobiellen Gemeinschaft für die Funktionalität hervorgehoben. Das Kapitel beinhaltet die Ergebnisse aus den Veröffentlichungen Schmidt et al. Freshwater Biology (2016), Schmidt et al. Research and Reports in Biology (2018b) und Thom et al. International Journal of Sediment Research (2015).

(5) Die meisten Studien über Biofilme konzentrieren sich auf die Analyse oder Visualisierung von Wachstum und Stoffwechselaktivität, Biomasse und Zusammensetzung der Gemeinschaft oder EPS-Matrix. Wenn Funktionalität überhaupt

untersucht wird, dann vor allem im Hinblick auf biogeochemische Prozesse, die vom Biofilm maßgeblich beeinflusst werden (Battin & Brumaghim, 2008; Hodl *et al.*, 2014). Hingegen gibt es nur wenige (siehe vorherige Kapitel) bis gar keine Informationen über die Adhäsionsfähigkeit eines Biofilmes, obwohl diese eng mit den mechanischen Eigenschaften und der Stabilität des Biofilm-Substratum-Komplexes verknüpft ist. Innovative Techniken wie die Atomkraftmikroskopie (Atomic Force Microscopy AFM) liefern gute Ergebnisse im Nanobereich, die aber kaum auf den mechanischen Widerstand der gesamten Biofilmmatrix extrapoliert werden können (Dugdale *et al.*, 2005). Das Erosionsverhalten von Biofilmen wird in Fließrinnen zwar auf der relevanten Skala untersucht, ist aber mit Unsicherheiten, gerade bei jungen, aufwachsenden Biofilmen, behaftet (Thom *et al.*, 2015; Pique *et al.*, 2016). Die Messung der Adhäsion mittels der Anziehungskraft magnetischer Partikel durch einen Elektromagneten (Magnetic Particle Induction MagPI, Larson *et al.*, 2009; Anderson *et al.*, 2011) agiert dagegen im mesoskaligen Bereich (mm-cm-Bereich) und ist in hoher räumlicher als auch zeitlicher Auflösung zerstörungsfrei möglich. Diese scheinbar einfache aber innovative Technik weist eine hohe Sensitivität gegenüber kleinsten Veränderungen auf und wurde daher in den vorhergehenden Experimenten erfolgreich eingesetzt. Da der MagPI eine „Junge Idee“ darstellt, ist hier noch Potential für Weiterentwicklungen (a) im Aufbau des Elektromagneten, (b) in der Kalibrierung, (c) bei der Messmethode (d), in der Automatisierung von Messungen und Datenauswertung sowie (e) der Umrechnung in ingenieursrelevante Einheiten gegeben. Das Kapitel VII. fokussiert sich auf die technischen Aspekte in (a) und (b) um zum einen die Leistungsfähigkeit dieses Gerätes weiter zu verbessern und zum anderen durch besseres Verständnis des Funktionsprinzips eine korrekte Kalibrierung zwischen unterschiedlichen Laboren zu ermöglichen. Dabei wurde der Einfluss von Material und Geometrie auf die

Leistungsfähigkeit demonstriert und mittels Variationen in der technischen Fertigung eine breite Palette unterschiedlich leistungsfähiger Elektromagneten hergestellt. Des Weiteren wurde die Bedeutung des Zusammenspiels von Magnetfeldstärke und Magnetfeldgradient für die Physik des MagPI-Ansatzes aufgezeigt. Durch dieses vertiefte Verständnis des Funktionsprinzips sowie der Zusammenhänge zwischen Fertigung und Leistung der Elektromagnete, kann sich für MagPI ein breiterer Anwendungsbereich in der ökologischen Forschung erschließen, aber auch darüber hinaus, z.B. in der Medizin oder Biotechnologie. Das Kapitel geht auf die Veröffentlichung von Gerbersdorf et al. zurück (kürzlich eingereicht im Journal of Biofouling 2017).

Diese Habilitationsschrift umspannt damit neue Erkenntnisse zur gegenseitigen Beeinflussung von Biofilmdiversität, Keyplayern, deren Lebensweise im Biofilm sowie bindungsrelevanten EPS Komponenten im Hinblick auf die Adhäsionskraft und deren Abhängigkeiten von abiotischen Randbedingungen wie Salinität, Nährstoffe, Licht, Hydrodynamik und nicht zuletzt Saisonalität. Dabei umfassen die Forschungsbeiträge der Habilitandin und ihres Teams auf dem Gebiet der mikrobiellen Biostabilisierung von Feinsedimenten neben inhaltlichen Aspekten auch methodische Weiterentwicklungen.

SUMMARY

Microbial biostabilization has increasingly received attention over the last years due to its significance for the dynamics of fine sediments in fluvial and coastal systems with implications for ecology, economy and human-health. This habilitation thesis highlights the contributions of the applicant and her team to this multi-disciplinary research area and is based on eight core publications that are presented in seven chapters. First, the topic of biofilm and biostabilization is introduced and second, the materials and methods applied are presented before own research findings are discussed. To start with, the stabilization potential of heterotrophic bacterial assemblages has been emphasised as well as the adhesive properties of the protein moieties within the EPS (extracellular polymeric substances) that are more significant than previously thought. Furthermore, the engineering potential of estuarine prokaryotic and eukaryotic assemblages has been studied separately and combined to reveal the effective cooperation of mixed biofilm that resulted in highest substratum stabilization although the effects were not clearly synergistic (=more than additive). The significance of biostabilization could be evidenced as well for freshwaters where highest adhesive capacity and sediment stability occurred during spring. Microbial community composition differed accordingly to result in mechanically highly diverse biofilm. Moreover, the importance of two of the most influential abiotic conditions, light intensity and hydrodynamics, was shown for biofilm growth, species composition and functionality – here biostabilization. In order to test adhesive properties at the relevant mesoscale (mm-cm) but non-destructively and highly sensitive, MagPI (Magnetic Particle Induction) has been applied. The last chapter concerns technical aspects to further improve its performance while demonstrating the impact of material and geometry and the importance of both, magnetic field strength and field gradient for the physics of the MagPI approach.

LIST OF FIGURES

Figure 1: The graphic illustrates the multicultural life within a biofilm consisting of heterotrophic bacteria, cyanobacteria, diatoms, green algae, fungi, and protozoa. The left circle indicates the trophic relations of the micro-organisms in the 'microbial loop' (Pomeroy et al., 2007). Source: Gerbersdorf and Wieprecht 2015 Geobiology. 20
Figure 2: The significance of biostabilization in the Erosion Transport Deposition Consolidation (ETDC) cycle of cohesive sediments. Microbial activity 'glues' fine sediment particles together to impact sediment stability, floc characteristics of the entrained material, and thus, further sediment transport and deposition. During consolidation processes, the biological matrix undergoes chemical changes that further enhance the binding forces. Source: Gerbersdorf and Wieprecht 2015 Geobiology. 22
Figure 3: The initial steps of microbial attachment to a surface: (A) reversible bridging between cell and surface via London forces, (B) overcoming repulsive forces and pulling the cell towards the surface by shooting fimbrae and/or flagellas at the surface and (C) irreversibly binding accompanied by extracellular polymeric substances (EPS) secretion and establishing short polar range forces. Source: Gerbersdorf and Wieprecht 2015 Geobiology. 26
Figure 4: The graphic contrasts two different sediment types and the typical microbial inhabitants: (A) sandy sediment colonized by epipsammic diatoms that attach via pads and stalks to the particles, as well as cyanobacteria gliding through and building a trichome network and some euglenoids and (B) muddy (silt clay) sediments dominated by epipelic (=moving) diatoms. Source: Gerbersdorf and Wieprecht 2015 Geobiology. 27
Figure 5: The graphic illustrates the effect of two different hydrodynamic scenarios: lower flow conditions (left) result in a pronounced DBBL (diffusive benthic boundary layer) and thicker, more fluffier biofilm while higher flow velocities (right) reduces the extension of both, DBBL and biofilm; the latter being more compact. 32
Figure 6: An oxygen bubble trapped in the filaments of the green algae Klebsormidium flaccidum. Source: Gerbersdorf and Wieprecht 2015 Geobiology. 35
Figure 7: LTSEM (low-temperature scanning electron microscopy, SERG-Lab of Prof. D.M.Paterson) Images. Left: glass beads embedded by the extracellular polymeric substances (EPS) matrix of naturally grown biofilm consisting mainly of heterotrophic bacteria and diatoms. Right: EPS strands and embedded microbes that surrounded the detached glass bead (empty space). Source: Gerbersdorf and Wieprecht 2015 Geobiology. 42
Figure 8: CSM measurements within esturarine biofilm grown in boxes on glass beads. Left: the test or erosion chamber (grey) in idle position above the beaker is connected to the yellow suitcase containing air supply and water bottles for the perpendicular water jets as well as the digital panel and keypad for the various erosion programs to apply and measure. Right: visualization of one CSM jet within the test chamber by applying a potassium permanganate solution (Image from SERG lab of Prof. D.M. Paterson). 64
Figure 9: Magnetic Particle Induction (MagPI). Left: the setup with the electromagnet positioned in a fixed distance (via micromanipulator) to the biofilm and connected to the power supply (not to be seen here). Middle: drawing of the electromagnet positioned above the biofilm surface with F=the "lifting" force, x the distance between surface and magnet, N=number of turns of cupper coils and V=voltage applied. Right: Ferromagnetic particles spread onto the surface (upper image) and re-captured by the electromagnet positioned above (lower image). Source: right and left: DFG project Gerbersdorf, middle: Keybioeffect project Gerbersdorf. 66

Figure 10: Left: Schematic view of SETEG erosion flume, modified after Witt &Westrich (2003): (a) pressure duct, (b) sediment cartridge fitted into a frame (c) pump and magnetic inductive flow meter (d) laser triangulation system (e) jack with stepping motor (f) outflow weir. Right: view from above onto the sediment cartridge fitted into a frame to insert into the SETEG flume from below. Source: left: (Thom et al., 2015) and right: DFG project Gerbersdorf. 67
Figure 11: Cohesiveness in the treatments “bacteria” (grey triangles), and “bacteria+” (dark grey squares) versus the “controls” (black circles) over the course of the main experiment (five weeks). The cohesiveness is expressed as the vertical stagnation pressure in Nm^{-2} (=Pascal), which is needed to erode the substrate surface, determined by the CSM (Cohesive Strength Meter) (n=6). Gerbersdorf et al. 2008b FEMS. 76
Figure 12: Bacterial EPS concentrations over the course of the experiment; mean values (n=6) with standard deviation are given for the “bacteria” without nutrients (grey triangles), the “bacteria+” with nutrients (dark grey squares) and the “controls” (black circles) for EPS protein (left) and EPS carbohydrates (right). Source: Gerbersdorf et al. 2008b FEMS.....78
Figure 13: Different EPS ratios over the course of five weeks: EPS protein/carbohydrate P/C ratio for “bacteria” (black circles) and for “bacteria+” (black triangles) as well as the EPS C/C (grey circles) and P/P (grey triangles) ratio between the treatment “bacteria” and “bacteria+” (n=6). Source: Gerbersdorf et al. 2008b FEMS. 78
Figure 14: EPS protein concentrations in 10 substrate layers (between the top 500µm–10mm depth); mean values (n=6) with standard deviation are given for each layer (1-10) and each week (1-5). Source: Gerbersdorf et al. 2008b FEMS. 79
Figure 15: EPS carbohydrate concentrations in 10 substrate layers (between the top 500µm–10mm depth); mean values (n=6) with standard deviation are given for each layer (1-10) and each week (1-5). Source: Gerbersdorf et al. 2008b FEMS. 80
Figure 16: Bacterial cell numbers in the top 500µm substrate over the course of the experiment; mean values (n=3) with standard deviation are given for the treatments “bacteria” (grey triangles), “bacteria+” (dark grey squares) versus the “controls” (black circles). Source: Gerbersdorf et al. 2008b FEMS. 81
Figure 17: Regression between the bacterial cell numbers and the EPS proteins in the top 500µm substrate layer [cm^3]. The grey circles indicate the relation for “bacteria” and the black circles for “bacteria+”. Each circle is representing a mean value for one week (n=6; five weeks in total). Source: Gerbersdorf et al. 2008b FEMS. 83
Figure 18: Regression between the EPS proteins and the stagnation pressure in the top 500µm substrate layer [cm^3]. The grey circles indicate the relation for “bacteria” and the black circles for “bacteria+”. Each circle is representing a mean value for one week (n=6; five weeks in total). Source: Gerbersdorf et al. 2008b FEMS. 84
Figure 19: LTSEM (Low Temperature Scanning Electron Microscope) images of the bacteria nutrient treatment (left side) and the control (right side) substratum using different magnifications. Frozen water on the surface resulted in some artificial vertical cover lines on the glass beads (left and right); otherwise the glass beads of the controls are sparkling clear while the glass beads in the bacteria nutrient treatment are heavily covered in EPS which also fills the intermediate space. Source: Gerbersdorf et al. 2008b FEMS.....85
Figure 20: Mean values of the different treatments: mixed assemblages (BD), diatoms (D), bacteria (B), control (C): A. chlorophyll a (n=21). B. bacterial cell numbers (n=24). C. bacterial division rates (n=18). D. bacterial specific division rates (n=18). Source: Lubarsky et al. 2010 PLoS ONE. 100

Figure 21: EPS concentrations within different assemblages. A-B: Mean values (n=3 per treatment, based on n=3 replicates per box + SE) of EPS concentrations in the treatments bacteria and diatoms (BD, ▲), diatoms (D, ♦), bacteria (B, □) and controls (C, ●) for carbohydrates (A) and proteins (B). C-D: The EPS concentration of the mixed cultures (BD) relative to the contribution of the single cultures (B and D) such that the value "[BD]-[B+D]" is reported for carbohydrates (C) and proteins (D). Source: Lubarsky et al. 2010 PLoS ONE. 102
Figure 22: Mean values of MagPI and CSM measurements of different assemblages. A. Mean values (n=6) of MagPI over the time of the experiment. B. Mean values (n=6) of CSM over the time of the experiment. The treatments were bacteria and diatoms (BD, ▲), diatoms (D, ♦), bacteria (B, □) and controls (C, ●). Substratum stability by the mixed BD treatment relative to the stability of the single B and D treatments is given for MagPI (C) and CSM (D). Source: Lubarsky et al. 2010 PLoS ONE. 104
Figure 23: Relationship between MagPI (mTesla) and CSM (Nm^{-2}). Source: Lubarsky et al. 2010 PLoS ONE. 105
Figure 24: Relations between biofilm adhesion and sediment stability (MagPI, CSM) and EPS components. A-B: The relations between surface adhesion (MagPI) and EPS carbohydrates and proteins concentrations. C-D: The relations between substratum stability (CSM) and EPS carbohydrates and proteins concentrations. Source: Lubarsky et al. 2010 PLoS ONE. 106
Figure 25: Low-temperature scanning electron microscope images using different magnifications. A-B: The mixed assemblages bacteria + diatom. C-D: The diatom treatment. E-F: The bacteria treatment. G-H: The control substratum. Frozen water (ice) on the surface produces a solid matrix around the glass beads in the controls. In the other treatments with microorganisms, the EPS matrix is visible, heavily covering the glass beads and permeating the intermediate pore space. Source: Lubarsky et al. 2010 PLoS ONE. 112
Figure 26: Experimental setup. Top: image of three equivalent straight flumes installed in one container. Bottom: schematic image of one straight flume with (a) outflow tank, (b) pump, (c) inlet flow section with baffles, (d) biofilm cultivation section, (e) outlet flow section, (f) weir, (g) fluorescent tubes, (h) sediment cartridges, (i) bypass, (j) current abatement, and (k) fine-tuning valve. Source: Thom et al. 2012 Wasserwirtschaft. 118
Figure 27: Temporal development of selected biofilm features (mean values with corresponding STDev): spring (▲), summer (●), autumn (■). Upper left: EPS carbohydrate contents; upper right: EPS protein contents; lower left: chlorophyll a contents; lower right: biofilm adhesiveness (T3) with logarithmic ordinate. Source: Schmidt et al. 2016 Freshwater Biology. 128
Figure 28: Sediment stability over time for different seasons: black circles-spring (May 2013), red circles-summer (August 2013) and green circles-autumn (November 2013). The biofilm stability of one cartridge has been determined in the SETEG flume and each data point represents the mean values of four eroded cartridges originating from two flumes with the same boundary conditions of medium light (50µE m^{-2} s^{-1}) and low discharge (0.02Nm^{-2}) (n=4).....129
Figure 29: The two dominant types of biofilm-impacted entrainment as observed during the experiments. Source: Thom et al. 2015a International Journal of Sediment Research. 129
Figure 30: Temporal development of the bacterial community. Inverted image of DGGE band patterns taken during spring (May 2013). The indicated numbers represent days of growth. The developing specialization of the bacterial community and dominance of single bands became very plain. Source: Schmidt et al. 2016 Freshwater Biology. 133

Figure 31: DCA of the diatom communities. Triangles: spring; circles: summer; squares: autumn. Numbers represent sampling days. A: “August 2012”, J: “July 2013”, M: “May 2013”, m: “March 2014”, N: “November 2013”. The additional “a” and “b” represent the two different flumes sampled during one experiment. Source: Schmidt et al. 2016 Freshwater Biology. 134
Figure 32: Relative proportions of diatom genera [%] of early and late successional biofilm stages during all seasons. Genera with a relative abundance of less than 3.0% were summarized as 'others'. Source: Schmidt et al. 2016 Freshwater Biology. 135
Figure 33: Microalgal biomass, bacterial cell numbers and EPS carbohydrates as well as EPS proteins at different light intensities (LI) and separated in early (young) and late (matured) biofilm stages (pairwise per LI). Source: Schmidt et al. 2018 Research and Reports in Biology. 158
Figure 34: Microalgal biomass, bacterial cell numbers and EPS carbohydrates as well as EPS proteins at different flow velocities/bed shear stress (BSS) and separated in early (young) and late (matured) biofilm stages (pairwise per BSS level). Source: Schmidt et al. 2018 Research and Reports in Biology. 159
Figure 35: Range-weighted richness (Rr) of early and late biofilm stages. Left: at different levels of LI; right: at different levels of BSS. Source: Schmidt et al. 2018 Research and Reports in Biology. 160
Figure 36: Dynamics (Dy) of the bacterial community of early and late biofilm stages. Left: at different levels of LI; right: at different levels of BSS. Source: Schmidt 2017 PhD Thesis University Stuttgart.....161
Figure 37: Functional organization (Fo) of the bacterial community of early and late biofilm stages. Left: at different levels of LI; right: at different levels of BSS. Source: Schmidt 2017 PhD Thesis University Stuttgart. 161
Figure 38: Temporal development of the diatom community at medium and high light intensities (LI) at the days 14, 21, 28 and 35. Note: no microalgal growth could be detected at darkness. Genera with relative proportions less than 3% are summarized as “others”. Source: Schmidt 2017 PhD Thesis University Stuttgart. 165
Figure 39: Composition of early (day 14) and late (day 35) diatom communities at different levels of bed shear stress (BSS). Genera with relative proportions less than 3% are summarized as “others”. Source: Schmidt et al. 2018 Research and Reports in Biology. 166
Figure 40: Adhesiveness of early (1) and late (2) biofilm stages. Left: at different levels of light intensity LI. Right: at different levels of bed shear stress (BSS) (logarithmic ordinate). Source: Schmidt et al. 2018 Research and Reports in Biology. 167
Figure 41: The impact of hydrodynamics on the biofilm stability at spring (March and May 2013) and autumn (November 2013). The critical shear stress of erosion [T_{crit}] and BI is determined by eroding four cartridges from two flumes run at the identical boundary conditions. Each graph shows the data from two flumes (flume A triangles n=2 and flume B squares n=2) separately, but thicker symbols indicate the availability of only one cartridge. The light intensity has been constant at 50µE m^{-2} s^{-1} while the bed shear stress level varied. Source: Thom et al. 2015a International Journal of Sediment Research. 168
Figure 42: The impact of light on the biofilm stability addressed in two summer experiments (July and August 2013). The critical shear stress of erosion [T_{crit}] and BI is determined by eroding four cartridges from two flumes run at the identical boundary conditions. Each graph shows the data from two flumes (flume A triangles n=2 and flume B squares n=2) separately, but thicker symbols indicate the availability of only one cartridge. The bed shear stress has been constant at 0.02Nm^{-2} while the light

intensity varied. Source: Thom et al. 2015a International Journal of Sediment Research. 169
Figure 43: (A) The setup of the MagPI (from left to right: electromagnet positioned by micromanipulator, multimeter, power supply) and **(B)** Stepwise attraction of the ferromagnetic particles by the overlying electromagnet (4mm distance from the surface) at increasing currents. Image 3 marks threshold 2 (first particle is attracted), image 4 resembles threshold 3 (few particles attracted) and image 9 indicates threshold 4 (total clearance).....184
Figure 44: The magnetic field B_z [mT] in dependence of the current I [mA] for MagPIs with different core material: “MagPI_Original” with iron core and “MagPI_200_1” as well as “MagPI_200_1 + PM” (permanent magnet) with permalloy as core material. Due to the permanent magnet, the “MagPI_200_1 + PM” causes a finite magnetic field strength at zero current; the same is true for the “MagPI_Original” after repeated measurements, indicating its remanence in contrast to “MagPI_200_1”. The remanence can be clearly seen in the inset. 195
Figure 45: The magnetic field B_z [mT] versus I [mA] for various MagPIs with different number of turns (from 200 up to 1500 turns), measured at a fixed position (z=4mm, x=y=0mm) with respect to the pole of the MagPI core. With increasing number of turns, the slope of the initial linear relation becomes steeper, and the saturation level (where the linear relation finishes) is achieved already at lower currents. 196
Figure 46: The magnetic field B_z [mT] at a fixed current of 1000mA and varying heights z while x=y=0mm using two MagPIs with varying numbers of turns, with and without (remanence=R) current. 198
Figure 47: The magnetic field B_z [mT] at a fixed current of 1000mA and varying horizontal positions x (up to 10mm away from the centre) while z=4mm and y=0mm using two MagPIs with varying numbers of turns, with and without (remanence=R) current. 198
Figure 48: Threshold T3 (retrieval of few particles) is determined for four different substrates with increasing adhesion from 1-4 (1=petridish, 2=5g/l Agar Agar, 3=3g/l Xanthan Gum, 4=7,5g/l Xanthan Gum) with an electromagnet at a fixed height (4mm). Image A (above) shows the relation between T3 values and the corresponding magnetic field; image B (below) indicates the relation between T3 values and the corresponding magnetic gradient. 200
Figure 49: Hysteresis curves for one ferromagnetic particle (“A1”) from the size class 200–250µm with 15,5µg weight. (A) is showing the full hysteresis loop, while (B) presents a detailed view on the magnetic momentum which is zero before applying an external magnetic field (ellipse at starting point) and differs from zero after the field is reduced from finite values to zero again, thus indicating remanence after magnetisation (above and below ellipse). 203
Figure 50: Hysteresis curves for three ferromagnetic particle (“A3”, “B4”, “C1”) from three different sizes classes (200–250µm, 250–315µm,>315µm), respectively, before (A) and after (B) correction for their individual mass [mg].....204

LIST OF TABLES

Table 1: The two sectioning pattern of the frozen mini-cores followed for the depth-dependent distribution of EPS and the total quantity of EPS. Source: Gerbersdorf et al. 2008b FEMS.....74
Table 2: Oligonucleotides used in this study. Source: Gerbersdorf et al. 2008b FEMS. 75
Table 3: One-way ANOVA to test effects of treatments and time. Signifcance levels are given for EPS sugars, EPS proteins, bacterial cell numbers and sediment stability. Source: Gerbersdorf et al. 2008b FEMS.....75
Table 4: Extracellular sugar concentrations in the treatment „bacteria“ and „bacteria+“ over the course of five weeks. Mean value [mg cm^3] is given for n=6. Source: Gerbersdorf et al. 2008b FEMS.....77
Table 5: Extracellular protein concentrations in the treatment „bacteria“ and „bacteria+“ over the course of five weeks. Mean value [mg cm^3] is given for n=6. Source: Gerbersdorf et al. 2008b FEMS.....77
Table 6: Percentage of the specific bacterial groups (marked by the oligonucleotide probes named on the left) of the total eubacterial counts; given for the treatments bacteria and diatoms (BD) as well as bacteria (B) for the beginning (1) and the end (2) of the experiment. Source: Lubarsky et al. 2010 PLoS ONE. 99
Table 7: Differences between days 1 and 14 where most of the variables showed their maximum value as well as differences between the treatments (mixed BD, Bacteria B, Diatom D); both times expressed as quotient/factors for EPS carbohydrates, EPS proteins, MagPI and CSM. Source: Lubarsky et al. 2010 PLoS ONE.....103
Table 8: Pearson's correlation coefficients between surface adhesion (MagPI), substratum stability (CSM), EPS carbohydrates as well as EPS proteins in the different treatments with the significance levels: *** $p<0.001$. ** $p<0.01$. * $p<0.05$. Source: Lubarsky et al. 2010 PLoS ONE.....106
Table 9: Boundary conditions applied in the experiments. 119
Table 10: Overview over the performed experiments with BSS = benthic shear stress and LI = light intensity. Source: Schmidt 2017 PhD Thesis University Stuttgart. Note: in March 2013 there was one additional experiment on varying BSS (low, medium, high) which were only sampled for SETEG data without biochemical analysis. 122
Table 11: Intra-flume comparison. Mean values of EPS (carbohydrates and protein), chlorophyll a contents (n=144), bacterial cell counts (n=24) and surface adhesiveness (n=162) from six flumes combined for each region over the whole experimental time (with STDev). Source: Schmidt et al. 2015 ESEU. 125
Table 12: Inter-flume comparison. Mean values of EPS (carbohydrates and protein), chlorophyll a contents (n=120), bacterial cell counts (n=40) and surface adhesiveness (n=135) from each of the five flumes over the whole experimental time (with STDev). Source: Schmidt et al. 2015 ESEU.....125
Table 13: Results of the Kruskall-Wallis tests. Intra-flume and inter-flume comparisons of the measured data that indicated no significant differences. Source: Schmidt et al. 2015 ESEU.....125
Table 14: Seasonal and growth stage comparison of biofilm EPS matrix, microbial community and adhesiveness (mean values and corresponding StDEV). N=non-significant, S=significant. Source: Schmidt et al. 2016 Freshwater Biology. 132
Table 15: Correlations of biofilm parameters during spring (abbreviations see in text). Source: Schmidt et al. 2016 Freshwater Biology. 133

Table 16: Detected diatom species with minimal abundance of 1% of total counted frustules. Source: Schmidt et al. 2016 Freshwater Biology.....136
Table 17: Possible differences in biofilm growth and functionality due to different boundary conditions of shear stress and light intensity. n=number of samples, N=non-significant, S=significant. Source: Schmidt 2017 PhD Thesis University Stuttgart. 154
Table 18: Possible differences in biofilm growth and functionality over time at darkness and varying light intensities. n=number of samples. Source: Schmidt 2017 PhD Thesis University Stuttgart. 155
Table 19: Possible differences in biofilm growth and functionality over time at varying flow velocity intensities as the basis for bed shear stress calculations (BSS). n=number of samples. Source: Schmidt 2017 PhD Thesis University Stuttgart. 156
Table 20: Growth and functionality of biofilm grown at different levels of light intensity: mean values given for microbial parameter and adhesiveness, both for the different stages of young (early) and matured (late) biofilm. N=non-significant, S=significant. Source: Schmidt et al. 2018 Research and Reports in Biology. 163
Table 21: Growth and functionality of biofilm grown at different levels of bed shear stress: mean values given for microbial parameter and adhesiveness, both for the different stages of young (early) and matured (late) biofilm. N=non-significant, S=significant. Source: Schmidt et al. 2018 Research and Reports in Biology. 164
Table 22: Overview of the tested MagPIs and their main features. Note 1: MagPI “1000_3a” has a flat end while MagPI “1000_3b” possesses a conically shaped end, but with little variations as to the magnetic field beneath the core. Note 2: the solenoids length refers to the part of the core where the copper wire is coiled around.....191

I. INTRODUCTION

I.1. LIFE IN CONFINED SPACES: BIOFILM

It was not long ago that single cells floating in their aqueous habitat were regarded as the dominant lifestyle of microorganisms, while conglomerations of microbes were considered of minor importance in microbiology (Bender *et al.*, 1994; Pereira *et al.*, 2002; Flemming, 2011). Nowadays, it is well-known that microbes commonly prefer a social life, flourishing in multicellular and often multispecies communities embedded in their self-secreted three-dimensional matrix of polymeric substances (Costerton *et al.*, 1978; Stoodley *et al.*, 2002). These microbial assemblages ("biofilm") preferentially develop at all kinds of interfaces (e.g. sediment surface-water, water surface-air) (Characklis & Cooksey, 1983). While one might immediately think of microphytobenthos or even more coherent and stratified microbial mats that are both clearly visible to the naked eye, epiphyton on macrophytes, biofouling within pipes and on implants, dental plaque as well as flocs, aggregates and activated sludge (attached or floating) are biofilm too (Flemming & Wingender, 2010). Nevertheless, the constituent assemblages and functionality are as varied as their appearance. Already on the bacterial level, fundamental differences have been unveiled between attached biofilm and floating aggregates originating from the same source. Planktonic microorganisms that differentiated into aggregates comprised higher species richness, constant evenness, higher percentage of exclusively occurring OTUs (operational taxonomic units) as well as different functional profiles related to adhesion, cell communication and motility as compared to biofilm attached (Niederdorfer *et al.*, 2016). Moreover, biofilm might range from single species mono-layers of heterotrophic bacteria (e.g. in the lungs of cystic fibrosis patients) to multi-taxa and multi-species communities including

prokaryotic cyanobacteria, eukaryotic green algae, and diatoms, complemented by protozoa (e.g. natural biofilm in fluvial ecosystems, Figure 1). The growth, metabolic activity, and survival of these biofilm members exceed by far the capabilities of their free-living companions. Enhanced food availability along with co-metabolisms within the social microbial community boost their development significantly while the biofilm matrix *inter alia* effectively protects the microorganism from extremely varying environmental conditions (e.g. pH or dehydration) or toxins (e.g. antibiotic doses) (Flemming & Wingender, 2010).

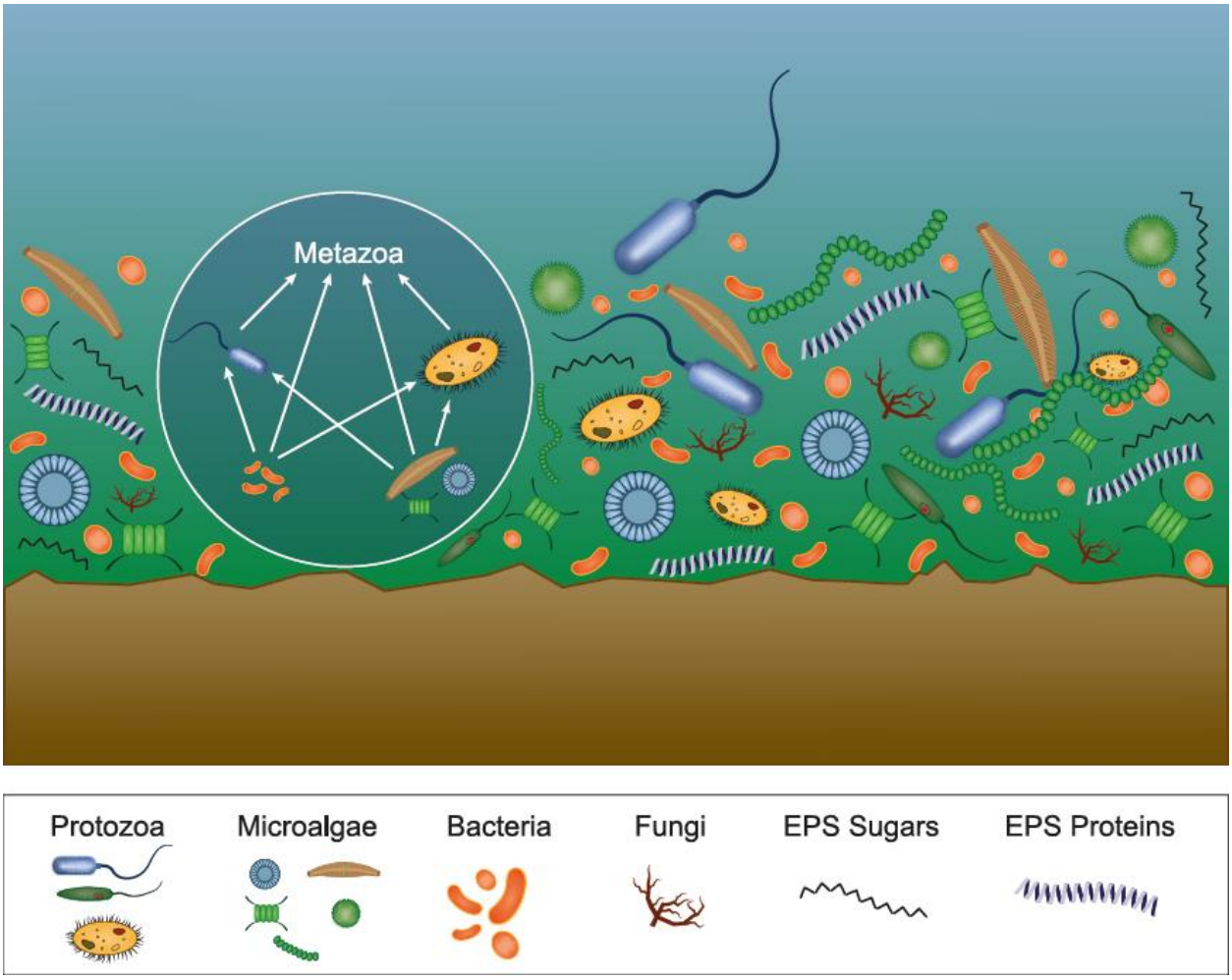

Figure 1: *The graphic illustrates the multicultural life within a biofilm consisting of heterotrophic bacteria, cyanobacteria, diatoms, green algae, fungi, and protozoa. The left circle indicates the trophic relations of the micro-organisms in the 'microbial loop' (Pomeroy* et al.*, 2007). Source: Gerbersdorf and Wieprecht 2015 Geobiology.*

I.2. Hazards and Services of "Microbial Cities"

As advantageous as the life in a biofilm is to its inhabitants, biofilm can have quite diverse effects on their natural or artificial environments; these range from the beneficial (e.g. self-purification, waste-water treatment) to the troublesome or even harmful (e.g. biofouling, biocorrosion, medical infections), incurring high costs (Flemming & Wingender, 2001b; Liu & Fang, 2003; Parsek & Tolker-Nielsen, 2008). With the increased awareness of the widespread nature and resilience of biofilm, the numbers of studies on these microbial assemblages have skyrocketed in biotechnology and biomedicine during recent decades (Pennisi, 2002; Jain *et al.*, 2007; Vu *et al.*, 2009). While this research boosted with a clear focus on monospecies bacterial cultures over the last decades, a shift towards investigations on multispecies bacterial biofilm can be recognized in the more recent years (Hibbing *et al.*, 2010; Elias & Banin, 2012; Hodl *et al.*, 2014). However, research on multitaxa biofilm in their natural habitats has received much less attention, which is surprising given the functional relevance of biofilm, notably at the sediment-water interface (Singer *et al.*, 2006). Biofilm are essential features of rivers and lakes that provide important ecosystem services, such as being the base of the food chain, transferring carbon to higher trophic levels, controlling self-purification of organic compounds and biodegrading anthropogenic pollutants (Gerbersdorf *et al.*, 2011). Moreover, the microbes significantly mediate the erosive response of sediment particles to hydrodynamic forcing (Paterson *et al.*, 2000; Black *et al.*, 2002; Vardy *et al.*, 2007; Gerbersdorf *et al.*, 2008a; Lubarsky *et al.*, 2010). While settling at the grain surfaces, the microbes virtually glue the sediment particles together, mainly by secreting extracellular polymeric substances (EPS) such as polysaccharides, proteins or lipids to form the biofilm matrix (Decho, 1990; Donlan, 2002; Flemming, 2011). In this respect, the microbial mats, up to a few centimeters thick, are important in covering and

protecting large areas of sedimentary surfaces against erosion (Noffke & Paterson, 2008), a phenomenon called “biostabilization” (Paterson, 1989) (Figure 2). Given the right environmental conditions, initial biofilm or mats can develop further into solid, often reef-like structures such as the stromatolites, by trapping sediment particles and mineral precipitation (“biomineralization”) (Noffke & Paterson, 2008; Phoenix & Konhauser, 2008; Paterson *et al.*, 2008).

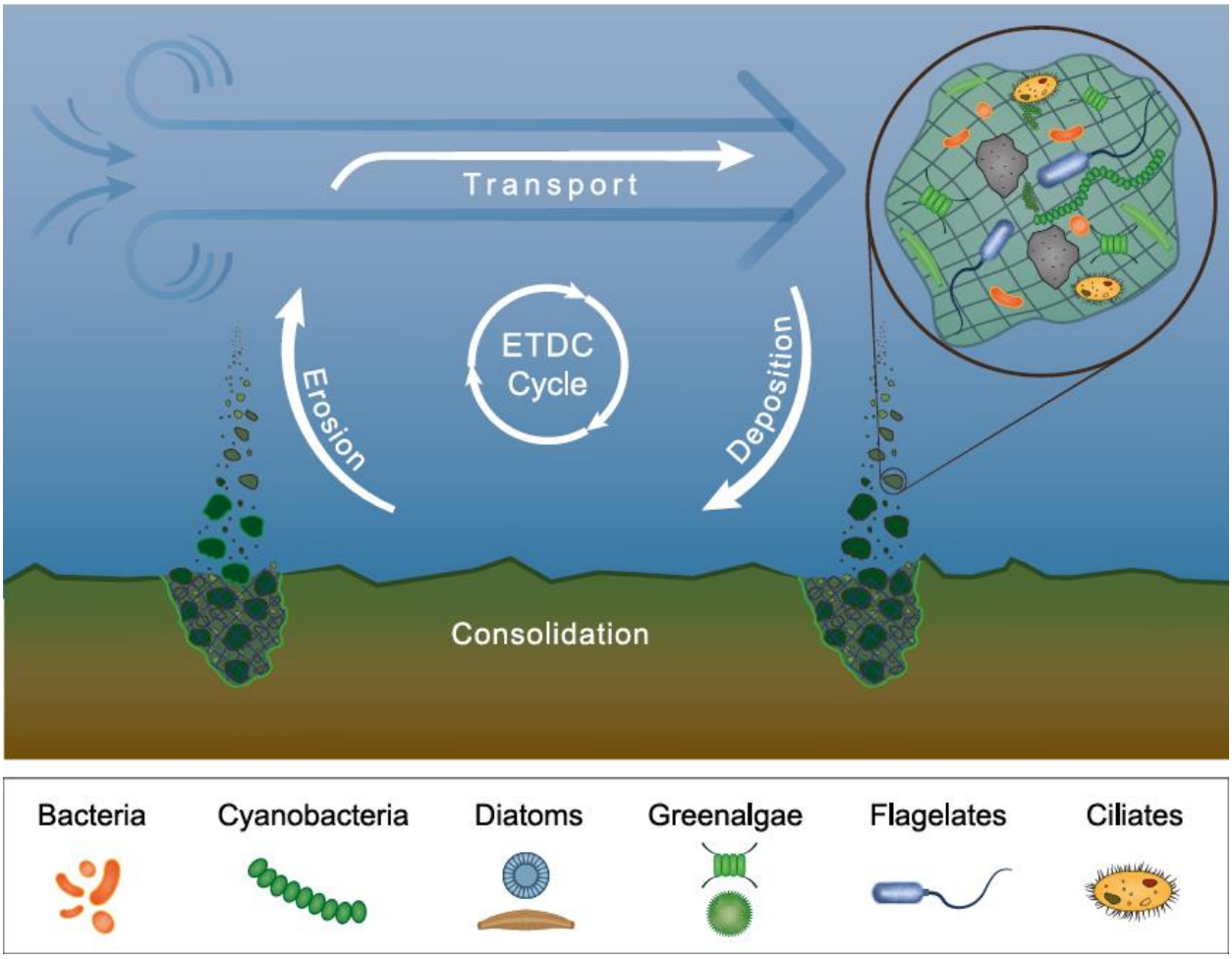

Figure 2: *The significance of biostabilization in the Erosion Transport Deposition Consolidation (ETDC) cycle of cohesive sediments. Microbial activity ‘glues’ fine sediment particles together to impact sediment stability, floc characteristics of the entrained material, and thus, further sediment transport and deposition. During consolidation processes, the biological matrix undergoes chemical changes that further enhance the binding forces. Source: Gerbersdorf and Wieprecht 2015 Geobiology.*

In this habilitation thesis, however, we focus on the stabilization capacity of micro- to macroscopically thin biofilm that coat, bridge or permeate with their hydrated polymeric

mucilage single grains and porous media. Consequently, biostabilization is not restricted to surfaces, but also encompasses deeper sediment/subsurface layers that are likely to be mobilized at flood events or reservoir flushing. The activity of these (ubiquitous) biofilm further extends to the pelagic environment and changes the characteristics of eroded sediment flocs in terms of their size, form, density and settling velocity, affecting sediment transport and deposition (Droppo, 2001, 2004) (Figure 2).

I.3. BIOSTABILIZATION: AN IMPORTANT ECOSYSTEM FUNCTION

Biofilm formation impacts the whole cycle of cohesive sediments, from erosion, transport, deposition to consolidation (ETDC cycle) (Figure 2). For a long time, sediment dynamics has been at the focus of management strategies in terms of “too much” (Netzband *et al.*, 2002), or “too little” (Kondolf, 1997), and the significance of this dynamics in coastal protection will increase with sea level rise (beach nourishment costs on the island Sylt, Germany, 1972–2012: >180 million Euros, GFA–News 2013). In addition to the economic and ecological aspects, we are increasingly concerned about human health related issues, since numerous anthropogenic pollutants tend to bind to fine sediments, coupling their fate closely to sediment deposition (temporary sink for pollutants) and resuspension (secondary source for pollutants) (Haag *et al.*, 2001; Gerbersdorf *et al.*, 2005a, 2007, 2015). Altogether, this explains the intense research efforts of hydraulic engineers to understand and predict sediment dynamics better, but the complexity of fine cohesive sediments (and the strong impact by biological processes) still precluded the definition of a general valid theory to explain their movements (Black *et al.*, 2002; Gerbersdorf *et al.*, 2011). Addressing these cohesive forces in sedimentology (Baas *et al.*, 2013), will ultimately require the implementation of biological processes, as is increasingly recognized by

geomorphologists and hydraulic engineers (Haag *et al.*, 2001; Black *et al.*, 2002). Research at this interface is not exactly new, but disciplinary specialization in recent decades now requires the adoption of mutually accepted methods and approaches (Rice *et al.*, 2010). Nowadays, we see a strong trend towards this type of collaborative work from complementary disciplines (Hannah *et al.*, 2004); however, most investigations on "ecohydraulics" or "ecogeomorphology" concern macroscale processes (Le Hir *et al.*, 2007; Rice *et al.*, 2010). It is one of the future challenges to include the role of microorganisms in this new paradigm since the latter pioneer biological settlement and are prevalent in all substrates and hydraulic regimes (Characklis & Cooksey, 1983; Flemming & Wingender, 2010).

I.4. STATUS QUO IN BIOSTABILIZATION RESEARCH

To better understand the ecosystem function biostabilization, it is essential to learn about biofilm, their development, needs and composition, both in terms of their inhabitants and the EPS matrix, and in reciprocal interaction with abiotic and biotic conditions prevailing in their close environment. The following paragraph gives an update on the knowledge available and the gaps remaining concerning the above mentioned points.

I.4.1. ATTACHMENT AND SETTLEMENT OF BIOSTABILIZING BIOFILM

Landing is not trivial. When approaching the sediment surface, microbial cells are initially transported by eddy diffusion in turbulent flow conditions until they enter the diffusive benthic boundary layer (DBBL) where laminar flow prevails. Depending on size, density and motility, the microbes may travel within this viscous layer by molecular diffusion, gravity, increasing their buoyant density or self-propulsion, and occasionally

by downsweeps (Characklis & Cooksey, 1983; Tuson & Weibel, 2013). Although higher flow velocities could hamper the “touch down” of small organisms, hydrodynamic torque imparted by local shear within porous media or tubes has been shown to trap and accumulate motile bacteria in high-shear regions in close proximity to the surfaces and thus, promoting biofilm formation (Rusconi *et al.*, 2014). Striking the surface does not necessarily lead to permanent attachment of the microbes since shear forces, upsweeps or taxis might result in immediate detachment (Characklis & Cooksey, 1983). However, when given the chance, the microbes possess strategies to successfully adhere to surfaces: they bridge distances to the surface greater than 50nm by weak intermolecular (London dispersion) forces, overcome the electrostatic repulsion barrier at closer distances by increasing the non-polar nature of their cell surface or using appendages/flagella and finally, at closer proximity (< 1.5nm), bind irreversibly by short-range polar forces (e.g. hydrogen bonds, ionic bonds, hydrophobic interaction) and through secreting exopolymeric substances (EPS) (further details in Gerbersdorf & Wieprecht, 2015) (Figure 3). Furthermore, ubiquitously present organic macromolecules with hydrophobic or amphiphilic compounds (e.g. glycoproteins, humic acids, polysaccharides) constitute a so-called conditioning film on the substratum surface which acts to facilitate microbial adhesion by offering a much wider variety of chemical groups as docking stations and to reduce the repulsive forces (Marshall, 1985; Nichols & Nichols, 2008). Consequently, conditioning layers often rendering the underlying surface properties (sometimes specifically modified by material scientist to prevent biofouling) irrelevant (Tuson & Weibel, 2013). Therefore microbes eventually find means to attach to all kind of surfaces although they prefer hydrophobic substrata and enhanced surface roughness with a higher surface area for settlement, shelter from shear forces and increased convective mass transport (Donlan, 2002).

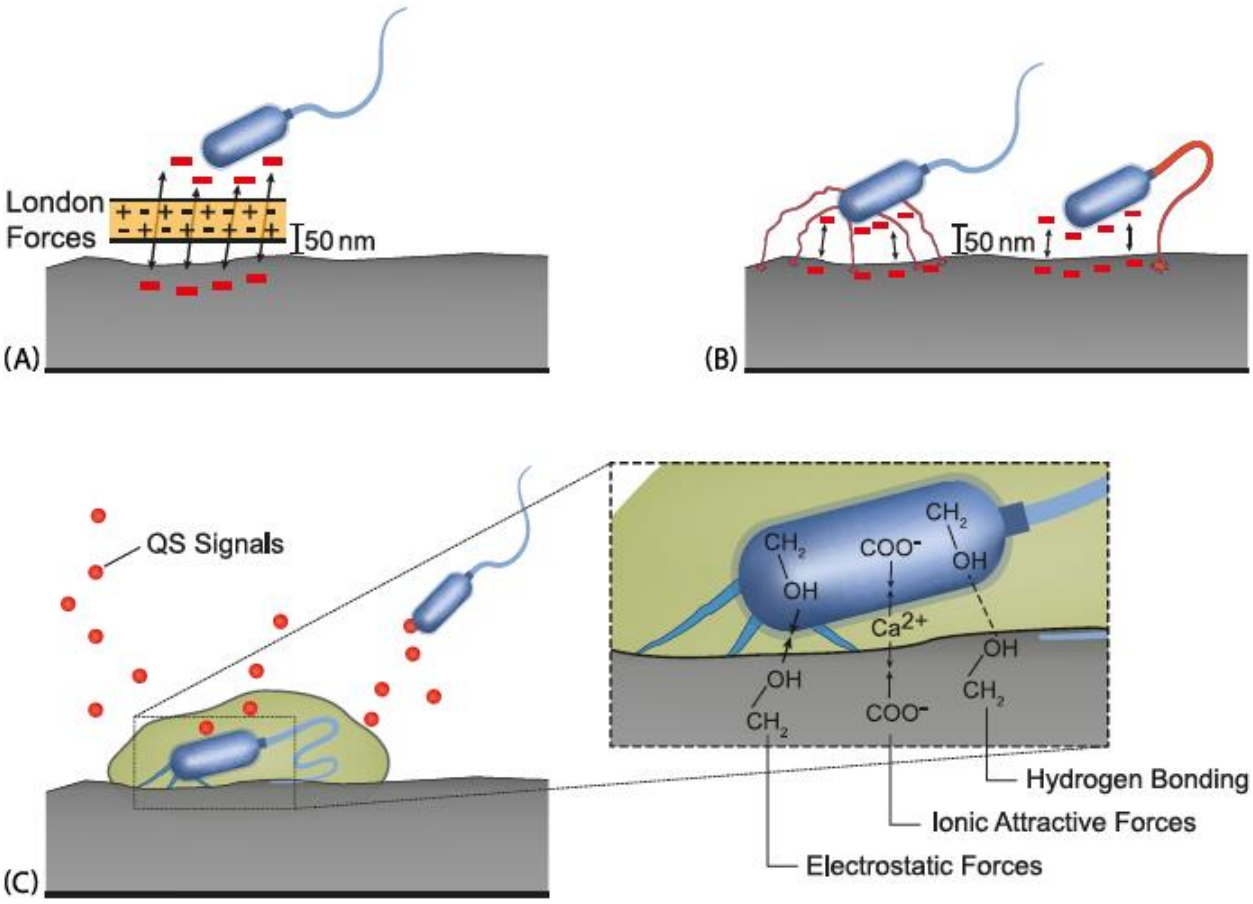

Figure 3: *The initial steps of microbial attachment to a surface: (A) reversible bridging between cell and surface via London forces, (B) overcoming repulsive forces and pulling the cell towards the surface by shooting fimbrae and/or flagellas at the surface and (C) irreversibly binding accompanied by extracellular polymeric substances (EPS) secretion and establishing short polar range forces. Source: Gerbersdorf and Wieprecht 2015 Geobiology.*

Fine-grained sediment: an ideal place to settle. In the benthic environment, highest bacterial numbers and chlorophyll a values are associated with small particle size classes that offer large surface areas for settlement (de Brouwer *et al.*, 2002; Meyer-Reil, 2005). Furthermore, the high surface to volume ratio of fine-grained particles such as clays and silts results in comparatively high surface loadings. This creates so called inter-particle forces that constitute the “cohesive” properties of fine sediments (Paterson & Black, 1999); it remains a challenge to distinguish them from the ubiquitously present and biologically-induced binding forces in natural sediments. This charged nature of fine sediments offers plenty of binding sites that are not restricted to microbes but entrap

organic materials as well as anthropogenic pollutants (Flemming & Wingender, 2001a). Both might serve as nutrient resources for microbes, making the settlement within fine sediments even more attractive (Meyer-Reil, 2005; Gerbersdorf *et al.*, 2011). In contrast, the surface charge in fine or coarse sand is negligible in relation to particle mass; thus these size fractions have less reactive surfaces (Stal, 2003) (Figure 4).

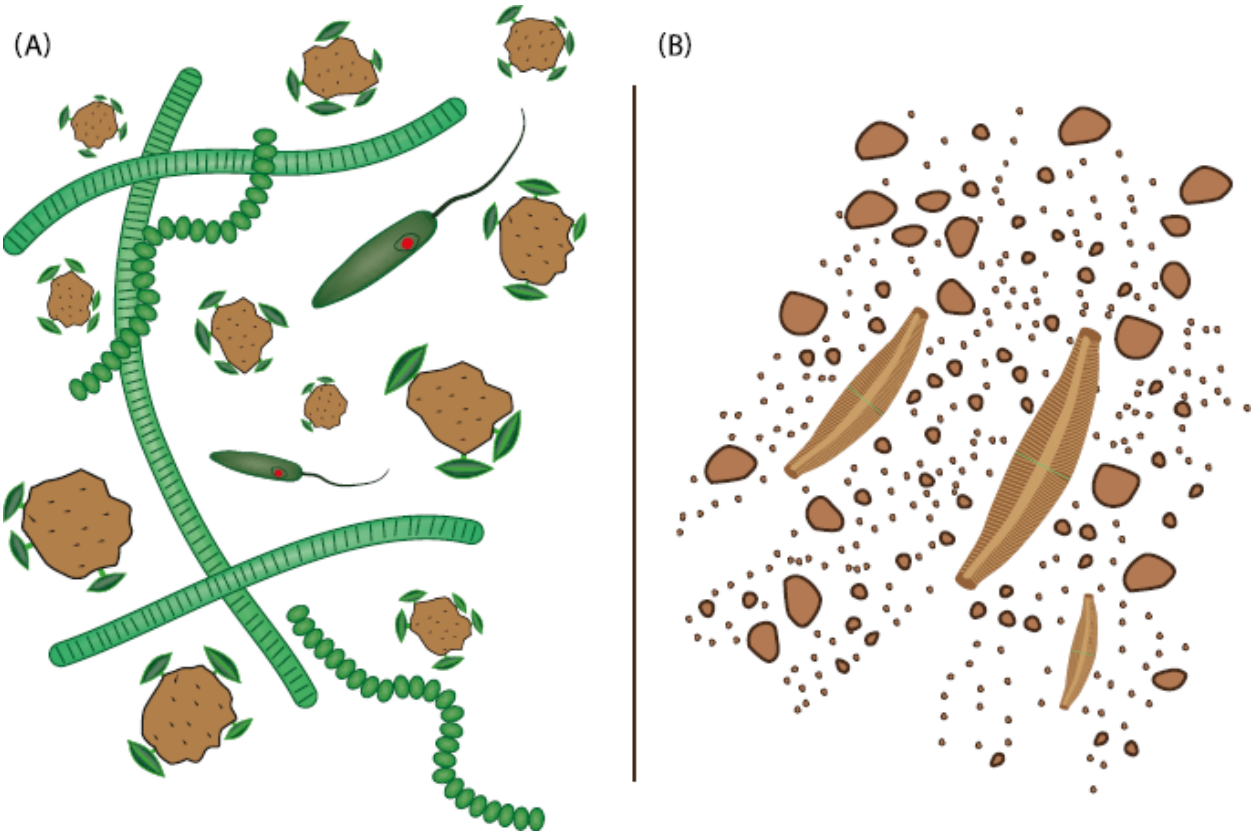

Figure 4: *The graphic contrasts two different sediment types and the typical microbial inhabitants: (A) sandy sediment colonized by epipsammic diatoms that attach via pads and stalks to the particles, as well as cyanobacteria gliding through and building a trichome network and some euglenoids and (B) muddy (silt clay) sediments dominated by epipelic (=moving) diatoms. Source: Gerbersdorf and Wieprecht 2015 Geobiology.*

Nevertheless, pronounced bacterial biofilm growth has been observed in sandy subsurface layers (Leon-Morales *et al.*, 2004). Another important aspect relates to hydraulic conditions and the mobility of particles: coarser sediments deposit in highly energetic habitats where frequent collisions of sand particles (“rolling”) might damage the fragile microorganisms, even the silicate frustules of diatoms (Delgado *et al.*, 1991; Stal, 2003). That said, rapid microbial colonization and sediment binding has still been

observed on very coarse beds with high flow velocities (Battin *et al.*, 2003a; Vignaga *et al.*, 2012). The stromatolites are another example of ecosystem engineering in sandy habitats by cyanobacteria (Noffke & Paterson, 2008; Phoenix & Konhauser, 2008). In contrast to coarse material, cohesive sediments usually settle in waters with low energy impact, hence the likelihood for a microbe of being immediately washed away is actually limited to more extreme events. Still, fine-grained particles are usually far more easily resuspended than coarser sediments; however the microbes can bind silt and clay particles, thus stabilizing their own environment with their growth and activity (Stal, 2003).

Communication and cooperative ecosystem engineers. There is evidence that the successful attachment of one microbe induces further settlement of other companions, whether from the same species or totally different taxa. This is done by means of communication via chemical compounds (autoinducers) that alter the gene expression of the receptor bacteria when the signaling agent passes a certain threshold level (Pasmore & Costerton, 2003). Alterations in these signals subjected to the physico-chemical milieu and biological influences might be used by microbes as an extracellular sensor to get information about their proximal environment, a phenomenon named “efficiency sensing” (Hense *et al.*, 2007). This communication, called “quorum sensing”, has been shown to be vital not only for biofilm formation but also for biofilm morphology (Decho *et al.*, 2010). Obviously, bacterial cells settling closest to the solid surface or deep within a biofilm could quickly become limited for nutrients since diffusion is constrained by the restricted pore space and tight linkages between adjacent polymers of a dense EPS matrix. This seems to be counteracted by the construction and maintenance of flow channels within the EPS matrix and it is speculated that regulation of biofilm morphology occurs via quorum sensing (Pasmore & Costerton, 2003; Nadell

et al., 2008). It seems intuitive that the morphology of the biofilm should not only be closely linked to functionality for the biofilm itself, but also beyond, e.g. in terms of the biostabilization capacity. However, there is not yet enough proof to support this hypothesis. Apart from the significant role of bacterial communication in biofilm, the signals also attract other organisms, including different species and even different taxa, from the micro- to macro-scale. For instance, bacterial settlement facilitates the recruitment of fungi, spores of micro- and macroalgae, protozoa and invertebrate larvae of macrofouling organisms (Mieszkin *et al.*, 2013). Thus, through habitat modification, one ecosystem engineer (here bacteria) promotes the settlement of another engineering species (Passarelli *et al.*, 2014). These sometimes successional, but often rather dynamic shifts in biofilm species composition are addressed in antifouling science (Mieszkin *et al.*, 2013) but have not yet received much attention in biostabilization research, despite their obvious significance for biofilm functionality.

I.4.2. GROWTH REQUIREMENTS OF THE MATURING BIOFILM

After the successful adhesion and attachment, further biofilm growth is largely controlled by nutrient and light provision which are closely linked to hydrodynamics. Biofilm growth along with flow conditions and conductivity determines biofilm strength and thus, biostabilization capacity. In turn, the development of the "microbial city" affects the abiotic conditions both via metabolic activity and by shaping surface roughness and stickiness.

Food availability is vital both in quantity and quality. Nutrients are a prerequisite for cell maintenance and growth and it is thus no surprise that we find nutrient concentrations being well correlated with the number of attached bacterial cells and microalgae (Cowan *et al.*, 1991; Underwood & Paterson, 2003). It is still a matter of debate whether

the first step in biofilm formation, the bacterial attachment, is stimulated by food limitation to enhance long-term access by trapping nutrients and co-metabolism (Poindexter, 1981; Costerton *et al.*, 1995; Meyer-Reil, 2005; Tuson & Weibel, 2013). However, most of our aquatic habitats offer plenty of nutrients and despite of this, or possibly because of that, new surfaces are quickly colonized by microbes. Concerning further growth, thick confluent biofilm are known from nutrient-rich subsurface layers, whereas thin and patchy biofilm are associated with pristine conditions (Leon-Morales *et al.*, 2004). This is in line with observations in estuarine sediments where high nutrient load increased bacterial biofilm growth as well as their EPS production and sediment stabilization (Gerbersdorf *et al.*, 2008b). However, limitation of nutrients has been shown to enhance EPS secretion of diatoms in microbial mats. This has been explained by the stimulation of the locomotive ability enabling the cells to migrate to more favorable conditions and/or by the accumulation of excess carbon during unbalanced growth (Smith & Underwood, 2000; Staats *et al.*, 2000). In many bacterial cultures, large EPS yields could be detected when grown specifically in a high carbon/low nitrogen medium (Decho, 1990). Nutrient composition may not only induce quantitative but also qualitative changes in EPS. For instance, bacteria produced either more EPS proteins or more EPS sugars under carbon or nitrogen starvation, respectively (Durmaz & Sanin, 2001; Sanin *et al.*, 2003). Nutrient-depleted diatoms secreted higher cellular rates of water-soluble carbohydrates, along with a shift towards high-molecular weight fractions within the EPS (Underwood *et al.*, 2004) that could imply a higher binding strength. It has already been assumed that these changes in EPS quality seem to be more decisive for the biostabilization potential of the biofilm than variations in EPS quantity alone (Gerbersdorf *et al.*, 2008b; Lubarsky *et al.*, 2010). Nevertheless, it remains to be answered whether nutrient depletion or -excess via varying EPS

chemistry or movement pattern (“micro-bioturbation”) has an altogether positive or negative influence on sediment stability.

Hydrodynamics is key: shear forces and DBBL. One thing seems to be sure though: hydrodynamics have a vital role in shaping biofilm architecture, composition and functionality. First of all, the shear forces impact biofilm attachment as well as further colonization up to possible cell dispersal and biofilm dissolution (McDougald *et al.*, 2012). Second, flow velocity determines largely the expansion of the diffusive benthic boundary layer (DBBL) that again influences the diffusion path length of nutrients and thus, their availability to the microbial community (Figure 5). Consequently, at low flow conditions, the pronounced thickness of the DBBL may restrain nutrient diffusion towards the biofilm surface while greater shear forces evidently enhance the metabolic and kinetic behaviour of biofilm (Liu & Tay, 2002). During growth in the benthic environment, bacterial settlement will be smoothing the sediment surface to reduce turbulence (Graba *et al.*, 2010) but subsequent algae development producing long filaments is then again roughening the surface (Nikora *et al.*, 1998). This patchy grow of biofilm might counteract impending nutrient depletion by maximizing the sinuosity of advective flow across the biofilm surface (Battin *et al.*, 2003b). Thus, the two extremes in biofilm structures, the compact and close-to-each-other bungalow type colonies in turbulent conditions as opposed to the fluffy skyscraper-type settlements (that project through the laminar layers into areas with greater food supply) in calm waters, are mostly reasoned because of two important features for biofilm growth: protection from detachment and sufficient nutrient supply (Figure 5).

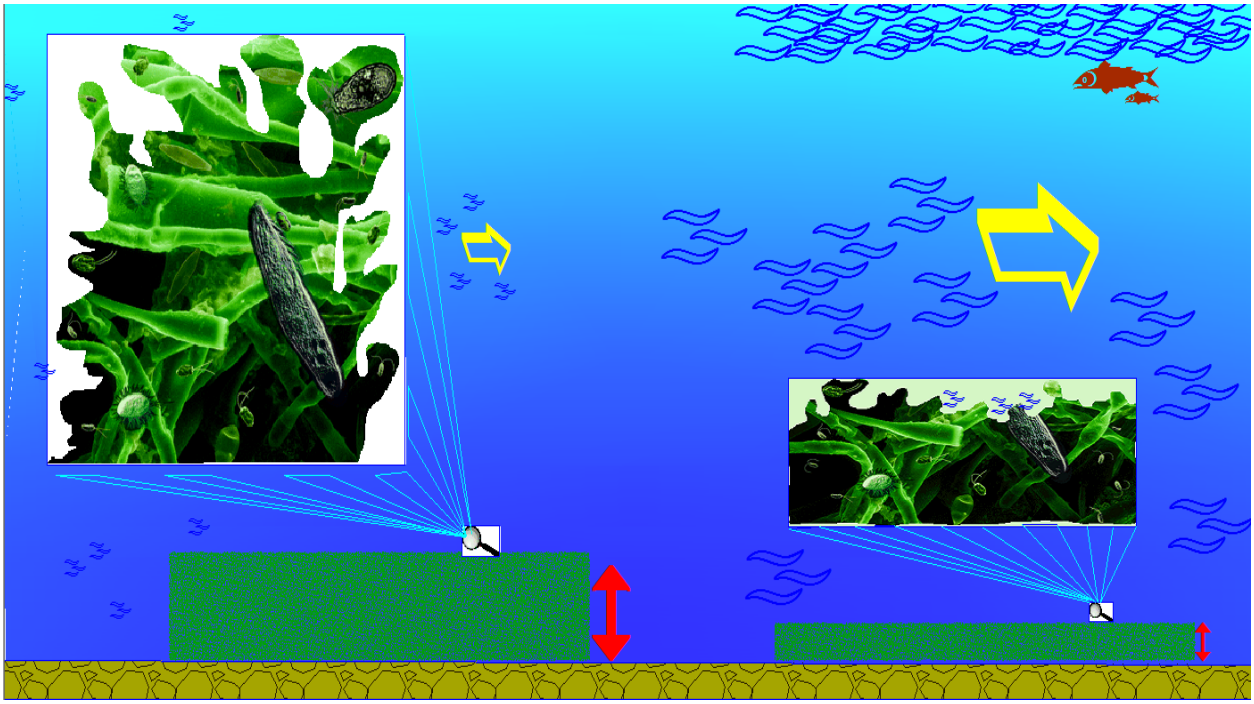

Figure 5: *The graphic illustrates the effect of two different hydrodynamic scenarios: lower flow conditions (left) result in a pronounced DBBL (diffusive benthic boundary layer) and thicker, more fluffier biofilm while higher flow velocities (right) reduces the extension of both, DBBL and biofilm; the latter being more compact.*

The resulting biofilm structures have again implications for their own compactness and stability: both increase with turbulent conditions (Pereira *et al.*, 2002; Graba *et al.*, 2013). Apparently a higher stability might be explained by enhanced exopolymeric secretion within the biofilm that is subjected to higher fluid velocities (Brading *et al.*, 1995). Moreover, the whole architecture and the microbial assemblages vary significantly at different hydrodynamic regimes (Besemer *et al.*, 2007). Despite enhanced EPS production, it now seems generally accepted that flow velocity and the thickness of the biofilm are negatively related (Pereira *et al.*, 2002; Graba *et al.*, 2013). Since diffusion limitation is negligible within thinner biofilm, this might have implications for a higher efficiency in microbial turnover rates and a more effective EPS production. Besides affecting a range of vital functionalities provided by the biofilm, a thinner structure might relate to biostabilization capacity. While it is intuitive to assume significant effects for biostabilization by these different types of biofilm, hardly any study

crosses disciplinary boundaries to link structural parameters such as biofilm architecture to functionality such as adhesive capacity and sediment stabilization, neither at the surface nor in subsurface layers.

Light and photosynthesis - essential in autotrophic biofilm. Light is certainly a prerequisite for autotrophic biofilm members to grow; still too much light can severely harm. Photosynthesizing organisms have developed various strategies to cope with either too little or too much light, which in turn, impacts biostabilization. Most phototrophs show relatively low light saturation values at 5–150µE m^{-2} s^{-1}, especially those of prokaryotic origin such as cyanobacteria, purple or some green sulfur bacteria (<0.1µE m^{-2} s^{-1}) (Gerbersdorf *et al.*, 2005a; Franks & Stolz, 2009). Nevertheless, a common problem is eutrophication of aquatic systems favoring phytoplankton blooms and increasing light attenuation in the water body that suppresses microphytobenthic life as well as reducing their ecosystem functions (Gerbersdorf *et al.*, 2005b). Another issue in calm waters where microbes settle is the continuous coverage by newly deposited fine material, which might further limit light penetration into the biofilm and hampers photosynthesis. On the other hand, ultraviolet (280–400nm) or photosynthetic active radiation (400–700nm) might reach locally harmful intensities that are counteracted e.g. by biomineralization or physiological responses such as non-photochemical quenching via the xanthophyll cycle (Phoenix *et al.*, 2006; Jesus *et al.*, 2009). Whether too little or too much light, most of the microalgae are able to migrate towards optimum light conditions; thereby orientating themselves by gravity, light or chemical gradients while showing a circadian and - where applicable - tidal rhythm (Friend *et al.*, 2003; Stal, 2003). The important point is: all of the strategies to cope with the varying light fields have implications for biostabilization which is obvious for the impact of silicified biofilm but expands to physiological adaptation and migration that

both concern the EPS production and secretion. Epipelic diatoms that are common in muddy sediments move for instance on those polymers which are secreted through their raphes (Paterson, 1989; Underwood & Paterson, 2003) (Figure 4). This colloidal EPS carbohydrate fraction contributes significantly to sediment binding, especially in “deeper” sediment horizons due to de-watering and degradation processes (Yallop *et al.*, 2000; Gerbersdorf *et al.*, 2008a). The gliding motility of cyanobacteria may as well enhance the stability of sandy substrates (Stal, 2003, 2010) (Figure 4). Moreover, cyanobacteria are highly capable to trap fine sediments in their trichome network by their “baffling and trapping” strategy (Noffke & Paterson, 2008) or release EPS sugars to act as bioflocculants that additionally trap sediments and contribute to water clarity and sediment stability (Bender *et al.*, 1994). It is thus surprising that cyanobacteria are hardly addressed in biostabilization research.

With the focus being on stabilizing microalgae in recent years, there have been huge efforts to prove the link between photosynthetic activity and EPS production. Orvain et al. (2003) reported an increase of extracellular carbohydrates during the day due to photosynthesis. However, there is evidence for additional EPS release during dark phases related to algae movements. Whether the latter is due to utilization of internal storage such as glucan (Underwood & Smith, 1998; Smith & Underwood, 2000) or facilitated by fresh EPS production during heterotrophic phases (Staats *et al.*, 2000), photosynthesis seems to be the prerequisite to this direct or indirect release of extracellular material which emphasizes again the role of light for biofilm growth and biostabilization. Since photosynthesis cannot be shut down, continuously high light intensities might eventually lead to an overflow of photo-assimilates, thus further increasing the amount of (colloidal and low-molecular weight) EPS to sometimes extremely high rates on e.g. tropical sand and mudflats (Perkins *et al.*, 2001; Wolfstein

& Stal, 2002; Underwood, 2002). Whether this excess of water-extractable carbohydrates that are usually released at the sediment surface, is washed away or contributes to sediment stability, is still a matter of debate. Nevertheless, too much light will eventually rather destabilize the upper sediment layers, for instance by the photosynthesis-driven oversaturation of oxygen resulting in the formation of bubbles (Sutherland *et al.*, 1998a) (Figure 6).

Figure 6: *An oxygen bubble trapped in the filaments of the green algae Klebsormidium flaccidum. Source: Gerbersdorf and Wieprecht 2015 Geobiology.*

Gas formation could be one explanation why some biofilm are more strongly adhered to sediment in the beginning of the succession than in later stages with substantial algal growth (Droppo *et al.*, 2007; Gerbersdorf *et al.*, 2009). In addition to oxygen bubbles at the surface derived by photosynthesis, anaerobic respiration processes by bacteria will contribute to the formation of gases (methane, carbon dioxide) in deeper layers. These bubbles might ascend towards the surface, but their effect on stability can only be speculated on (Amos *et al.*, 2003).

I.4.3. SPECIES COMPOSITION - INTERNAL COMPETITION AND EXTERNAL FORCING

While environmental parameters drive the physiological response and growth, this will vary in a species-specific manner. In turn, the species composition of the microbial

community depends on abiotic as well as biotic (competition, predation/grazing) conditions. This shows the high extent of feedback mechanisms between abiotic/biotic conditions, metabolic activity, growth, and diversity of microorganisms to influence biostabilization.

Bacteria as Pioneers. Given the right abiotic conditions, natural biofilm will rarely be assembled by just one taxa or even one single species as it is sometimes seen in rather extreme “habitats” (e.g. different heterotroph bacterial biofilm in drinking water pipes, *Pseudomonas* biofilm in the lungs of fibrocytosis patients). After microbes initiate the first settlement on a surface, they will soon experience neighbors of the same or different kind in a more or less predictable succession or via dynamic shifts, mediated by quorum sensing. Usually bacteria are the pioneers able to secrete copious amounts of EPS and to establish elaborate biofilm of impressive thickness and rigidity, as we have known for a long time from medicine, biotechnology and waste-water treatment (Flemming & Wingender, 2001a; Liu & Fang, 2003; Parsek & Tolker-Nielsen, 2008). Dade and Nowell (1991) calculated that one single bacterium can produce enough EPS to cover more than 500 particles of about 0.4µm per day, with significant effects on the entrainment of clay/water suspensions (Dade *et al.*, 1990, 1996). Bacteria occur ubiquitously and in high numbers (10^9-10^{12} cells g^{-1} dry weight) in fine sediments, thus being the dominant microbial genera (Meyer-Reil, 2005). While this holds especially true in vertical terms where bacteria can contribute to sediment stabilization in deeper layers, it has been largely overlooked (Gerbersdorf *et al.*, 2005a). Just recently, the high stabilizing potential of natural bacterial assemblages growing on artificial glass beads has been shown, with substratum stability being up to 11 (in some cases even up to 20) times higher as compared to the abiotic controls (Gerbersdorf *et al.*, 2008b, 2009). This high stabilization potential of bacteria might be explained by their tendency to secrete a

tenaciously adhesive EPS for permanent attachment since staying put requires especially strong and epoxy-like glues (Svensater *et al.*, 2001; Pennisi, 2002). However, there is still a paucity of information on the role of bacteria in biofilm succession and the consequences for sediment stability.

Microalgae - the second phase of biofilm formation. In natural habitats with sufficient light availability, phototrophic microorganisms that occur as single cells, in colonies or as filaments, are soon complementing the biofilm: prokaryotic cyanobacteria, eukaryotic green algae and diatoms (mainly pennate, epipsammic/attached or epipelic/motile species, some centric). In comparison to bacteria (mostly 0.5-1µm), microalgae are larger in size (10-200µm) and need to create macromolecular bridges to connect to particles, thus adding to binding forces by interconnecting sheets and strands of EPS (Black *et al.*, 2002). Like the bacteria, epipsammic diatoms firmly attach to sand grains via appropriate EPS strands or pads that consist of highly complex insoluble EPS, similar to the polymers secreted by filamentous cyanobacteria (Hoagland *et al.*, 1993; Wustman *et al.*, 1997; Underwood & Smith, 1998; de Winder *et al.*, 1999; Stal, 2003; Molino & Wetherbee, 2008). In addition, the net-like structures formed by the filamentous sheaths of cyanobacteria can significantly add to sediment stability (Grant & Gust, 1987; Noffke *et al.*, 2003; Amos *et al.*, 2004; Vignaga *et al.*, 2012). Much more common in intertidal areas as well as in freshwater sediments are motile or epipelic diatoms. Their EPS secretion is largely depending on size because larger cells such as *Nitzschia sigma* (100-200µm) may require proportionally more EPS to propel them through the sediment as compared to the smaller species *Nitzschia frustulum* and *Surirella ovata* with lower EPS yields (Underwood & Smith, 1998; Smith & Underwood, 2000). However, quantity is not necessarily decisive for the binding effects observed.

De Brouwer et al. (2005) substantiated this by two times higher sediment-stabilizing effects of *Nitzschia brevissima* creating three-dimensional matrix structures as opposed to the tychoplanktonic *Cylindrotheca closterium*, although both secrete similar quantities of EPS carbohydrates. Furthermore, microalgal species secreting the comparatively lowest EPS (sugar and protein) content created biofilm of highest viscosity (Hu *et al.*, 2003). These findings point to the significance of the composition and structural consistency of the EPS matrix for the stability of the biofilm that also varies significantly among the different species, and even among the same strains (Decho, 1990). Motile diatoms have in common that the binding must be more of the temporarily kind to allow movement through the substratum (Decho, 1990; Underwood & Paterson, 2003; Gerbersdorf *et al.*, 2008a). Hence, they produce rather labile EPS fractions which are the preferred subject for bacterial mineralization. This again might result in refractory EPS compounds with higher binding capacity, especially in deeper layers as explained above (Yallop *et al.*, 2000; Gerbersdorf *et al.*, 2008a; McKew *et al.*, 2013).

Bacteria and microalgae - symbiosis or competition? Generally it is assumed that the coexistence of heterotrophic bacteria and microalgae leads to positive biostabilization effects since both parties benefit from each other, which results in increased EPS yields. Bacteria can exploit microalgal exudates (van Duyl *et al.*, 1999; Goto *et al.*, 2001; Hofmann *et al.*, 2009) and as a reward, microalgae are supplied with essential vitamins/minerals and recycled nutrients by bacterial metabolism (Klug, 2005). That way, both taxa will become less depend on external nutrient sources. Bruckner et al. (2011) proposed the presence of bacteria as even vital for diatom growth and EPS secretion. On the other hand, only specific types of bacteria seem to be tolerated in close proximity to microalgae (“satellite bacteria”) (Schäfer *et al.*, 2002). Microalgae can

secret polyunsaturated aldehydes against unwanted company with strong bactericidal effects (Wichard *et al.*, 2005; Ribalet *et al.*, 2008). In return, bacteria might suppress microalgal growth by releasing algicidal compounds into the medium (Fukami *et al.*, 1997; Jung *et al.*, 2008). Moreover, there is biochemical and genetic evidence of the expression of valine, one of the aliphatic amino acids, by many gram-negative bacteria within the biofilm to reduce interspecies competition (Valle *et al.*, 2008). Whether one or the other “wins” the competition strongly depends on the abiotic settings: for instance, the addition of nutrients favored diatom growth and suppressed bacterial growth, while bacteria were soon dominating at low nutrient levels (Gerbersdorf *et al.*, 2009). Although the overall interplay between bacteria and diatoms is not truly understood in all its complexity, it is interesting to note that the dominance of a certain taxa or species has strong implications for biostabilization. Undoubtedly, a large proportion of the variations in EPS quantity and quality are due to the environmental settings, the physiological state as well as growth phase of the microbes (Hoagland *et al.*, 1993). However, the paper of Bahulikar and Kroth (2008) strongly emphasizes the close relationship between EPS characteristics and species type, since the carbohydrate composition mirrored the phylogenetic relationship of the respective (freshwater) diatom under the same defined culture conditions. While it can thus be concluded that species composition matters for biostabilization, attempting to unravel the relationship is near to impossible in the complex natural environments. With the new molecular techniques available such as next-generation sequencing (NGS), it is high time to relate pro- and eukaryotic species in a complex sample (metagenomic approach) to their gene expression (from metatranscriptomics addressing RNA molecules to proteomics and EPS secretion) to identify the conditions and EPS components that are significant for biostabilization, thus providing a better link to functionality.

Predators in the Micro-Range. One of the main external forcing parameters that biofilm inhabitants and the EPS matrix experience is grazing pressure. First of all, extraordinary large populations of bacteriophages and to lesser extent eukaryotic algal viruses, control bacterial growth as well as microalgal blooms, respectively. This “bottom-up control” has significant impacts on the nutrient recycling within the microbial loop but also induces severe shifts in the aquatic microbial species composition with likely effects on biofilm functionality (Wommack & Colwell, 2000; Pomeroy *et al.*, 2007). Second, there is a “top-down control” by sessile protozoa and lower metazoans which are important grazers within natural biofilm (Wimpenny *et al.*, 2000; Parry, 2004). Heterotrophic flagellates (HF) and ciliates are the most abundant predators that control bacterial abundances and species composition direct or indirectly. For instance, bacterivorous suspension feeders such as peritrichous ciliates might either support benthic bacterial growth by producing a water (and nutrient) current or conversely, lead to the detachment of sessile bacteria by hydrodynamic stress (Parry, 2004; Ackermann *et al.*, 2011). In contrast, the omnivorous heterotrich *Stentor* was able to exert a great grazing pressure on bacteria and microalgae, as well as on flagellates and small ciliates within the biofilm (Ackermann *et al.*, 2011). HF can also significantly reduce bacterial cells, but at the same time they stimulate the abundance of matrix-embedded bacterial microcolonies that are better protected against feeding (Matz & Kjelleberg, 2005; Wey *et al.*, 2008). Some grazers, however, might effectively get access to bacteria even within matured biofilm by their specialized feeding mode (Weitere *et al.*, 2005). There are no hints that ciliates would influence the build-up of biofilm structures, but they keep the HF in check; thus their presence might lead to a net increase in single bacterial cells (Wey *et al.*, 2008; Hofmann *et al.*, 2009). Altogether, research focusing on protozoa abundances, species distribution and feeding behaviour has very recently gained

momentum but possible impacts on bacterial taxonomy, EPS secretion pattern, and resulting sediment biostabilization are largely uncharted territory. It is timely to consider all relevant groups of organisms in biofilm since the multitude of their interactions imposes great consequences for biofilm functionality.

I.4.4. THE EPS MATRIX - KEY TO FUNCTIONALITY?

The EPS matrix forms the streets and houses of the microbial city in which their inhabitants flourish, move and interact, but at the same time acts as the essential glue to bridge sediment particles, change their erosional behaviour and thus to stabilize the outer surrounding of the biofilm (Figure 7). With up to 90%, the matrix is the dominating part of the biofilm while only 10% of the dry mass relates to the inhabiting microorganisms (Flemming & Wingender, 2010). Considering this importance in functionality and quantity, it is worthwhile to have a closer look at the current knowledge on EPS origin, components, composition and structural elucidation related to biostabilization.

Making-of-EPS Matrix. Within this matrix, water is by far the dominating component, thus biofilm were named “stiff water” by K.C. Marshall. Interesting to note that 99.8% of the water has similar features in comparison to the bulk water, indicated by similar diffusion coefficients, while only 0.2% interact with EPS components to reduce significantly permeability (Vogt *et al.*, 2000).

Thus water seems to be retained just by lowered entropy through mixing with non-interacting polymers (Flemming, 2011). It is well-known that water content of the sediment is negatively correlated to sediment stability; for instance, consolidation with depth enhances the inter-particle forces between sediment particles by reducing sediment porosity (Paterson *et al.*, 2000; Haag *et al.*, 2001; Orvain *et al.*, 2003).

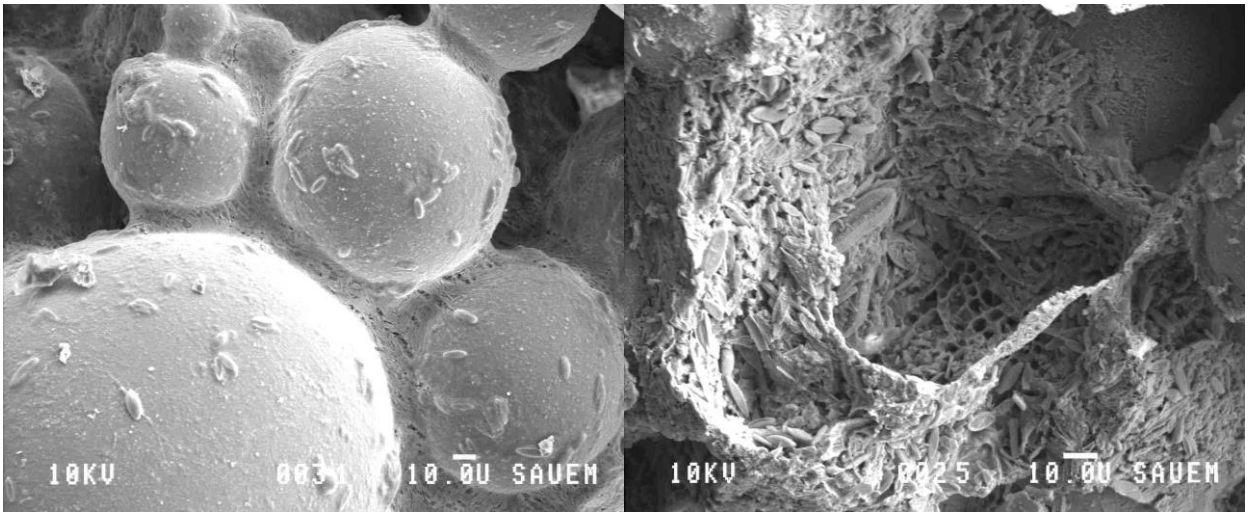

Figure 7: *LTSEM (low-temperature scanning electron microscopy, SERG-Lab of Prof. D.M.Paterson) Images. Left: glass beads embedded by the extracellular polymeric substances (EPS) matrix of naturally grown biofilm consisting mainly of heterotrophic bacteria and diatoms. Right: EPS strands and embedded microbes that surrounded the detached glass bead (empty space). Source: Gerbersdorf and Wieprecht 2015 Geobiology.*

It also seems that the EPS moieties show a higher binding capacity with sediment depth (Perkins *et al.*, 2003; de Brouwer *et al.*, 2005). Similarly, it can be expected that desiccation within the EPS matrix brings potential binding sites of the biopolymers closer together to enhance biofilm stability; this is largely unexplored (Flemming & Wingender, 2010). Although the actual polymers represent the smallest proportion of the EPS matrix, their binding capacity is significant. The biopolymers have charged residues that interact among each other as well as with water to effectively hold the biofilm together. Surprisingly, these bonds create individually weak forces such as hydrogen and ionic bonds as well as London forces and hydrophobic interactions. In terms of the overall binding capacity however, these forces add up to bond values equivalent to those of the covalent type, explaining the high integrity of the biofilm matrix that extends towards the effective connection of external sediment particles (Flemming *et al.*, 2000). Thereby, the rather freshly-secreted and loosely-attached moieties (colloidal or water-extractable) are to be distinguished from more matured refractory pool of firmly-bound (e.g. cation-exchange-resin extractable) EPS. Since the

first fraction seems to be related to migration or an overflow of photo-assimilates, these water-extractable compounds might be easily washed away (Paterson, 1989; de Brouwer *et al.*, 2005). Apart from direct secretion of more firmly attached EPS (Pennisi, 2002), degradation processes along with de-watering transforms part of the colloidal into bound moieties that contribute significantly to adhesion and sediment binding (Yallop *et al.*, 2000; Gerbersdorf *et al.*, 2008a). Within the conglomerate of various biopolymers in both fractions, the best investigated constituents related to biostabilization are carbohydrates, proteins, and nucleic acids.

EPS sugars might be homopolysaccharides constructed from one monomer only (such as dextran, cellulose, curdlan), but the majority consists of heteropolysaccharides (such as kefiran, gellan, alginate, xanthan). While homopolysaccharides are mostly neutral, heterosugars can be either polyanionic by the presence of uronic acids, ketal-linked pyruvate, phosphate or sulphate, or polycationic due to amine moieties that are protonated or acetylated/deacetylated (Flemming & Wingender, 2010). For microalgae, there is evidence that the monomer glucose largely dominates the freshly produced, photosynthesis-linked and less binding colloidal EPS fraction. During the transition from colloidal to bound fractions (Taylor *et al.*, 1999; Pierre *et al.*, 2010) as well as from log to stationary growth phase (Hofmann *et al.*, 2009; Aslam *et al.*, 2012), this glucose content decreases along with an increasing share of structural more relevant monosaccharides. The changing proportion towards e.g. mannose, rhamnose, xylose or galacturonic acid, has been related to enhanced attachment as well as binding properties of the biofilm (Hu *et al.*, 2003; Willis *et al.*, 2013). First, the increase in heterogeneity among the monosaccharides towards the more bound EPS fractions (Bahulikar & Kroth, 2008; Pierre *et al.*, 2010) emphasizes the importance of monosaccharide variety for the binding potential (Hu *et al.*, 2003). In contrast to microalgae, it appears that most

bacterial sugars consist of few monomers only (three to four instead of six to ten for microalgae); these monomers are arranged in groups of ten or less to form repeating units (Nichols & Nichols, 2008). Nevertheless, bacteria usually attach permanently and thus, their EPS has a high degree of tensile strength and structural relevance (Zeng *et al.*, 2015a). This point to the second important feature: bacterial EPS sugars show a great conglomeration of substituents (phosphate, pyruvate, acyl groups), functional groups (carboxyl-group) and linkages to proteins (glycoproteins, proteoglycans) that are all clearly linked to adhesive properties, permanent attachment and biofilm formation (Decho, 1990; Vu *et al.*, 2009). This underlines the importance of hydrophobicity and polyionic nature of the secreted heterosugars to facilitate adhesive capacity via ionic bridging (Staats *et al.*, 1999; Donlan, 2002) and explains the higher binding potential of species secreting polymers with a high degree of substitutions (Hu *et al.*, 2003). Third, EPS polysaccharides often show various degrees of branching to form complex networks and architectures resulting in sheets, spirals, and single/triple helices (Dumitriu, 2004; Delattre *et al.*, 2016): all of which adds further to structural integrity (Pennisi, 2002; Wotton, 2004). Nevertheless, even unbranched polymers like alginate can be responsible for the mechanical stability of the matured biofilm (Flemming & Wingender, 2010). Hence, EPS sugars seem to have their share in the observed binding effects, although they are also preferentially hydrolyzed by bacteria in contrast to proteins, the latter becoming enriched during biofilm aging (Nielsen *et al.*, 1997; van Duyl *et al.*, 1999; de Brouwer & Stal, 2001; Goto *et al.*, 2001).

EPS Proteins. In the past, EPS protein moieties were solely regarded as an external digestive system secreted by bacteria to break down biopolymers and organic particles in close proximity to their cell and facilitate cellular uptake (Flemming & Wingender, 2010). Although the link of these proportionally-wise significant EPS enzymes to binding

capacity is not directly obvious, they eventually promote growth of microbes and help biofilm formation as well as enable microbial dispersal and the colonization of new habitats where biostabilization can occur (Characklis & Cooksey, 1983; McDougald *et al.*, 2012). Furthermore, there is increasing evidence on the structural role of proteins (Pennisi, 2002). Proteinaceous appendages of bacteria and eukaryotes such as pili, fimbriae and flagella are important for adhesion and mobility, respectively, but might also act as structural elements to influence matrix stabilization (Flemming & Wingender, 2010). Recently, the formation of bacterial amyloids fibrils has been linked to a more rapid surface colonization, alterations in biofilm morphology and stiffness as well as mechanical robustness (Dueholm *et al.*, 2013a;b; Zeng *et al.*, 2015a). In addition, these amyloids are entangled in a net-like structure that is able to bind small metabolites such as nutrients or quorum-sensing molecules; both vital for biofilm growth (Seviour *et al.*, 2015; Zeng *et al.*, 2015a). Earlier AFM (Atomic force microscopy) investigations as well as staining techniques and spectroscopy on diatom mucilages (e.g. pads) identified proteins as being the primary component of their adhesives (Dugdale *et al.*, 2005; Chiovitti *et al.*, 2008). For ovoid benthic (attached) forms, a considerable portion of the cell frustule was enveloped in proteins (Willis *et al.*, 2013). EPS proteins intertwined with carbohydrates (so-called lectins) are important in the formation and stabilization of the matrix to form epoxy resin-like structures, as well as help flocculation and floc stability (Long & Azam, 1996; Pennisi, 2002; Czaczyk & Myszka, 2007; Lynch *et al.*, 2007; Park & Novak, 2009). In line with these insights, it has become apparent that sediment stability is significantly related to EPS proteins (Gerbersdorf *et al.*, 2008b, 2009; Lubarsky *et al.*, 2010; Schmidt *et al.*, 2016). Thus, non-enzymatic EPS proteins seem to be strongly involved in attachment as well as in the structural integrity of the

biofilm and its immediate surroundings to boost biostabilization. However, this needs to be followed up in more detail.

Extracellular DNA. In the past, extracellular DNA (eDNA) was regarded as a residue of previous cell lyses, but it became clear that eDNA is also actively secreted or released via vesicles from living cells to fulfill a wide range of functions (Dominiak *et al.*, 2011). The relatively abundant eDNA (up to 300mg g^{-1} organic matter) is *inter alia* linked to quorum sensing (which is decisive for biofilm build-up and maintenance) and represents an important structural component within the EPS matrix (Whitchurch *et al.*, 2002; Allesen-Holm *et al.*, 2006; Dominiak *et al.*, 2011). Despite the fact that the eDNA from various bacterial cultures revealed major similarities to their whole-genome DNA, distinct differences have been detected that support the concept of the structural function of eDNA (Böckelmann *et al.*, 2006; Allesen-Holm *et al.*, 2006). Apart from the genetic evidence, Böckelmann et al. (2006) showed for the first time the formation of an extracellular filamentous network of eDNA (by bacteria isolated from river snow) that might contribute to particle trapping or interactions within the biofilm community, not to mention bonding. Moreover, there are hints that the flexible eDNA matrix is embedding the relatively stiff bacterial amyloid fibrils to combine elasticity with rigidness (Zeng *et al.*, 2015a) like it is known from spider dragline silk (Hagn, 2012). Although the eDNA is normally highly susceptible to DNase, the eDNA may be adsorbed and stabilized in fine sediments by generating cationic bridges between the clay surfaces and the phosphate groups of the nucleic acids, both negatively-charged (Nielsen *et al.*, 2006). In this way, the eDNA becomes partially resistant to degradation by nucleases and might add to sediment stabilization, but this has not been addressed yet.

Behind the scenes - structural elucidation of EPS. To understand the mechanistic behaviour behind the effects of biostabilization that we record, modern analytical studies on nature and conformation of EPS biopolymers are required that go beyond the quantitative determination of the above mentioned major EPS constituents. So far, the monomer characterization of the diatom and bacterial EPS components gave the first valuable hints to certain fractions and functional groups, as well as residues, which are possibly prerequisites for adhesion within the biofilm matrix and beyond. Even so, the observed phenomenon of biostabilization is far from being explained by examining the analytically separated single monomers of EPS only. For instance, the diatom mucilages of the benthic ovoid and planktonic fusiform *Phaeodactylum tricornutum* cells (diatom) have similar profiles of monosaccharides, but only the EPS of the ovoid type shows adhesive properties (Willis *et al.*, 2013). Similarly, the cyanobacteria *Microcoleus vaginatus* and *Scytonema javanicum* are significantly different in stabilizing sand grains, but their EPS is largely similar in protein content and monosaccharides composition (Hu *et al.*, 2003). It thus seems to be timely and important to know more about the order in which the monomers occur, the type and stereochemistry of linkages and branching, to better understand adhesive capacity. Pursuing the above presented examples, linkage analysis by Willis et al. (2013) suggests an important role for 4-linked fucose and 3,4-linked rhamnose in the adhesive mucilage of the ovoid type whereas terminal xylose and 2-linked fucose is more common in non-adhesive EPS of the fusiform cells. Likewise, Hu et al. (2003) successfully revealed the main difference between the two cyanobacterial EPS: *N*-linkages of sugars and proteins to form proteoglycans in the highly stabilizing species *M. vaginatus*, while *S. javanicum* EPS showed *O*-linkages that were alkali-labile. These are just two examples where, besides the effects of monomer

variety, degree of substituents and intertwining of proteins and carbohydrates, the evaluation of the linkages seems important for explaining biostabilization.

Nowadays we have highly sophisticated techniques available, ranging from MS (mass spectrometry) in different specifications (Maldi-ToF Matrix-Assisted-Laser-Desorption/Ionization-Time-of-Flight, ESI Electro-Spray Ionization, Pyrolysis-MS), NMR (nuclear magnetic resonance) to spectroscopy (Infrared IR, Fourier transform infrared FTIR, UV/VIS, Raman) to allow the separation/identification of molecules according to their mass/loading, resonance information on position and distances of magnetic isotopes as well as the detection of functional groups by characteristic vibrational modes, respectively. Hence, quantitative determination and most of all, structural elucidation, is possible but only a few investigations go beyond the monomer composition or visualization of EPS components in biostabilization research. This is mainly reasoned by the high complexity of the EPS matrix that constantly changes with species and boundary conditions and thus requires sophisticated adaptation of selected methods (Delattre *et al.*, 2016). Most of the studies available usually origin from biotechnology to decipher complete structures for novel products or to find suitable enzymes to prohibit or constrain unwanted biofilm (Vu *et al.*, 2009; Kolodkin-Gal *et al.*, 2010; Hochbaum *et al.*, 2011). It remains difficult to retrieve valuable information regarding EPS features important for biostabilization because (a) structural evaluation rarely relates to adhesive properties, (b) the data usually originate from single species cultures with limited natural relevance, (c) targeted EPS fractions are often not comparable and (d) the suitability of the techniques applied is difficult to assess. It is therefore still a considerable challenge to better link structural composition of EPS of natural and complex biofilm to its functionality or adhesive capacity in the future.

This introduction (including Figures) is largely based on the review paper Gerbersdorf and Wieprecht (2015) in Geobiology.

I.5. TOPICS OF THIS HABILITATION THESIS

Research on biostabilization itself has gained momentum during the last decades due to the significant microbial impact on fine sediment and pollutant dynamics that qualifies biostabilization as one important ecosystem function. This thesis will highlight the contributions of the applicant and her team to this truly multidisciplinary research area while focusing on the following topics approached in five chapters:

(1) The stabilization potential of heterotrophic bacterial assemblages in estuaries
(2) Synergistic effects by mixed versus single taxa biofilm for biostabilization
(3) The significance and seasonality of microbial biostabilization in freshwaters
(4) The impact of light and hydrodynamics on biostabilization in riverine waters
(5) Taking a promising device further: Magnetic Particle Induction (MagPI)

(1) Biofilm members are considered “ecosystem engineers” since they cause changes in aquatic ecosystem structure, function, and biodiversity by modulating the availability of resources to other species (Boogert *et al.*, 2006). It was believed that microalgae (microphytobenthos) play the most crucial role in stabilizing fine sediments with EPS carbohydrates as their main secretion product. Consequently, research concentrated on the highly visible microbial mats in the intertidal areas (e.g. Smith & Underwood, 2000) and on the compositional as well as structural elucidation of microalgal EPS carbohydrates involved in migration, stalks, mucilage pads or capsules (e.g. Wustman *et al.*, 1997; Bahulikar & Kroth, 2008). Conspicuously absent from this research was the

role of the heterotrophic bacteria despite their ability to secrete copious amounts of EPS and their ubiquitous occurrence in fine sediments (Flemming & Wingender, 2001a; Liu & Fang, 2003). The chapter III. emphasizes the great stabilization potential of natural benthic bacterial assemblages and the adhesive properties of bacterial EPS proteins that are more significant than previously thought. The publication of Gerbersdorf et al. in FEMS Microbiological Letters (2008b) represents the original source for this chapter.

(2) With these new insights on the importance of heterotrophic bacteria for sediment stability, earlier results on the microalgal stabilization potential require new interpretation since natural microalgal mats are not devoid of bacteria. This can be addressed by studying separately and combined the engineering potential of prokaryotic and eukaryotic assemblages. In biofilm, there is evidence of an advantageous co-existence or symbiosis between heterotrophic bacteria and microalgae that is mainly reasoned by nutrient recycling (Schäfer *et al.*, 2002; Grossart & Simon, 2007). However, some studies revealed mutual suppression by producing compounds with bactericidal (secreted by microalgae) or algicidal (secreted by bacteria) effects (Mu *et al.*, 2007; Ribalet *et al.*, 2008). The chapter IV. addresses these bacteria-microalgae interactions to show that the individual engineering capability of heterotrophic bacterial assemblages was two times higher as compared to axenic diatom cultures. The mixed assemblages of autotrophic and heterotrophic members resulted in highest biostabilization values, but the data did not suggest clear synergistic (=more than additive) effects. This chapter is mainly based on the publication of Lubarsky et al. in PLoS ONE (2010).

(3) It was predicted that biostabilization would be more influential in marine habitats due to the high ion concentrations that help in this binding process (Spears *et al.*, 2008); although the EPS concentrations known from freshwater habitats, e.g. lakes are quite impressive (Hirst *et al.*, 2003; Cyr & Morton, 2006). In order to fully pursue and understand the biostabilization potential in freshwaters, it is crucial to take seasonal effects into account. Biological processes show huge variations over the year in e.g. terms of succession processes within the biofilm or by affecting aquatic food webs (Lyautey *et al.*, 2005; Power *et al.*, 2008); still the implications for biostabilization can be only speculated on. The chapter V. introduces a mesocosm that was newly-designed to allow reproducible biofilm growth under quasi-natural and controlled conditions while combing engineering and biological expertise. Furthermore, the significance of biostabilization has been proven for the first time in freshwaters. The highest adhesion as well as sediment stability occurred both during spring and were clearly linked to microbial community composition to result in mechanically highly diverse biofilm. This chapter combines the most relevant content from the publications within Environmental Sciences Europe ESEU (Schmidt *et al.*, 2015) and Freshwater Biology (Schmidt *et al.*, 2016), as well as within the International Journal of Sediment Research (Thom *et al.*, 2015).

(4) Environmental conditions strongly affect biofilm structure (Blenkinsopp & Lock, 1994) or metabolic pathways (Romani *et al.*, 2004; Marcarelli *et al.*, 2009; Kendrick & Huryn, 2015) to name but a few. There is a consensus that light is one driving factor for biostabilization since it could be linked to photosynthetic activity and migration of microalgae (Smith & Underwood, 2000; Orvain *et al.*, 2003). The effects of hydrodynamics on biofilm growth are understood as a balance between enhanced mass transfer rates (e.g. of nutrients into the biofilm) and possibly detachment (by e.g.

promoting biofilm erosion); however, effects on biostabilization are a matter of theoretical debate. The chapter VI. links for the first time the most influential abiotic conditions - light and hydrodynamics - to this biofilm functionality. While adhesion and sediment stability both increased with increasing light intensities, heterotrophic bacterial growth in the dark was delayed, presumably due to the limited nutrient supply in the oligotrophic river waters. Higher discharges and resulting bed shear stresses caused as well a delayed development of biofilm with significant effects on biostabilization. Shifts in the microbial community and species characteristics could be clearly related to the induced binding force. This chapter summarizes the most important parts from the publications of Schmidt et al. in Freshwater Biology (2016) as well as Research and Reports in Biology (2018b), and Thom et al. in International Journal of Sediment Research (2015).

(5) Most biofilm studies focus on the analysis or visualisation of growth and metabolic activity, biomass and community composition or EPS matrix. If functionality is addressed at all, it is mostly on how biofilm orchestrate biogeochemical processes (Battin & Brumaghim, 2008; Hodl *et al.*, 2014), but little to none information is given on the adhesive capacity (=attachment) and the physical properties of a biofilm. Techniques such as Atomic Force Microscopy (AFM) produce results on the nanoscale that cannot be extrapolated to the mechanical resistance of the entire biofilm matrix (Dugdale *et al.*, 2005). On the other hand, testing biofilm potential failure and sloughing-off so far involved (macro- to microscale) entrainment experiments within erosion flumes with critical sensitivity and uncertainty (Thom *et al.*, 2015; Pique *et al.*, 2016). Measuring adhesion by MagPI (Larson *et al.*, 2009; Anderson *et al.*, 2011) is quick, non-destructive and highly sensitive with a small footprint to determine adhesive

capacity at the mesoscale (mm–cm range) but over reasonable large areas. The chapter VII. concerns several technical aspects to further improve the performance of this powerful experimental approach and enhance the range of MagPI applications. Thereby, the influence of material and geometry on performance was demonstrated and the importance of both, the magnetic field strength and the magnetic field gradient for the physics of the MagPI approach could be shown. The chapter origins from the publication of Gerbersdorf et al. (recently submitted to Journal of Biofouling 2017).

II. MATERIAL AND METHODS

II.1. SUBSTRATUM, BIOFILM GROWTH AND SAMPLING

Inert glass beads (size range 100–200µm) were used as an artificial, non-cohesive substratum to focus on the binding capacity potential of the biofilm. Biofilm were grown using natural water from various sources (estuarine and freshwater) and allowing the resuspended microbes to settle on the artificial substratum and built biofilm under natural nutrient conditions. Thereby, in the first experiments, the biofilm were cultured in boxes supplied with aeration but later on in highly sophisticated flumes with precisely defined hydrodynamics conditions (the specific experimental settings for one particular experiment are described in the appropriate chapters below). Important environmental conditions such as temperature and light were controlled in all cases.

Sampling took place by taking water samples for nutrient analysis and withdrawing mini-cores of the biofilm-encrusted substratum at various growth stages. For the latter, a 2ml cut-off syringe is pushed carefully into the sediment and the mini-cores are hold inside by under-pressure. After retrieving the sample, the piston of the syringe is gentle pushed upwards until only the first 0.5cm³ of substratum including the surface remains inside. This 0.5cm^3 is then used for further chemical and biological analysis (see below).

II.2. CHEMICAL ANALYSES

II.2.1. EPS EXTRACTION AND DETERMINATION

EPS was extracted from the upper 0.5cm³ of biofilm-grown substratum mini-cores (taken by a 2ml cut-off syringe and transferred into 2ml safety-lock Eppendorf caps) by adding 1.5ml of distilled water (water-extractable=colloidal EPS). The samples were then continuously rotated for 1.5h by a horizontal mixer (Denley Spiramix 5 or Stuart

Roller Mixer SRT9D from Bibby Scientific) at room temperature (25°C) and 60rpm. After centrifugation (10.743g, 5 minutes, Thermo Scientific Espresso Centrifuge, rotor 12x1.5/2.2ml) the supernatants of two mini-cores/Eppendorf caps containing the colloidal EPS fraction were pipetted and merged into a new 2ml Eppendorf cap. In most experiments, the determination of colloidal EPS was sufficient, and the remaining pellets were dried to relate the EPS concentrations to the sediment dry weight. However in some experiments, the more firmly bound EPS moieties were analysed as well. In these cases, the remaining pellets were further extracted by adding 1ml distilled water + 100g/g volatile solids cation exchange resin (CER, Dowex, APA-1, 16-45 mesh, Fluka 44445). After continuous rotation by the horizontal mixer (see above) for 18h at room temperature (25°C) (modified after Frolund *et al.*, 1996), the CER extracted samples were centrifuged for 10 minutes (see above), the supernatant was retained and the pellet dried. Prior to use, the cation exchange resin was washed three times in PBS (Gerbersdorf *et al.*, 2007).

Whether for colloidal (water-extractable) or bound (resin-extractable) EPS fractions, the supernatants were always well-mixed before taking three subsamples (triplicates) each for EPS carbohydrates and proteins, following the Phenol Assay protocol (Dubois *et al.*, 1956), and the modified Lowry procedure (Raunkjaer *et al.*, 1994), respectively. Briefly, for carbohydrates analysis, 200µl supernatant was mixed with 200µl phenol (5%) plus adding carefully 1ml sulphuric acid (98%). The samples were incubated for 35 minutes at 30°C and the carbohydrate concentration was measured by spectrophotometer (CECIL CE3021) at a wavelength of 488nm (Dubois *et al.*, 1956; Gerbersdorf *et al.*, 2008a). For protein analysis, 250µl supernatant was incubated for 15 minutes with 250µl of 2% sodium dodecyl sulphate salt (SDS) and 700µl of chemical reagent 4 (Reagent 1: 143mM NaOH, 270mM Na_2CO_3, Reagent 2: 57mM $CuSO_4$, Reagent 3:

124mM Na-tatrate, Reagent 4: a mixture of Reagent 1, 2 and 3 in a ratio of 100:1:1) and incubated for a further 45 minutes at 30°C with 100µl Folin reagent (diluted with distilled water 5:6) (Raunkjaer *et al.*, 1994; Gerbersdorf *et al.*, 2008a). The protein concentration was measured by spectrophotometer (CECIL CE3021) at a wavelength of 750nm.

The EPS carbohydrates and proteins concentrations are given in microgram per cubic centimeter [µg cm^{-3}]. In parallel, the sediment dry weight was determined for the extracted mini-cores to calculate EPS carbohydrates and proteins contents [µg g^{-1} DW].

II.3. BIOLOGICAL ANALYSES

II.3.1. CHLOROPHYLL A AND PHEOPHYTIN

Chlorophyll a and pheophytin were measured as a proxy for living and dead microalgal biomass, respectively, following the DIN 38 412/16 protocol. Similar to EPS, the pigments were extracted from the upper 0.5cm^3 of mini-cores taken by a 2ml cut-off syringe but transferred into 15ml centrifuge tubes. The samples were frozen until further processing upon which they were defrosted and incubated with 10ml 96% ethanol while being rotated for 24h in the dark by a horizontal mixer (Denley Spiramix 5 or Stuart Roller Mixer SRT9D from Bibby Scientific) at room temperature (25°C). After centrifugation (1.434g, 10min, Hettich Universal 2 S Centrifuge) the supernatant was transferred into a new centrifuge tube and determined in triplicates spectrophotometrically before and shortly after (3–10 minutes) acidification with 120µl of 1N HCl per 1ml cuvette sample at the wavelengths 665nm and 750nm, respectively. Chlorophyll a and pheophytin data are given as concentration [µg L^{-1}] and content [per sediment dry weight DW, µg g^{-1} DW] according to the following calculations:

$$chla = \frac{(E_{665(korr.)} - E^{acid}_{665(korr.)}) \cdot \frac{R}{R-1} \cdot V_{extr}}{e_c \cdot l \cdot V_p} \quad (1)$$

$$pheaoa = \frac{(R \cdot E^{acid}_{665(korr.)} - E_{665(korr.)}) \cdot \frac{R}{R-1} \cdot V_{extr}}{e_c \cdot l \cdot V_p} \quad (2)$$

with:

$chl\ a$	=	$\left[\frac{\mu g\ chl\ a}{cm^3}\right]$	Concentration of *chlorophyll a* of sediment sample
$pheao\ a$	=	$\left[\frac{\mu g\ pheao\ a}{cm^3}\right]$	Concentration of *pheaopigment a* of sediment sample
$E_{665(korr)}$	=	$E_{665} - E_{750}$	Corrected extinction at the absorption maxima before acidification
$E^{acid}_{665(korr)}$	=	$E^{acid}_{665} - E^{acid}_{750}$	Corrected extinction at the absorption maxima after acidification
e_c	=	$\left[\frac{cm^3}{\mu m \cdot cm}\right]$	Specific extinction coefficient of *chlorophyll a* at absorption maxima in red spectral range. In 96 % Ethanol: $83\frac{l}{g \cdot cm} = 83 \cdot 10^{-3}\frac{cm}{\mu m \cdot cm}$
V_{extr}	=	cm^3	Amount of extraction agent
l	=	cm	Length of cuvette
R	=	1.7	Ratio of extinction
V_p	=	cm^3	Volume of sediment sample

II.3.2. DIATOM COMMUNITY

Again, the upper 0.5cm³ of mini-cores taken by a 2ml cut-off syringe were transferred to one 2ml Eppendorf cap and fixed with 1ml of Lugol's iodine to a final concentration of about 2%. The organic content of the samples was removed by boiling them in H_2O_2 (30%) followed by three washes with MilliQ water. The diatom frustules were embedded

in Naphrax (Northern Biological Supplies, England) for species determination (Battarbee, 1986; Krammer & Lange-Bertalot, 1986; Hofmann *et al.*, 2011) at 1000x magnification using a Zeiss Avioscope (Carl Zeiss, Oberkochen, Germany) with differential interference contrast. At least 300 valves were identified per sample and the relative abundance of each taxon was recorded. Data were evaluated by calculation of Bray-Curtis dissimilarity (BCD) (Somerfield, 2008) and Shannon diversity index (Shannon & Weaver, 1963).

II.3.3. BACTERIAL CELL NUMBERS

The upper 0.5cm³ of mini-cores was fixed for bacterial cell counts with 1ml paraformaldehyde in PBS (phosphate buffered saline, 130mM NaCl and 10mM $NaHPO_4/NaH_2PO_4$, pH 7.4) at a final concentration of 4%. After 1h incubation, the samples were washed twice in 1ml PBS and the pellet was resuspended in 1ml PBS. After shaking the sample and waiting for 1 minute, to allow the glass beads to settle, a sub-sample of 20µl was taken from the middle of the supernatant. The sub-sample was mixed with an equal amount of SYTO Green 13 (1µl of stain mixed in 1ml distilled water, Molecular Probes) for 15 minutes in the dark. SYTO dyes are non-fluorescent unless bound to nucleic acids, thus no excess stain had to be removed.

Bacterial cells were determined in two ways: first via epifluorescence image analysis and later by using a flow cytometer. For epifluorescence, two sub-samples of 1.5µl were placed on gelatin-coated microscope slides, and an equal amount of glycerol (1.5µl, Vectashield H-1400, Vector Laboratories, Burlingame) was added. After sealing the cover slip (nitrocellulose), images of at least 10 randomly chosen microscopic fields (330x440µm) were taken per sample with at least 1000 bacterial cells and evaluated for bacterial enumeration with the software “Volocity”.

Triplicates of the bacterial cell samples were counted at 488nm excitation using a flow cytometer (FACScalibur, BD Bio Science, New Jersey, USA) and the data were recorded until 10.000 events were acquired and/or 1 minute had passed. Bacteria were detected by plotting the side light scatter (SSC) versus green fluorescence (FL1). An internal standard was added to some samples (PeakFlow™ reference beads, 6µm size, 515nm, Molecular Probes) to distinguish bacterial cells from debris and mineral particles. The data were analyzed using the "Cellquest" software. Bacterial abundance was calculated by multiplying the acquisition rates (between 160 and 640 bacteria per sec) by the flow rate (fixed to 60ml min^{-1}). Bacterial cell numbers are given as cells per sediment volume [cm^{-3}] and calculated as cells per sediment dry weight DW [g^{-1} DW].

II.3.4. BACTERIAL COMMUNITY

Basically, two lines of analyses were followed: 1. Amplifying DNA via PCR (polymerase chain reaction) and separating discrete fragments of various sequences within an electrophoresis gel that contains a gradient of a denaturing agent (DGGE, Denaturing gradient gel electrophoresis). This way, the resulting banding patterns visualize variations in microbial genetic diversity as well as the abundance of predominant microbial members ("community fingerprinting"). 2. Applying fluorescence probes that bind specifically to parts of the bacterial chromosomes with a high degree of sequence complementarity in order to identify certain prokaryotic species as well as localize them within a biofilm (FISH, Fluorescence *in situ* hybridization). The following description originates from Schmidt (2017) and Schmidt *et al* (2015, 2016, 2018b) where further details are given.

For (1), DNA was isolated from the samples with Nucleospin Kit for Soil (Macherey and Nagel, Düren, Germany) following manufacturer's instructions. Bacterial 16S rRNA genes were amplified via PCR assay using the universal primers 27f (5′-AGA GTT TGA

TCM TGG CTC AG-3′) and 517r (5’-ATT ACC GCG GCT GCT GG-3’) (Lane, 1991; Emtiazi *et al.*, 2004). For subsequent DGGE (Denaturing Gradient Gel Electrophoresis), a GC-clamp (5’-CGC CCG CCG CGC CCC GCG CCC GTC CCG CCG CCG CCC CCG CCC C-3’) was attached to the primer 27f. Each PCR reaction (25µL) amplifying 15ng DNA consisted of: 16.38µL sterile PCR water (Merck Millipore, Darmstadt, Germany), 2.5µL 10x PCR buffer (QIAGEN, Venlo, Netherlands) provided by the enzyme manufacturer, 0.125µL dNTPs (200µM), 0.25µL of each primer (40µM) and 0.13µL Taq DNA polymerase (HotStart™ Polymerase, 5U/µL, QIAGEN, Venlo, Netherlands). Amplification was carried out in a GeneAmp PCR system 9700 (Applied Biosystems, Carlsbad, CA, USA) with the following specifications: 30s at 94°C, 35 cycles of 30s at 94°C, 30s at 55°C and 60s at 72°C. The final extension lasted 7 minutes at 72°C. The PCR products were loaded onto 1% agarose gels in 1xTAE buffer (pH 8.0), stained with GelRed (GeneON, Ludwigshafen, Germany) and studied under UV illumination (600nm). DGGE was performed as described by Muyzer et al. (1993) using a Bio Rad DCode system (Bio-Rad Laboratories, Hercules, CA, USA): a 1.5mm thick vertical gel containing 7.5% (w/v) polyacrylamide (37.5:1 acrylamide: bisacrylamide) with a linear denaturing gradient of urea and formamide (40%-70%) was loaded with similar-sized PCR products. After electrophoresis in a 1x TAE buffer (pH 8.5) for 17h at 70V and 56°C, gels stained with GelRed (GeneON, Ludwigshafen, Germany) for 15 minutes were analyzed under a Lumi-Imager F1 Working Station (Roche Diagnostics, Mannheim, Germany). Images of each gel were taken with a CCD camera system (The Imager, Appligene, Illkirch, France) and processed with the software Lumi Analyst 3.1 for DGGE banding patterns analysis. After processing with the programs GelCompar II (6.0) and ImageJ (148a), range-weighted richness (Rr), community dynamics (Dy) and functional organization (Fo) were calculated as

described by Marzorati et al. (2008). Thereby, the Rr value is derived from the number of DGGE bands within a certain gradient section to reflect the microbial diversity and carrying capacity of an ecosystem. High Dy values indicate a high “rate of change” in a healthy microbial community within a defined time interval (by comparing consecutive DGGE bands from different sampling times). In contrast, higher Fo values indicate a highly specialized, low-diversity microbial community by calculating the ratio between dominant and resilient microorganisms derived from Pareto–Lorenz evenness curves (Lorenz, 1905). Additionally, DGGE bands of interest were excised from GelRed stained gels and re-amplified via PCR (see above) using the same DGGE primers without GC clamp. 73 DNA fragments of appropriate length were purified with the Wizard ® Genomic DNA Purification Kit (Promega, Fitchburg, USA). Cloning of the purified DGGE bands was performed using the TOPO TA Cloning® kit (Invitrogen Inc. Carlsbad, CA) with the pCR® 4-TOPO® vector and One Shot Chemically Competent *E. coli* cells following the instructions of the manufacturer. Three to five clones per band were selected and grown overnight in 5mL LB broth containing 100µg ml^{-1} ampicillin. The transformed *E. coli* clones were sent to GATC Biotech AG (Constance, Germany): after plasmid purification, the primers M13 forward and reverse were used to sequence cloned DGGE bands. Obtained sequences were manually edited in Chromas Lite (Technelysium, South Brisbane, Australia), compared to sequences in the BLAST database (NCBI, Bethesda; USA) (bacterial strains of the analysed DGGE bands in Schmidt (2017)) and aligned using the SINA aligner of the ARB software package (v 5.2) and the corresponding SILVA SSU Ref 102 database (Pruesse *et al.*, 2007).

For FISH (2), samples were fixed as described above in 4% (w/v) paraformaldehyde in PBS. Because the permeability of gram-positive paraformaldehyde-fixed cells might be seriously limited, an additional set of samples was fixed in 70% ethanol according to

Roller *et al.* (1994) and incubated for 4h at 8°C (Manz, 1999). Samples were washed in PBS, then resuspended in 500µl PBS and stored in a mixture with equal parts of PBS and ice-cold absolute ethanol at -20°C as described by Amann *et al.* (1990). Prior to total cell count determination and hybridization, sediment-associated bacteria were detached and homogenized by 5 minutes of sonication at 35kHz (Sonoplus GM70, Bandelin Electronics, Berlin, Germany), thoroughly mixed for 1 minute and centrifuged at 12.200g^{-1} (Hettich Rotanta 460R, Rotor 4489, Tuttlingen, Germany). 50µm aliquots of the cell suspensions were filtered through polycarbonate membranes (0.2µm pore size, Millipore, Eschborn, Germany) and stained with 15µl DAPI solution (4',6-diamidino-2-phenylindole, Sigma, Deisenhofen, Germany, 10µgml^{-1}). FISH was performed as described by Manz *et al.* (1992) using oligonucleotide probes (listed below in III. Table 2). The samples (sonicated and centrifuged as described above) were incubated in hybridization buffer containing 0.9M NaCl and formamide, 20mM Tris-HCl, 0.01% SDS (sodium dodecyl sulphate), and the oligonucleotide probe at a concentration of 20-50ng ml^{-1} for at least 4h at 46°C. Following hybridization, slides were washed, carefully avoiding contamination under stringent conditions for 20min, and air-dried. In the washing solution (20mM Tris-HCl, pH 8; 0.01% SDS), the stringency was maintained by lowering the sodium chloride concentration according to the formamide concentration used in the hybridization buffer. All hybridization probes were labelled with the indocarbocyanine dye Cy3. Unlabelled competitor oligonucleotides for BET42a, GAM42a, were used to improve the specificity of the hybridization as previously described (Manz *et al.*, 1992).

An epifluorescence microscope (Zeiss Axioplan II, Carl Zeiss, Jena, Germany) fitted with Zeiss light filter set no. 1 for DAPI (exciter 365nm, dichroic mirror 395nm, emission filter 397nm) and for Cy3 (exciter 535/50nm, dichroic mirror 565nm, emission filter

610/75nm) was used for total cell count determination and FISH analysis. Samples were evaluated by enumerating at least 10 randomly chosen microscopic fields (100x100µm) and counting a minimum of 1.000 cells per sample. Probe-specific cell counts were given as percentages to the total of eubacterial cell counts as determined by hybridization with a molar mixture of probes EUB338, EUB338II, and EUB338III.

II.3.5. BACTERIAL DIVISION RATE

Cores were incubated for 20 minutes immediately after sampling with [methyl-3H] thymidine (final concentration 300nmol L^{-1}, S.A., 50 $Cimmol^{-1}$) according to Fuhrman and Azam (1982). The incorporation of radioactive thymidine was stopped by adding 5ml of 80% ethanol. All samples were collected on a filter (0.2µm) after the incubation time and washed several times with 80% ethanol and 5% trichloroacetic acid (TCA) to remove excess radioactivity. The filters (containing bacteria and glass beads) were mixed with 5ml of 0.5mol l^{-1} HCl and incubated at 95°C over 16h (Garet & Moriarty, 1996) allowing the settlement of the glass beads and the solubilisation of the stained bacteria into the supernatant. A subsample of the supernatant was taken, cooled and mixed with 3ml of the scintillation cocktail Ultima Gold MV.

The bacterial division rate (cells cm^{-3} h^{-1}) was calculated according to an internal standard quenching curve (Liquid scintillation analyzer “TRI-CARB 2000”) while assuming that 1 mol^{-1} incorporated thymidine is equivalent to the production of $2x10^{18}$ bacterial cells (Lee & Fuhrman, 1987; Cho & Azam, 1990). The saturating concentration of ^{3}H-thymidine was derived from previous experiments. The thymidine incorporation was linear under the range of chosen concentrations (Hubas *et al.*, 2007a;b). For each replicate, the radioactivity of the samples was corrected against a blank which corresponded to the pre-fixed cores submitted to the protocol described above.

II.4. Determination of Adhesion and Sediment Stability

The terminology around adhesion and cohesion is confusing and inconsistent. In the following text “adhesion” is used to describe active bacterial attachment to a substratum while “cohesion” is used to describe the attraction/bonding strength between sediment particles, whether caused by electrostatic forces or by EPS.

II.4.1. Cohesive Strength Meter (CSM)

Within the first experiments on microbial biostabilization in estuarine sediments (chapter III. and IV.), the Cohesive Strength Meter (CSM) was applied as described in Paterson (1989). The CSM can determine small-scale spatial and temporal variations in sediment stability with high sensitivity. The test chamber (30mm in diameter) is positioned at the substratum surface and filled with water. Within this chamber, a sequence of perpendicular water jets are fired onto the substratum with gradually increasing force/stagnation pressure according to the programm (Vardy *et al.*, 2007) (Figure 8).

Figure 8: *CSM measurements within esturarine biofilm grown in boxes on glass beads. Left: the test or erosion chamber (grey) in idle position above the beaker is connected to the yellow suitcase containing air supply and water bottles for the perpendicular water jets as well as the digital panel and keypad for the various erosion programs to apply and measure. Right: visualization of one CSM jet within the test chamber by applying a potassium permanganate solution (Image from SERG lab of Prof. D.M. Paterson).*

Sediment resuspension is recorded by changes in transmission above the bed and a 10% drop in transmission from the original undisturbed bed is taken as the indication of bed failure (Tolhurst *et al.*, 1999; Vardy *et al.*, 2007). The most sensitive test program "Fine1" was chosen given the expected range of low stagnation pressure values. Prior to the use in the experiments, the CSM was calibrated after Vardy *et al*. (2007) and the relative substratum stability was expressed as stagnation pressure at the bed surface (Nm^{-2}). The minimum operation depth for the CSM is about 3cm sediment depth.

II.4.2. MAGNETIC PARTICLE INDUCTION (MAGPI)

Mechanical properties of the biofilm were studied with a new method based on the magnetic attraction of specially-produced test particles: MagPI (Larson *et al.*, 2009). This method is suitable for sensitive recording of changes of the surface adhesion of sediments or biofilm. Briefly, a known volume of ferromagnetic fluorescent particles (Partrac Ltd, UK, 180-250μm) is spread onto a defined area of the sediment surface. The particles are then recaptured by an overlying electromagnet and the force (magnetic flux) needed to retrieve the particles is determined as a measure of the retentive capacity of the substratum, a proxy for adhesion (Figure 9). In order to quantify the particle attraction by the electromagnet from surfaces with varying adhesive properties, four thresholds were defined:

Threshold 1–The particles align towards the overlaying electromagnet

Threshold 2–The first particle is attracted by the electromagnet

Threshold 3–Few particles (around 5) are retrieved by the electromagnet

Threshold 4–All particles are retrieved by the electromagnet–total clearance

The electromagnetic force applied is controlled by a precision power supply and the particle movements are precisely monitored at each increment of voltage/current. The MagPI was calibrated using a Hall probe and the results can be thus given in Ampere and in mTesla (Larson *et al.*, 2009). The adhesive properties of the biofilm were either studied parallel to the CSM (experiments in estuarine sediments, chapter III. and IV.) or to the SETEG ("Strömungskanal zur Ermittlung der tiefenabhängigen Erosionsstabilität von Gewässersedimenten", see next paragraph) measurements (experiments on freshwater biofilm, chapter V. and VI.). The MagPI itself was further studied and developed in terms of geometric properties and the physical working principle behind. The results are presented in chapter VII.

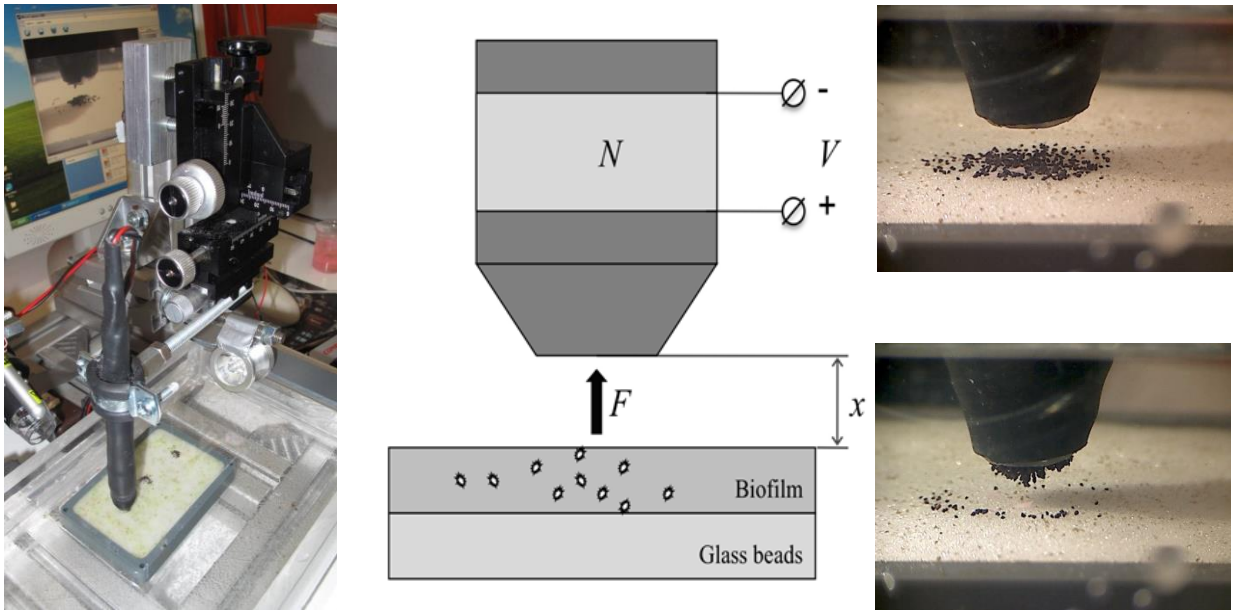

Figure 9: *Magnetic Particle Induction (MagPI). Left: the setup with the electromagnet positioned in a fixed distance (via micromanipulator) to the biofilm and connected to the power supply (not to be seen here). Middle: drawing of the electromagnet positioned above the biofilm surface with F=the "lifting" force, x the distance between surface and magnet, N=number of turns of cupper coils and V=voltage applied. Right: Ferromagnetic particles spread onto the surface (upper image) and re-captured by the electromagnet positioned above (lower image). Source: right and left: DFG project Gerbersdorf, middle: Keybioeffect project Gerbersdorf.*

II.4.3. EROSION MEASUREMENTS IN THE SETEG FLUME

The determination of the critical bed shear stress for biostabilized freshwater sediments has been conducted in the “Strömungskanal zur Ermittlung der tiefenabhängigen Erosionsstabilität von Gewässersedimenten” SETEG-flume (Witt & Westrich, 2003) (Figure 10 left). The SETEG flume is a pressure duct (length l x width w x height h = 8.3m x 0.15m x 0.1m) where samples (here: the sediment cartridges) are inserted from beneath while being carefully lifted up by a jack-stepping motor until the surface of the sample is on the same height as the flume bottom (Figure 10 right). That way, the sample is now exposed to the flow within the flume and the discharge (each level maintained for one minute) is increased stepwise in small increments.

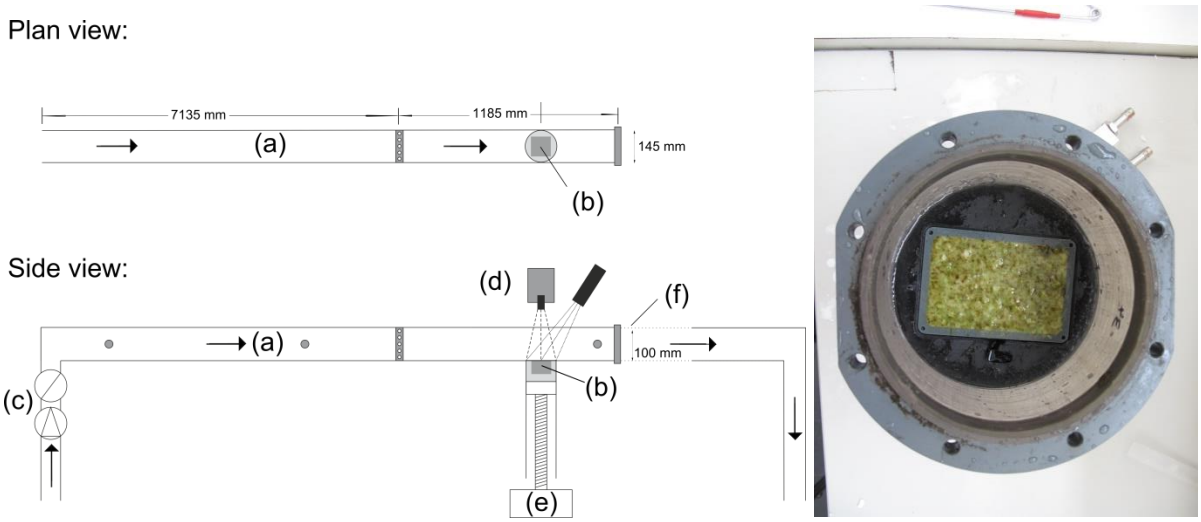

Figure 10: *Left: Schematic view of SETEG erosion flume, modified after Witt &Westrich (2003): (a) pressure duct, (b) sediment cartridge fitted into a frame (c) pump and magnetic inductive flow meter (d) laser triangulation system (e) jack with stepping motor (f) outflow weir. Right: view from above onto the sediment cartridge fitted into a frame to insert into the SETEG flume from below. Source: left: (Thom* et al.*, 2015) and right: DFG project Gerbersdorf.*

In the study of biostabilized substratum, the critical bed shear stress is defined as the point of incipient particle/aggregate motion where the detachment exposes the underlying abiotic sediment. This definition is basically identical with the erosion type Ib

after Amos et al. (2003). By focussing on the morphologically relevant de-armouring of the sediment, the release of the surficial fluffy layers is not taken into account here.

A critical bed shear stress of 0.23Nm^{-2} has been determined for the abiotic sediment used in the experiments on freshwater biofilm which is slightly higher than the one derived from the Shields' equation (=0.15Nm^{-2} after Shields (1936)). In the chapters V. and VI., the determined 0.23Nm^{-2} for abiotic sediment serves as the reference value to classify the effects of biostabilization.

II.5. STATISTICS

Data sets were first assessed for normality (Shapiro-Wilk *W*-Test) and homogeneity of variance by visual assessment of the frequency histogram and the normality plot as well as by Kolmogorov-Smirnov and Barlett tests. Normal-distributed data were further evaluated by one-way ANOVA to test the hypothesis that the means of the treatments were equal (significance levels $p<0.05$ and $p<0.001$). Rejection of this hypothesis was followed by the *post hoc* Dunett Test to determine which treatment groups showed significant differences. If the data violated assumptions of normality and homogeneity of variance, differences between treatments were assessed using a non-parametric Kruskal-Wallis (χ^2) test (KW), followed by the non-parametric Student-Newman-Keuls (SNK) test to correct for multiple comparisons.

Regression analysis was used for modeling and for analysis of numerical data consisting of values of a dependent variable (response variable) and of one or more independent variables; while correlation analysis was used to indicate the strength and direction of a linear relationship between two random variables.

III. THE BIOSTABILIZATION POTENTIAL OF NATURAL BENTHIC BACTERIAL ASSEMBLAGES FROM AN ESTUARY

III.1. ABSTRACT

The secretion of extracellular polymeric substances (EPS) by bacteria has been recognized as important across a wide range of scientific disciplines, but in natural sediments EPS production by microalgae as a mechanism of sediment stabilization has received much more attention than bacterial products. In the present study, the stabilization potential of a natural benthic bacterial assemblage was tested in cultures growing on non-cohesive glass beads. The surface erosion resistance as determined by CSM (Cohesive Strength Meter) was significantly enhanced over time compared to controls. Nutrient enrichment of the bacterial assemblages by a general broth (bacteria+) resulted in enhanced stabilization (x3.6) as compared with nutrient-depleted (bacteria) assemblages (x1.8). This correlated with higher bacterial biomass and EPS concentrations in enriched cultures. Substratum stability was closely related to bacterial cell numbers (R^2=0.75/0.78) and EPS protein concentrations (R^2=0.96/0.53) (for bacteria/bacteria+ treatments, respectively), but not with EPS carbohydrates. This study implies greater significance for extracellular proteins in substratum cohesion within the EPS complex than previously recognized. The data shows the importance of bacterial assemblages for microbial sediment stabilization and secondly, that a change in abiotic conditions can significantly affect sediment stabilization.

III.2. BACKGROUND

Bacterial secretion of extracellular polymeric substances (EPS) is a well-studied phenomena in medical research (e.g. bacterial resistance to antibiotics and biocides (Foley & Gilbert, 1996; Morton *et al.*, 1998)), in waste-water treatment (e.g. biofouling,

flocculation, binding site for pollutants/water purification, water retention (Flemming & Wingender, 2001a; Liu & Fang, 2003)) and in biotechnology (e.g. biocorrosion of metal, use in food industry, cosmetics, pharmaceuticals (Sutherland, 1998; Flemming & Wingender, 2001a)). In recent years, microbial EPS have been linked with a number of important ecological functions such as representing a nutritional source (Cyr & Morton, 2006), accumulating pollutants (Wolfaardt *et al.*, 1998) or stabilizing sediments (reviewed in Stal, 2003; Underwood & Paterson, 2003; Gerbersdorf & Wieprecht, 2015). Biogenic stabilization by the EPS matrix of diatoms has received particular attention through numerous studies on microphytobenthic mats in the marine environment (reviewed in Stal, 2003; Underwood & Paterson, 2003). Most of these studies have concentrated on microalgae/diatoms as the main EPS producers and on the polysaccharides as their most important product with respect to biostablization (e.g. Paterson *et al.*, 2000; Riethmüller *et al.*, 2000; de Brouwer *et al.*, 2005; Hanlon *et al.*, 2006). In contrast, the role of bacteria has been investigated with respect to the degradation and modification of the labile EPS components (van Duyl *et al.*, 1999; Goto *et al.*, 2001), while the importance of their ability to excrete copious amounts of EPS was generally overlooked (Decho, 1990).

Bacterial EPS consists of polysaccharides but also contains a high proportion of proteins (up to 60% in bacterial biofilms, Flemming & Wingender, 2001; EPS_P: EPS_C ratios between 0.5 – 21.2 in waste water flocs, Liu & Fang, 2003). Most of the proteins may function as extracellular enzymes (Flemming & Wingender, 2010) but may also play a crucial structural role (Pennisi, 2002). Negatively-charged groups within the proteins can be bridged in saline (ion-rich) media by divalent cations enhancing the stability of flocs and biofilm (Flemming *et al.*, 2000). Although this also applies to the anionic carboxyl groups of carbohydrates, dibasic amino acids have been shown to be

quantitatively more important constituents of EPS in bacteria-dominated environments such as activated sludge (Dignac *et al.*, 1998). In contrast to carbohydrates, proteins are known to be involved in the hydrophobic properties of EPS (Jorand *et al.*, 1998) and there is evidence that hydrophobicity is important for attachment and thus, possibly for stabilization (Sanin *et al.*, 2003). Earlier work has indicated possible synergistic effects between EPS constituents since protein may enhance the adhesion of polysaccharide fibres or strengthen polysaccharide complexes (Costerton *et al.*, 1978; Pennisi, 2002). Recent results point to bacterial amyloids as important EPS components in biofilm robustness (Zeng *et al.*, 2015a). Still, the structural role of extracellular proteins, possible interactions between EPS proteins and carbohydrates or other EPS moieties as well as their effects on stabilization, is not yet understood.

Given the numerous studies showing that bacterial settlement and bacterial EPS production increases sediment flocculation and alters floc characteristics (reviewed in Liu & Fang, 2003), it can be assumed that the binding capacity of bacteria directly (cell surface loading) or indirectly (via EPS) affects sediment stability. To our knowledge, only Yallop *et al.* (2000) have investigated the relationships between natural microalgal biomass/primary production and bacterial cell numbers/secondary production with sediment stability, reporting a set of positive inter-correlations for natural intertidal sediments. The contribution of the bacteria to the observed effects and the potential impact bacteria have remains largely unexplained. Pioneering studies on the entrainment of sand and clay-seawater suspensions by Dade *et al.* (1990, 1996) reported significant effects of bacterial exopolymer on sediment behaviour. Dade *et al.* (1996) also demonstrated that nutrient-depleted *Alteromonas* cultures caused a relative increase in Bingham yield stress of 60%, in contrast to the nutrient-enriched *Alteromonas* cultures. Bacteria can change from a mobile to a sessile lifestyle under

metabolic stress (such as nutrient limitation), accompanied by enhanced EPS production (Marques *et al.*, 1986). However, starvation can have very different effects on the quantity and quality of bacterial EPS depending on the nature of the limiting resource (Sanin *et al.*, 2003). So far, there is little information on bacterial binding dynamics relevant to sediment erosion and almost no information on how environmental variables (such as nutrition) affect EPS quantity and quality and thus, attachment and stabilization. The presented study provides an empirical analysis of the impact of bacterial assemblages and associated EPS (carbohydrates and proteins) on substratum stability as a function of nutrient availability.

III.3. EXPERIMENTAL SETTINGS

III.3.1. BACTERIAL CULTURES

The use of natural bacterial assemblages was preferred over monocultures. Subsurface (5-20mm depth) sediments were sampled from a mudflat in the southern part of the Eden Estuary (South East of Scotland, 56° 22' N, 2° 50' W). 1000ml of 0.2µm filtered seawater was mixed with the same volume of sediment and the slurry was ultrasonicated for 5–10 minutes to enhance detachment of bacteria from the sediment grains. The mixture was transferred to Pyrex centrifuge bottles (Sigma-Alderich, 500ml) and centrifuged for 10 minutes at $1.590g^{-1}$ (Beckman Centrifuge, Model J2-21 M/E, rotor JA-10). The supernatant was further centrifuged for 10 minutes at $17.700g^{-1}$ and the supernatant discarded. The pellet was resuspended and filtered through a 1.6µm filter (glass microfibres filter, Fisherbrand MF100) to exclude microphytobenthos. This was confirmed by epifluorescence microscopy. All the equipment used after this filtration step was acid-washed (15% 2M HCL). Standard autoclaved nutrient broth (Fluka, including peptone 15g/l, yeast 3g/l, sodium chloride 6g/l and glucose 1g/l) was added to

the filtered supernatant (V/V, 1:1) containing the bacteria. The cultures were established in 200ml Erlenmeyer flasks under constant aeration and at room temperature in the dark for two weeks. After two weeks, the cultures were centrifuged for 10 minutes at 6.030g^{-1} (Mistral 3000E) and the pellet washed twice in 0.2µm filtered seawater. The pellet was finally resuspended in 150ml of 0.2µm filtered seawater for inoculation.

III.3.2. EXPERIMENTAL SET-UP

Rotilabo deep-freeze boxes (l x w x h = 20.8cm x 20.8cm x 9.4cm) were filled to a height of 3cm with glass beads (Ballotini balls, cf diam 150µm) that served as non-cohesive substratum. A layer of buoyant plastic was placed onto the surface to protect the bed during the addition of 1.6L of 0.2µm filtered seawater. The treatments established were: three controls (covered additionally by a lid), six bacteria (bacteria) and six bacteria plus nutrients (bacteria+). Bacteria were added via a 10ml inoculum of the bacterial concentrate while nutrients were added with an additional 50ml of nutrient broth. All boxes were gently aerated (water column height of 2-3cm) and kept in a dark room at constant room temperature of 20°C for five weeks. The bacterial cultures with added nutrients are henceforth referred to as the "bacteria+" treatment to distinguish them from bacteria cultured without nutrients "bacteria" or the controls.

III.3.3. SAMPLING

Sampling took place after 3, 7, 14, 21, 28 and 35 days. The samples of sediment were obtained by gently pushing steel corers (1.45 and 1.6cm diameter, area of 1.65 and 2.02cm^2, respectively) into the substratum. Most of the overlying water was removed by syringe (1cm water layer left on top to protect the culture surface) and liquid nitrogen was gently added to the steel core until the inner core and outer surroundings were frozen. The frozen core was carefully removed and stored (-80°C). In order to determine

the depth penetration of different EPS fractions, the frozen cores were sectioned before analysis using a freezing microtom (Kryomat 1703, Leitz). Prior to sectioning, the cores were trimmed down to a maximum height of 1.5cm using a grinding machine (Wilmac, Stirling). Two sectioning patterns were followed (see Table 1).

Table 1: *The two sectioning pattern of the frozen mini-cores followed for the depth-dependent distribution of EPS and the total quantity of EPS. Source: Gerbersdorf et al. 2008b FEMS.*

Depth-dependent EPS profile			**Total EPS quantity**		
Layers	Depth of layer (µm)	Cumulative depth (mm)	Layers	Depth of layer (µm)	Cumulative depth (mm)
1-5	200	1	1-2	500	1
6-9	500	3	3	1000	2
10-11	1000	5	4	2000	4
12-13	2500	10	5-6	3000	10

Apart from the analyses of colloidal as well as bound EPS carbohydrates and proteins in all fine-sectioned layers, bacterial cell counts were determined and FISH performed within each top layer of 500µm (analyses see II.2. and II.3.,Table 2).

III.4. RESULTS

III.4.1. THE STABILITY AND COHESION OF THE SUBSTRATUM

The stability of the sediment surface in both bacterial treatments increased against controls from week one to three and was significantly different in the weeks three–five (Table 3, Figure 11). The increase was also significantly greater for treatments with nutrients (up to 107Nm^{-2}) over those without (up to 72Nm^{-2}) (Table 3, Figure 11). The control systems did not show any significant changes in stability over the entire five week period (Figure 11). Epifluorescence microcopy did not reveal any microalgae contamination of treatments or controls during the experiment.

***Table 2**: Oligonucleotides used in this study. Source: Gerbersdorf et al. 2008b FEMS.*

Target organisms	Oligonucleotides	Sequence (5`- 3`)	Reference
Bacteria	S-D-Bact-0338-a-A-18, EUB338	GCTGCCTCCCGTAGGAGT	Amann *et al.*, 1990
Planctomycetales	S-D-BactP-0338-a-A-18, EUB338 II	GCAGCCACCCGTAGGTGT	Daims *et al.*, 1999
Verrucomicrobiales	S-D-BactV-0338-a-A-18, EUB338 III	GCTGCCACCCGTAGGTGT	Daims *et al.*, 1999
Archaea	S-D-Arch-0915-a-A-20, ARCH915	GTGCTCCCCCGCCAATTCCT	Amann *et al.*, 1990
Crenarchaeota	S-K-Cren-0499-a-A-18, CREN 499	CCAGRCTTGCCCCCCGCT	Burggraf *et al.*, 1994
Euryarchaeota	S-K-Eury-0498-a-A-14, EURY 498	CTTGCCCRGCCCTT	Burggraf *et al.*, 1994
Alphaproteobacteria	S-Sc-aProt-0968-a-A-18, ALF968	GGTAAGGTTCTGCGCGTT	Neef, 1997
Betaproteobacteria	L-Sc-bProt-1027-a-A-17, BET42a	GCCTTCCCACTTCGTTT	Manz *et al.*, 1992
Gammaproteobacteria	L-Sc-gProt-1027-a-A-17, GAM42a	GCCTTCCCACATCGTTT	Manz *et al.*, 1992
Flavobacteria, Bacteroidetes, Sphingobacteria	S-P-CyFla-0319-a-A-18, CF319a	TGGTCCGTGTCTCAGTAC	Manz *et al.*, 1996
Actinobacteria	S-P-HGC-1901-a-A-18, HGC69a	TATAGTTACCACCGCCGT	Roller *et al.*, 1994
Desulfovibrionales and other Bacteria	S-F-Srb-0385-a-A-18, SRB385	CGGCGTCGCTGCGTCAGG	Amann *et al.*, 1990
Desulfobacterales, Desulfuromonales, Syntrophobacterales, Myxococcales	S-F-Srb-0385-b-A-18, SRB385Db	CGGCGTTGCTGCGTCAGG	Rabus *et al.*, 1996

***Table 3:** One-way ANOVA to test effects of treatments and time. Signifcance levels are given for EPS sugars, EPS proteins, bacterial cell numbers and sediment stability. Source: Gerbersdorf et al. 2008b FEMS.*

Variables	Treatments/Week					Treatments	Time
	Week 1	Week 2	Week 3	Week 4	Week 5	All data	All data
EPS sugars	0.2167	0.0237	0.0300	0.0093	0.0315	<0.0001	0.9020
EPS proteins	0.3268	0.2930	0.0470	0.0510	0.0382	0.0126	0.6762
Bacteria	<0.0001	<0.0001	0.0010	0.0246	0.0002	<0.0001	0.0059
Stability/CSM	0.0200	0.5500	0.0008	0.0125	0.0006	0.0020	0.0022

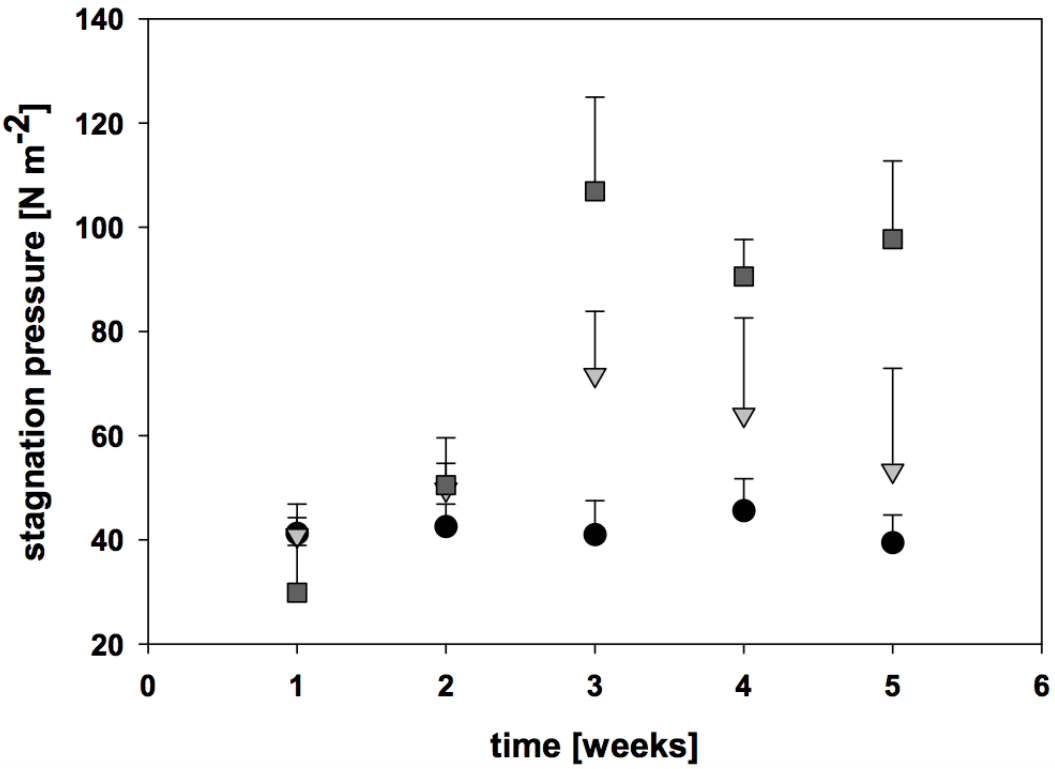

***Figure 11**: Cohesiveness in the treatments "bacteria" (grey triangles), and "bacteria+" (dark grey squares) versus the "controls" (black circles) over the course of the main experiment (five weeks). The cohesiveness is expressed as the vertical stagnation pressure in Nm^{-2} (=Pascal), which is needed to erode the substrate surface, determined by the CSM (Cohesive Strength Meter) (n=6). Gerbersdorf et al. 2008b FEMS.*

III.4.2. BACTERIAL EPS (EXTRACELLULAR POLYMERIC SUBSTANCES)

Water-extractable carbohydrate concentrations varied between 0.08–0.32mg cm^{-3} and 0.09–1.70mg cm^{-3} in the top 500µm of sediment of the bacteria and nutrient cultures, respectively. Over the total depth of 10mm, the colloidal carbohydrate concentrations ranged between 0.43–1.56mg cm^{-3} (bacteria) and 0.21–3.39mg cm^{-3} (bacteria+) (Table 4). The water-extractable protein concentrations ranged between 0.04–1.71mg cm^{-3} and 0.06–4.02mg cm^{-3} in the top 500µm for bacteria and nutrient treatments, respectively. Over the total depth, the proteins reached concentrations between 0.45–9.66 and 0.19–8.18mg cm^{-3} for bacteria and bacteria+, respectively (Table 5).

***Table 4**: Extracellular sugar concentrations in the treatment „bacteria“ and „bacteria+“ over the course of five weeks. Mean value [mg cm³] is given for n=6. Source: Gerbersdorf et al. 2008b FEMS.*

Layer	**Bacteria**					**Layer**	**Bacteria+**				
Week	1	2	3	4	5		1	2	3	4	5
500 µm	0.14	0.15	0.16	0.18	0.15	500µm	0.55	0.42	0.56	0.41	0.36
1000µm	0.22	0.25	0.22	0.30	0.24	1000µm	0.96	0.76	1.06	0.63	0.61
3000µm	0.51	0.81	0.46	0.90	0.56	3000µm	1.02	1.10	1.63	1.02	1.02
10000µm	0.65	0.92	0.55	1.03	0.66	10000µm	1.09	1.16	1.71	1.07	1.09

***Table 5:** Extracellular protein concentrations in the treatment „bacteria“ and „bacteria+“ over the course of five weeks. Mean value [mg cm³] is given for n=6. Source: Gerbersdorf et al. 2008b FEMS.*

Layer	**Bacteria**					**Layer**	**Bacteria+**				
Week	1	2	3	4	5		1	2	3	4	5
500µm	0.16	0.19	0.38	0.50	0.43	500µm	1.00	1.14	1.74	1.22	1.24
1000µm	0.24	0.34	0.70	0.82	0.58	1000µm	1.89	1.61	2.54	1.80	1.72
3000µm	0.80	1.31	3.05	2.91	1.49	3000µm	2.49	2.46	3.76	3.09	2.15
10000µm	0.95	1.56	3.76	3.51	1.78	10000µm	2.73	2.82	4.28	3.58	2.41

The resin-extractable EPS fractions accounted for 30–115% (mean value 85%) of the colloidal EPS concentrations in the top 500µm. Over the total depth of 10mm, the ratio of colloidal to bound EPS fractions was almost 1 for the proteins (R^2=0.87, P<0.0001, n=100) and much higher but variable for the sugars (R^2=0.25, p=0.0002, n=100).

EPS protein concentrations were significantly higher than EPS carbohydrates for the bacteria+ (1-way ANOVA, p=0.01 for top 500µm and p<0.001 for 10mm) but not for the bacteria. The EPS protein and carbohydrates concentrations in the top 500µm layer were significantly higher for the bacteria+ compared to bacteria (Table 3, Figure 12). Differences in EPS contents between treatments only became significant in the weeks three-five (Table 3). The averaged EPS P/C (Protein/Carbohydrate) ratio was >1 for both treatments and increased over the course of the experiment from 1.1-2.8 and 1.8-3.5 for the bacteria and nutrient treatments, respectively (Figure 13). Carbohydrates were below detection levels in the controls, and only minor traces of proteins could be determined (1% of the values for bacterial treatments).

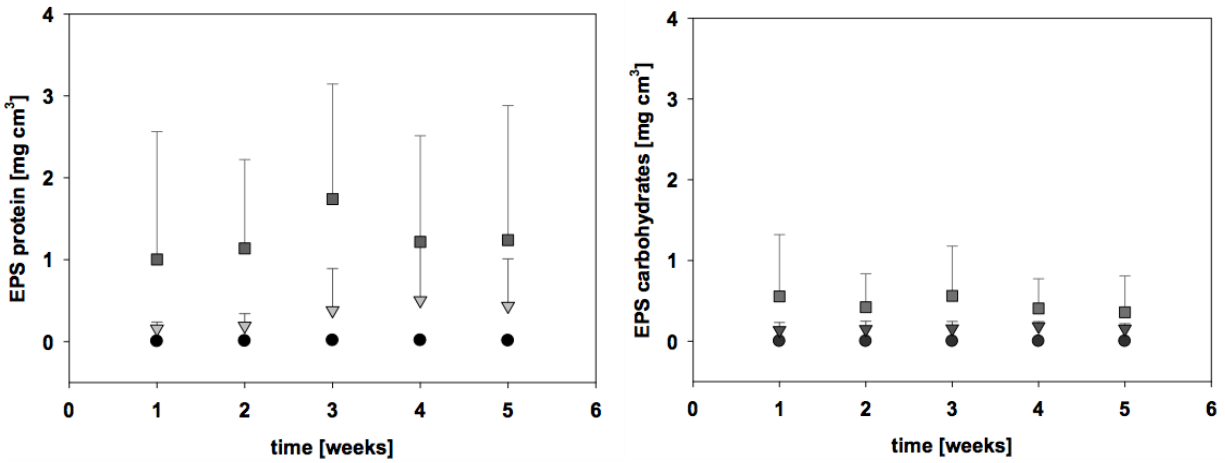

Figure 12: *Bacterial EPS concentrations over the course of the experiment; mean values (n=6) with standard deviation are given for the "bacteria" without nutrients (grey triangles), the "bacteria+" with nutrients (dark grey squares) and the "controls" (black circles) for EPS protein (left) and EPS carbohydrates (right). Source: Gerbersdorf et al. 2008b FEMS.*

Both EPS fractions increased over the first three weeks and showed a decrease thereafter. The carbohydrate concentrations in week five were similar or lower than at the beginning of the experiment while the protein concentrations were higher despite a decline after weeks three or four (Figure 12).

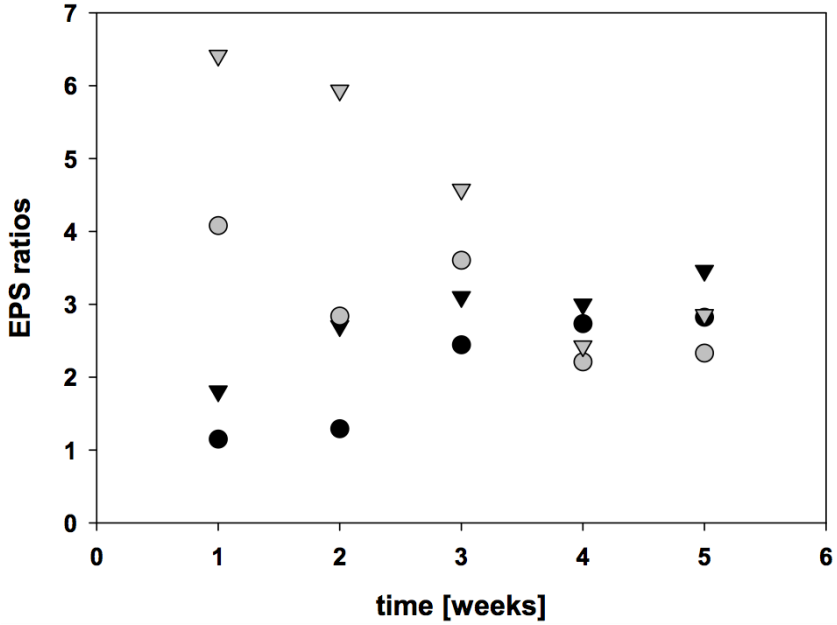

Figure 13: *Different EPS ratios over the course of five weeks: EPS protein/carbohydrate P/C ratio for "bacteria" (black circles) and for "bacteria+" (black triangles) as well as the EPS C/C (grey circles) and P/P (grey triangles) ratio between the treatment "bacteria" and "bacteria+" (n=6). Source: Gerbersdorf et al. 2008b FEMS.*

The bacterial EPS penetrated the total measured depth of the sediment from week one onwards (Figure 14 and Figure 15). The increase in total EPS (sum of EPS over all layers) towards week three, and the decrease after that, was reflected by the changes in the EPS concentrations in the single layers of the vertical depth profiles.

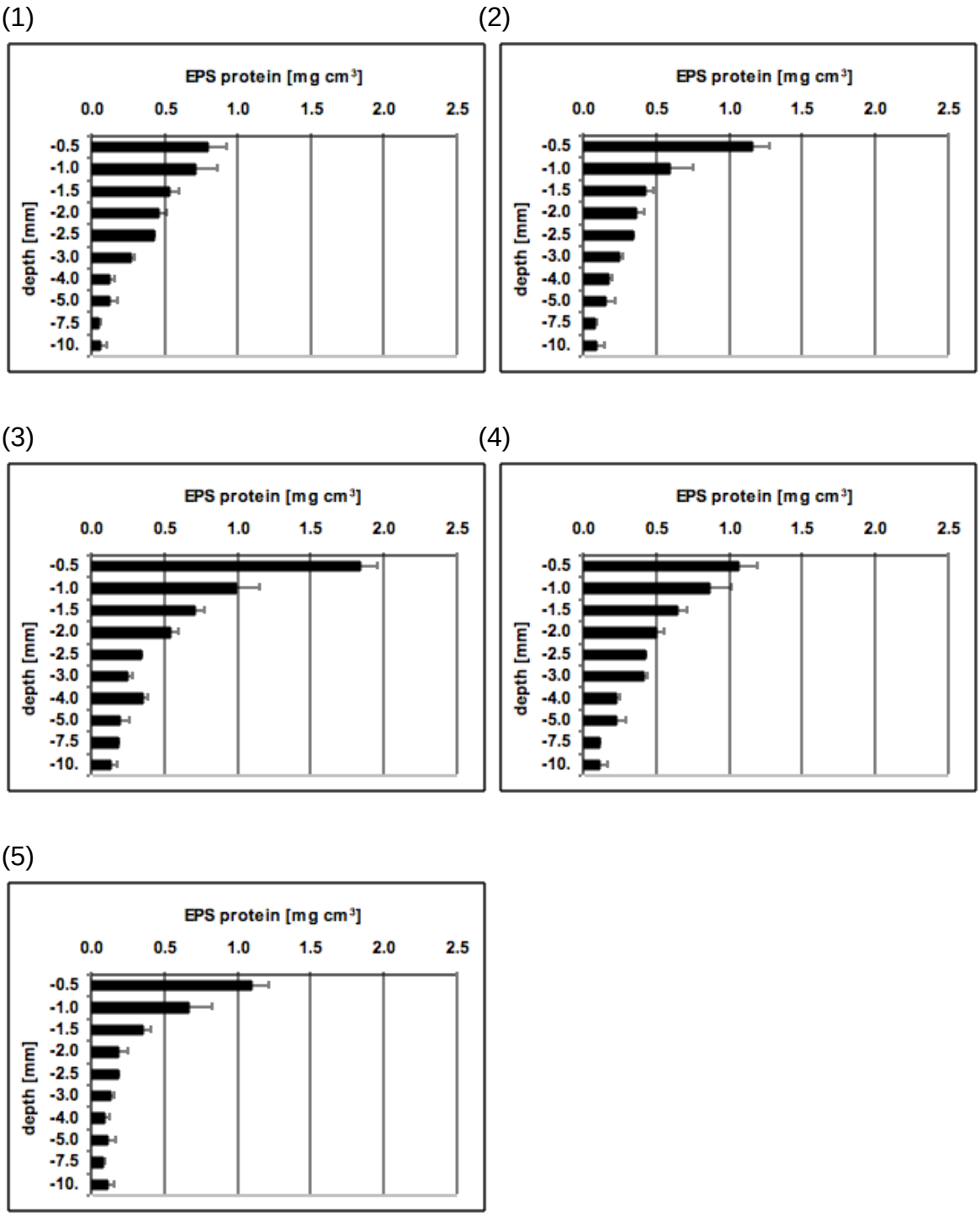

Figure 14: *EPS protein concentrations in 10 substrate layers (between the top 500µm–10mm depth); mean values (n=6) with standard deviation are given for each layer (1-10) and each week (1-5). Source: Gerbersdorf et al. 2008b FEMS.*

The patterns of temporal variation were much more pronounced for proteins (Figure 14) than for carbohydrates (Figure 15). The pronounced decrease of EPS with depth held for all weeks, so that most of the EPS protein and carbohydrate was always contained within the upper 2-3mm of sediment (Table 4, Table 5).

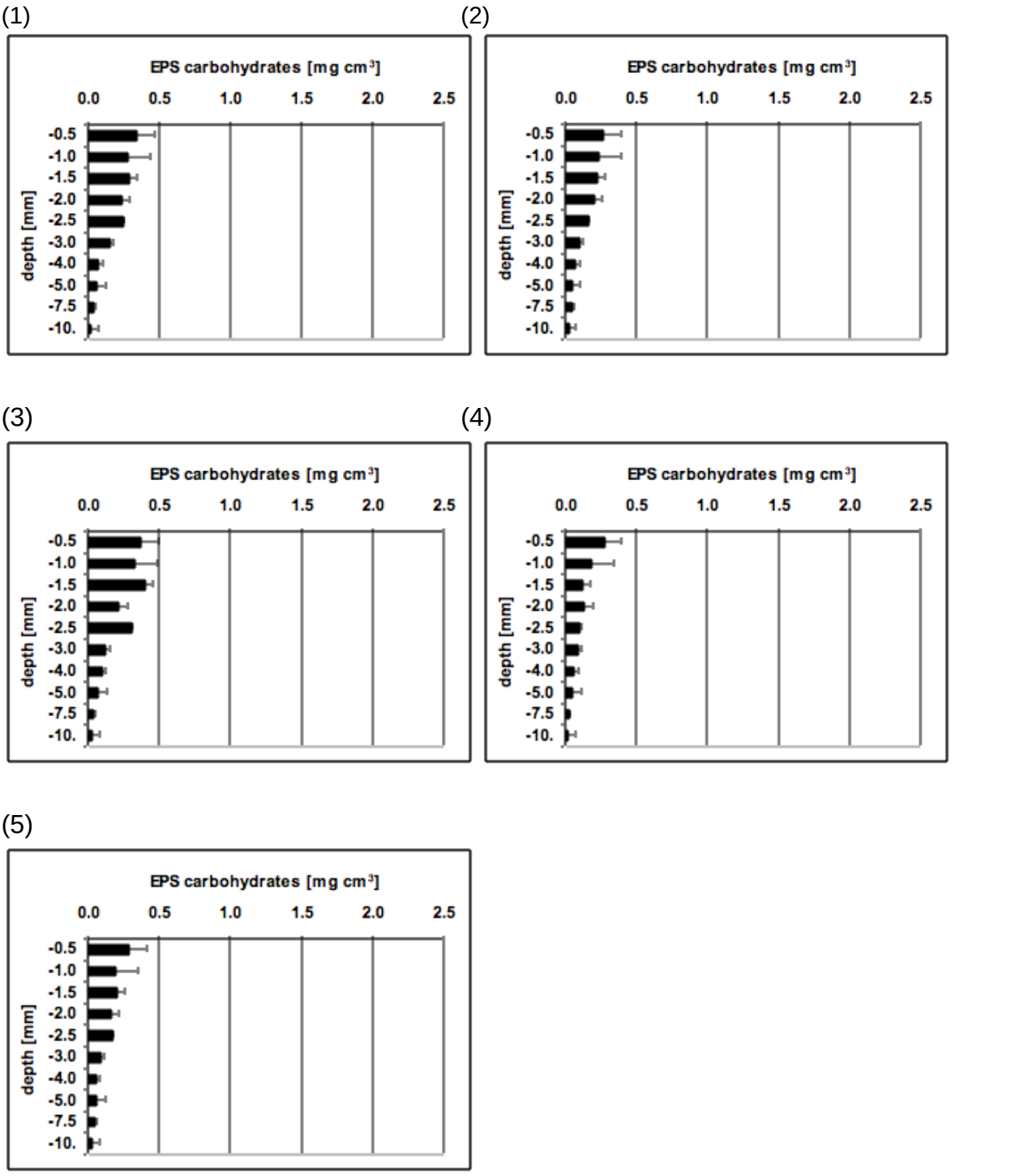

Figure 15: *EPS carbohydrate concentrations in 10 substrate layers (between the top 500µm–10mm depth); mean values (n=6) with standard deviation are given for each layer (1-10) and each week (1-5). Source: Gerbersdorf et al. 2008b FEMS.*

III.4.3. BACTERIAL CELL NUMBERS

The bacterial cell numbers determined in top 500µm layer ranged between $5.30x10^7$-$5.08x10^8$ cells cm^{-3} (mean value $1.41x10^8$ cells cm^{-3}, n=30) for the bacterial treatment and $1.44x10^8$-$8.34x10^8$ cells cm^{-3} (mean value $3.74x10^8$ cells cm^{-3}, n=30) for the nutrient treatment. Thus, the bacteria+ had significantly higher cell numbers (up to factor 10 for single replicates) than the bacteria (Table 3). Under both conditions, the bacterial cell numbers increased towards week 3 and decreased afterwards (Figure 16).

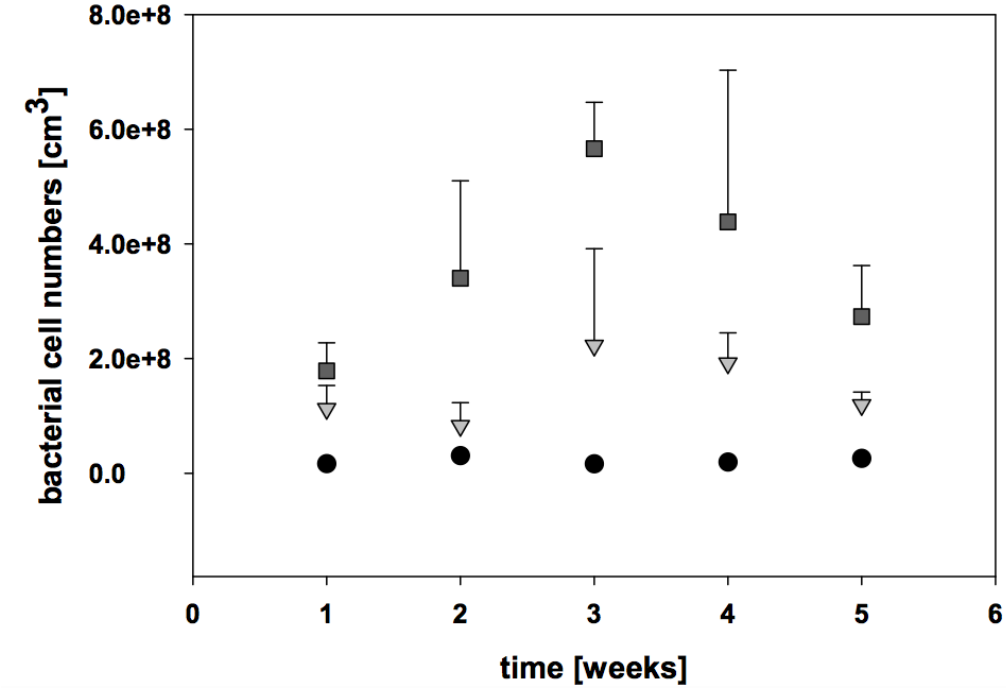

Figure 16: *Bacterial cell numbers in the top 500µm substrate over the course of the experiment; mean values (n=3) with standard deviation are given for the treatments "bacteria" (grey triangles), "bacteria+" (dark grey squares) versus the "controls" (black circles). Source: Gerbersdorf et al. 2008b FEMS.*

III.4.4. BACTERIAL COMPOSITION: PHYLOGENETIC ANALYSIS BY FISH

Within both experimental treatments, the average detection yield with the bacterial probe set EUB338 I-III ("probe active counts" - PAC) - normalized to total cell counts - ranged from 47%-79%, indicating that more than 50% of the bacterial community was usually metabolically active at sampling time. FISH analysis using specific probes for

major taxonomic units of bacteria indicated a predominance of gram-negative *Proteobacteria* covering more than 90% of probe active counts in both treatments. In contrast, the gram-positive *Actinobacteria* and *Firmicutes* occurred at a relative low *in situ* abundance of 2-4%, and 1-3% of probe active counts, respectively. Hybridization with a probe set specific for *Archaea* (ARCH915, CREN499 and EURY498) produced very few fluorescent cells (relative abundance below 1%).

In the bacteria samples, 74.5% of the probe active counts could be assigned to *Gammaproteobacteria,* 12.3% to *Alphaproteobacteria*, and 7.5% to *Betaproteobacteria*. 3.3% of probe active counts hybridized with probe SRB385, covering *Desulfovibrionales* and other bacteria. The relative abundance of *Desulfobacterales*, *Desulfuromonales*, *Syntrophobacterales*, and *Myxococcales* (as shown by hybridization with probe 385Db) was very low, ranging from 1-2% in all samples. *Flavobacteria, Bacteroidetes* and *Sphingobacteria* (members of the subphylum *Cytophaga-Flexibacter*) were present at low relative abundance (1-2% of probe active counts). The nutrients supplied to the nutrient treatment induced a shift within the population structure, reflected by an increase of the relative abundance of *Alphaproteobacteria* (up to 18%) and cells hybridizing with probe SRB385 (14.3%). The relative abundance of *Betaproteobacteria* was enhanced slightly (9.8% PAC). In contrast, the relative abundance of *Gammaproteobacteria* declined to 55%.

III.4.5. Relations between Bacterial Cell Numbers, EPS and Sediment Stability

Bacterial numbers showed a significant relationship with EPS protein concentrations in the top 500µm layer for both treatments (Figure 17). Using the mean values of bacterial numbers and EPS protein for both treatments combined, a regression relationship of R^2=0.74 (p=0.0014) was determined (Figure 17). In contrast to EPS proteins, no relation was found between bacterial cell numbers and EPS carbohydrates for the single

treatments. However, combining the mean values for both treatments resulted in a regression of R^2=0.51 (p=0.0199).

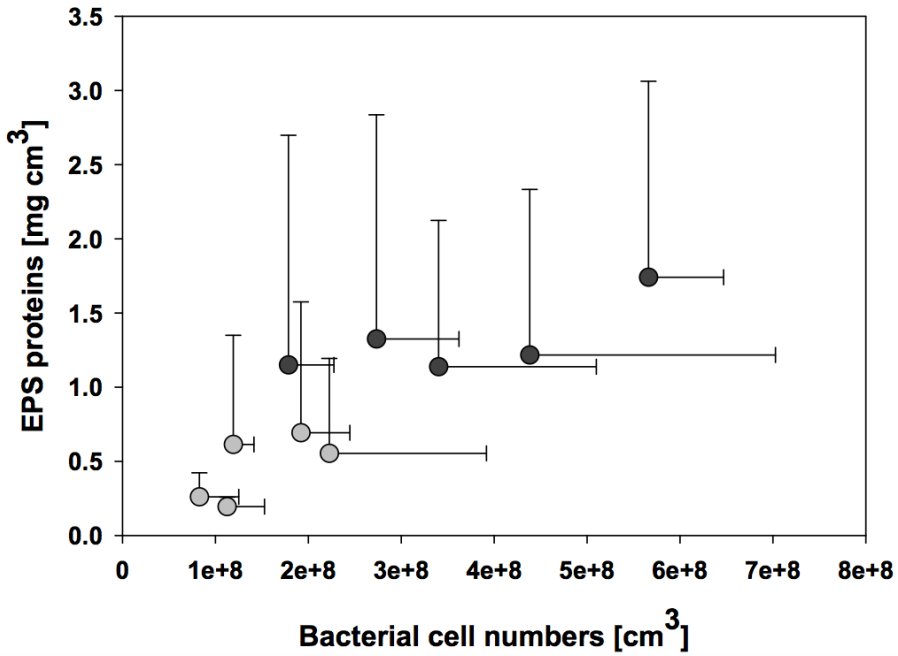

***Figure 17**: Regression between the bacterial cell numbers and the EPS proteins in the top 500µm substrate layer [cm³]. The grey circles indicate the relation for "bacteria" and the black circles for "bacteria+". Each circle is representing a mean value for one week (n=6; five weeks in total). Source: Gerbersdorf et al. 2008b FEMS.*

The variation of surface cohesion over five weeks was closely mirrored by the bacterial cell numbers and EPS concentrations (Figure 11, Figure 12, Figure 16). Hence, a regression between stagnation pressure and bacterial cell numbers in the top 500µm of the substratum was determined (single values: R^2=0.41, p=0.0002, n=60; mean values of combined treatments: R^2=0.58, p=0.0105, n=10). A significant relationship was also noted between stagnation pressure and the water-extractable EPS protein concentrations (single values: R^2=0.31, p<0.0001, n=60; mean values of combined treatments: R^2=0.44, p=0.0374 (Figure 18), but not with carbohydrates (e.g. for mean values of combined treatment: R^2=0.05, p=0.5349).

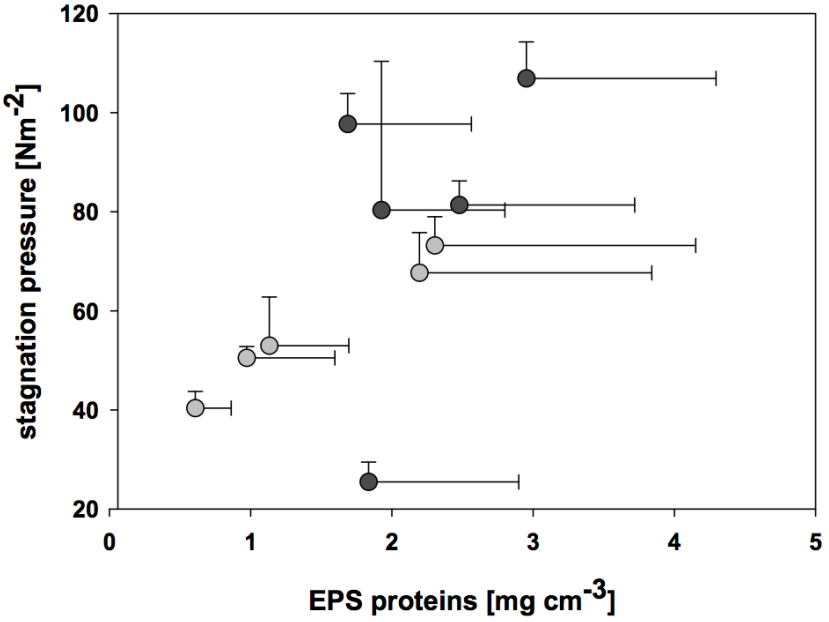

***Figure 18**: Regression between the EPS proteins and the stagnation pressure in the top 500µm substrate layer [cm^3]. The grey circles indicate the relation for "bacteria" and the black circles for "bacteria+". Each circle is representing a mean value for one week (n=6; five weeks in total). Source: Gerbersdorf et al. 2008b FEMS.*

III.5. DISCUSSION

III.5.1. BACTERIAL STABILIZATION POTENTIAL

Bacterial colonization resulted in the development of a biofilm which significantly stabilized the test substratum. Since the chosen substratum was composed of non-cohesive glass beads, the binding force must have been entirely due to bacterial attachment and the secretion of a polymeric matrix (Figure 19). Although the CSM data did not indicate significant differences between the treatments and controls until week three, the crater edges left behind by the CSM jet after one week were distinct in the bacterial treatments in contrast to the controls indicating the onset of stabilization below the CSM detection limits. The biofilm can only resist the vertical force of the CSM when a certain critical strength is developed.

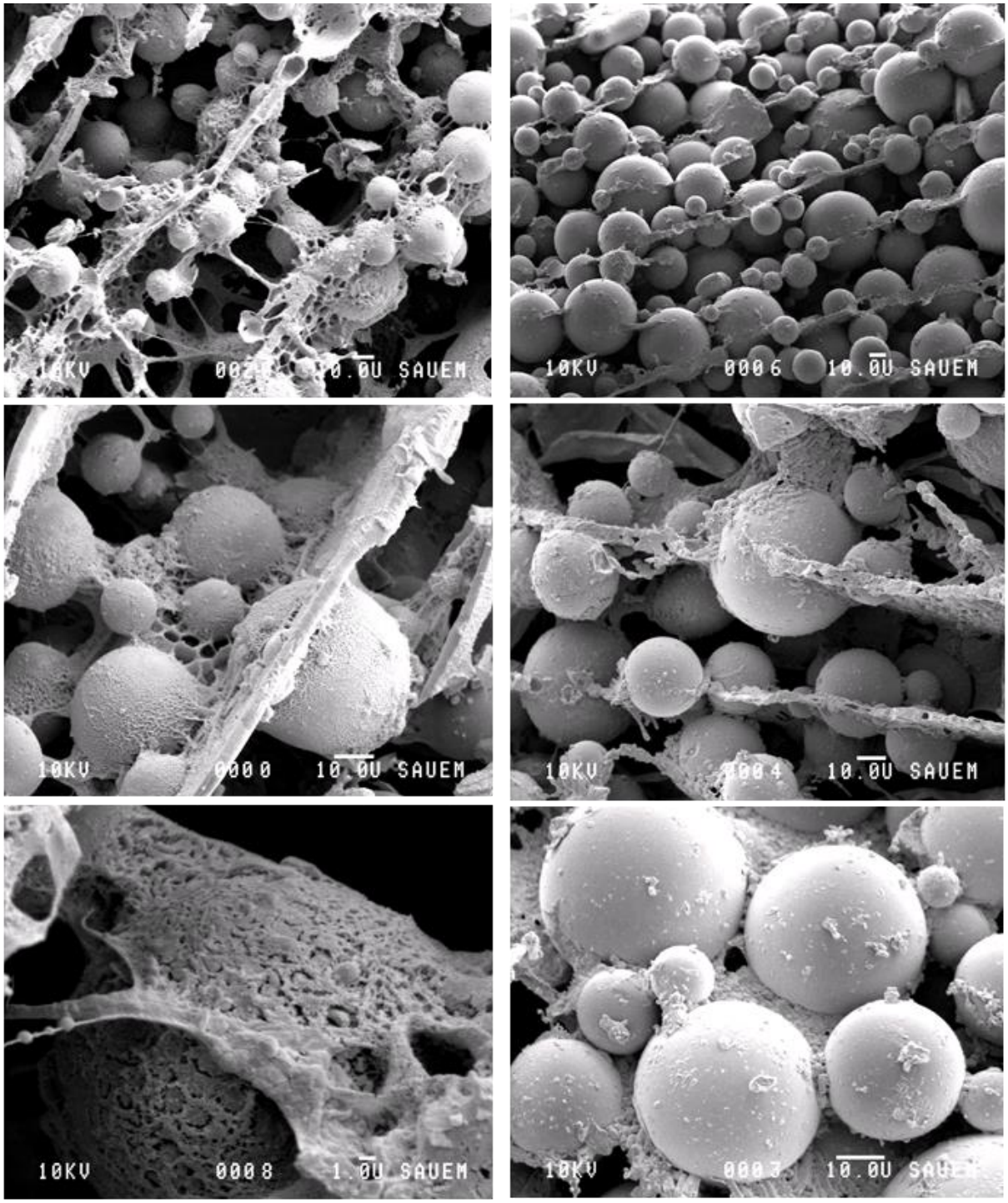

Figure 19: *LTSEM (Low Temperature Scanning Electron Microscope) images of the bacteria nutrient treatment (left side) and the control (right side) substratum using different magnifications. Frozen water on the surface resulted in some artificial vertical cover lines on the glass beads (left and right); otherwise the glass beads of the controls are sparkling clear while the glass beads in the bacteria nutrient treatment are heavily covered in EPS which also fills the intermediate space. Source: Gerbersdorf et al. 2008b FEMS.*

In the literature, it has been shown that “natural” assemblages kept in the dark and under antibiotic treatment, imitating bacterial and diatom dominance, respectively,

increased the erosion threshold by 20% and 120% relative to the physico-chemical binding (Lundkvist *et al.*, 2007b). However, these results include some uncertainties due to the antibiotic treatment and its potential effect on stabilization. In the present experiment, the increase in cohesive strength in the nutrient-enriched bacterial community was impressive and even comparable to the stabilization effects of epipelic diatom assemblages on glass beads (factor 4, Paterson, 1990).

III.5.2. The Effect of Nutrient Addition for bacterial Biostabilization

The stabilization effects were significantly more pronounced for the bacterial treatments with nutrients (factor 3.6) compared to bacteria without nutrients (factor 1.8). Dade *et al.* (1996) reported an increase in Bingham yield stress of 60% for nutrient-depleted *Alteromonas* inoculated clay suspensions, while nutrient-enriched treatments showed no significant difference to controls. Although the stabilization effect of bacteria without nutrients was comparable to our data, the nutrient-enriched treatment showed opposite effects. The failure of nutrient-enriched *Alteromonas* suspensions to stabilize was explained by Dade *et al.* (1996) as due to the fact that EPS are mainly produced under metabolic stress (e.g. by nutrient limitation). This was contrary to our results where additional nutrient supply stimulated bacterial cell division along with significantly enhanced EPS proteins and EPS carbohydrates. Moreover, nutrient supply from the water column seems to induce vertical profiles of EPS contents where bacterial EPS production is concentrated in the surface millimetres and gradually declining with depth. This is similar to the EPS profiles known from microalgae where light is the limiting factor. For the bacteria water column nutrients may be limiting bacterial development. Our data is supported by Jorand *et al.* (1994) where easily assimilable substrates were supplied to bacterial cultures. Nutrient depletion may be more important in inducing

qualitative rather than quantitative changes in EPS (Sanin *et al.*, 2003) and may be very context-dependant. Under carbon starvation, excess nitrogen is channelled into EPS protein formation, while under nitrogen starvation, excess carbon is channelled into the EPS matrix (Durmaz & Sanin, 2001). The current study showed enhanced EPS production per cell for bacteria under nutrient enrichment but this was similar for proteins (3x) and carbohydrates (2.5x). This implies that the nutrient-depleted treatments were not limited for a specific nutrient, but had a lower supply of C-source/energy (glucose), amino acids/NSP (Peptone) or vitamins/growth factors (yeast) as provided to the enriched treatments.

III.5.3. THE EFFECT OF NUTRIENT ADDITION ON THE BACTERIAL COMMUNITY

The nutrient treatment produced higher total EPS concentrations as compared to the bacterial treatment, but the differences were most pronounced for EPS proteins, especially in the surface layers of sediment and for the early part of the experiment. There is a consensus that bacterial extracellular proteins are largely exo-enzymes deployed to solubilize external organic matter and bacteria react quickly to additional nutrient supply by increasing the expression of α- and β-glucosidase activity (van Duyl *et al.*, 1999; Goto *et al.*, 2001). This is also said to induce shifts in bacterial community structure, presumably favouring "r-strategists" which are often affiliated to *Gammaproteobacteria*, as shown for waste-water treatment plants (Wagner *et al.*, 1993). In this study, the bacterial assemblages were dominated by gram-negative bacteria affiliated to the *Gammaproteobacteria* in both treatments, as often reported from marine habitats (Nold & Zwart, 1998). Interestingly, the results of FISH analysis also indicate indeed a shift of microbial assemblages between bacteria and nutrient treatment samples. While the "r-strategists" *Gammaproteobacteria* showed a decrease

of probe-active counts for the nutrient-enriched assemblages, the increase of probe-active cells hybridizing with probe SRB385 reflected the activation of further bacterial species (e.g. *Alphaproteobacteria*). In this context, the activation of sulphate-reducing bacteria commonly present in marine sediments cannot be confirmed by the hybridization results with probe SRB385Db. The shift in bacterial community structure shown in this study could potentially change the net stabilization effect, but to date little is known to what extent specific microbial groups contribute to qualitative and quantitative aspects of EPS production. Further studies should elucidate whether increase/decrease in relative abundance of certain bacterial species might be outbalanced by parallel shifts in total cell numbers (see also chapters V. and VI.).

III.5.4. THE POTENTIAL ROLE OF PROTEINS FOR ADHESION

While in natural sediments the bound EPS fraction exceeds the colloidal/water-extractable EPS fraction significantly (e.g. Gerbersdorf *et al.*, 2005a, 2007), the quantities of both protein fractions were comparable and the bound carbohydrates negligible. The relatively low fraction of bound EPS might be a result of the non-cohesive substratum compared to the natural sediments where inter-particle forces might retain the secreted polymeric substances more strongly. Thus, the present study focused on colloidal EPS only.

Substratum stability showed a strong relationship to bacterial cell numbers and proteins in both treatments, but not to carbohydrates. In the large body of literature on stabilization by microalgae, carbohydrates were often positively correlated with sediment stability (reviewed in Stal, 2003; Underwood & Paterson, 2003) although there is still no agreement on the responsible carbohydrate fraction (e.g. Wigglesworth-Cooksey *et al.*, 2001). Carbohydrate carboxyl-groups contribute to the anionic

properties of the biofilm, and might enhance the binding significantly when bridged by divalent cations (Flemming *et al.*, 2000). However, proteins with a high content of acidic negatively-charged amino acids can be even more involved in electrostatic bonds, especially because there is evidence that cations tend to bind preferentially to proteins over carbohydrates (Dignac *et al.*, 1998). In waste-water flocs, it has been shown that hydrophilic carbohydrates had a negative effect on flocculation while hydrophobic proteins increased hydrophobicity and surface charge (Jorand *et al.*, 1998; Liao *et al.*, 2001), which seems to be crucial for attachment/binding (Liu & Fang, 2003; Sanin *et al.*, 2003). Synergistic effects between the proteins and carbohydrates could strengthen the cohesion of substrata substantially. Earlier work of Costerton *et al.* (1978) argued that the adhesion of bacteria by “spinning a mat of polysaccharide fibers” is likely to be enhanced by lectins.

The majority of EPS polysaccharides have been largely regarded as a labile carbon source for benthic microbes and infauna (Decho, 1990; van Duyl *et al.*, 1999; Goto *et al.*, 2001). This is supported by the relative increase in EPS protein over EPS carbohydrate in aging biofilm, giving evidence that proteins are more resistant to degradation than carbohydrates (Laspidou & Rittmann, 2002). Some authors suggest that EPS enriched in proteins enhances longevity while pure carbohydrate production can lead to the disintegration of biofilm matrix because of their vulnerability to degradative enzymes, especially after local cell lysis (Davis, 1999; Sutherland, 1999). The present data set did not support that bacterially produced EPS carbohydrates were preferentially degraded compared to proteins or under nutrient starvation. Both EPS components, proteins and carbohydrates, were decreasing in both treatments after the third week of the experiment. While the bacterial cell numbers under nutrient addition showed a greater increase to week three (320%) compared to bacteria (200%), both

treatments showed a similar decrease to 50% of original values between weeks three and five, indicating senescence of the bacterial community. The data suggest that the total EPS concentrations were affected as a result of this decline in bacterial population. However, it cannot be ruled out that EPS production rates changed within the aging biofilm or that shifts in bacterial assemblages may lead to lower EPS contents. At the end of the experiment and along with lower bacterial cell numbers and lower EPS content, the substratum became more susceptible to erosive forces.

III.6. CONCLUSIONS

In natural sediments the bacteria have been largely regarded as decomposers while microalgae - mainly diatoms - have been identified as sediment stabilizers, even considered as important ecosystem engineers (Boogert *et al.*, 2006). This is despite the common knowledge that benthic assemblages invariably incorporate a significant biomass of heterotrophic bacteria. In this chapter, it could be shown that a natural benthic bacterial assemblage significantly stabilized the test substratum, clearly surpassing the effects reported in the few other relevant investigations.

Unlike previous studies based on microphytobenthos assemblages, sediment stabilization was more closely associated with EPS proteins than EPS carbohydrates. This implies more significance for the proteins in substratum cohesion within the bacterial EPS complex than previously recognized. The structural role of proteins in the EPS complex and its interactions with other EPS components concerning the stability of natural sediments is worth further attention. There is now a consensus that the natural biota often provides the important ecosystem function of “biostabilization” for depositional habitats. The improved understanding of this functional capacity is necessary to improve models of sediment dynamics and optimize coastal management

strategies. The current study data show that bacterial assemblages should not be neglected when considering microbial sediment stabilization and secondly, that a change in abiotic conditions (here represented by nutrients) can significantly affect the composition and the stabilization potential of bacterial assemblages. This is of particular importance when considering the expected changes in abiotic factors (e.g. temperature, CO_2) along with higher frequencies of storm events due to climate change.

IV. SYNERGISTIC EFFECTS BY MIXED VERSUS SINGLE TAXA BIOFILM COMMUNITIES FOR BIOSTABILIZATION

IV.1. ABSTRACT

Little is known about the individual engineering capability of the main biofilm components (heterotrophic bacteria and autotrophic microalgae) in terms of their individual contribution to the pool of naturally adhesive material (EPS: extracellular polymeric substances) and their relative functional contribution to substratum stabilization. This chapter investigates the engineering effects on a non-cohesive test bed as the surface was colonised by natural benthic assemblages (prokaryotic, eukaryotic and mixed cultures) of bacteria and microalgae. Magnetic Particle Induction (MagPI) and Cohesive Strength Meter (CSM) determined the adhesive capacity and the cohesive strength, respectively, of the culture surface. Stabilization was significantly higher for the bacterial assemblages (up to a factor of 2) than for axenic microalgal communities. The EPS concentration and composition (carbohydrates and proteins) were both important in determining stabilization. The engineering effect was significantly higher in the mixed assemblage as compared to the bacterial (x1.2) and axenic diatom (x1.7) cultures. Nevertheless, the results did not suggest clear synergistic (=more than additive) effects for biostabilization by the interaction of autotrophic and heterotrophic biofilm consortia. The overall stabilization potential of the various assemblages was impressive (x7.5 and x9.5, for MagPI and CSM, respectively, as compared to controls). This information contributes to the conceptual understanding of the microbial sediment engineering as an important ecosystem function in aquatic habitats.

IV.2. BACKGROUND

Microalgae have been put forward as important “ecosystem engineers” (Boogert *et al.*, 2006) due to their influence on the structure and behaviour of sedimentary habitats. While biostabilization by microalgae has been researched extensively in the marine habitat, the ubiquitous heterotrophic bacteria have largely been ignored, even in conceptual models, as we have learned in the previous chapter. Pioneering work on the entrainment of a clay-water suspension by Dade et al. (1996) and on the stability of experimentally-derived biofilm by Leon-Morales et al. (2007) inspired our recent work which has shown that natural benthic bacterial assemblages from estuarine areas significantly stabilized a test substratum (Gerbersdorf *et al.*, 2008b, 2009). The former work on the sediment stabilization potential of microalgae appears in a new light, since the natural “microalgal mats” investigated were certainly not devoid of heterotrophic bacteria. Hence, the question of the functional role and origin of EPS in microbial mats requires further interpretation and can initially be addressed by separate studies of the engineering potential of prokaryotic and eukaryotic assemblages.

There is evidence that the co-existence of bacteria and microalgae might be of mutual advantage mainly in terms of nutrient recycling (Goto *et al.*, 2001; Klug, 2005). Some microalgal species depend on association with certain bacteria groups (Schäfer *et al.*, 2002) and in some pelagic diatoms, the presence of specific bacteria is crucial for their growth and EPS secretion (Grossart & Simon, 2007). Bruckner et al. (2008) showed that the monomer composition of microalgal EPS carbohydrates varied along with the presence of different bacterial groups. On the other hand, some microalgae species suppress bacteria by producing polyunsaturated aldehydes that have strong bactericidal effects (Wichard *et al.*, 2005; Ribalet *et al.*, 2008). Bacteria can also influence microalgal growth and EPS secretion through the release of specific algicidal

compounds (Fukami *et al.*, 1997; Mu *et al.*, 2007). There is evidence that these bacteria-microalgae interactions are highly species-specific and help to shape the composition of the biofilm assemblages (Boivin *et al.*, 2007), again with possible implications for EPS secretion and sediment binding. Presumably, the various bacteria - microalgae interactions are strongly driven by abiotic and biotic conditions both within and outside the biofilm. For instance, external nutrient addition caused shifts within the natural microbial assemblage which influenced EPS concentration, EPS composition and sediment stability (Gerbersdorf *et al.*, 2008b, 2009). Still, the mechanisms and species interactions inducing these shifts in biofilm are far from understood and nutrients are not the only influential environmental variable.

This chapter compares the individual and combined engineering capability of natural heterotrophic bacterial assemblages ("B"), axenic autotrophic microalgal assemblages ("D") and mixed assemblages of both ("BD") in terms of EPS secretion and substratum stabilization. The adhesive capacity of the surface as well as the resistance to erosion, both proxies for sediment stability, were monitored regularly by MagPI and CSM, respectively, and related to microbial growth (bacterial cell numbers, bacterial division rate, microalgal biomass) and EPS secretion (concentrations/composition of carbohydrates and proteins). It was hypothesized that the coexistence of bacteria and microalgae might show synergistic effects on EPS secretion, cell growth and the net engineering potential.

IV.3. EXPERIMENTAL SETTINGS

IV.3.1. BACTERIAL CULTURES

Subsurface sediment was sampled to a depth of 5–10mm from an intertidal mudflat in the Eden estuary located in the southeast of Scotland (56°22'N, 2°51'W). One litre of

1µm filtered seawater was mixed with the same volume of sediment and the sediment slurry was sonicated (Ultrasonic bath XB2 50-60Hz) for 10 minutes. The sediment slurry was centrifuged twice (10min, 6.030g, Mistral 3000E, Sanyo, rotor 43122-105) to separate sediment (pellet) and bacteria (supernatant). The supernatants were further centrifuged (10min, 17.700g, Sorval RC5B/C) and this time the supernatant was discarded, while the remaining pellet with associated bacteria was re-suspended and filtered through a 1.6µm filter (glass microfiber filter, Fisherbrand MF100). The filter size was chosen to exclude the smallest expected microalgae from the Eden estuary. Equipment was acid-washed and microalgal contamination was checked regularly by epifluorescense microscopy. Standard nutrient broth (Fluka, Peptone 15g l^{-1}, yeast extract 3g l^{-1}, sodium chloride 6g l^{-1}, D (+) glucose 1g l^{-1}) was autoclaved and added (1:3) to the filtered supernatant. The bacterial stock cultures were established in 200ml Erlenmeyer flasks under constant aeration in the dark at room temperature (15°C) and fresh nutrient broth was added once a week during two weeks cultivation.

IV.3.2. DIATOM CULTURES

Sediment surface samples (0–5mm) were taken from the same location on the Eden estuary and were initially processed as described for the bacterial cultures. However, the remaining pellet was resuspended in F/2 culture media without the filtration step. To exclude bacteria, antibiotics were added (150mg l^{-1} streptomycin, 20mg l^{-1} chloramphenicol, final concentrations) and the effective exclusion of bacteria was confirmed regularly by epifluorescense microscopy. The microalgal cultures were incubated under constant temperature (15°C) and at ambient light conditions in the laboratory for two weeks with fresh nutrients added regularly (Ribalet *et al.*, 2008).

IV.3.3. EXPERIMENTAL SET-UP

A 3cm layer (minimum operation depth of the Cohesive Strength Meter, CSM) of 0.04-0.07mm glass beads was placed in Rotilab deep-freeze boxes (l x w x h = 20.8cm x 20.8cm x 9.4cm). Two litres of autoclaved seawater were carefully added to each box (Gerbersdorf *et al.*, 2008b). Bacteria and diatom cultures (see above) served as inocula to initiate biofilm on the non-cohesive artificial substratum. The following treatments were established (six replicates of each): controls (C), bacterial cultures (B), diatom cultures (D), as well as mixed assemblages of bacteria and diatoms (BD). The controls containing glass beads and seawater were regularly treated (once a week) with a mixture of antibiotics (150mg l^{-1} streptomycin and 20mg l^{-1} chloramphenicol, final concentrations) to prevent bacterial colonisation. The other boxes were initially inoculated from the stock cultures with 15ml each for bacterial and diatom cultures, and 30ml (15/15ml, B/D) for the mixed cultures. All treatments were gently aerated and kept at constant temperature (15°C) over a period of four weeks. The diatoms and the mixed assemblages were illuminated at 220–250µE m^{-2} s^{-1} with a light/dark cycle of 10/14h.

IV.3.4. SAMPLING

Sampling took place on every third day during the experiment. For each treatment, three boxes out of the six replicates were randomly selected and sampled in turns at each measurement. From each sample box, four sediment cores of 5mm depth were taken with a cut-off syringe (10mm diameter) to determine bacterial cell numbers, bacterial assemblage (two cores for two fixation protocols) and EPS. For the treatments diatoms (D) and the mixed assemblage (BD), two additional cores were taken to determine chlorophyll a and the microphytobenthic species composition. For bacterial division rate, one more sediment core (depth 10mm) was taken from the box and the

three cores per treatment pooled before analysis; all other sediment cores were processed individually.

IV.4. RESULTS

IV.4.1. MICROPHYTOBENTHOS COMPOSITION

In the mixed assemblage (bacteria + diatoms, BD), diatoms of the genera *Achnanthes*, *Caloneis*, *Navicula* and *Nitzschia* were the initial colonizers of the substratum at the beginning of the experiment (day 1). While the species *Achnanthes longipes* (~ 50µm length, on stalks) and *Caloneis amphisbaena* (~ 70µm length) were dominant, the majority of species were represented by the genus *Navicula* (*N. cinta, N. digitoradiata, N. flanatica N. gregaria N. crytocephala, N. perminuta/diserta, N. phyllepta, N. salinarum*) and *Nitzschia (N. epithemioides, N. frustulum, N. hungarica, N. sigma*). Over time, smaller species from the genus *Navicula* became increasingly dominant together with *Nitzschia* and *Cymbella* species. After four weeks, only small *Navicula* species remained in the culture. In the diatom assemblage (D), treated with antibiotics to inhibit bacterial colonization, the species composition was quite similar to the mixed assemblage with *Achnanthes*, *Cylindrotheca*, *Cymbella*, *Navicula* and *Nitzschia* species present but smaller *Navicula* species were dominant from the beginning. *Achnanthes*, *Cymbella*, and *Nitzschia* species were characteristic for this treatment for about three weeks. By the end of the experiment, only small *Navicula* species remained.

Most of the diatom species were typically from poly- and hypertrophic environments, except for some species of *Achnanthes* and *Cymbella* that prefer mesotrophic conditions. Although the benthic diatom community was isolated from natural sediments, species richness seemed becoming less diverse during culturing.

IV.4.2. BACTERIAL ASSEMBLAGES

The proportion of the active cells, as determined by EUB mix, was higher at the start of the incubations for the pure bacterial assemblage (B, 58%) as compared to the mixed assemblage (BD, 38%) but similar in both treatments (54%, B and 55%, BD) at the end of the experiment. This indicated that most of the bacterial community was metabolically active at the relevant sampling time. In the controls (C) and in the diatom assemblage (D), hybridization with oligonucleotide probes was below levels of detection.

The application of domain, phylum, and subphylum specific oligonucleotide probes (Table 2) revealed that gram-negative Proteobacteria dominated the samples, while gram-positive Actinobacteria were less than 1% of the total bacteria (Table 6).

In the mixed assemblage, the Alphaproteobacteria accounted for 18%, the Betaproteobacteria for 35%, the Gammaproteobacteria for 15%, the Delta-subclass for 5% and the Cytophaga Flexibacter Subphylums for 15%. Over time, a noticeable shift was determined within the assemblage: while the Alphaproteobacteria increased to 20%, the Betaproteobacteria decreased to 18%, and the Sulphate deoxidizer/Delta-subclass decreased below detection limits. The Actinobacteria accounted for less than 1% and were thus negligible.

The pure bacterial assemblage showed similar proportions of the subphyla (Alphaproteobacteria 10%, Betaproteobacteria 30%, Gammaproteobacteria 10%, Cytophaga/Flexibacter 13%), but the Delta-subclass could not be detected. Over time, Alphaproteobacteria increased (to 12%) and the Betaproteobacteria decreased, but to a much lesser extent (to 25%) as compared to the mixed assemblage. Noticeably different to the BD treatment was the increase in Gammaproteobacteria (to 25%) and Cytophaga/Flexibacter (to 18%) over time. Like in the mixed assemblage, the gram-positive Actinobacteria were present at relatively low abundance of <1% (Table 6).

Table 6: *Percentage of the specific bacterial groups (marked by the oligonucleotide probes named on the left) of the total eubacterial counts; given for the treatments bacteria and diatoms (BD) as well as bacteria (B) for the beginning (1) and the end (2) of the experiment. Source: Lubarsky et al. 2010 PLoS ONE.*

	BD, 1 FA (%)	**BD, 2 FA (%)**	**B, 1 FA (%)**	**B, 2 FA (%)**
ALF968	18	20	10	12
BET42a	35	18	30	25
GAM42a	15	15	10	25
HGC69a	<1	-	-	<1
SRB385Db	5	-	-	<1
CF319a	15	15	13	18

IV.4.3. MICROBIAL BIOMASS, CELL NUMBERS AND GROWTH RATE

The chlorophyll a (Chl a) and pheophytin concentrations were significantly different between the treatments for most of the sampling days (Kruskal-Wallis (χ^2) test (KW), $p<0.05$). Chl a concentrations in the mixed treatment ranged between 1.5 and 2.17µg cm^{-3} and were significantly higher than in the axenic microalgal assemblages (Figure 20A) with values ranging between 1.38 and 1.97µg cm^{-3} (for example, day 14: KW, $\chi2=6.77$ df=2, $p<0.05$, with post-hoc Student-Newman-Keuls (SNK) test).

The bacterial cell numbers determined by flow cytometry significantly differed between the treatments on most of the days too (KW, $p<0.05$). The bacterial cell numbers in the treatments B and BD varied between $1.44x10^7$ and $5.56x10^7$ cells cm^{-3} as well as $0.34x10^6$ and $1.19x10^7$ cells cm^{-3}, respectively (Figure 20B). Thus, the bacterial cell numbers were significantly higher in the pure bacterial culture (for example, day 14: KW, $\chi2=3.8$, df=3, $p<0.05$, with post-hoc SNK test).

Based on the calculated [*methyl*-^{3}H] thymidine incorporation, there was no significant difference for bacterial division rate between the bacterial and mixed assemblages (Figure 20C). Like the bacterial cell numbers, the bacterial division rates were negligible

in the controls and in the axenic diatom assemblage. The specific rate of bacterial division per cell per hour can be calculated by dividing the division rate of the bacterial community (cells cm^{-3} h^{-1}) by the bacterial cell numbers (cells cm^{-3}). The specific rate of bacterial division was significantly higher for BD as compared to B (Figure 20D); especially on day three (BD 18.2 times higher than B, KW, $\chi 2=6.2$ df=2, $p<0.05$, with post-hoc SNK test).

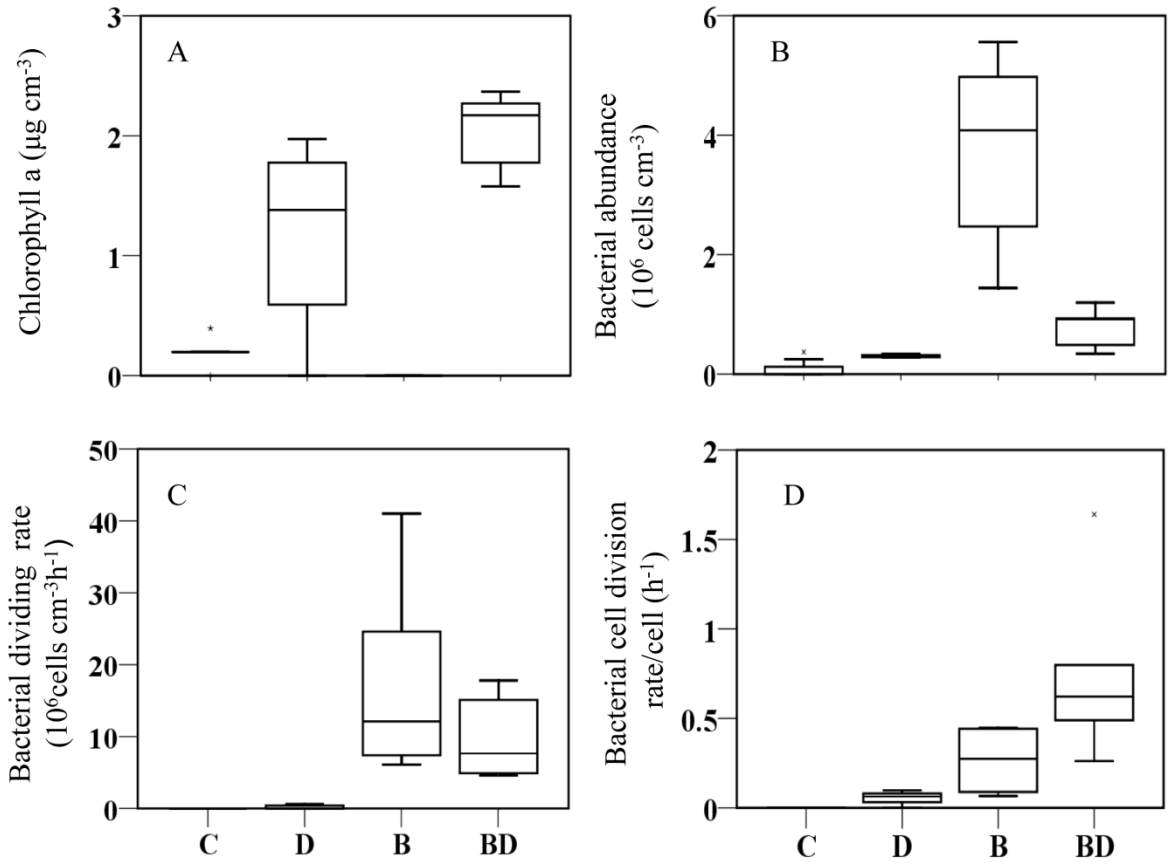

Figure 20: *Mean values of the different treatments: mixed assemblages (BD), diatoms (D), bacteria (B), control (C): A. chlorophyll a (n=21). B. bacterial cell numbers (n=24). C. bacterial division rates (n=18). D. bacterial specific division rates (n=18). Source: Lubarsky et al. 2010 PLoS ONE.*

There was no significant correlation between the bacterial cell division rates and bacterial cell numbers in the bacterial treatment or in the mixed assemblage. Despite ongoing growth of microalgae and bacteria, no significant relationships between

chlorophyll a as a proxy for microalgal biomass and the bacterial cell numbers or division rates could be determined within the mixed assemblage.

IV.4.4. CHANGES IN EPS COMPONENTS

Over time, the colloidal EPS carbohydrate concentrations increased in all treatments to a maximum on day 14 (Figure 21 A, Table 7), but the increase was most pronounced for the mixed assemblage. The carbohydrate concentrations varied between 13-147.3µg cm^{-3}, 7.3-40.5µg cm^{-3} and 15.9–56.6µg cm^{-3} for BD, B and D, respectively (Figure 21 A) with significantly different means in the treatments for all sampling dates except at the beginning of the experiment (KW, $p<0.05$). The carbohydrate concentrations were significantly higher in BD as compared to D and B (for example, day 14: KW, $\chi2=9.66$, $df=3$, $p<0.05$, followed by post-hoc SNK test) (Figure 21 A, Table 7). The treatments B and D were not significantly different from each other. The controls showed negligible concentrations of EPS carbohydrates.

The pattern of the water-extractable protein concentrations over time was similar to that of the carbohydrates, with an increase towards day 14 in all treatments (Figure 21 B, Table 7). The protein concentrations for the treatments BD, B and D varied between 20.9-213.1µg cm^{-3}, 9.8-120.6µg cm^{-3} and 27.8-112.8µg cm^{-3}, respectively (Figure 21 B), with significantly different means in the treatments for most of the sampling dates (KW, $p<0.05$). The protein concentrations in the treatment BD were significantly higher than in the treatments B and D (for example, day 14: KW, $\chi2=9.67$, $df=3$, $p<0.05$, followed by post-hoc SNK test). The treatments B and D were not significantly different from each other and the EPS proteins in the controls were below detection limits.

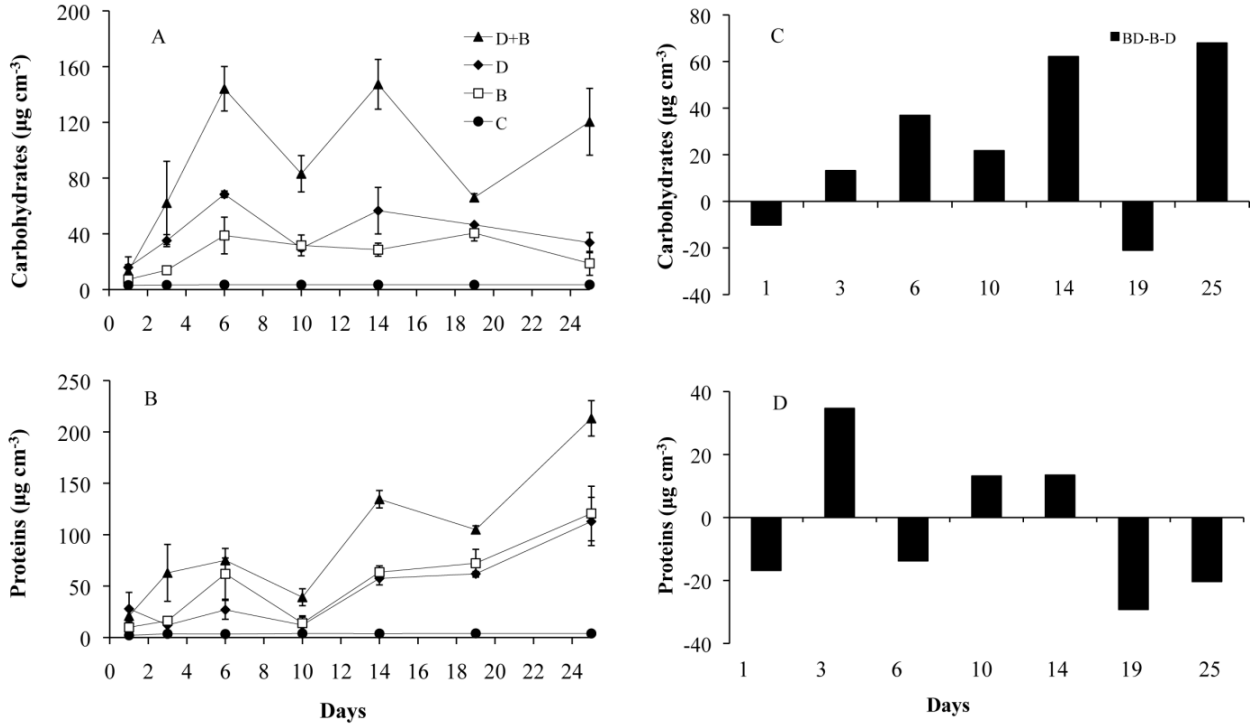

Figure 21: *EPS concentrations within different assemblages. A-B: Mean values (n=3 per treatment, based on n=3 replicates per box + SE) of EPS concentrations in the treatments bacteria and diatoms (BD, ▲), diatoms (D, ♦), bacteria (B, □) and controls (C, ●) for carbohydrates (A) and proteins (B). C-D: The EPS concentration of the mixed cultures (BD) relative to the contribution of the single cultures (B and D) such that the value "[BD]-[B+D]" is reported for carbohydrates (C) and proteins (D). Source: Lubarsky et al. 2010 PLoS ONE.*

To explore possible inhibitory, additive or synergistic effects by the liaison of bacteria and microalgae, the amount of EPS produced in each single assemblage (B and D) was assessed relative to the amount of EPS produced in the mixed assemblage ([BD]-[B+D], (Figure 21 C and D). Where the production of carbohydrate or protein from mixed cultures (BD) exceeds that of the added single cultures (B and D) the value is positive (synergistic effect) and vice versa (inhibitory effect). If the added values of the single cultures exactly equal the mixed cultures then there is an additive effect. For EPS carbohydrates, the value was strongly positive for most of the sampling days suggesting a synergistic effect (Figure 21 C). The results in terms of EPS protein production were more equivocal with a balance in response across the sampling dates (Figure 21 D).

Table 7: *Differences between days 1 and 14 where most of the variables showed their maximum value as well as differences between the treatments (mixed BD, Bacteria B, Diatom D); both times expressed as quotient/factors for EPS carbohydrates, EPS proteins, MagPI and CSM. Source: Lubarsky et al. 2010 PLoS ONE.*

Factors		***Carbohydrates***	***Proteins***	***MagPI***	***CSM***
between day 1-14	B	5.5	6.4	3.4	4
	D	3.6	2.1	2.6	2.8
	BD	11	6.4	2.9	1.8
between treatments	BD/B	5.1	1.7	1.4	2.6
	BD/D	2.6	1.9	2.5	4.1
	B/D	0.714	-	1.7	1.3

A strong positive correlation was determined between colloidal EPS carbohydrates and proteins (Pearson correlation coefficient, $r=0.607$, $n=78$, $p<0.001$). The colloidal carbohydrates and proteins showed a significant positive relation to microalgal biomass ($r=0.385$, $n=56$, $p<0.001$ and $r=0.310$, $n=57$, $p<0.01$, respectively) as well as to the bacterial cell numbers ($r=0.649$, $n=18$, $p<0.01$ and $r=0.518$, $n=18$, $p<0.01$, respectively).

IV.4.5. THE STABILITY OF THE SUBSTRATUM

The surface adhesion of the substratum as determined by MagPI increased for all treatments over time to a maximum value on day 14 (Figure 22 A, Table 7). Cohesion of the substratum as indicated by CSM increased continuously for all treatments (Figure 22 B, Table 7) over the four weeks. The control treatments (C) did not show any significant changes in adhesion/stability over the 25 days of the experiment. There was a significant difference in the means of the treatments for the surface adhesion and cohesion ($p<0.05$) for all dates except at the beginning of experiment.

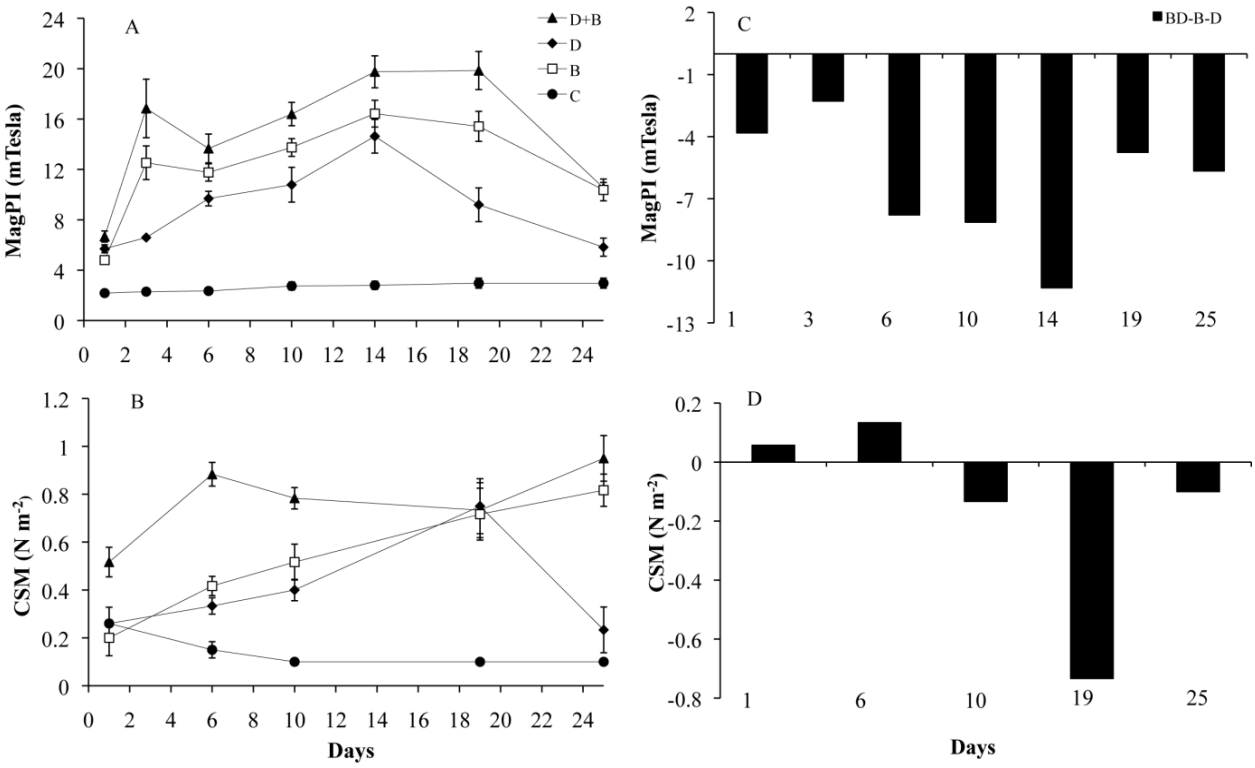

Figure 22: *Mean values of MagPI and CSM measurements of different assemblages. A. Mean values (n=6) of MagPI over the time of the experiment. B. Mean values (n=6) of CSM over the time of the experiment. The treatments were bacteria and diatoms (BD, ▲), diatoms (D, ♦), bacteria (B, □) and controls (C, ●). Substratum stability by the mixed BD treatment relative to the stability of the single B and D treatments is given for MagPI (C) and CSM (D). Source: Lubarsky et al. 2010 PLoS ONE.*

The mixed assemblage (BD) showed the highest surface adhesion of the sediment followed by the bacterial culture (B) and finally, the diatom biofilm (D). The CSM measurements confirmed the MagPI results with significantly higher sediment surface stability in treatment BD followed by B and D (for example, day 24: KW, $\chi 2=10.2.$, df=3, $p<0.05$, followed by a post hoc SNK test). There was a strong linear relationship between CSM (erosion threshold) and MagPI (surface adhesion) (Pearson correlation coefficient: r=0.785, n=20, $p<0.001$, Figure 23).

In order to visualize possible additive/synergistic effects of bacteria-diatom assemblages, this time for sediment stability, their absolute value of adhesion was compared to the values for the pure bacterial and diatom cultures ([BD]-[B+D], (Figure

22 C and D). There was a stronger case for interference in the mixed assemblage since the results were much lower than would be expected from the additive effects of the two cultures B and D, as was particularly evident for surface adhesion (Figure 22 C and D).

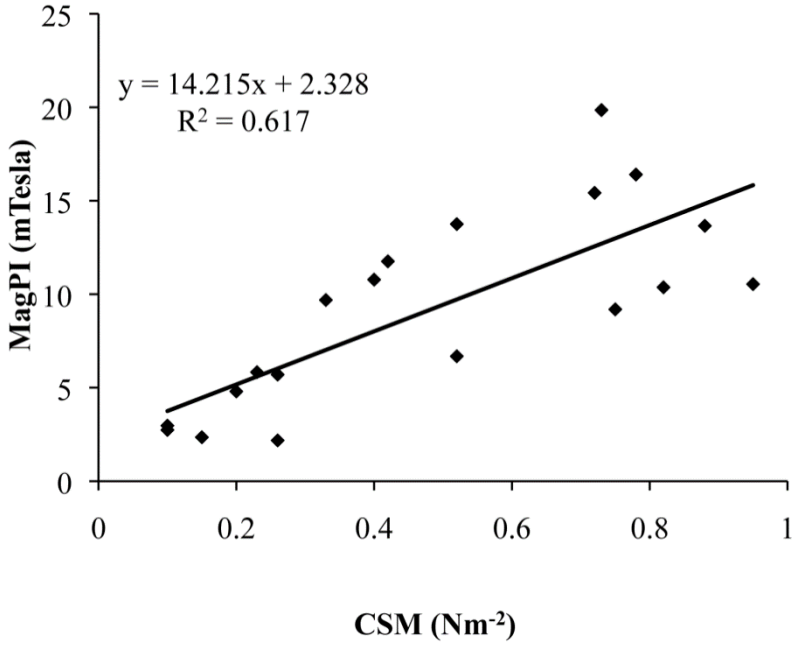

Figure 23: *Relationship between MagPI (mTesla) and CSM (Nm^{-2}). Source: Lubarsky et al. 2010 PLoS ONE.*

IV.4.6. RELATION BETWEEN BIOLOGICAL VARIABLES AND SURFACE ADHESION AND STABILITY

There was a strong positive relationship between sediment stability measurements and chlorophyll a concentrations (MagPI: r=0.395, p<0.001; CSM: r=0.501, p<0.001). Similarly, EPS carbohydrates concentrations were highly significantly correlated with MagPI and CSM measurements for all treatments. The same applied for the relation of EPS proteins concentrations to adhesion (MagPI) and cohesion (CSM) of the surface for B and BD, while for D the relationships were not significant (Figure 24, Table 8).

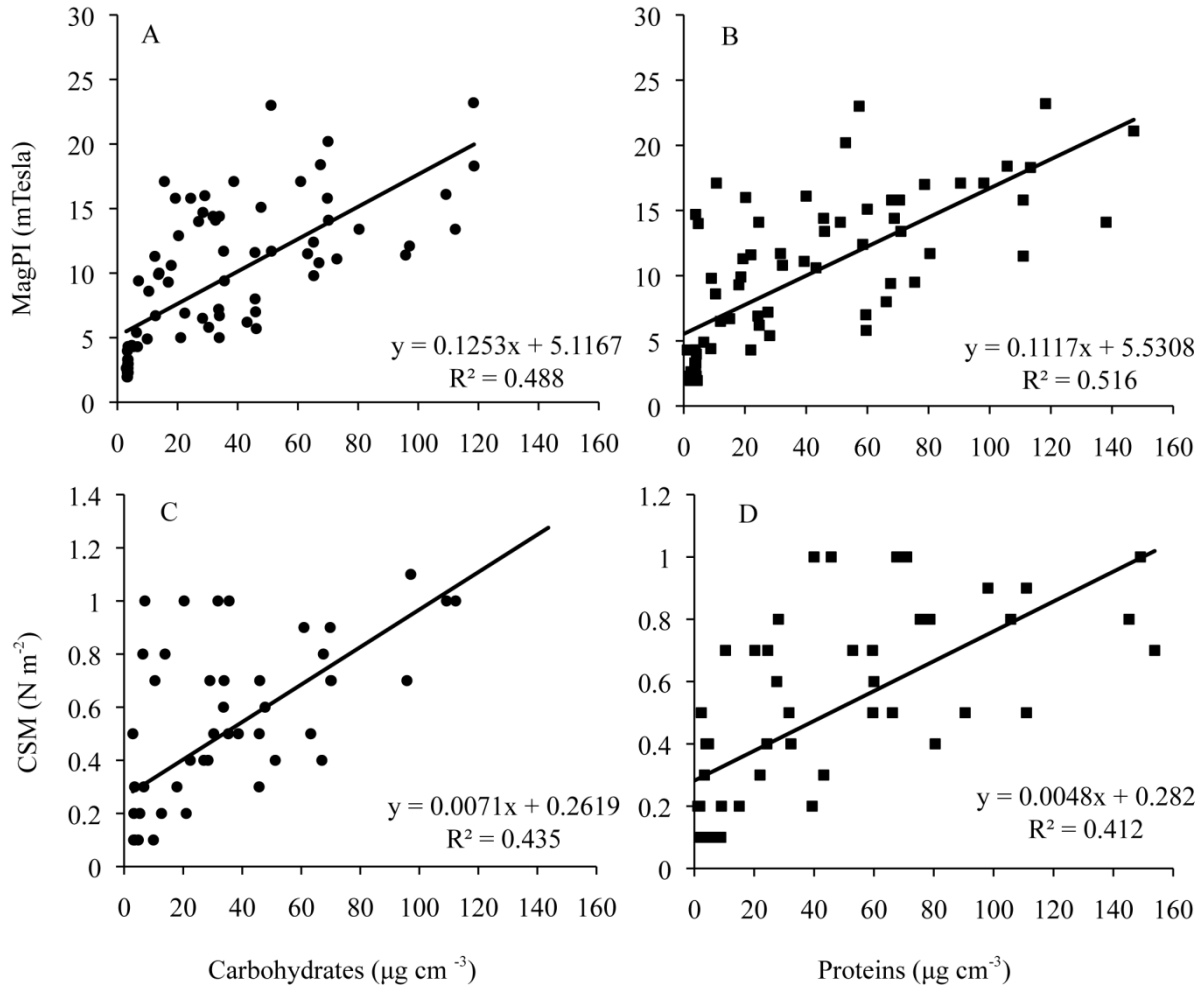

Figure 24: *Relations between biofilm adhesion and sediment stability (MagPI, CSM) and EPS components. A-B: The relations between surface adhesion (MagPI) and EPS carbohydrates and proteins concentrations. C-D: The relations between substratum stability (CSM) and EPS carbohydrates and proteins concentrations. Source: Lubarsky et al. 2010 PLoS ONE.*

Table 8: *Pearson's correlation coefficients between surface adhesion (MagPI), substratum stability (CSM), EPS carbohydrates as well as EPS proteins in the different treatments with the significance levels: *** p<0.001. ** p<0.01. * p<0.05. Source: Lubarsky et al. 2010 PLoS ONE.*

Treatments	***Techniques***	***Carbohydrates***			***Proteins***		
Diatom	MagPI	0.882	17	***	-0.189	21	
	CSM	0.869	11	***	0.321	15	
Bacteria	MagPI	0.861	15	***	0.770	14	**
	CSM	0.753	9	*	0.902	10	***
Bacteria+ Diatom	MagPI	0.706	15	**	0.741	15	**
	CSM	0.617	12	*	0.494	12	*

IV.5. DISCUSSION

IV.5.1. BIOSTABILIZATION BY MICROBIAL ASSEMBLAGES FROM ESTUARINE SEDIMENTS

This study has shown impressive biostabilization of non-cohesive material by microbial assemblages, as determined by Magnetic Particle Induction (MagPI) and Cohesive Strength Meter (CSM). These devices determine slightly different surface properties of the test bed. With MagPI, an increase in adhesion (a proxy for particle capture potential and interface stability) was determined from day 1 onwards in all microbial assemblages. MagPI does not require the erosion of the surface and therefore is a repeatable, sub-critical stress measurement with a high sensitivity that has been shown suitable for measuring the surface properties of young, developing biofilm. The CSM is a well-established device to measure erosion resistance; it requires bed failure and can operate over a range of values beyond that of most linear flumes. The CSM is not designed to mimic the processes of natural erosion since the eroding pressure is perpendicular to the bed but provides an accepted relative measure of surface stability. It also requires a surface that has some initial resistance to erosion or the lightest jet pulse causes a 10% reduction in transmission, and therefore it is not as sensitive as MagPI for highly unconsolidated systems. However, these devices were found to complement each other, increasing the range of measurements that could be made and showed a strong correlation in the overlapping portion of the data (R^2=0.62, $p<0.001$).

IV.5.2. THE INDIVIDUAL AND COMBINED ENGINEERING CAPABILITY OF MICROBIAL ASSEMBLAGES

The comparison of pure bacterial, axenic microalgal and mixed (bacteria + microalgae) assemblages was designed to provide insights into the individual and combined functional capacity of the heterotrophic and autotrophic biofilm components in terms of substratum properties. While this is a limited suite of measurements, they demonstrate

the functional development of these assemblages in a new light. Bacterial assemblages stabilized the substratum significantly more than axenic microalgal assemblages (x2). This work supported earlier findings (Gerbersdorf *et al.*, 2009) but are in contrast to most of the literature (Yallop *et al.*, 2000; Lundkvist *et al.*, 2007a), where the contribution of bacteria to sediment stabilization is usually regarded as less significant or even negligible as compared with diatom assemblages. Separation of the influence of component assemblages of bacteria and diatoms in nature is problematic. Our approach was to use assemblages derived from natural systems but manipulated to create the segregation of bacteria and diatoms. We used a mixture of antibiotics to inhibit bacterial growth and we understand there are some potential problems with this. Chloramphenicol has been reported to suppress the growth of microalgae in general and diatoms in particular (Campa-Córdova *et al.*, 2006; Lai *et al.*, 2009). It is also known that some microalgae, among them diatoms, require an association with bacteria to thrive (Fukami *et al.*, 1997; Guerrini *et al.*, 1998; Grossart & Simon, 2007; Bruckner *et al.*, 2008; Levy *et al.*, 2009). In this study, the microalgal biomass was significantly lower in the axenic diatom assemblage (D) as compared to the assemblage associated with bacteria (BD) which may be an indication of antibiotic treatment effects or the influence of bacteria/diatom association. In contrast, the bacterial growth in the pure culture without microalgae was good.

It was first hypothesized that the grouping of bacteria and diatoms in the mixed assemblages might result in synergy in community EPS secretion and therefore substratum stabilization. The first of these concepts is supported by the data in terms of EPS carbohydrate production but not for EPS protein production. However, the synergism in EPS carbohydrate was not reflected in surface stability by either method of determination (MagPI, CSM). While the adhesive capacity and the cohesion of the test

surfaces were significantly higher in the mixed assemblage, the differences against the pure cultures were less than expected. This may be because the shape of the relationship between EPS concentration and surface stability is not linear and may reach an asymptote as EPS increases. This makes logical sense since by adding more EPS the strength of the surface cannot increase beyond the fundamental binding capacity of the polymer. The improved binding by the mixed culture may reflect the contribution of different types of EPS with varied properties and the nature of the micro-spatial arrangement of the EPS deposited by bacteria (largely attachment to grains) and diatoms (mainly for locomotion) (Figure 25).

It is often suggested that diatom growth and EPS secretion is promoted by nutrient recycling by bacteria (Guerrini *et al.*, 1998; Elifantz *et al.*, 2005; Klug, 2005; Grossart & Simon, 2007). Over the first ten days of the experiment, the greater growth of microalgae in the natural assemblage, as compared to the axenic microalgal culture, seemed to support this possibility. However, with time, the microalgal biomass decreased to comparable levels in both treatments. Furthermore, the microalgal community composition was quite similar over time in both biofilm and thus gave no support to the suggestion of selection or inhibition of microalgae by these bacteria. The natural and axenic microalgal assemblages were both dominated by typical poly- to hypertrophic species found in fresh-brackish waters. In the last week of the experiment, species diversity declined similarly in both biofilm until only small *Navicula* species remained suggesting laboratory conditions were not ideal (Defew *et al.*, 2002). Surprisingly, the bacterial cell numbers, along with the bacterial division rates, were significantly lower in the mixed assemblage as compared to the pure bacterial culture. In the literature, it is reported that bacteria development is often concomitant with benthic microalgae (Bowen *et al.*, 2009) and they adapt quickly to the different organic

microalgal exudates with substrate-specific responses regarding enzyme activity, usually resulting in compositional shifts and stimulated bacterial growth and metabolic activity (Schäfer *et al.*, 2002; Haynes *et al.*, 2007). However, the bacteria consortia that developed in our systems did not seem to profit from the presence of diatoms. There is a possibility that the diatoms actively suppressed the bacteria since it is known that marine bacteria are very sensitive to polyunsaturated aldehydes (PUAs) produced by a range of microalgae species (Wichard *et al.*, 2005; Ribalet *et al.*, 2008). This possibility requires further study in benthic systems. However, it is perhaps more likely that we observed a selection/adaptation process as the natural microbial biofilm adapted to culture conditions, and populations capable of co-existing or exploiting algal/bacterial species were promoted, as has been shown for floodplains and estuaries (Boivin *et al.*, 2007; Haynes *et al.*, 2007). Indeed, the bacterial community showed pronounced compositional shifts with the presence of diatoms during the experiment. While the gram-negative Proteobacteria constituted the majority of the bacterial community, the percentage of α, β, γ-Proteobacteria changed over time. Members of α-Proteobacteria as well as the *Cytophaga-Flavobacterium-Bacteroides* (CFB) phylum have been identified as “satellite bacteria” for marine diatoms (Schäfer *et al.*, 2002). Interestingly, α-Proteobacteria were more prominent in the mixed assemblage than in the bacterial culture, although the absolute increase over time was similar in the two relevant treatments. However, the hybridization to the CFB phylum did not increase over time in the mixed assemblage. β-Proteobacteria decreased in both treatments, but this was more pronounced in the natural assemblage where the presence of diatoms might have been a factor. The γ-Proteobacteria increased solely in the bacterial assemblages and remained unchanged in the mixed biofilm, and thus seem to have a lesser prominence

in the presence of diatoms. Hence, the composition of the bacterial assemblage was responsive to the presence of diatoms.

IV.5.3. THE EPS MATRIX - KEY TO SUBSTRATUM STABILIZATION?

It has generally been reported that diatoms secrete mainly polysaccharide EPS while bacteria secrete a greater proportion of proteins in their EPS (Flemming & Wingender, 2001a, 2002). This is supported by the significantly higher carbohydrate concentrations in the axenic microalgal assemblage as opposed to the bacterial biofilm. Despite this, the stabilization effect of the bacterial assemblage was significantly higher than in the microalgal biofilm, although the EPS protein concentrations were quite similar. This strongly suggests that EPS quantity *per se* cannot be predictive of substratum stabilization. The ecological function of the microbial EPS secretion has to be considered: for instance, bacteria attach firmly to a substratum with the help of EPS while diatoms secrete EPS for locomotion (Edgar & Pickett-Heaps, 1983) and only few species stay put by stalks (e.g. *Achnanthes* spec.) (Chiovitti *et al.*, 2008; Willis *et al.*, 2013). Thus, it seems logical to suggest that the EPS secreted by bacteria and diatoms must generally differ in their characteristics and mechanical properties.

These variations in EPS rigidity and robustness secreted by different taxa/species might explain the unexpectedly greater stabilization capability of bacterial cultures as compared to the axenic diatom cultures - despite similar proteins and higher carbohydrate quantities in the latter. The axenic diatom cultures were indeed dominated by smaller highly mobile species of *Navicula* in contrast to the initial dominance of stalk-building sessile *Achnanthes* in the mixed assemblage. Since the mixed assemblage had the highest all overall higher stabilization potential this functional effect might be related to the different EPS binding structures.

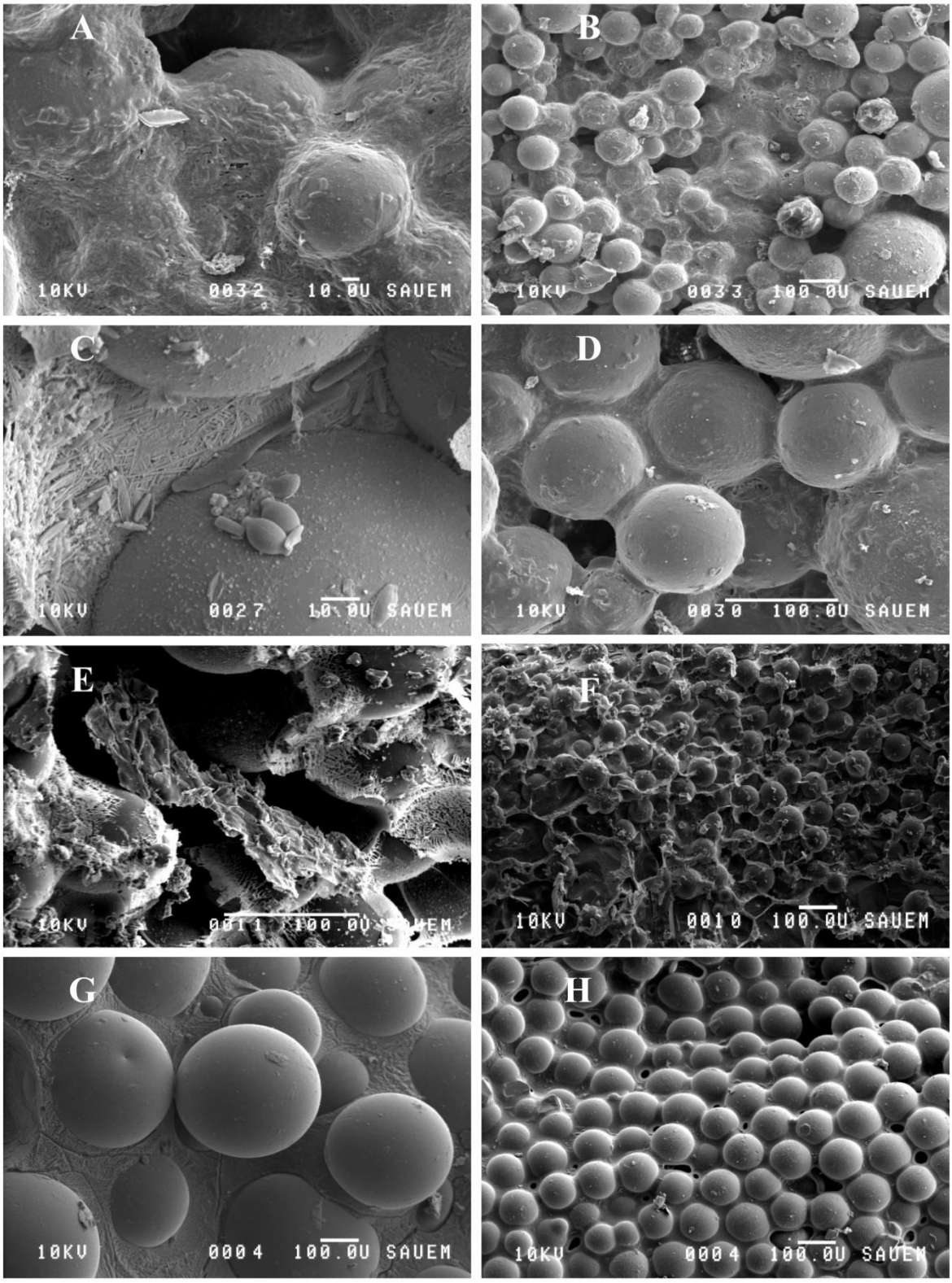

Figure 25: *Low-temperature scanning electron microscope images using different magnifications. A-B: The mixed assemblages bacteria + diatom. C-D: The diatom treatment. E-F: The bacteria treatment. G-H: The control substratum. Frozen water (ice) on the surface produces a solid matrix around the glass beads in the controls. In the other treatments with microorganisms, the EPS matrix is visible, heavily covering the glass beads and permeating the intermediate pore space. Source: Lubarsky et al. 2010 PLoS ONE.*

Nevertheless, highest biostabilization in the mixed assemblage also coincided with significantly higher quantities of microbial produced colloidal EPS carbohydrates and EPS proteins as compared to the other treatments (Figure 25).

Although our initial hypothesis of synergistic effects in a combined prokaryotic and eukaryotic biofilm community in terms of stability was not supported, the functional capacity for adhesion and cohesion by the liaison between bacteria and microalgae was still impressive. This biostabilization is an important “ecosystem service” since it affects processes beyond the biofilm, such as nutrient fluxes, pollutant retention and sediment erosion/transport.

IV.6. CONCLUSIONS

The stabilization of the substratum by estuarine microbial assemblages was due to the secreted EPS matrix, and both EPS concentrations (quantity) and EPS components (quality) were important. In this context, it became again apparent that EPS proteins play a more crucial role for adhesion/cohesion of the substratum than previously thought. Bacterial assemblages had a significantly higher stabilization potential as compared to the axenic microalgal cultures. The explanation is probably in the conformation of the polymeric matrix and may reflect the functional roles (attachment, movement) that the EPS provides. The mixed assemblages were more stable than either community on its own and this suggests both assemblages have an important role in substratum stabilization and are more effective together. The tendency in the literature to exclude the contribution of bacterial EPS to sediment stability in the field should be re-addressed and the importance of bacterial assemblages recognized.

V. The Significance and Seasonality of Biostabilization in Freshwaters

V.1. Abstract

The stabilization of fine sediments via biofilm ('biostabilization') has various economic and ecological implications but has been long unaddressed within lotic waters. To investigate natural biofilm growth and functionality in freshwater sediments under controlled boundary conditions, a unique mesocosm was constructed and tested that combines established know-how from engineering and natural sciences and consists of six straight flow-through flumes.

Over three consecutive years, six long-term experiments were performed with fluvial water under identical boundary conditions over different seasons. Highest biofilm adhesion and biostabilization occurred during spring (in average 8-10 and 3-5 times greater than during autumn and summer, respectively) and coincided with highest EPS production - especially extracellular proteins indicating the essential role of adhesive proteins for substratum stability. Furthermore, not biomass but microbial community composition and the life-style of the dominating species differed significantly between seasons to result in mechanically highly diverse biofilm. These findings emphasize the importance to link insights into the microbial community and EPS matrix to functionality, here biostabilization.

The unique mesocosm allows comparable biofilm growth under controlled natural-like conditions - an important requisite for future research on the impact of biostabilization for ecosystem functioning at varying environmental scenarios. The first data demonstrated the importance of microbial biostabilization for fine sediment dynamics in freshwaters and their seasonality - both of which has implications for future modeling and management strategies of riverine sediments.

V.2. BACKGROUND

In contrast to limnic systems, biostabilization has been extensively investigated within the marine and brackish environment, which revealed a high microbial binding capacity within fine sediments. For example, Tolhurst et al. (1999) reported a five-fold increase of critical bed shear stress in an intertidal flat colonized by diatoms as compared to bare sediments. The dynamics of fine sediments is not just important for the transport of suspended material in intertidal zones and for coastal erosion processes, but also essential for the bioavailability of associated pollutants as well as for maintaining waterways, dams and harbours. Consequently, knowledge on biostabilization potential is crucial in freshwaters too, but it was long believed that it might be of minor importance due to the lack of high ion concentrations to stabilize microbially-induced polymeric binding (Spears *et al.*, 2008). This chapter is about addressing biostabilization in freshwaters for the first time.

That again requires a sophisticated setup which, ideally, combines the advantages of field (natural relevance) and laboratory (controlled reproducible settings) measurements while teaming engineering and biological expertise. Hence, a novel mesocosm has been developed that consists of six straight flow-through flumes with unique features: (1) the flume dimensions guarantee fully developed turbulence, uniform water flow and constant discharge as important requirements in hydraulic research; (2) the inoculation and development of biofilm from natural water on natural-like substratum minimizes behavioural artefacts of the microorganisms as a response to a more artificial physical environment and (3) microbial growth and development can be linked to biofilm functionality, here biostabilization as one important ecosystem service. The mesocosm has been tested in a first experiment for its suitability, namely whether biofilm grown in different parts of one single flume as well as in different flumes, and at the same

conditions, are representative despite the well-known heterogeneity of biofilm and natural water.

Five long-term experiments then served to unravel the influence of abiotic conditions; the focus of this chapter is on seasonality effects in biostabilization as they have been reported from intertidal flats. For instance, Widdows et al. (2000) determined a varying biostabilization capacity over the course of one year with higher values in June as compared to September. *In situ* measurements in the Venice Lagoon by Amos et al. (2004) confirmed that bed strength in summer exceeded winter stability up to five times. It is well-known that seasonal shifting abiotic environmental parameters such as temperature, nutrients or underwater light intensity have a significant impact on the biocoenosis resulting in clearly visible succession processes within the benthic biofilm (Gamier *et al.*, 1995; Sekar *et al.*, 2004; Lyautey *et al.*, 2005). While knowledge of this seasonal effect upon benthic and biofilm organisms is steadily increasing (Coma *et al.*, 2000; Olapade & Leff, 2004; Moss *et al.*, 2006) and some implications for biofilm functionality (e.g. on aquatic food webs) have been studied (Yoshioka *et al.*, 1994; Power *et al.*, 2008), the link to biostabilization of fine sediments is still to be examined.

In the experiments, one focus was on the structures and mechanical properties that biofilm-stabilized sediments develop since this is an important prerequisite for a unifying equation to predict erodibility (Grabowski *et al.*, 2011). Unfortunately, very little information is available on the relation between environmental conditions and the mechanical structure of the biofilm/sediment matrix and its response to increasing bed shear stress. One exception is Vignaga et al. (2013) who investigated cyanobacterial mats exposed to increasing bed shear stress and compared their mechanical behaviour to an elastic, oscillating membrane that suddenly fails.

Altogether, the intention of this chapter is to (1) test the novel mesocosm developed (2) prove the significance of biostabilization in lotic freshwaters (3) investigate the seasonality of microbially-induced sediment stability and (4) to address the mechanical processes and erosional pattern of the biofilm-substratum tandem while combining biological and engineering science.

V.3. Experimental Settings

V.3.1. Mesocosm: six straight Flumes with own Circuit

The mesocosm consists of six straight identical glass flumes, each with an individual, separate water and cooling circuit, regulated discharges, and adjustable light intensities (Thom *et al.*, 2012, 2015). Two containers encase three flumes each to avoid any possible contamination and the influence of ambient light (Figure 26). The individual flumes (l x w x h = 3.00m x 0.15m x 0.15m) provide an inlet flow section and a biofilm cultivation section. The design allows a homogeneous fully-turbulent flow field and constant shear stress across the biofilm growth section (length 1.32m). This section contains 16 cartridges (l x w x h = 0.08m x 0.06m x 0.02m) fitted into PVC frames that are planar with the flume bottom to ensure minimal disturbance of the hydraulic regime. The cartridges are filled with glass beads as an artificial non-cohesive substratum in the sizes of 100-200µm diameter (Mühlmeier, Germany), which is well in the range where binding forces of EPS can dominate gravitational forces (Fang *et al.*, 2014). The cartridges can be taken out of the flume for further measurements.

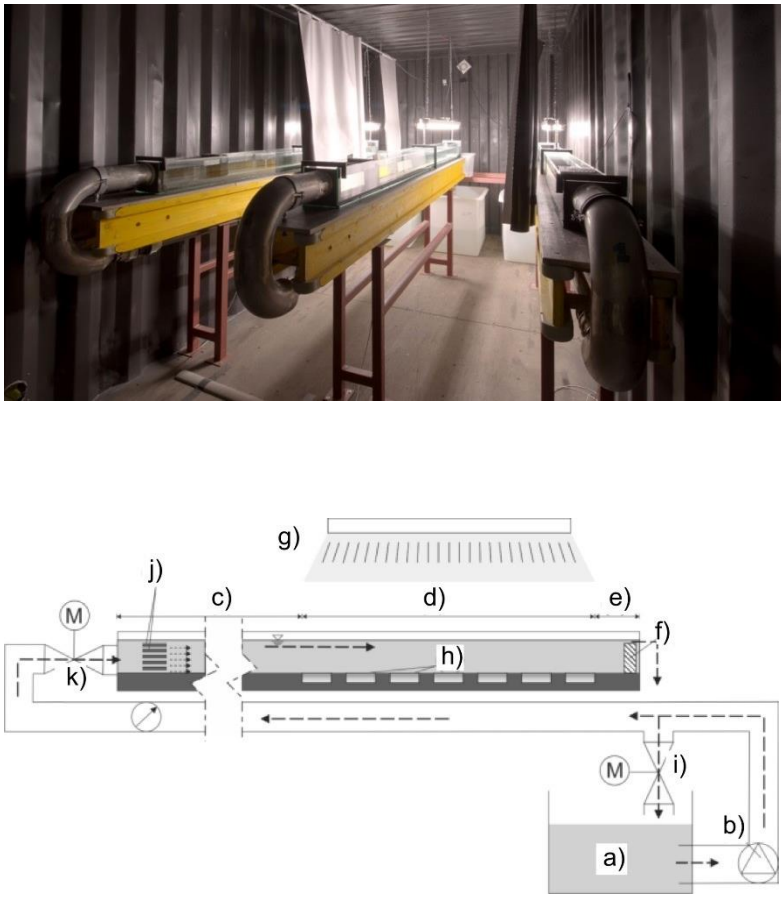

Figure 26: *Experimental setup. Top: image of three equivalent straight flumes installed in one container. Bottom: schematic image of one straight flume with (a) outflow tank, (b) pump, (c) inlet flow section with baffles, (d) biofilm cultivation section, (e) outlet flow section, (f) weir, (g) fluorescent tubes, (h) sediment cartridges, (i) bypass, (j) current abatement, and (k) fine-tuning valve. Source: Thom et al. 2012 Wasserwirtschaft.*

V.3.2. CONTROL OF TEMPERATURE, LIGHT INTENSITY AND HYDRODYNAMICS

The water temperature that is vital for biological processes was kept at 15°C ± 0.3°C (for comparison: mean water temperature in the River Enz: during spring 9°C, during summer 14-20°C and during autumn 12°C) by heat exchangers supplied with colder water (8°C). This initial temperature is needed to compensate for the additional heating by the activity of the pumps.

Cartridges were illuminated by two parallel fluorescent tubes (Osram Biolux; 480–665nm). The distance of these light sources to the sediment surface was adjustable resulting in different illumination intensities with 8/16 hours day/night cycle for the

sediment and biofilm surface. Homogenous irradiation over the whole growth section was confirmed by measurements of light intensity and wavelength irradiance of the photosynthetic active radiation (PAR) spectrum using a high resolution spectroradiometer (SR-9910, Macam Photometric Ltd., Livingston, Scotland) (Gerbersdorf & Schubert, 2011). During the experiments, both darkness and two different light intensities were established according to Table 9 (left column) to mimic natural illumination in various niches.

Table 9: *Boundary conditions applied in the experiments.*

	Light intensity [µmol m^{-2} s^{-1}]	**Bed shear stress [Nm^{-2}]**
Low	0	0.02
Medium	50	0.04
High	100	0.08

As the hydrodynamic regime controls two important parameters for biofilm formation, namely mass transfer and drag forces (Stoodley *et al.*, 1999a; Stewart, 2012), special attention was paid to the establishment of well-defined hydraulic boundary conditions. Since near-bed mass transfer (of e.g. nutrients to the biofilm surface) is primarily driven by turbulence (Nikora, 2010), direct measurements of the flow velocity components and calculated fluctuations were conducted using a LDA system (Laser Doppler Anemometry, Coherent, USA) at different positions while applying various discharges and a constant water level (due to the relatively low discharges the flow can be assumed to be uniform in the following considerations). The turbulent shear stress (τ) can be calculated as the time-averaged product of velocity fluctuations (after Reynolds decomposition, in longitudinal (v'_s) and normal (v'_n) directions) from the mean velocity multiplied with the fluid density:

$$\tau = -\rho \cdot \overline{v'_s \cdot v'_n} \qquad [Nm^{-2}]$$

To determine the bed shear stress (τ_{bed}) in the flumes, the turbulent shear stresses measured at 5, 6, 8, and 10mm height above the bed were averaged. As τ_{bed} was constant in the rearward-half of the flumes, fully-turbulent conditions are assumed here. Consequently, the biofilm growth section including the cartridges and illumination was placed into this area. Reproducibility of the hydraulic boundary conditions in all flumes was confirmed by ADV (Acoustic Doppler Velocimetry, Sontek, USA) measurements.

The following empirical relationship was established to describe the relation between the discharge Q [L s^{-1}] (regulated adjusting the by-pass and continuously measured by a flow meter from Buerkert 8030, Ingelfingen, Germany) and the bed shear stress τ_{bed} [Nm^{-2}] over the biofilm growth section (R^2=0.9968):

$$\tau_{bed} = 0.00119 \cdot Q^2 + 0.0079 \cdot Q \ [Nm^{-2}]$$

The three levels of τ_{bed} that were applied during the experiments are listed in Table 9 (right column). It is important to note that the investigations were solely carried out at turbulent conditions since laminar flow can rarely be found in a natural stream. Since light intensities and -quality may vary at different water depths, the water level is kept constant (8.1cm) in the setup, i.e. in all flumes and at different discharges. This is achieved by deploying weirs positioned at the end of the flumes that are adapted to the designated discharges by varying their height.

V.3.3. BIOFILM CULTIVATION

1.2m^3 of natural freshwater was taken from the River Enz (county of Baden-Württemberg, Germany, 48°56'0.63''N 8°55'3.54''E), transported to the laboratory, filtered (removing larger particles) and transferred well-mixed into the outflow tanks of the flumes. While adjusted to constant temperature (15.0°C ± 0.3°C) by the cooling

water circuit, 200L were circulated in each flume by a circulatory pump (BADU Eco Touch, Speck Pumpen, Neunkirchen am Sand, Germany) for the duration of one experiment. Thus, indigenous microorganisms within the river water eventually settled on the substratum surface (=inert glass beads of a diameter of 100–200µm) to form a biofilm over the following days and weeks. The abiotic conditions mimicked natural settings in terms of temperature, nutrients (no further addition), oxygen, light and hydrodynamics (see above).

V.3.4. EXPERIMENTS AND SAMPLING

Within three consecutive years, six long-term experiments were conducted from spring to autumn to test the influence of seasonality as well as underwater light intensity (LI) and bed shear stress (BSS) (see also chapter VI. and overview in Table 10). While the first experiment served for a detailed inter–and intra-flume comparison during biofilm cultivation at identical boundary conditions (Schmidt *et al.*, 2015), the other five experiments varied in light or flow conditions. Thereby, always one pair of flumes was exposed to the same settings which allowed for three different treatments in the six flumes available. The treatment differed in either LI or BSS adjusted to three different levels, hereinafter described as “low”, “medium” and “high” (see Table 9), while the other was kept constant in all six flumes („medium“ in terms of light, „low“ in terms of flow). Consequently, in each experiment always two of the flumes were run at identical conditions of (medium) light and (low) flow velocity: 50µmol $m^{-2}s^{-1}$ in an 8/16 hours day/night circle and a discharge of 0.80 ± 0.10L s^{-1} resulting in a flow velocity of 0.07 ± 0.008m s^{-1}. From these flumes, the data that were gained during the six experiments served as the basis for the season comparison as presented in this chapter.

Table 10: *Overview over the performed experiments with BSS = benthic shear stress and LI = light intensity. Source: Schmidt 2017 PhD Thesis University Stuttgart. Note: in March 2013 there was one additional experiment on varying BSS (low, medium, high) which were only sampled for SETEG data without biochemical analysis.*

Experiment	Duration	Flume	BSS	LI	Sampling days
"August12"	01.08.–28.08.2012	1	low	medium	4, 7, 11, 14, 18, 21, 25, 28
		2			
		3			
		4			
		5			
		6			
"May"	30.04.–07.06.2013	1	high	medium	4, 7, 11, 14, 18, 21, 25, 28, 32, 35
		2	medium		
		3	low		
		4	low		
		5	medium		
		6	high		
"July"	28.06.–06.08.2013	1	low	low	4, 7, 11, 14, 18, 21, 25, 28, 32, 35
		2		medium	
		3		high	
		4		low	
		5		medium	
		6		high	
"August"	23.08.–30.09.2013	1	low	high	4, 7, 11, 14, 18, 21, 25, 28, 32, 35
		2		medium	
		3		low	
		4		high	
		5		medium	
		6		low	
"November"	22.11.–20.12.2013	1	medium	medium	4, 7, 11, 14, 18, 21, 25, 28
		2	low		
		3	high		
		4	high		
		5	low		
		6	medium		
"March"	18.03.–29.04.2014	1	low	medium	4, 7, 11, 14, 18, 21, 25, 28, 32, 35, 39
		2		high	
		3		low	
		4		medium	
		5		high	
		6		low	

Sampling of the biofilm and water in the flumes took place on days 4, 7, 11, 14, 18, 21, 25, 28 during all experiments; additional samples were taken on days 32, 35 and 39 during “May”, “July”, “August” and “March” and again on day 42 during “March”. The previous study performing detailed inter–and intra-flume comparisons (Schmidt *et al.*, 2015) displayed no significant differences in biofilm features such as biomass, EPS contents or composition of the microbial community, but showed that the well-known patchiness and heterogeneity of biofilm on the microscale (Battin *et al.*, 2007) should be addressed when sampling. Therefore, at each sampling day, mini-cores of biofilm-substratum samples were withdrawn by using a 2mL cut-off syringe (diameter 0.01m) and the material of one cartridge was pooled afterwards to obtain representative results. From this pooled material, subsamples were taken for biochemical and microbiological parameters (1.0cm^3 for chlorophyll a and 0.5cm^3 for all other analyses) and transferred into centrifuge tubes (15ml) or Eppendorf tubes (2ml) for chlorophyll a and all other biochemical analyses, respectively. In this context, samples/cartridges from single flumes exposed to the same treatment were considered as statistical replicates. Hence, the total number of replicates (n) was a result of multiplying the number of cartridges in all flumes with comparable settings and combining them for corresponding seasons; either separated by days or incorporating all different sampling times. For chemical analyses, additionally 1L of water was collected from the flumes.

The analyses to be conducted were: EPS carbohydrates, EPS proteins, bacterial cell numbers, bacterial community composition, chlorophyll/pheophytin, and diatom community composition (see II.2 and II.3). Additionally, the concentration of ammonia and chloride ions in the water samples was analyzed according to DIN 38406-E5-1 and DIN EN ISO 10304, respectively. Moreover, a quick test (Hach Lange GmbH, Berlin, Germany) was used to determine the concentrations of nitrate, phosphate, fluoride and

sulfate ions (detection limits: nitrate 1mg l^{-1}, phosphate 0.1mg l^{-1}, fluoride 0.1mg l^{-1} sulfate 5.8mg l^{-1})*.*

In parallel to the sampling, biofilm adhesion and substratum stability were determined with Magnetic Particle Induction (MagPI) and within the SETEG flume, respectively; both methods are described in detail in II.4. For the MagPI results, the focus was on the data gained by threshold 3 named “T3” hereafter (II.4.).

V.4. RESULTS

V.4.1. WATER CHEMISTRY

Water samples were tested thoroughly for nutrients during the entire experiment I. The nutrient concentrations were constant over the experimental time and, except for nitrate, at the detection limit (according to LAWA 1998): phosphate < 0.2mg L^{-1}, ammonium and nitrate approx. 0.04 ± 0.03 and 2.9 ± 0.1mg L^{-1}, respectively, and sulphate with 48.1 ± 0.4mg L^{-1}. Concentrations of fluoride and chloride were below 0.2 and around 58.7 ± 0.7mg L^{-1}, respectively. The nutrient concentrations continued to be low without proof of exhaustion during the other experiments.

V.4.2. INTER- AND INTRA-FLUME COMPARISON IN EXPERIMENT I

Comparison of the data from experiment I on biochemical analysis, microbial biomass and surface adhesiveness (T3) showed no significant difference neither between the different regions within one flume nor between the different flumes (Table 11, Table **12**, Table 13). Due to pump failure and flow stagnation in the sixth flume during the first week, this flume was excluded from inter-flume comparison (Table **12**) but still served for intra-flume comparison (Table 11).

Table 11: *Intra-flume comparison. Mean values of EPS (carbohydrates and protein), chlorophyll a contents (n=144), bacterial cell counts (n=24) and surface adhesiveness (n=162) from six flumes combined for each region over the whole experimental time (with STDev). Source: Schmidt et al. 2015 ESEU.*

Flume region	Carbohydrates (µg*gDW^{-1})	Proteins (µg*gDW^{-1})	Chlorophyll (µg*gDW^{-1})	Bacterial cells (10^{7}*gDW^{-1})	Adhesiveness (mA)
Front	27.9 ± 12.5	2.4 ± 1.6	1.3 ± 1.6	1.5 ± 0.8	618 ± 99
Middle	27.3 ± 14.7	2.9 ± 2.2	1.4 ± 1.7	1.6 ± 0.9	603 ± 115
Back	27.0 ± 13.3	2.9 ± 2.1	1.4 ± 1.8	1.7 ± 1.0	599 ± 104

Table 12: *Inter-flume comparison. Mean values of EPS (carbohydrates and protein), chlorophyll a contents (n=120), bacterial cell counts (n=40) and surface adhesiveness (n=135) from each of the five flumes over the whole experimental time (with STDev). Source: Schmidt et al. 2015 ESEU.*

Flume	Carbohydrates (µg*gDW^{-1})	Proteins (µg*gDW^{-1})	Chlorophyll (µg*gDW^{-1})	Bacterial cells (10^{7}*gDW^{-1})	Adhesiveness (mA)
1	23.1 ± 9.9	2.0 ± 1.7	1.1 ± 1.0	2.2 ± 1.7	630 ± 107
2	26.5 ± 11.2	2.7 ± 1.2	1.0 ± 1.0	1.9 ± 1.7	600 ± 96
3	25.5 ± 8.2	3.1 ± 1.6	1.4 ± 1.5	1.9 ± 1.0	558 ± 91
4	31.0 ± 16.5	2.5 ± 2.0	1.6 ± 2.1	2.0 ± 1.4	623 ± 132
5	32.7 ± 18.0	3.4 ± 3.0	2.1 ± 2.5	1.5 ± 0.9	623 ± 88

Table 13: *Results of the Kruskall-Wallis tests. Intra-flume and inter-flume comparisons of the measured data that indicated no significant differences. Source: Schmidt et al. 2015 ESEU.*

Comparison	Carbohydrates	Proteins	Chlorophyll	Bacterial cells	Adhesiveness
Intra-Flume	p=0.8203 (n=144[1])	p=0.5865 (n=144)	p=0.9492 (n=144)	p=0.8540 (n=24[2])	p=0.7670 (n=162[3])
Inter-Flume	p=0.3364 (n=120[4])	p=0.1223 (n=120)	p=0.5432 (n=120)	p=0.9522 (n=40[5])	p=0.0631 (n=135[6])

[1]: 3 regions * 6 flumes * 8 sampling points; [2]: 3 regions * 1 flume * 8 sampling points
[3]: 3 regions * 6 flumes * 9 sampling points; [4]: 3 regions * 5 flumes * 8 sampling points
[5]: 1 region (middle) * 5 flumes * 8 sampling points; [6]: 3 regions * 5 flumes * 9 sampling points

V.4.3. THE BIOFILM EPS MATRIX AND MICROBIAL BIOMASS OVER TIME

For this aspect, only the data from the flumes that were run at identical conditions of (medium) light and (low) flow velocity during the six experiments were considered and

pooled for the matching seasons such as spring (two experiments), summer (three experiments), autumn (one experiment); either separated for the single days of growth or combining all sampling times. For EPS, mean carbohydrate contents displayed fluctuating values in all experiments. While increases over time (not significant) were detected in each experiment during spring and summer, autumn biofilm showed approximately stable EPS carbohydrate content. In contrast, a significant increase in EPS protein content (KWT: p=0.0041; n=45) from 2.9 ± 0.6µg gDW^{-1} on day two to 27.6 ± 7.4µg gDW^{-1} on day 28 was detected during spring, but neither summer nor autumn showed a significant rise (Figure 27). Biofilm chlorophyll a content increased over time in each season; this was highly significant for spring and summer (KWT: spring: p=0.0010; n=45; summer: p< 0.0001; n=44) and a strong trend was observed in autumn (KWT: p=0.0488; n=16). On day 28, mean chlorophyll a content reached 2.3 ± 0.3µg gDW^{-1} during spring, 2.6 ± 0.7µg gDW^{-1} during summer and 1.4 ± 0.3µg gDW^{-1} during autumn. Bacterial cell counts (BCC) also increased significantly during spring and summer (KWT: spring p=0.0233; n=20; summer p=0.0156; n=20) and showed a similar trend during autumn (KWT: p=0.0611; n=16) (data not shown). This resulted in mean BCC value of 2.3 ± 1.2 x $10^7 gDW^{-1}$ during spring, 4.3 ± 1.6 x $10^7 gDW^{-1}$ during summer and 1.8 ± 0.8 x $10^7 gDW^{-1}$ during autumn on day 28.

V.4.4. Biofilm Adhesiveness, Substratum Stability, mechanical Failure Types

In accordance with the chlorophyll a contents, biofilm adhesiveness showed two distinctly different developmental phases manifesting in a significant difference between early (until day 18) and later biofilm growth stages (from day 21 onwards; Figure 27). Adhesiveness (T3) showed a highly significant increase during spring and summer (KWT: spring: p< 0.0001; n=45; summer: p< 0.0001; n=44) and a similar trend in autumn (KWT: p=0.0547; n=16). However, maximal mean values were clearly different:

in spring mean T3 was 543.3 ± 102.3mA on day 28, while it was 263.9 ± 49.8mA in summer and 78.4 ± 18.8mA in autumn (Figure 27). Considering only the mean values, the adhesion was in spring up to eight times and five times higher as compared to autumn and summer, respectively. Altogether, the biostabilized substratum showed an impressive increase in adhesion as compared to the abiotic control - for instance up to 25 times in the spring experiments.

The critical shear stress determined in the SETEG flume gave similar results: firstly, the two distinct stages were confirmed with no or low changes over the first two weeks, followed by a significant increase hereafter; secondly, the biostabilization reached highest values in spring followed by summer and autumn (Figure 28). The calculated biostabilization indices (after Manzenrieder 1985: ratio between critical bed shear stress of biostabilized bed and the abiotic reference which was here 0.23 Nm^{-2}) were the following: up to 10 in spring, around 3 in summer and with a maximum of 1.5 in autumn.

In the first days of the experiments, before the biofilm growth influences the mechanical behaviour, the entrainment mechanism is predominantly covered by the movement of individual particles as bed load (characteristic for abiotic non-cohesive sediments). However, in later stages, the direct visual observations of each individual erosion process revealed two dominant types of biofilm-influenced entrainment: (a) crust-like erosion with smaller aggregates that are released subsequently and (b) elastic carpet-like erosion where the biofilm rolls off and leaves the bare substratum exposed (see Figure 29 for an illustration). The crust-like erosion type has been commonly observed over all seasons while linked to a wide range of bed stabilities. In contrast, the carpet-like erosion has been detected mainly in spring (but also in summer) related to more pronounced biostabilization. Hence, these two types seemed related to varying microbial community composition and substratum stability.

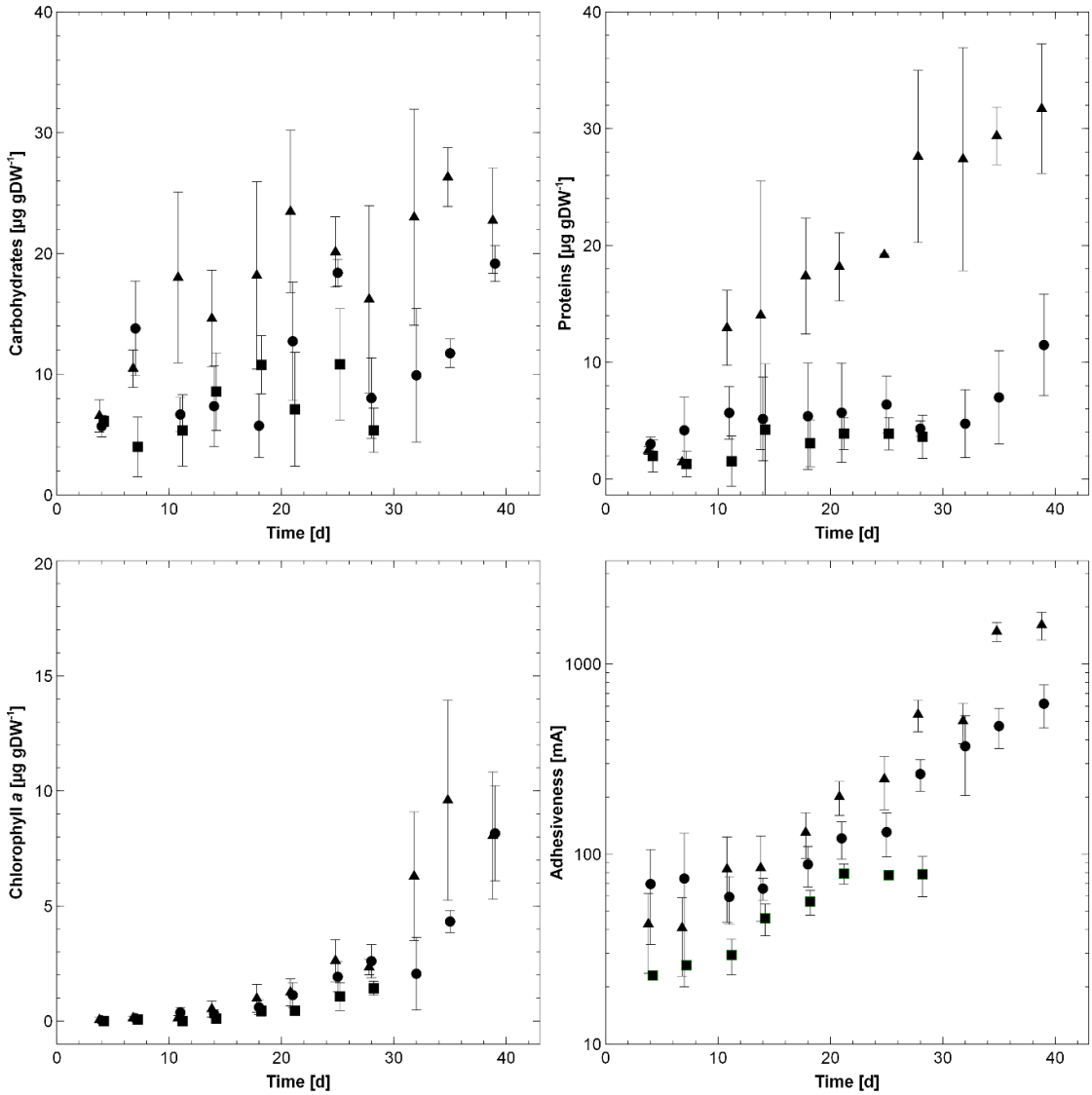

Figure 27: *Temporal development of selected biofilm features (mean values with corresponding STDev): spring (▲), summer (●), autumn (■). Upper left: EPS carbohydrate contents; upper right: EPS protein contents; lower left: chlorophyll a contents; lower right: biofilm adhesiveness (T3) with logarithmic ordinate. Source: Schmidt et al. 2016 Freshwater Biology.*

Altogether, it was found that the measurements by SETEG were less sensitive as compared to the MagPI adhesion determination when accounting for subtle changes in biofilm features – especially in early stages of biofilm growth. Since MagPI is a non-destructive method, the pool on data and replicates tested is much larger than for SETEG, where bed failure of a whole cartridge is required to get just one value. Thus, in

the following, most of the interlinkages between biofilm and functionality were statistically tested for the adhesive capacity.

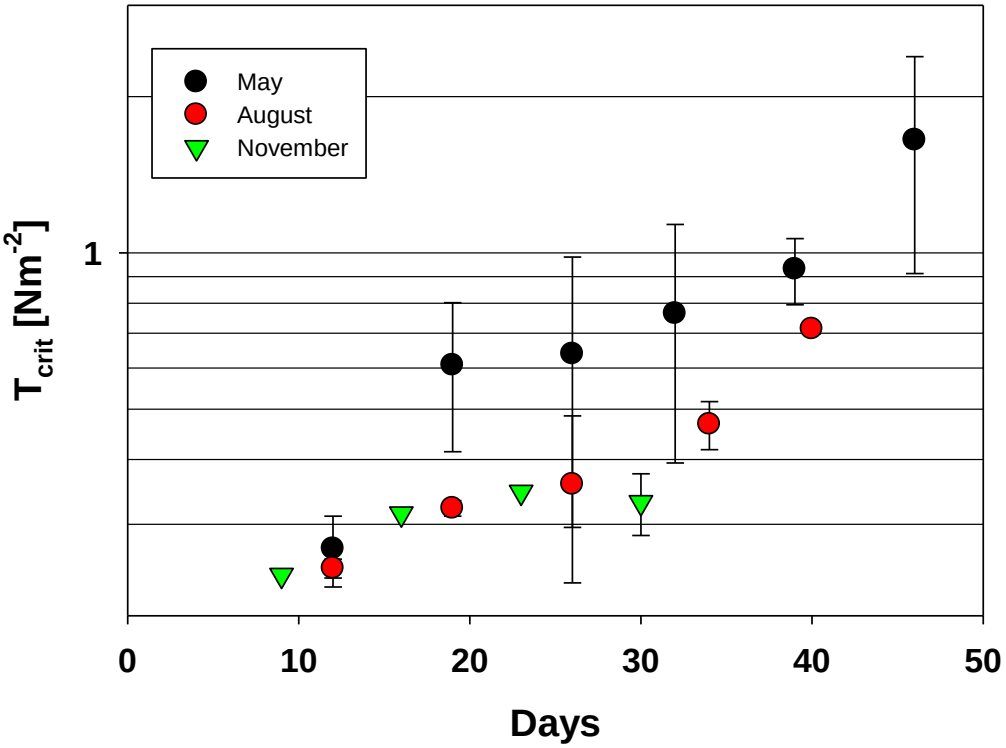

Figure 28: *Sediment stability over time for different seasons: black circles-spring (May 2013), red circles-summer (August 2013) and green circles-autumn (November 2013). The biofilm stability of one cartridge has been determined in the SETEG flume and each data point represents the mean values of four eroded cartridges originating from two flumes with the same boundary conditions of medium light (50µE m^{-2} s^{-1}) and low discharge (0.02Nm^{-2}) (n=4).*

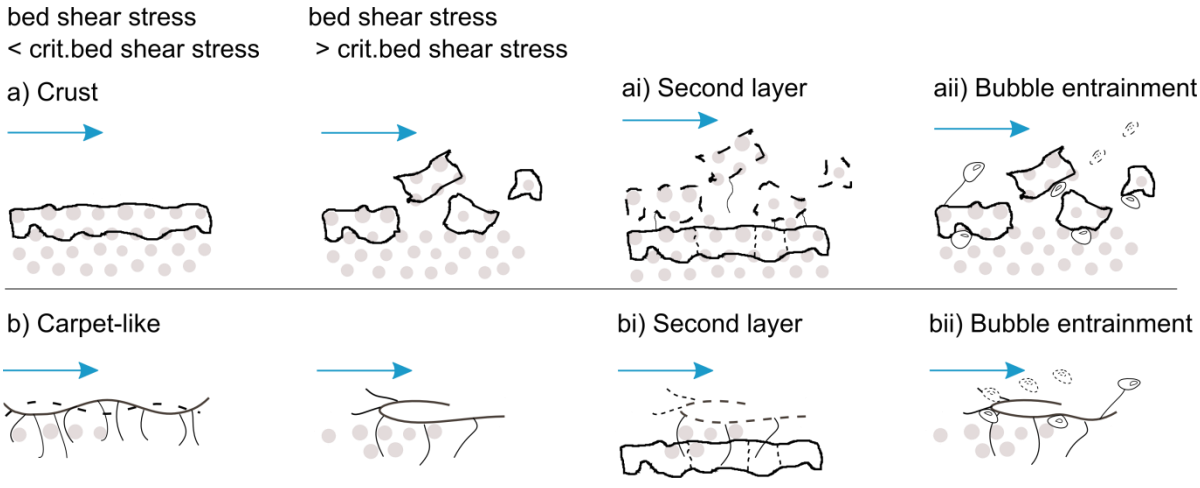

Figure 29: *The two dominant types of biofilm-impacted entrainment as observed during the experiments. Source: Thom et al. 2015a International Journal of Sediment Research.*

V.4.5. Seasonal Aspects and Interactions of Biofilm Features

The overview of the analyzed biofilm parameters in Table 14 reflects the two distinct biofilm developmental stages: early phase with transparent surface and bacteria-dominated until day 18 and the later phase with greenish-brownish surface that was diatom-dominated from day 21 onwards. Although no significant differences were detected in microalgal biomass and cell numbers (that is chlorophyll a content and bacterial cell counts BCC, respectively) between the seasons, spring biofilm were clearly distinguishable. For instance, biofilm adhesiveness and EPS contents were significantly higher in spring (KWT; $p=0.0013$; $n=80$ for T3; $p< 0.0001$; $n=64$ for both carbohydrates and proteins) as compared to summer or autumn. In contrast, diatom diversity on day 28 (mean Shannon index 1.7 ± 0.8 compared to 2.0 ± 0.8 in summer and 2.5 ± 0.3 in autumn) and the dynamics within the bacterial community were lowest during spring (KWT; $p< 0.0001$; $n=68$ for dynamics).

Since biostabilization was highest during spring, the analysis of interactions between different biofilm features and biofilm stability focused on this season. EPS protein content, biofilm chlorophyll a content and BCC showed high correlations to biofilm adhesiveness T3 (Spearman; proteins-T3: $rs=0.73$; $p<0.0001$; $n=45$; chlorophyll a-T3: $rs=0.71$; $p<0.0001$; $n=45$; BCC-T3: $rs=0.75$; $p=0.0001$; $n=45$; Table 15). Furthermore, high correlations between EPS protein content and chlorophyll a as well as BCC were detected (Spearman; proteins-chlorophyll: $rs=0.75$; $p<0.0001$; $n=45$; proteins-BCC: $rs=0.72$; $p=0.0004$; $n=20$). Evidence for the importance of the development within the bacterial community was suggested as its functional organization (Fo) showed high correlations to chlorophyll a content and biofilm adhesiveness T3 (Spearman; Fo-chlorophyll a: $rs=0.82$; $p<0.0001$; $n=42$; Fo-T3: $rs=0.78$; $p<0.0001$; $n=42$; Table 15).

V.4.6. MICROBIAL COMMUNITY: HETEROTROPHIC BACTERIA

For the bacterial community, the temporal development of the three ecology indices “range weighted richness” (Rr), “dynamics” (Dy) and “functional organization” (Fo) showed distinct differences over the seasons (Figure 30). While for the summer no significant changes were observed in any index, the autumn experiments revealed significantly increasing Rr over time (KWT; p=0.0430; n=14) and a trend towards increasing Dy (KWT; p=0.0514; n=12). Spring biofilm showed a highly significant increase in Fo (KWT; p=0.0005; n=42) where the initial mean Fo approximately doubled until the end of the experiments (from 40.02 ± 5.75 to 79.75 ± 7.07).

Further 16S rRNA gene-based identification of the total of 211 prominent bacterial DGGE bands/sequences from all experiments yielded 77 different bacterial species. It was revealed that the number of species exclusively detected in one particular season varied to a great extent: while 51 species were solely associated with spring, only 7 species were specific for summer biofilm and even less, 3 species, were unique in autumn. Typical freshwater species that were determined during spring were *Aquabacterium sp*. (Kalmbach *et al.*, 1999), *Brevundimonas diminuta* (Vancanneyt *et al.*, 2009) or *Gemmatimonas phototrophica* (Zeng *et al.*, 2015b, 2016). For a more detailed analysis considering the different boundary conditions of light and hydrodynamics over the varying seasons, see also chapter VI.

Table 14: *Seasonal and growth stage comparison of biofilm EPS matrix, microbial community and adhesiveness (mean values and corresponding StDEV). N=non-significant, S=significant. Source: Schmidt et al. 2016 Freshwater Biology.*

		Spring		**Summer**		**Autumn**		**Difference between seasons**
		Early Day 0-18	**Late Day 21-28**	**Early Day 0-18**	**Late Day 21-28**	**Early Day 0-18**	**Late Day 21-28**	
EPS	Carbohydrates [µg gDW^{-1}]	15.9 ± 8.1	19.3 ± 5.7	10.2 ± 9.2	11.8 ± 8.4	6.0 ± 2.6	8.5 ± 3.7	S
	Proteins [µg gDW^{-1}]	8.1 ± 8.9	10.2 ± 10.4	4.2 ± 3.1	5.5 ± 3.6	2.3 ± 2.7	3.6 ± 1.3	S
Biomass	Chlorophyll a [µg gDW^{-1}]	0.2 ± 0.3	2.4 ± 1.5	0.2 ± 0.2	1.9 ± 0.9	0.1 ± 0.1	0.7 ± 0.5	N
	Bacterial cells [$*10^7$ gDW^{-1}]	1.2 ± 1.8	3.0 ± 2.2	0.9 ± 0.7	4.2 ± 2.4	0.7 ± 0.3	1.5 ± 0.9	N
Bacterial Community	Range-weighted richness	18.7 ± 3.1	26.2 ± 13.9	13.7 ± 5.2	12.9 ± 8.1	13.9 ± 5.4	27.9 ± 7.7	N
	Functional organization	45.3 ± 7.3	61.1 ± 7.9	50.8 ± 11.1	49.9 ± 10.1	51.2 ± 2.7	39.8 ± 3.8	N
	Dynamics	10.2 ± 6.1	10.8 ± 5.7	13.7 ± 6.0	16.5 ± 10.5	22.0 ± 2.1	34.9 ± 2.2	S
Diatom community	Shannon Index	2.9 ± 0.1	1.7 ± 0.8	2.8 ± 0.2	2.0 ± 0.8	3.1 ± 0.1	2.5 ± 0.3	N
	Evenness	0.7 ± 0.1	0.5 ± 0.2	0.7 ± 0.1	0.6 ± 0.2	0.8 ± 0.1	0.7 ± 0.1	N
Biofilm Stability	Adhesiveness [mA]	64.2 ± 34.6	294.4 ± 210.8	63.2 ± 33.4	171.8 ± 76.3	31.1 ± 10.3	72.8 ± 13.5	S

Table 15: *Correlations of biofilm parameters during spring (abbreviations see in text). Source: Schmidt et al. 2016 Freshwater Biology.*

		EPS		**Biomass**		**Bacterial community**		**Adhesiveness**	
		Carb	Prot	Chl a	BCC	Rr	Fo	Dy	T3
EPS	Carb	1							
	Prot	0.55	1						
Biomass	Chl a	0.18	0.75	1					
	BCC	0.54	0.72	0.55	1				
Bacterial community	Rr	0.15	-0.42	-0.10	-0.06	1			
	Fo	0.21	0.70	0.82	0.65	0.08	1		
	Dy	-0.09	0.38	0.24	0.40	-0.48	0.18	1	
Adhesiveness	T3	0.40	0.73	0.71	0.75	0.01	0.78	-0.02	1

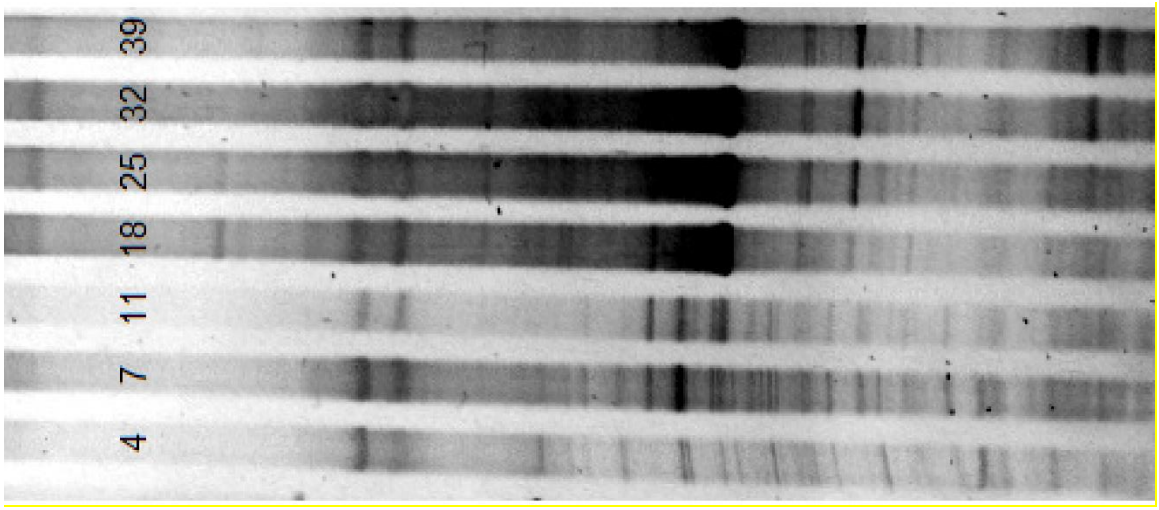

Figure 30: *Temporal development of the bacterial community. Inverted image of DGGE band patterns taken during spring (May 2013). The indicated numbers represent days of growth. The developing specialization of the bacterial community and dominance of single bands became very plain. Source: Schmidt et al. 2016 Freshwater Biology.*

V.4.7. MICROBIAL COMMUNITY: DIATOMS

Biofilm were dominated by a variety of different diatoms (see Table 16), while only few green algae such as *Scenedesmus sensu lato* were detected in low abundances. Hence, the analysis is focused on the diatom community: Statistical analysis of the complete data set for Bray-Curtis dissimilarity (BCD) indices of the diatom communities displayed no significant differences between the single flumes of one single experiment or between the two corresponding experiments representing one

season (KWT: p=0.934, p=0.3928 resp.; for both n=132). However, significantly increasing BCD indices were detected comparing the diatom communities of day 11 with days 18 and 28 (KWT: days 11 vs. 18: p=0.0054; days 18 vs. 28 and days 11 vs. 28: p<0.0001; for all n=132). On day 28, BCD indices obtained from the comparison of the diatom communities of spring and autumn were significantly higher than the ones between summer and autumn or between spring and summer (ANOVA: p=0.0185; n=44) reflecting the annual succession in riverine waters. The Detrended Correspondence Analysis (DCA) including all diatom samples (Figure 31) confirms this seasonal succession as it indicated three distinct clusters for the different seasons, where spring and summer are divided along the ordinate, while summer and autumn as well as autumn and spring are separated along the abscissa.

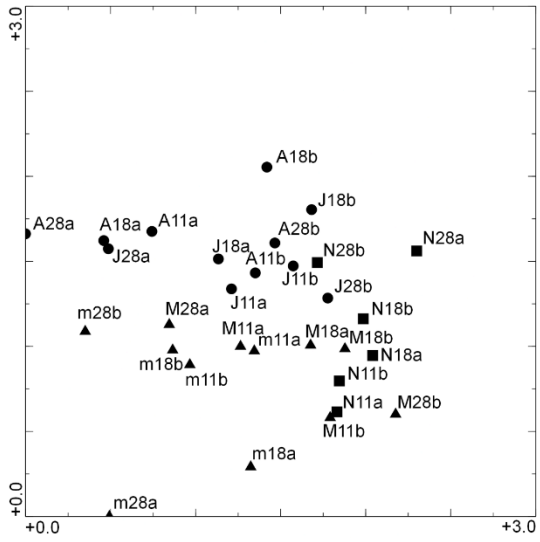

Figure 31: *DCA of the diatom communities. Triangles: spring; circles: summer; squares: autumn. Numbers represent sampling days. A: "August 2012", J: "July 2013", M: "May 2013", m: "March 2014", N: "November 2013". The additional "a" and "b" represent the two different flumes sampled during one experiment. Source: Schmidt et al. 2016 Freshwater Biology.*

Late successional biofilm (day 28) were always dominated by a combination of the four diatom species *Achnanthidium minutissimum var. minutissimum (A. min.)*, *Sellaphora seminulum (S. sem.)*, *Nitzschia fonticola (N. font.)* and *Nitzschia dissipata*

var. dissipata (N. diss.) with varying proportions over the course of one year (Figure 32). During spring, *A. min.* and *S. sem.* dominated late successional biofilm while other diatom species such as *Mayamaea atomus var. permitis* or *Eolimna minima (E. min.)* were subdominant. In summer biofilm, *S. sem.* developed strongly while the fractions of other diatom species such as *Nitzschia paleacea* and *Eolimna subminuscula* were lower. In contrast to spring and summer, autumn diatom communities were dominated by *N. font.* and *N. diss.* representing almost half of the diatoms in the late biofilm.

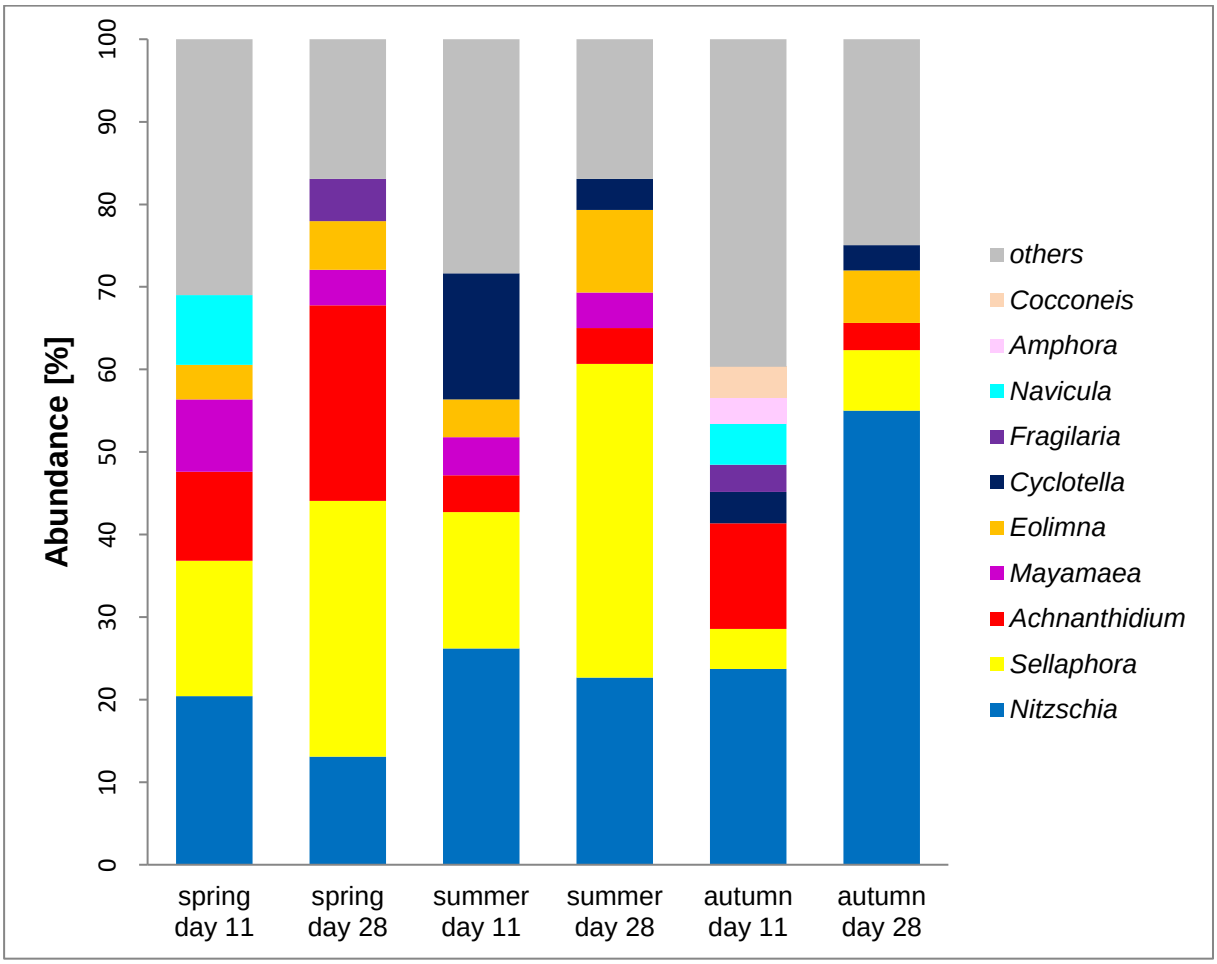

Figure 32: *Relative proportions of diatom genera [%] of early and late successional biofilm stages during all seasons. Genera with a relative abundance of less than 3.0% were summarized as 'others'. Source: Schmidt et al. 2016 Freshwater Biology.*

Table 16: *Detected diatom species with minimal abundance of 1% of total counted frustules. Source: Schmidt et al. 2016 Freshwater Biology.*

Taxon	Spring		Summer		Autumn	
	Day 11	Day 28	Day 11	Day 28	Day 11	Day 28
Achnanthidium minutissimum var. minutissimum	+	+	+	+	+	+
Amphora pediculus	+	+	+	+	+	
Cocconeis placentula					+	
Cyclotella menighiana			+	+	+	+
Cyclotella sp.			+	+	+	+
Diatoma moniliformis var. moniliformis	+					
Diatoma vulgaris	+					
Encyonema silesiacum	+	+			+	
Eolimna minima	+	+	+	+	+	+
Eolimna subminuscula	+		+	+		+
Fragilaria construens f. venter		+			+	
Fragilaria pararumpens		+			+	
Fragilaria pinnata					+	
Gomphonema olivaceum					+	
Mayamaea atomus var. permitis	+	+	+	+	+	+
Navicula gregaria	+	+	+		+	+
Navicula lanceolata	+				+	
Navicula reichardtiana					+	+
Navicula veneta					+	
Nitzschia abbreviata			+	+	+	+
Nitzschia acicularis	+		+	+	+	
Nitzschia amphibia						+
Nitzschia capitellata	+		+	+		
Nitzschia constricta			+		+	
Nitzschia dissipata var. dissipata	+	+	+	+	+	+
Nitzschia fonticola	+	+	+	+	+	+
Nitzschia inconspicua					+	
Nitzschia linearis	+			+		+
Nitzschia palea var. debilis	+		+	+	+	+
Nitzschia palea var. palea			+	+	+	
Nitzschia paleacea	+		+			+
Nitzschia sp.						+
Nitzschia supralitorea	+		+		+	+
Pennate unident.	+				+	
Planothidium frequentissimum	+		+	+	+	
Sellaphora seminulum	+	+	+	+	+	+
Surirella brebissonii var. brebissonii						+
Surirella brebissonii var. kuetzingii	+	+	+			+
Surirella minuta			+		+	+

V.5. DISCUSSION

V.5.1. THE SUITABILITY OF THE NEW MESOCOSM FOR BIOFILM STUDIES

One of the main purposes of this chapter was to put the new design of straight flumes to the test in terms of nature-like biofilm settlement and cultivation. Despite the absolutely identical setup of the six flumes, biofilm development could still differ due to smallest, possibly undetected variations in, e.g., the light or flow field, to result in deviations of biofilm growth along the test section of one single flume or between individual flumes. Moreover, biofilm have even been described as microbial landscapes that are *per se* characterized by high spatial heterogeneity (Battin *et al.*, 2007). Not surprisingly, biofilm settling in the flumes exhibited high small-scale heterogeneity (on a single cartridge), but these pattern were clearly similar over the test section in one flume and across all single flumes. This reflects the identical settings of temperature, illumination and, most importantly, hydrodynamics in every flume to provide the same growth conditions for biofilm. The exact determination of near-bed turbulences and bed shear stress directly at the sites of interest is especially important because this impacts the erosive forces acting on biofilm as well as their nutrient replenishment to affect biofilm morphology, metabolic activity (e.g. EPS secretion) and functionality (here biostabilization). Hence, the turbulence distribution was determined via high resolution Laser Doppler Anemometry (LDA) in the prototype flume and later on checked with Acoustic Doppler Velocimetry (ADV) (Thom *et al.*, 2012). The measurements on hydrodynamics indicated the need of a long inlet flow section and a sufficient distance of the cartridges from the flume walls. Apart from the homogenous turbulence distribution over the biofilm growth section, constant discharges ensured identical bed shear stresses over the test section. The highly resolved discharge measurements were performed in all flumes throughout the

present and the following experiments. These data gave evidence on the constant and similar discharges in all six flumes, and thus on the identical bed shear stress levels over all biofilm growth sections.

Furthermore, the PAR (photosynthetic active radiation) distribution and composition has been tested and arranged to ensure a homogeneous light field over the whole test section and flumes. All of these efforts have been rewarded with the results from the first experiment that gave evidence on the comparability of biofilm growth and composition within and between the flumes - an essential prerequisite for studies on the impact of environmental parameters on biofilm ecology and functionality.

V.5.2. Significance of Biostabilization in Freshwaters

The second important objective of this chapter concerned the importance of microbial biostabilization within riverine sediments; a phenomenon that has been insufficiently studied in contrast to marine and estuarine habitats. That was reasoned by the fact that biostabilization largely depends on the amount of ions that help binding between the microbially-secreted polymers and the sediment particles (Spears *et al.*, 2008). This would imply that the stabilization potential in freshwater is significantly lower than in the marine environment. Recent investigations at the Rivers Elbe, Neckar and Rhine gave first hints to the involvement of microbial activities but could not unravel their contributions in the highly complex natural sediment cores (Gerbersdorf *et al.*, 2008a). The experiments conducted here were the first to clearly demonstrate the high biostabilization potential with significant increases in sediment stability/biostabilization index (determined by the SETEG flume) and in adhesive capacity (determined by MagPI). The biostabilization indices between 1.5 up to 10 after five weeks of growth were well within the range of highest indices calculated in

marine habitats by, e.g., Amos et al. (2004) (BImax: 2.4), de Brouwer & Bjelic (2000) (BImax: 3) and Tolhurst et al. (1999) (BImax: 6.2). For the adhesive capacity, top values were even 25 times higher as compared to the abiotic control over five weeks of growth.

Consequently, despite observing significantly lower EPS values as well as microbial biomass (as compared to brackish/marine biofilm), a significant biostabilization effect was detected. This emphasized the meaning of biostabilization in lotic freshwaters for sediment dynamics, contradicting the current doctrine on the solely importance of large ion quantities for sediment stabilization processes.

V.5.3. SEASONAL EFFECTS UPON BIOSTABILIZATION

The maximum of biostabilization capacity was clearly detected during spring, followed by summer and autumn; verified by determining the point of mass erosion within the standardized SETEG flume as well as by evaluation of the adhesive capacity with MagPI. Seasonal differences in sediment stability have been reported from various field studies in intertidal environments and riverine sites (Widdows *et al.*, 2000; Tena *et al.*, 2014). Dickhudt et al. (2009), for example, found a higher erodibility in winter and spring than in summer and autumn. A five-fold increase of the BI in summer as compared to winter was reported by Amos et al. (2004). Our results confirm seasonal trends, possibly indicating a cyclic behaviour of erodibility in freshwaters. The highest sediment stability during spring might be an evolutionary adaptation in rivers of mid-to-high latitude temperate regions: during spring, snow melting in higher regions of the catchment regularly leads to rising discharge resulting in elevated flow velocity and bed shear stress, which can dislodge benthic biofilm. Possible adaptation strategies of biofilm microbes facing this situation could

be either to resist the increased mechanical stress by attaching tightly to the sediment surface or to colonize uncovered sediment very quickly. Thus, the annual repetition of a stressful hydraulic regime during spring could favour rapidly growing biofilm (i.e. early succession stages of the diatom community). In the epipotamal (downstream) region of a river, the combination of high illumination intensities (lacking riparian vegetation) and high nutrient availability (lacking macrophyte concurrence) may additionally enhance diatom growth, their EPS production and the resulting biostabilization capacity. In this context, the annual successional process not only shapes the benthic community but also the functionality of the overall biofilm system, in this case biostabilization. Although the used experimental set-up constitutes a great simplification of the natural system, it was necessary to guarantee that the only variable parameter influencing biostabilization was the investigated seasonal changing composition of the microbial community.

V.5.4. Driving Factors for Biofilm Growth and Biostabilization

Extracellular polymeric substances. EPS carbohydrates are considered a driving factor for biofilm formation and stability (Sutherland *et al.*, 1998b; Underwood & Paterson, 2003; Tolhurst *et al.*, 2006); hence, the composition of diatom EPS carbohydrates and its influence upon the viscosity of the cell coating mucilage and biofilm structure have been studied intensively (Staats *et al.*, 1999; Sutherland, 2001; Khandeparker & Bhosle, 2001; Higgins *et al.*, 2002; Magaletti *et al.*, 2004). Furthermore, Svetlicic et al. (2013) highlighted the importance of the EPS carbohydrate network and its role during colony formation of diatoms. The present study confirmed the reported high correlation between biofilm stability and EPS carbohydrate content (Yallop *et al.*, 2000) with the highest values for both parameters

detected during spring. However, it also indicated that EPS carbohydrates are not the only important extracellular components influencing biostabilization since biofilm stability was also strongly correlated to EPS protein content. Becker et al. (1996) noted that a high EPS carbohydrate content does not necessarily result in stronger diatom adhesion to a surface and showed that the relation between EPS and biofilm stability is much more complex, as the production of extracellular carbohydrates has a number of functions for microbes that are not necessarily linked to biofilm stability. For example different carbohydrates from the group of acyl-homeserine lactones are used by a broad range of different bacteria for intra- and inter-species quorum sensing (Waters & Bassler, 2005). Additionally, diatoms can produce EPS carbohydrates to avoid photo-oxidative stress due to high illumination intensities (Fogg, 1983). They also produce relatively fragile extracellular carbohydrates for their locomotion through the sediment (Smith & Underwood, 1998). In general, the production and composition of EPS carbohydrates has been found to reflect the physiological and nutritional state of diatoms, the developmental stage of their colonies and the level of environmental stress (Smith & Underwood, 2000; Haralampides *et al.*, 2003; Underwood *et al.*, 2004). These influencing factors may cause clear shifts in content and composition of extracellular carbohydrates. These fluctuations were hinted at during this study but apparently had no direct effect on biofilm stability. On the other hand, the detection of strongly correlating biofilm adhesiveness and EPS protein content during spring indicated the importance of extracellular proteins. Extracellular proteins also have been identified as important structural elements in bacteria e.g. linking together the strands of the extracellular matrix (Lind *et al.*, 1997; Chiovitti *et al.*, 2003, 2006) and as specific adhesive proteins produced by diatoms in order to attach to a surface (Dugdale *et al.*,

2006a;b). Thus, extracellular proteins are important for the mechanical strength of the EPS matrix to strongly influence the stability of the biofilm and its biostabilization capacity. Furthermore, the results of this study suggest a much more complex relationship between the microbes in the biofilm and biofilm EPS content than the reported correlation between microbial biomass and EPS production (Yallop *et al.*, 2000; Underwood & Paterson, 2003): on the one hand, EPS protein contents showed high correlation with microbial biomass during spring, while, on the other hand, the highest EPS contents were not reflected in microbial biomass when comparing among seasons. Moreover, the seasonal changes in microbial biomass were not mirrored by the varying biofilm adhesiveness and stability either. All of these emphasize the great importance of analyzing the microbial community to derive a comprehensive understanding of the driving factors influencing biostabilization.

Microbial community: heterotrophic bacteria. The observed Rr values pointed to similar “carrying capacities” of the biofilm during all seasons and they were well in the range of the results from Lubarsky et al. (2012). These rather medium levels of Rr values (Marzorati *et al.*, 2008) indicated that all biofilm in the oligotrophic water of the River Enz could harbour a moderate diversity of bacteria. However, the functional organization and dynamics appeared to be of importance as maximal biostabilization during spring was reflected by higher Fo and significantly lower Dy compared to autumn with minimal stabilization capacity. The Fo and Dy values during spring gave hints to a stable habitat in which a more specialized bacterial community could evolve. The high correlation between chlorophyll a content and Fo during spring might suggest an adaptation process of the bacterial community to the developing diatom dominance known to shape the biochemical and physical microenvironment

of biofilm (Besemer *et al.*, 2007). The fact that diatoms have a range of specific satellite bacteria was outlined by Amin et al. (2012). Furthermore, bacteria and their secreted substances were shown to influence diatom growth and EPS production (Bruckner *et al.*, 2011). Other studies stated the important role of bacteria during diatom attachment (Gawne *et al.*, 1998) and the formation of diatom aggregates (Gärdes *et al.*, 2011). Furthermore, Lubarsky et al. (2010) demonstrated that this symbiosis between diatoms and bacteria had a direct impact on the overall biofilm network and was an essential driving factor for biofilm stability and biostabilization. Considering both the maximum in biofilm stability during spring and the high correlation between Fo and T3, this study could be the first to report a specialized bacterial community with high stabilization potential. The trigger for this specialization might be the influence of the diatoms. However, parallel to the diatom community, the bacterial community in the inoculum is probably even more essential because its composition is also significantly influenced by seasonality (Karrasch *et al.*, 2001; Yannarell & Triplett, 2005). In addition, it directly impacts species composition in "river snow" (Böckelmann *et al.*, 2000) as well as in biofilm (Brümmer *et al.*, 2000, 2003; Lyautey *et al.*, 2005). Altogether, these findings emphasize the importance of a comprehensive observation of the temporal development within the microbial community.

Microbial community: diatom species. The diatom community showed typical representatives of European freshwater habitats (Battarbee, 1986; Krammer & Lange-Bertalot, 1986; Hofmann *et al.*, 2011) with *A. min.*, *S. sem.* and *E. min.* being considered typical pioneer species that are primary colonizers of virgin sediment (Peterson, 1996). During the course of the year, clear evidence for the seasonal

succession process within the diatom community was detected. In this context, the morphologies and life forms of the different diatom species in the biofilm appear to be essential for biostabilization. Many studies have examined the process of diatom locomotion through the biofilm and sediment via EPS secretion (Paterson, 1989; Smith & Underwood, 1998; Wang *et al.*, 2013), as well as its importance as a survival mechanism in a dynamic habitat of e.g. shifting sediment surfaces, water depths or underwater light intensities (Stal, 2003; Underwood & Paterson, 2003; Apoya-Horton *et al.*, 2006). However, while knowledge on the physiological and molecular biological reaction of selected diatoms to their environment and stress such as nutrient limitation or trace elements is constantly growing (McKay *et al.*, 1997; Kudo *et al.*, 2000; Dyhrman *et al.*, 2012), the various effects of their movement upon the biofilm matrix and biostabilization are currently barely addressed. Nevertheless, parallel to the observations that macrozoobenthos migration can disturb biofilm stability (de Deckere *et al.*, 2001), it can be assumed that the movement of large motile diatoms may impact the overall biofilm structure. Besides a potential positive effect upon the growth of heterotroph microbes degrading the mucilage trails, this micro-bioturbation can increase the micro-roughness of the biofilm surface to destabilize the biofilm (Gerbersdorf & Wieprecht, 2015). To investigate possible effects of the diatom community compositions during the different seasons upon the biofilm structure, surface area and volume of the detected diatoms were calculated (Hillebrand *et al.*, 1999; Sun & Liu, 2003). It became clear that *N. font.* and *N. diss.* dominated autumn biofilm, with up to eightfold higher biovolume and up to sevenfold higher surface area than smaller diatoms (e.g. *A. min.*, *S. sem.* or *E. min.*), which were more abundant during spring and summer. In contrast to *A. min.,* which represented a big fraction of the microphytobenthos during spring and which is known to be immotile and to attach

permanently to the sediment via short EPS stalks (Potapova & Hamilton, 2007), different *Nitzschia* species such as *N. font.* and *N. diss.* were described to be highly mobile (Lange *et al.*, 2011). Different studies could show that there are major differences in the composition of sugar monomers and the overall structure between adhesive stalks, the mucilage capsule and EPS strands involved in locomotion (Wustman *et al.*, 1997, 1998; Guo *et al.*, 2008). There are strong indications that the different forms of permanent (immotile diatoms that are fixed to sediment grains) or temporary (migrating specimens) attachment may be represented in EPS composition. Although the complex relationship between EPS composition and biofilm stability is not fully understood, this might constitute one possible explanation for the observed significantly different adhesive capacities and biostabilization of biofilm. Evidence for this is given by the results of recent studies: Higgins et al. (2003) described clear differences in EPS coating of different species of diatoms. While some species that are entirely covered in a thick compressible layer of EPS are known to be persistent fouling organisms such as *Crasepdostauros australis E. J. Cox*, the apparently more mobile *Nitzschia navis-varingica Lundholm et Moestrup* displayed only few EPS strands near the raphe region. It was suggested that this arrangement of EPS may play an important role for the biofilm network on a bigger scale and the connection of structural elements in the extracellular matrix – especially in a range very near to the cell surface. Other studies (de Brouwer & Stal, 2002; de Brouwer *et al.*, 2005; Molino *et al.*, 2006) demonstrated that the features of produced EPS are greatly influenced by the physiology and species of diatoms, i.e. distinct types of diatoms produced different quantities and compositions of EPS with diverse viscoelastic properties and adhesive features which can affect the structural stability of the whole biofilm. Even if these results were gathered via lab experiments

with some model diatoms and may not cover all processes in a natural system, these findings are essential as they indicate a link between species composition, EPS production and overall biofilm stability.

V.5.5. THE MECHANICAL PROCESS OF EROSION FOR BIOSTABILIZED SEDIMENTS

Differences in the mechanical structure and the resulting processes of erosion are often disregarded, but may be partly responsible for the wide range of stabilization potential observed. As highlighted by Grabowski et al. (2011), the development of a unifying equation to predict erodibility is limited by the absence of a complete mechanistic understanding of the biostabilization process and its interactions between key parameters. To get a better understanding of the fundamental processes, an analysis on the observed erosion processes was carried out, revealing significant differences between mechanisms and possible impacts on stability. Two predominant types of stabilizing structures were identified:

The most frequent mode of incipient motion in the experiments comprised the erosion of chunks or aggregates (Figure 29, denoted as crust-like erosion) that could be correlated to a wide range of stabilities. By gluing individual sediment particles together, a crust was formed on the top few millimetres. This type of structure was additionally detected below the surface of the sediment (i.e. a second underlying biofilm layer), adding even more resistance to the flow (Figure 29). In the event of erosion, this crust broke apart at the weakest spots (in the experiments cracks in the crust were frequently found already during cultivation) and aggregates of different sizes (up to mm scale) were resuspended. This led subsequently to a chain reaction where even more aggregates were exposed to the hydraulic forces and eroded. Righetti & Lucarelli (2007) ascribed the enhanced biostabilization potential to the

impact of changed aggregate sizes (and density) and adhesion forces between these aggregates and developed a promising model based on the Shields' equation (Shields, 1936) to account for the biogenic impacts.

The second type could be described as a carpet-like structure (Figure 29), which was largely detected at a more matured biofilm age, linked to different types of organisms and increasing sediment stability (mostly BI>3.5). Most striking was the formation of such a mat in one experiment (in May), with a BI of approximately 10. Loosely-bound to the underlying substratum via filaments, these biofilm formed an elastic mat armouring the river bed. Differences compared to classical erosion models are immense and until now only one model exists describing this behaviour, developed by Vignaga et al. (2013). For future experiments in the field of biostabilization these different mechanisms of erosion have to be considered, especially to interpret data from biological analysis and relate them to stabilizing effects.

V.6. CONCLUSIONS

The stabilizing effect of biofilm upon lotic fine sediment remained unaddressed until now despite its broad range of economic and ecological implications. To investigate the complex interactions between the biofilm and its environment, a sophisticated and unique setup consisting of six straight flow-through flumes was designed combining biological and engineering expertise. While running six long-term experiments during different seasons, three main issues were addressed that were described in this chapter:

Firstly, the evaluation of biological and biochemical features during biofilm growth in these new flumes demonstrated that representative biofilm (intra- and inter-flume-wise) could be cultivated while exposed to the same abiotic environment - an

essential prerequisite for further research into biostabilization processes. Secondly, the experiments under strictly controlled boundary conditions gave first evidence on the importance of biostabilization (known to be substantial in marine habitats) within lotic fine sediments. Thirdly, seasonal changes in biofilm adhesion and substratum stability became apparent - with a maximum during spring and a minimum during autumn/winter. Interestingly, this result was clearly reflected in shifting community composition of photosynthesizing diatoms as well as heterotrophic bacteria, in their various lifestyles, and in different EPS quantity and quality. Consequently, the mechanical properties of this biofilm-substratum tandem varied significantly to affect the type of erosion and thus vulnerability to the hydraulic forces. In summary, this comprehensive assessment could unravel various complex interactions of the EPS in the biofilm matrix, the responsible microbial producers, the resulting mechanical structures and the overall effect on the biofilm and sediment stability.

VI. The Effect of Light and Fluid Dynamics on Microbial Biostabilization in Freshwaters

VI.1. Abstract

Biofilm constitute a central issue in microbial ecology due to their high ecological and economic relevance but the impact of abiotic conditions and microbial key players on the development and functionality of a natural biofilm is still hardly understood. This study investigated the effects of light intensity (LI) and bed shear stress (BSS) and the role of dominant microbes during the formation of natural biofilm and particularly the process microbial biostabilization. A comprehensive analysis of microbial biomass, produced EPS, as well as the identification of dominant bacterial and algal species was correlated to the assessment of biofilm adhesiveness and substratum stability. LI and BSS impacted the biofilm in different ways: adhesion and stability both significantly increased with LI while higher BSS seemed to delay biofilm growth and biostabilization. Moreover, microbial biomass and the functional organization of the bacterial community increased with LI while the dynamics in the bacterial community increased with BSS. Most stable biofilm were dominated by sessile diatoms like *Achnanthidium minutissimum* or *Fragilaria pararumpens,* and bacteria with either filamentous morphology like *Pseudoanabaena biceps* or a potential high capacity for EPS production like *Rubrivivax gelatinosus*. In contrast, microbes with high motility like *Nitzschia fonticola* or *Pseudomonas fluorescens* and *Caulobacter vibrioides* dominated the least adhesive biofilm. Their movement and potential antibiotics production could have had a disruptive impact on the biofilm matrix which decreased its stability. This is the first study to unveil the link between abiotic conditions and resulting shifts in microbial key players to impact the ecosystem service microbial biostabilization.

VI.2. BACKGROUND

Numerous studies on the impact of environmental conditions, on the development and characteristics of biofilm as well as on their “performance” (such as the rate of nutrient cycling or contaminant retention) have been published. Thereby, environmental parameters were shown to affect biofilm structure (Blenkinsopp & Lock, 1994), metabolic pathways (Romani *et al.*, 2004; Marcarelli *et al.*, 2009; Kendrick & Huryn, 2015) and the development of the microbial community (Lawrence *et al.*, 2004; Wagner *et al.*, 2015). As a result, knowledge about the impact of important abiotic conditions upon biofilm systems is constantly increasing to unravel different feedback loops between biofilm and habitat.

However, the link to the process of microbial biostabilization within fine sediments is rarely given. An exception to this is the influence of light since the focus was largely on the photoautotrophic microalgae in intertidal areas where light availability varies greatly between high and low tide to result in varying patterns of microalgal EPS secretion and stabilization potential. EPS is generally considered as a driving factor for biostabilization and significantly linked to photosynthetic activity whether directly (e.g. freshly produced during illumination, Orvain *et al.*, 2003) or indirectly (e.g. release of formerly-produced EPS through the raphes for migration during darkness, Smith & Underwood, 2000). The good news in the benthic habitat: too much light can rarely harm the microalgae since they can migrate into the sediment or adapt physiologically to avoid photo-oxidative damages (e.g. Friend *et al.*, 2003; Jesus *et al.*, 2009). Nevertheless, there are hints that too much light might decrease sediment stability by photosynthesis-driven oversaturation of oxygen and bubble formation (Sutherland et al. 1998). The more common problem in sediments is the lack of light: eutrophication and phytoplankton blooms might increase light attenuation in the

water body and the deposition of new material can further decrease light availability for benthic algae (Gerbersdorf *et al.*, 2005b). On the other hand, sediment stabilization by heterotrophic bacteria under light exclusion can be impressive as has been shown for estuarine sediments (Gerbersdorf et al. 2008b); thus there is a possibility that the suppression of microalgae in darkness could even increase sediment stability.

Among others, there is an intense debate about the interactions between fluid flow pattern and biofilm, but again without a link to biostabilization (e.g. Stoodley *et al.*, 1999a;b; Manz *et al.*, 2005; Stewart, 2012). While it is well-known that microbes profit from the better nutrient availability due to higher mixing rates and thinner benthic boundary layers as flow rates increase (Nikora, 2010), high-energy impact by turbulent downsweeps might induce detachment ("sloughing-off") of biofilm (Characklis & Cooksey, 1983) with possible consequences for biostabilization. The resilience of biofilm to a sudden increase in hydrodynamic stress will certainly depend on its growth history and adaptation capacity. In this context, Pereira et al. (2002) could show that higher flow velocities during cultivation led to a reduction in biofilm thickness and simultaneously increased biofilm density which has implications for nutrient access and sediment stability. Hence, hydrodynamic forces shape the biofilm topography but the biofilm structure itself also impacts the adjacent physical environment by e.g. shifts in the displacement height and the roughness length to either reduce turbulence levels (Nikora *et al.*, 2002) or actively enhancing drag forces and nutrient transport by growing filamentous structures (Larned *et al.*, 2011).

While abiotic conditions such as light and hydrodynamic certainly impact biofilm growth and functionality, the link is via the microbial community. Shifts in species composition due to environmental settings have great implications for biofilm

architecture and functions. Clearly, different diatom species produce EPS with varying characteristics but even the same species can vary EPS quantity and quality according to their physiological adaptation (Wustman *et al.*, 1997, 1998; Wang *et al.*, 2000). The same is true for bacteria which exhibit different life styles, and thus vary EPS production that most likely has consequences for biofilm and sediment stability (e.g. Roeselers *et al.*, 2007; Brimacombe *et al.*, 2013). This suggests a significant influence of microbial key players and increases the complexity of the research on the stabilizing potential of biofilm.

To unravel the importance of single parameters in this highly complex process microbial biostabilization, an experimental setup was used whose design and reliability were previously demonstrated (see chapter V, Schmidt *et al.*, 2015). Biofilm was grown in these mesocosms under natural-like but controlled and reproducible conditions to assess the impact of two major abiotic environmental factors (light intensity and hydrodynamics) on the development of the biofilm and its functionality with special consideration of the microbial community composition and potential microbial key players in the process of biostabilization.

VI.3. Experimental Settings

The six long-term experiments performed in the novel straight flumes gave insights about the suitability of the mescosm, significance and seasonality (previous chapter) as well as on the influence of varying light and hydrodynamic conditions (this chapter) on biostabilization. The flow-through flumes as well as the experiments have already been described in the previous chapter (V.3.) and the same applies to sampling procedure, biochemical and molecular analyses as well as determination of biofilm adhesion and substratum stability. The three levels of light and hydrodynamic

regimes can be seen in Table 9. Generally, either light or hydrodynamic were varied in four flumes (Table 9) while two of the six flumes were always run at the same conditions of medium light and low flow (six flumes: three treatment levels for each experiment).

VI.4. RESULTS

VI.4.1. OVERVIEW ON THE EFFECTS OF LIGHT AND HYDRODYNAMIC TREATMENTS

Taking all data into account (over time, from young to matured biofilm), the three different levels of light intensity (LI) induced significant differences for the growing biofilm and all of the associated biochemical parameters (Table 17). This is also true for the three different levels of bed shear stress (BSS), however, not for biomass, bacterial cell numbers and EPS carbohydrates (Table 17).

VI.4.2. TEMPORAL BIOFILM DEVELOPMENT

The cultivation at different boundary conditions clearly influenced the temporal development of the analysed biofilm parameters. During darkness, only BCC (KWT; p=0.0023; n=30) and biofilm adhesiveness (KWT; p=0.0395; n=61) increased significantly over time. In contrast, biofilm cultivated at medium and high illumination displayed mostly significantly increasing microbial parameters and adhesiveness (Table 18, Figure 33). Exceptions to this were some parameters concerning bacterial community ecology and EPS carbohydrates for medium LI (Table 18). The three levels of BSS indicated various effects: while the contents of EPS carbohydrates showed fluctuating values without significant changes, EPS protein contents increased significantly at low and high BSS over time (Figure 34).

Table 17: *Possible differences in biofilm growth and functionality due to different boundary conditions of shear stress and light intensity. n=number of samples, N=non-significant, S=significant. Source: Schmidt 2017 PhD Thesis University Stuttgart.*

		Bed shear stress		Significance	Light intensity		Significance
		n	**p**		**n**	**p**	
EPS	**Carbohydrates**	175	p=0.7474	N	235	p=0.0004	S
	Proteins	175	p=0.0178	S	235	p=0.0002	S
Biomass	**Chlorophyll a**	177	p=0.1805	N	235	p<0.0001	S
	Bacterial cells	80	p=0.8905	N	121	p=0.0013	S
Bacterial community	**Range-weighted richness**	172	p=0.0001	S	226	p<0.0001	S
	Functional organization	162	p=0.0213	S	212	p=0.0005	S
	Dynamics	140	p=0.0047	S	174	p=0.0123	S
Biofilm stability	**Adhesiveness**	173	p=0.0398	S	229	p<0.0001	S

Table 18: *Possible differences in biofilm growth and functionality over time at darkness and varying light intensities. n=number of samples. Source: Schmidt 2017 PhD Thesis University Stuttgart.*

		Darkness		Medium LI		High LI	
		n	**p**	**n**	**p**	**n**	**p**
EPS	**Carbohydrates**	65	p=0.4069	105	p=0.0576	65	p=0.0199
	Proteins	65	p=0.2770	105	p=0.0002	65	p=0.0024
Biomass	**Chlorophyll a**	65	p=0.9523	105	p<0.0001	65	p<0.0001
	Bacterial cells	30	p=0.0023	48	p<0.0001	25	p=0.0143
Bacterial community	**Range-weighted richness**	62	p=0.8215	102	p=0.3665	62	p=0.6016
	Functional organization	54	p=0.8196	96	p<0.0001	48	p=0.0473
	Dynamics	44	p=0.1643	80	p=0.7847	62	p=0.0074
Biofilm Stability	**Adhesiveness**	61	p=0.0395	106	p<0.0001	62	p<0.0001

Table 19: *Possible differences in biofilm growth and functionality over time at varying flow velocity intensities as the basis for bed shear stress calculations (BSS). n=number of samples. Source: Schmidt 2017 PhD Thesis University Stuttgart.*

		Low BSS		Medium BSS		High BSS	
		n	**p**	**n**	**p**	**n**	**p**
EPS	**Carbohydrates**	105	p=0.0576	40	p=0.1981	30	p=0.4511
	Proteins	105	p=0.0002	40	p=0.0833	30	p=0.0424
Biomass	**Chlorophyll a**	105	p<0.0001	40	p=0.0005	32	p=0.0026
	Bacterial cells	48	p<0.0001	13	p=0.0853	12	p=0.0883
Bacterial community	**Range-weighted richness**	102	p=0.3665	40	p=0.0550	30	p=0.0721
	Functional organization	96	p<0.0001	38	p=0.0138	28	p=0.0183
	Dynamics	80	p=0.7847	32	p=0.0240	22	p=0.0347
Biofilm Stability	**Adhesiveness**	106	p<0.0001	40	p=0.0009	28	p=0.0643

Algal biomass significantly increased at all three flow velocity levels, but for BCC, this increase was only significant at low bed shear stress (Figure 34). The bacterial community displayed very variable reactions to the different levels of BSS over time: while a significant increase in Fo could be detected in all treatments, the Dy increased only significantly at medium and high BSS, and Rr did not change significantly in matured biofilm. At high BSS, the detected adhesiveness of biofilm was lowest and only the matured biofilm cultivated at low or medium BSS showed a significant increase (Table 19).

VI.4.3. Microbial Parameters: algal Biomass, bacterial Cell Numbers, EPS

Light. Cultivation in the dark (named “LI low”) resulted in chlorophyll values that were at the detection limit, significantly different from the other light levels (KWT; $p<0.0001$; $n=87$). Chlorophyll values were increasing with light intensity which was especially pronounced in matured biofilm. In the matured biofilm, the bacterial cell numbers were also clearly increasing with light intensity (Figure 33). Likewise, mean contents of EPS carbohydrates as well as proteins were significantly lowest in the dark when comparing the matured biofilm to the other two light levels (KWT; EPS carbohydrates: $p=0.0006$; $n=87$; EPS proteins: $p=0.0082$; $n=87$) (Figure 33).

Hydrodynamics. Highest BSS seemed to delay biofilm settlement and growth - both, bacterial cell numbers and microalgal biomass of the matured biofilm were clearly higher at low and medium flow velocities (Figure 34). However, the difference between the treatments was not significant (KWT; BCC: $p=0.2329$; $n=36$; Chlorophyll a: $p=0.1948$; $n=85$). Early biofilm stages that developed at high flow velocity displayed lower mean EPS contents as compared to biofilm at low and medium

levels of bed shear stress. In the matured biofilm, these differences were mitigated and EPS content was comparable for both, carbohydrates and proteins, at all BSS levels (Figure 34).

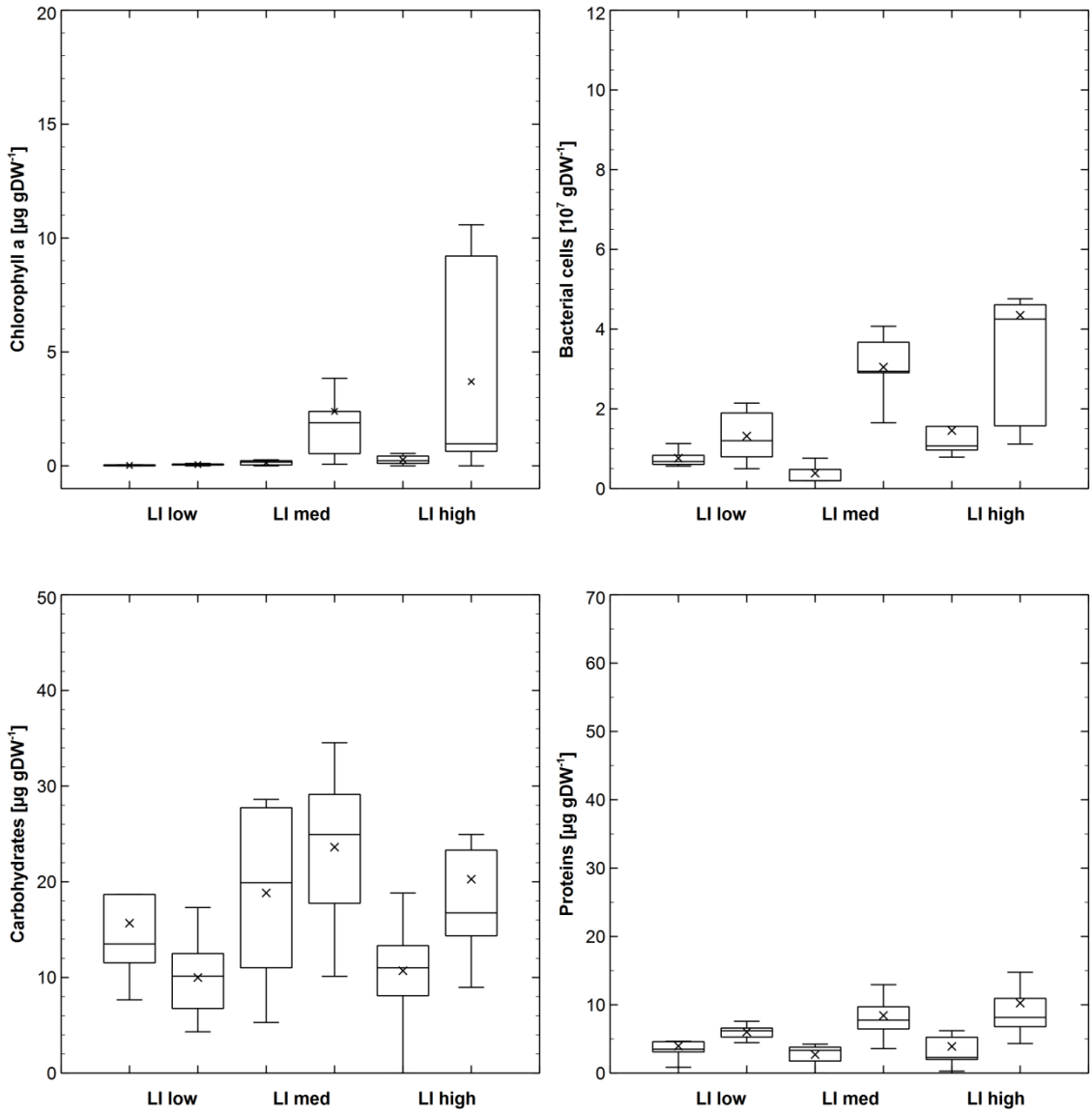

Figure 33: *Microalgal biomass, bacterial cell numbers and EPS carbohydrates as well as EPS proteins at different light intensities (LI) and separated in early (young) and late (matured) biofilm stages (pairwise per LI). Source: Schmidt et al. 2018 Research and Reports in Biology.*

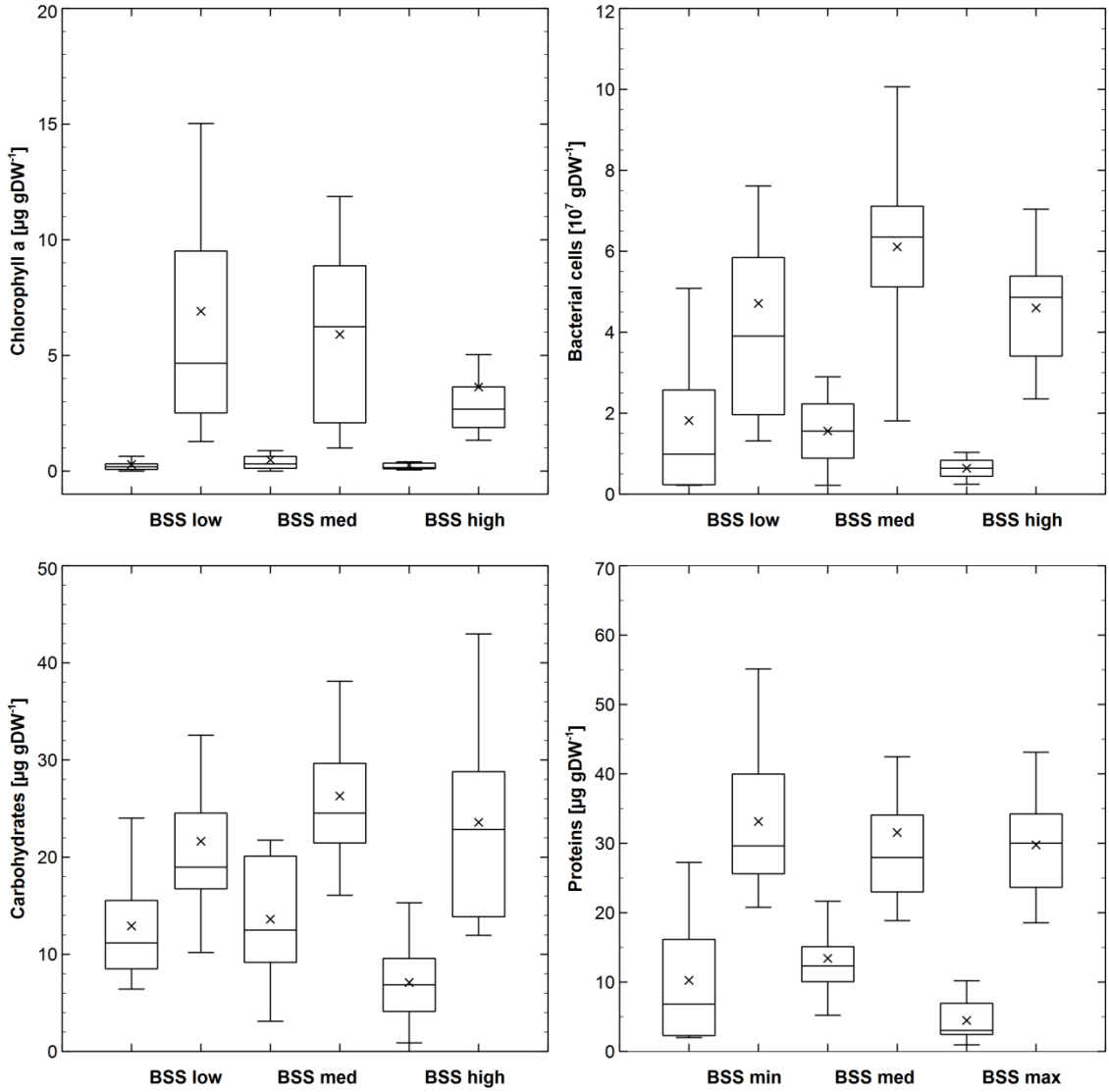

Figure 34: *Microalgal biomass, bacterial cell numbers and EPS carbohydrates as well as EPS proteins at different flow velocities/bed shear stress (BSS) and separated in early (young) and late (matured) biofilm stages (pairwise per BSS level). Source: Schmidt et al. 2018 Research and Reports in Biology.*

VI.4.4. BACTERIAL COMMUNITY

Light. In the dark, the range-weighted richness was significantly lowest (KWT; $p<0.0001$; n=84) while the dynamics was significantly highest (KWT; p=0.0158; n=68) as compared to the light treatments. When developing at medium and high LI, young as well as matured biofilm showed increasing richness while the dynamics decreased (Table 18, Figure 35, Figure 36). Furthermore, the functional organization of the bacterial community stagnated throughout the experiments and biofilm

development in the dark, while the bacterial communities at medium and high LI increased in their specialization leading to significantly higher mean values in matured biofilm (KWT; p=0.0026; n=82, Figure 37).

Hydrodynamics. The bacterial communities were clearly influenced by the different flow velocities. The range-weighted richness (Rr) was significantly lowest at the high BSS (KWT; p<0.0001; n=84) to display increasing values for low and medium BSS (Figure 35, Table 19). In young and matured biofilm, the dynamics of the bacterial communities increased significantly with increasing BSS, while the functional organization was only enhanced in young biofilm over the range of different BSS (KWT; p<0.0001; n=96) (Table 19, Figure 36, Figure 37).

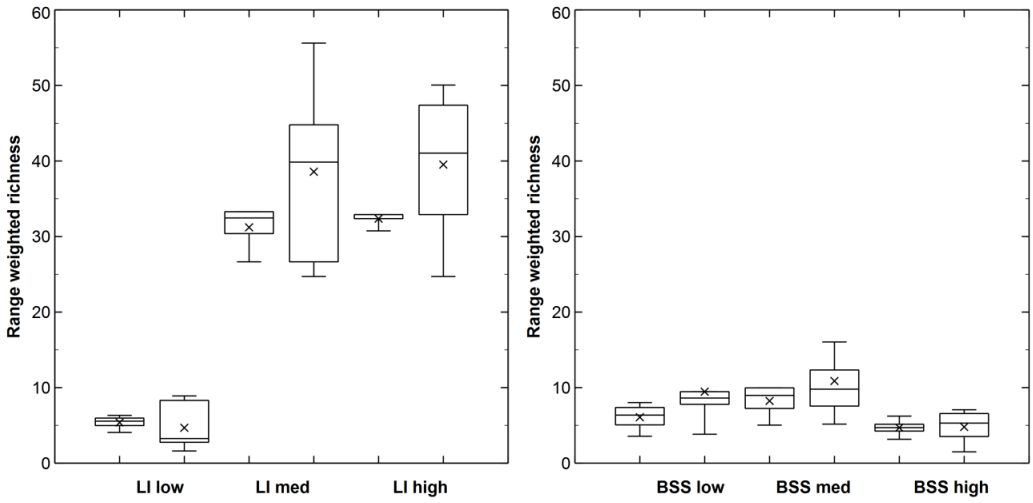

Figure 35: *Range-weighted richness (Rr) of early and late biofilm stages. Left: at different levels of LI; right: at different levels of BSS. Source: Schmidt et al. 2018 Research and Reports in Biology.*

Species Composition. Analysis of the 211 prominent bacterial DGGE bands/sequences yielded 77 different bacterial species. Microbial organisms generally considered as typical generalists and widely spread were detected in various seasons tested and at all different boundary conditions.

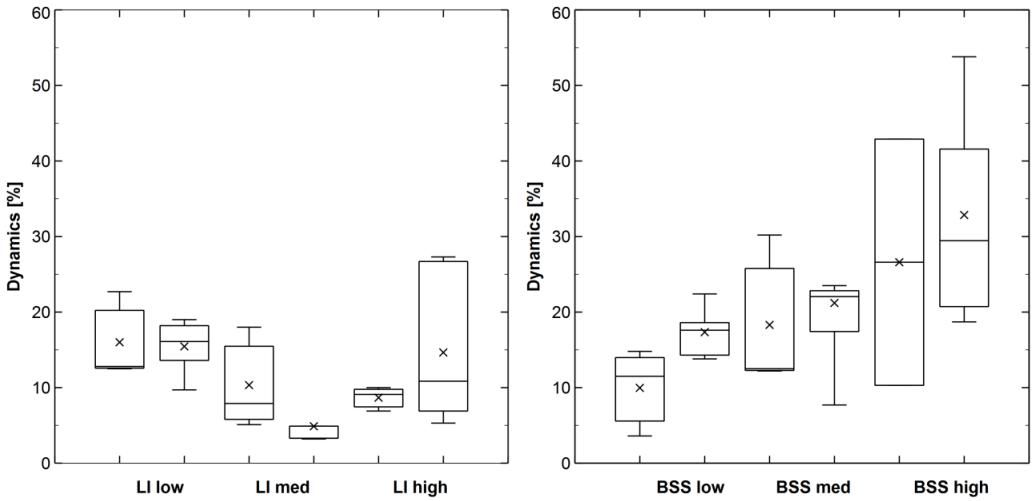

Figure 36: *Dynamics (Dy) of the bacterial community of early and late biofilm stages. Left: at different levels of LI; right: at different levels of BSS. Source: Schmidt 2017 PhD Thesis University Stuttgart*

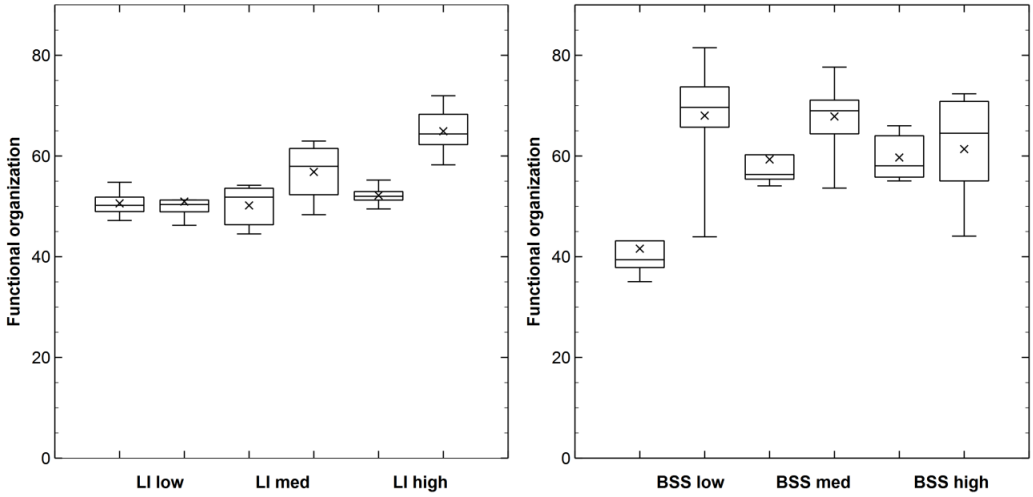

Figure 37: *Functional organization (Fo) of the bacterial community of early and late biofilm stages. Left: at different levels of LI; right: at different levels of BSS. Source: Schmidt 2017 PhD Thesis University Stuttgart.*

Apart from ubiquitously distributed species such as *Aquabacterium sp*. (Kalmbach *et al.*, 1999), *Brevundimonas diminuta* (Vancanneyt *et al.*, 2009) or *Gemmatimonas phototrophica* (Zeng *et al.*, 2015b, 2016) that were always detected in spring, four species dominated in biofilm grown at high light intensity: *Rubrivivax gelatinosus* (Wawrousek *et al.*, 2014) and *Rhodoferax saidenbachensis* (Kaden *et al.*, 2014) in early stages, *Neosynechococcus sphagnicola* (Dvorak *et al.*, 2014) and *Leptolyngbya sp.* (Kanellopoulos *et al.*, 2016) in matured biofilm. In contrast, the different levels of

shear stress displayed no significant influence upon the bacterial community composition - except for *Pseudomonas taeanensis* that appeared in higher proportions in biofilm cultivated at high flow velocity.

VI.4.5. DIATOM COMMUNITY

In total, 13 different diatom genera were present in relative abundances greater than 3% in the investigated biofilm. Among these, four different genera - *Fragilaria, Sellaphora, Nitzschia* and *Achnanthidium* appeared to dominate the biofilm in variable abundance ratios.

Light. The most apparent impact of the applied different levels of light intensity (LI) was, not surprisingly, the absence of algal development in dark conditions. Late biofilm stages were always dominated by a variable combination of *A. min*., *S. sem.* and members of the genus *Fragilaria* - mainly *Fragilaria construens* and *Fragilaria pararumpens* (*F. par*.) (Figure 38): *A. min.* clearly dominated biofilm grown at medium LI with a relative proportion of 65.2 ± 5.1% while *S. sem.* had the second biggest share of 24.7 ± 3.3%. In late biofilm which grew at the high LI, *A. min.* and *F. par.* both constituted the majority of the diatom community (44.6 ± 2.7% and 37.2 ± 3.3%, respectively) (Figure 38). The increasing dominance by a few species was reflected by decreasing diversity (Shannon index) and evenness of the diatom communities at medium and high LI (Table 20).

Table 20: *Growth and functionality of biofilm grown at different levels of light intensity: mean values given for microbial parameter and adhesiveness, both for the different stages of young (early) and matured (late) biofilm. N=non-significant, S=significant. Source: Schmidt et al. 2018 Research and Reports in Biology.*

		Darkness		Medium LI		High LI		Significance
		Early Day 0-18	Late Day 21-35	Early Day 0-18	Late Day 21-35	Early Day 0-18	Late Day 21-35	
EPS	**Carbohydrates [µg*gDW^{-1}]**	15.7 ± 7.1	10.3 ± 4.3	18.8 ± 9.1	23.6 ± 7.6	10.7 ± 5.8	20.3 ± 13.4	S
	Proteins [µg gDW^{-1}]	4.0 ± 2.1	6.1 ± 0.9	2.7 ± 1.5	8.4 ± 3.1	3.9 ± 3.5	10.2 ± 6.1	S
Biomass	**Chlorophyll a [µg gDW^{-1}]**	0.0 ± 0.0	0.1 ± 0.0	0.1 ± 0.1	2.4 ± 2.9	0.3 ± 0.2	3.7 ± 4.4	S
	Bacterial cells [*10^{7} gDW^{-1}]	0.8 ± 0.3	1.3 ± 0.7	0.4 ± 0.3	3.0 ± 0.9	1.5 ± 1.0	4.3 ± 4.0	S
Bacterial community	**Range-weighted richness**	5.4 ± 0.9	4.3 ± 2.8	31.2 ± 2.9	38.6 ± 11.1	32.4 ± 1.0	39.5 ± 9.0	S
	Functional organization	50.6 ± 2.9	50.9 ± 4.1	50.2 ± 4.5	56.8 ± 5.5	52.2 ± 2.2	64.9 ± 4.6	S
	Dynamics	16.0 ± 5.2	15.6 ± 3.4	10.3 ± 6.1	4.9 ± 2.6	8.7 ± 1.4	14.7 ± 9.4	S
Diatom community	**Shannon Index**	*	*	3.3 ± 0.2	1.0 ± 0.1	2.7 ± 0.2	1.4 ± 0.2	N
	Evenness	*	*	0.9 ± 0.1	0.4 ± 0.2	0.7 ± 0.1	0.5 ± 0.1	N
Biofilm Stability	**Adhesiveness [mA]**	71.2 ± 11.0	73.6 ± 28.4	55.5 ± 12.7	675.9 ± 837.8	58.0 ± 17.3	1001.7 ± 994.1	S

** at darkness, no significant algal development could be observed*

Table 21: *Growth and functionality of biofilm grown at different levels of bed shear stress: mean values given for microbial parameter and adhesiveness, both for the different stages of young (early) and matured (late) biofilm. N=non-significant, S=significant. Source: Schmidt et al. 2018 Research and Reports in Biology.*

		Low BSS		**Medium BSS**		**High BSS**		**Significance**
		Early Day 0-18	**Late Day 21-35**	**Early Day 0-18**	**Late Day 21-35**	**Early Day 0-18**	**Late Day 21-35**	
EPS	**Carbohydrates [µg gDW^{-1}]**	12.9 ± 6.1	21.6 ± 8.5	13.6 ± 6.7	26.3 ± 8.1	7.1 ± 5.0	23.6 ± 10.9	N
	Proteins [µg gDW^{-1}]	10.2 ± 9.6	33.1 ± 10.2	13.4 ± 6.3	31.5 ± 13.2	4.5 ± 3.2	29.8 ± 8.0	S
Biomass	**Chlorophyll a [µg gDW^{-1}]**	0.3 ± 0.3	6.9 ± 6.5	0.5 ± 0.5	5.9 ± 3.6	0.2 ± 0.2	3.6 ± 3.0	N
	Bacterial cells [*10^7 gDW^{-1}]	1.8 ± 2.3	4.7 ± 3.7	1.6 ± 1.9	6.1 ± 2.7	0.6 ± 0.6	4.6 ± 1.7	N
Bacterial community	**Range-weighted richness**	6.1 ± 1.8	9.5 ± 6.2	8.2 ± 2.2	10.9 ± 5.0	4.7 ± 1.2	4.8 ± 2.3	S
	Functional organization	41.6 ± 7.0	68.0 ± 11.4	59.3 ± 7.0	67.9 ± 7.3	59.7 ± 5.1	61.4 ± 12.0	S
	Dynamics	10.0 ± 5.1	17.3 ± 3.3	18.3 ± 9.2	21.2 ± 9.1	26.6 ± 18.8	32.9 ± 15.0	S
Diatom community	**Shannon Index**	1.8 ± 0.1	1.7 ± 0.8	3.1 ± 0.2	2.8 ± 0.8	2.6 ± 0.1	2.1 ± 0.3	N
	Evenness	0.5 ± 0.1	0.5 ± 0.2	0.8 ± 0.1	0.8 ± 0.2	0.8 ± 0.1	0.7 ± 0.1	N
Biofilm Stability	**Adhesiveness [mA]**	72.9 ± 47.3	810.3 ± 1044.6	73.5 ± 50.4	435.0 ± 316.7	84.8 ± 55.4	340.6 ± 270.8	N

Hydrodynamics. Biofilm cultivated at the low BSS were clearly dominated by *A. min.* with mean relative proportion of 52.0 ± 3.6% in early biofilm and 59.4 ± 4.2% in late biofilm. This strong dominance was also reflected by the lowest mean diversity and evenness (Table 21). At increasing BSS, the genus *Nitzschia* - mainly *Nitzschia fonticola, Nitzschia abbreviata* and *Nitzschia dissipata* - increased proportionally in matured biofilm: with 9.9 ± 0.2% in biofilm cultivated at low BSS up to 24.9 ± 3.3% and 40.8 ± 3.5% grown at medium and high BSS, respectively. Interestingly, the genus *Nitzschia* was less prominent in the experiments with varying light intensities. *S. sem*. reached a mean relative share of 22.1 ± 3.3% which was similar to the members of the genus *Nitzschia* in matured biofilm at medium BSS (see Figure 39).

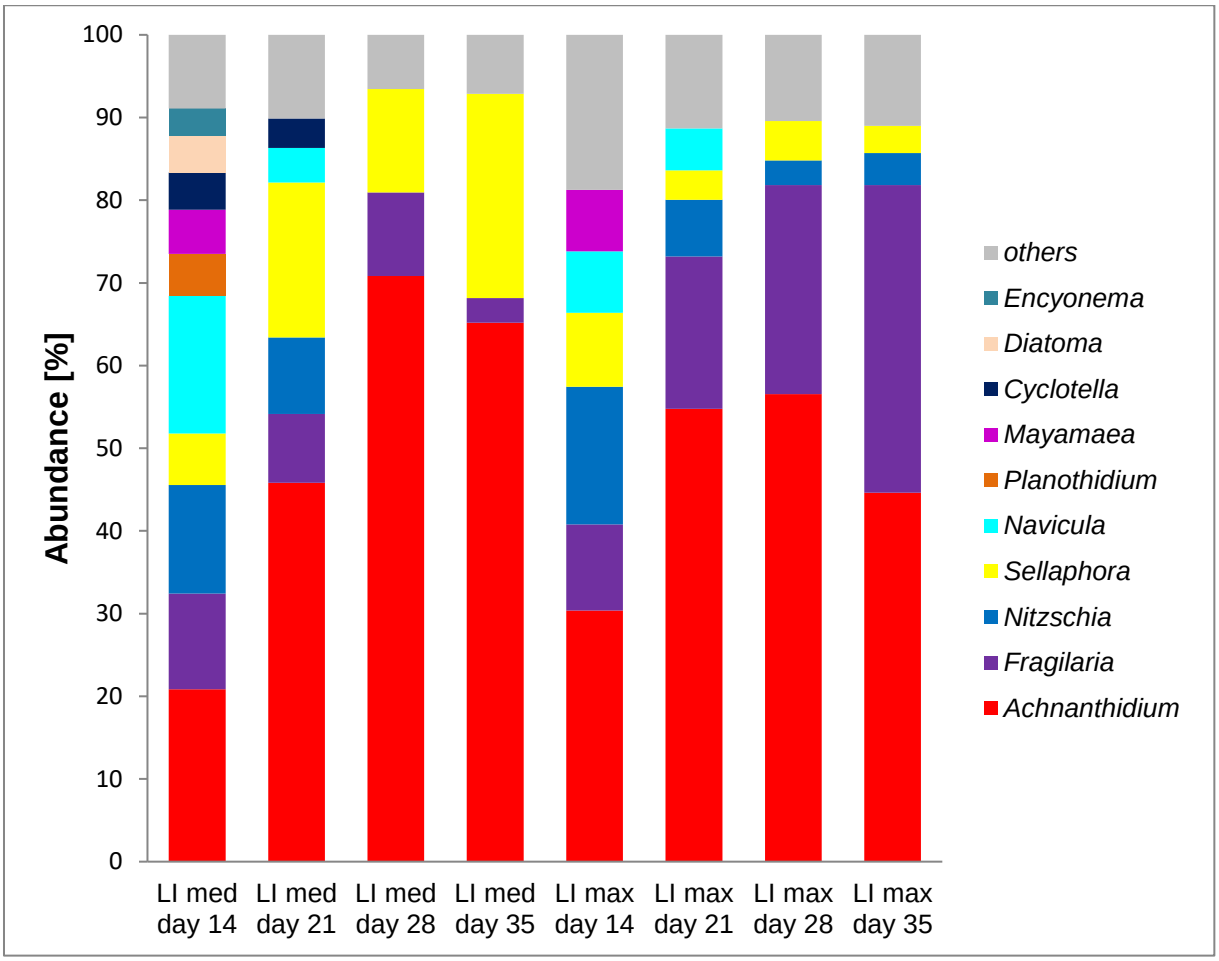

Figure 38: *Temporal development of the diatom community at medium and high light intensities (LI) at the days 14, 21, 28 and 35. Note: no microalgal growth could be detected at darkness. Genera with relative proportions less than 3% are summarized as "others". Source: Schmidt 2017 PhD Thesis University Stuttgart.*

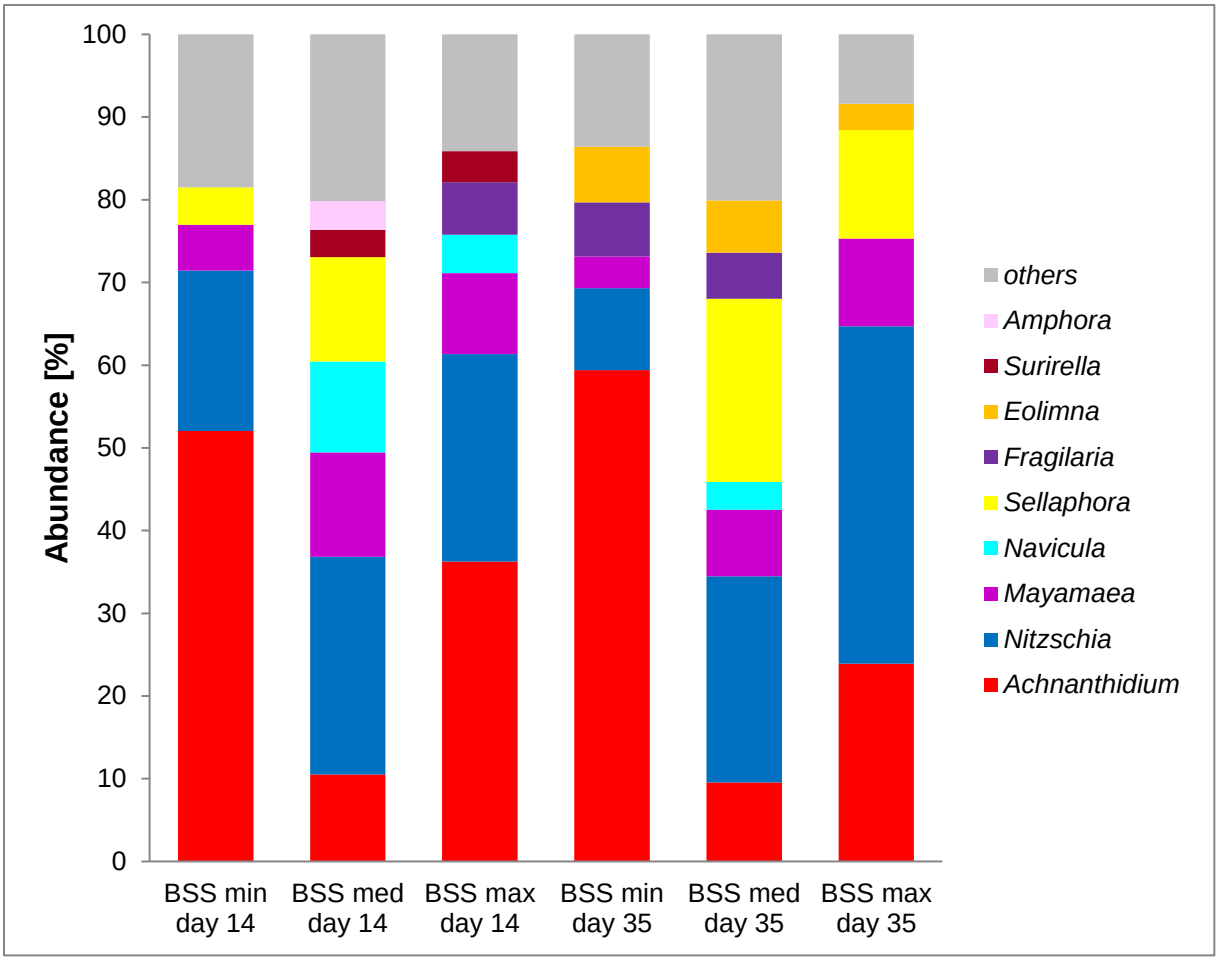

Figure 39: *Composition of early (day 14) and late (day 35) diatom communities at different levels of bed shear stress (BSS). Genera with relative proportions less than 3% are summarized as "others". Source: Schmidt et al. 2018 Research and Reports in Biology.*

VI.4.6. BIOFILM ADHESIVENESS

While initial levels of adhesiveness were very similar in all early biofilm stages (mean values of approximately 70.0mA), the highest increase and mean adhesiveness in late biofilm stages could be detected in biofilm grown at highest level of LI (1001.7 ± 994.1mA) and at lowest BSS (810.2 ± 1044.6mA) (Figure 40).

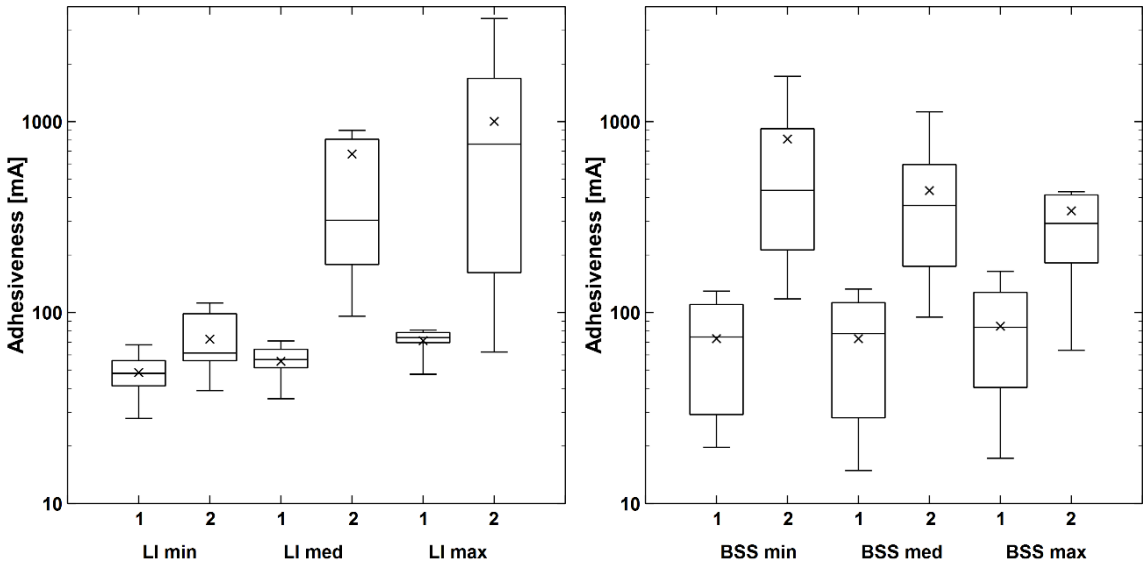

Figure 40: *Adhesiveness of early (1) and late (2) biofilm stages. Left: at different levels of light intensity LI. Right: at different levels of bed shear stress (BSS) (logarithmic ordinate). Source: Schmidt et al. 2018 Research and Reports in Biology.*

VI.4.7. BIOFILM STABILITY

Figure 41 and Figure 42 illustrate the temporal development of the biofilm stability, expressed as the critical shear stress needed to erode the biofilm, for two replicate flumes each that were run at the same boundary conditions over the different experiments and seasons. Like with the values on adhesiveness, the biofilm stability is largely comparable to abiotic sediments in the beginning (first two weeks) of the experiments to increase thereafter (with the exception of the July experiment at high light conditions, Figure 42). It has to be noted that the high heterogeneity of the biofilm growth partially gives quite remarkable differences in the critical shear stress despite identical boundary conditions (e.g. after six weeks in May at low BSS, Figure 41). This variability in biofilm development and appearance in the later stages as well as the mode of erosion might be responsible for the observed differences in the entrainment behaviour between single cartridges and flumes (Figure 41, Figure 42).

For the biofilm stability values, the biostabilization index (BI) was also calculated after

Manzenrieder (1985) as the ratio between the critical bed shear stress of the biostabilized sediment and the abiotic reference (here: $\tau_c = 0.23\ N/m^2$):

$$\mathrm{BI} = {}^{\tau_{c,bio}}/_{\tau_c}$$

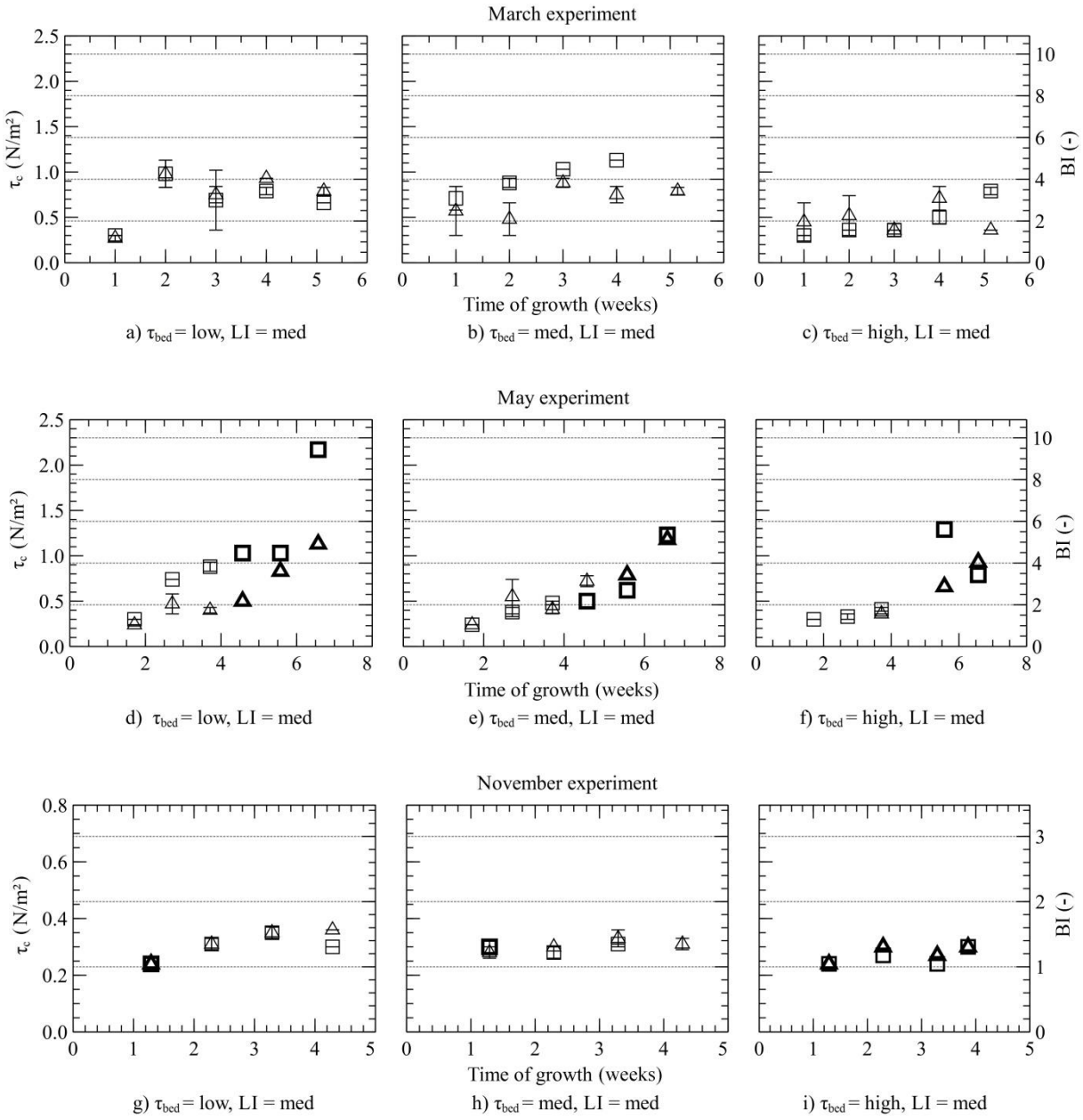

Figure 41: *The impact of hydrodynamics on the biofilm stability at spring (March and May 2013) and autumn (November 2013). The critical shear stress of erosion [T_{crit}] and BI is determined by eroding four cartridges from two flumes run at the identical boundary conditions. Each graph shows the data from two flumes (flume A triangles n=2 and flume B squares n=2) separately, but thicker symbols indicate the availability of only one cartridge. The light intensity has been constant at 50µE m^{-2} s^{-1} while the bed shear stress level varied. Source: Thom et al. 2015a International Journal of Sediment Research.*

The results of the experiments indicated ranges of the biostabilization index between 1 (no effect), 1–2 (first two weeks) and app. 10 (a tenfold increase of sediment stability in later biofilm stages) depending on applied boundary conditions and the investigated season.

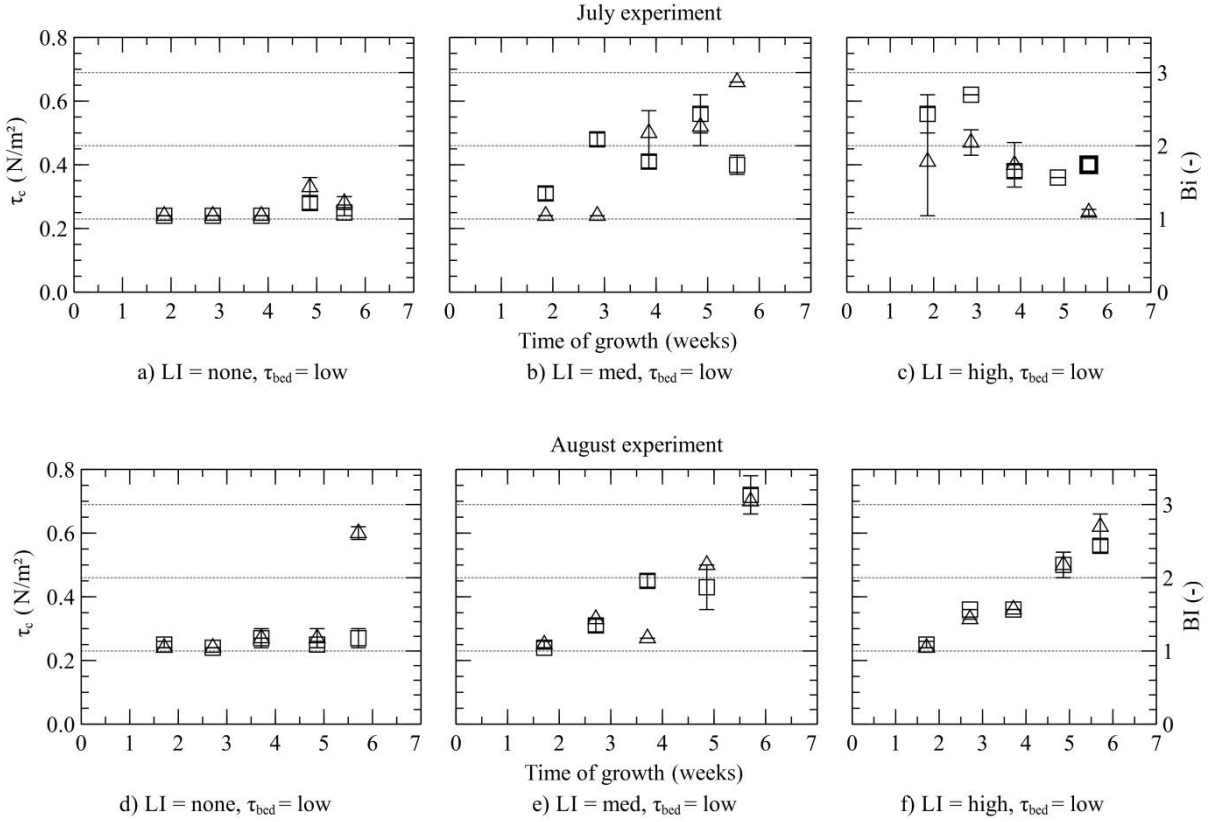

Figure 42: *The impact of light on the biofilm stability addressed in two summer experiments (July and August 2013). The critical shear stress of erosion [T_{crit}] and BI is determined by eroding four cartridges from two flumes run at the identical boundary conditions. Each graph shows the data from two flumes (flume A triangles n=2 and flume B squares n=2) separately, but thicker symbols indicate the availability of only one cartridge. The bed shear stress has been constant at 0.02Nm^{-2} while the light intensity varied. Source: Thom et al. 2015a International Journal of Sediment Research.*

VI.5. DISCUSSION

The mutual feedback mechanism between the microbial colonies and the present boundary conditions are decisive for microbial attachment, subsequent biofilm development and resulting functionality such as biostabilization. Changing one by one the two most influential parameters, that is light intensity and hydrodynamics, the

resulting net effects seemed to be easily assignable to the prevailing and controllable settings. However, the biochemical parameters such as microbial biomass or the functions such as adhesiveness that we measured were first of all impacted by the microbial community composition. The latter is strongly influenced by various complex interactions that go well beyond the addressed abiotic parameters, i.e. biotic conditions such as the competition of different taxa and species or prey-predator chains and grazing losses. This is the reason why this chapter includes as well an extended analysis of the bacterial and microalgal community in order to follow-up the identification of functional key players.

VI.5.1. ILLUMINATION INTENSITY AND NUTRIENTS

Light intensity on the sediment surface changes with shading riparian plants, macrophytes, water depth, turbidity and, last but not least, with the seasonally varying day/night cycle. While it is intuitive to assume that darkness supports a biofilm consisting solely of heterotrophic bacteria, the effects on biofilm functionality are less certain. In contrast to earlier work (Gerbersdorf *et al.*, 2008b, see chapter III) where the heterotrophic bacterial community stabilized the substratum in marine nutrient-rich waters significantly, the present experiments with oligotrophic freshwater gave no hints on the substantial influence by biofilm in the dark. However, in one summer experiment (Figure 42), a significant increase in stability was detected on the last measuring day. That could indicate that the bacterial community in the present experiments needs more time to develop and this might be directly linked to the low nutrient availability. The importance of nutrient limitation for riverine biofilm was recently demonstrated via a large comprehensive set of field experiments, where the type of land use and resulting nutrients runoff affected biofilm productivity (Reisinger *et al.*, 2016). However, the way in which nutrient competition between different

species and taxa impacts the community composition of biofilm is barely addressed. Jackson et al. (2001) suggested that resource competition may not be the primary driving force for the development of the bacterial community. However, the author´s own studies indicated that heterotroph bacteria do profit from sufficient nutrient supply with high metabolic rates and very fast development of their population, especially when microalgae are absent (Gerbersdorf *et al.*, 2009). That seems to be related to some competition for nitrogen, phosphorus and available organic carbon between bacteria and microalgae in the initial growth phase (Havskum *et al.*, 2003). In the presence of microalgae, bacterial growth was delayed but whether this is due to nutrient competition or active suppression by bactericidal compounds is still a matter of debate (Gerbersdorf *et al.*, 2009). The present study showed indeed partially lower bacterial cell numbers of young biofilm in the presence of light and developing diatoms but this was not consistent in all replicate flumes.

With increasing light intensity, the diatom-dominated microalgal community showed corresponding increases in their biomass. Although some studies emphasized that illumination is the most important driving factor for the development of the algal community structure (Lange *et al.*, 2011; Bowes *et al.*, 2012), the uptake of nutrients is equally important to further support photosynthesis and building up organic matter (e.g. Xin *et al.*, 2010; Prieto *et al.*, 2016). In this context, the attachment form of the algal cells was demonstrated to be of major importance since biofilm morphology and nutrient uptake influence each other in a complex reciprocal relation (Mulholland *et al.*, 1994). In the nutrient-poor to medium-rich waters of the River Enz erected species might have much better access to nutrients from the water column in contrast to species living adnate to the surface (Riber & Wetzel, 1987; Paul & Duthie, 1989; Burkholder *et al.*, 1990; Mulholland *et al.*, 1994). Other species adapt to this disadvantage by faster reproduction and the ability to colonize new habitats very

quickly, before they are suppressed by later successional stages which are more competitive (Peterson, 1996). In the present study, pioneering small diatom species, such as permanently attaching *Achnanthidium minutissimum*, had a competitive advantage on the fresh, un-colonized sediment surfaces due to their faster reproduction and possibly, their erected form. In contrast, later succession stages were rather dominated by larger and motile *Nitzschia* species. While it seems obvious that different life styles and attachment forms have an essential impact upon the overall biofilm stability, it is not clear yet whether rather flat-attaching microalgae species (Poff & Ward, 1995) or erected species (Schmidt *et al.*, 2016) exhibit greater resistance to mechanical forces. All overall, the species diversity was reduced compared to the natural setting, which might be due to the closed experimental setup without regular input of fresh natural water and replenishment by nutrients. This is similar to what has been described by Law et al. (2014) where two diatom species were dominant in oligotrophic conditions despite a high natural biodiversity. Interestingly, one cyanobacteria *Leptolyngbya* dominated in the present experiment with the ability to fix atmospheric nitrogen (Havens *et al.*, 1996).

Adhesiveness and biostabilization both increased with light and diatom development significantly. That supports the concepts from marine studies that claim the significant link between photosynthetic activity and microalgal EPS secretion - the latter being the driving factor for the observed biostabilization (Smith & Underwood, 2000; Orvain *et al.*, 2003). However, microalgae are not the only functional key players and the bacterial cell numbers eventually increased as well with enhanced light levels in the matured biofilm. Apart from substantial amounts of EPS secreted by heterotroph bacteria, the latter have a strong regulatory role on EPS quality and quantity produced by diatoms through their mineralization activity (Sack *et al.*, 2014; Agogué *et al.*, 2014). Thus, the complex interactions between autotrophic and heterotrophic

microbes have to be taken into account as they shape the overall biofilm system, the EPS matrix and finally biofilm functionality and biostabilization.

At the highest applied light intensity of about 100 $\mu Em^{-2}s^{-1}$, the present experiments did not gave any hint that too much light might decrease sediment stability although photosynthesis-driven oversaturation of oxygen and bubble formation has been observed as it is reported from other studies (Sutherland *et al.*, 1998a).

VI.5.2. THE IMPACT OF THE HYDRODYNAMIC REGIME

Hydrodynamic boundary conditions affect biofilm growth and biostabilization in complex ways by influencing the settlement of suspended microbes on the substratum and their subsequent attachment, the availability of nutrients, and the erosion (or detachment) of biofilm aggregates. In the initial phase of biofilm formation, the number of cells getting into contact with the sediment surface increases with higher turbulence intensities (Stoodley *et al.*, 1999a). In contrast to this, their attachment efficiency is reduced by higher bed shear stress (Bryers & Characklis, 1981); consequently, net attachment (difference between cells getting into contact with the surface and cells detached by the hydrodynamic forces) is also reduced. This is obviously despite the fact that bacterial cells can initiate within seconds multiple reversible bindings that later would trigger irreversible attachment (Hoffman *et al.*, 2015). In laboratory studies Stoodley et al. (1999a) confirmed that the colonization rate of bacteria was much higher in laminar flow than at turbulent conditions (and obviously higher than the detachment), resulting in an earlier development of biofilm. Although established bacterial biofilm may be able to react to present levels of shear stress and adapt their morphology (Peyton & Characklis, 1993; Choi & Morgenroth, 2003), the initial settlement is highly sensitive (Lemos *et al.*, 2015). This “conditioning layer” of bacterial pioneers is also essential for a

subsequent settlement of larger microbes such as diatoms (Blenkinsopp & Lock, 1994; Roeselers *et al.*, 2007). Consequently, high levels of shear stress can strongly delay the formation of natural complex biofilm on bare un-colonized sediment as it was reported by Coundoul et al. (2015) as well as Graba et al. (2013). These observations were confirmed in the present study while showing for the first time the impact of delayed biofilm growth on biostabilization capacity.

After settlement, the rate of biofilm growth depends on the availability of nutrients and substrate, along with light quantity and quality for photoautrotrophic biofilm as discussed above. Therefore, nutrients must be transported to the biofilm surface, and transport is significantly influenced by the near-bed turbulence. Increasing turbulence intensities reduces the thickness of the viscous benthic boundary layer (Characklis & Cooksey, 1983) and accelerates the mass transfer of nutrients from the overlaying water column (Horn & Hempel, 1998; Holtappels & Lorke, 2011) - especially mass transfer rates into and within biofilm voids (Rasmussen & Lewandowski, 1998). This diffusion limitation may be one reason why very thick biofilm (Rasmussen & Lewandowski, 1998) or biofilm developing in waters with low flow velocities tend to develop filamentous structures called “streamers” which undulate to increase turbulence and transport rate of nutrients to the biofilm cells (Stewart, 2012; Gashti *et al.*, 2015). On the other hand, high levels of shear stress on the sediment and biofilm surface can constitute a stressor for biofilm formation. Exceeding the critical shear stress level leads to bacterial detachment (Fink *et al.*, 2015) and was shown to promote biofilm erosion/sloughing-off phenomena (Moreira *et al.*, 2015). Considering these ambivalent impacts, a medium level of flow velocity appears to constitute an optimal situation for biofilm growth (sufficient nutrient supply and tolerable shear forces). This "trade-off" between enhanced mass transfer and possibly detachment (Stewart, 2012) at higher hydrodynamic stress is expected to result in a more or less

constant rate of biostabilization for matured biofilm as supported by the results of Fang et al. (2014). However, in the present study, the stability was still increasing over the experimental time which might support the initial conclusion that the biofilm did not reach full maturation over the monitored four to eight weeks.

VI.5.3. POSSIBLE KEY PLAYERS FOR BIOSTABILIZATION

The majority of bacterial species were found to be of the “generalist type” being independent of boundary conditions and within biofilm of varying biostabilization. However, a comprehensive investigation of the microbial community composition across the different seasons and boundary conditions revealed distinct dominance patterns that gave hints to possible key species in biostabilization. In biofilm with high stability indeces, a variable combination of six different bacteria dominated the community. Among these six organisms were two cyanobacteria - *Leptolyngbya sp.* and *Pseudoanabaena biceps,* two alpha proteobacteria - *Paracoccus aminophilus* and *Rhodobacter capsulatus* - and two beta proteobacteria - *Rhodoferax saidenbachensis* and *Rubrivivax gelatinosus.* Interestingly, these species were of minor relevance or even absent in biofilm with lower biostabilization capacity, where the following three bacterial species prevailed: *Pseudomonas fluorescens*, *Pseudomonas taeanensis* and *Caulobacter vibrioides*.

All bacterial species which were dominant in very stable biofilm had at least one of two common features: they were either phototrophic and/or had very versatile metabolisms. Besides the two cyanobacteria of the genus *Leptolyngbya* and *Pseudoananaena*, *Rhodobacter capsulatus* was shown to be capable of anoxic photosynthesis, N-fixation and various other metabolic pathways including different types of respiration (Tichi & Tabita, 2001). In addition, *Rubrivivax gelatinosus* was described as a very fast growing facultative photoheterotrophic microorganism

(Wawrousek *et al.*, 2014). *Paracoccus aminophilus* and *Rhodoferax saidenbachensis* can be considered as very adaptable microorganisms with a broad range of different respiration pathways (Urakami *et al.*, 1990) and the ability to utilize various algal secondary metabolites such as sugar alcohols (Kaden *et al.*, 2014) which can be considered as constantly present in the EPS matrix due to secretion by algal cells or as a result of cell death and lysis. This metabolic versatility might be an essential prerequisite for these microbes to utilize different niches, e.g. gradient zones, in the biofilm system which became increasingly complex due to diatom development. In this context, it is interesting to note that *Rubrivivax gelatinosus* apparently dominated early and maturing biofilm developing at high illumination intensity up to a point where diatom proliferated in the system. In matured biofilm *Rubrivivax gelatinosus* was apparently outcompeted which was clearly visible on DGGE fingerprints. This replacement may be a result of the increasing competition for light as primary energy source due to the multiplying diatoms and other phototrophic bacteria like the detected cyanobacteria. However, besides other bacterial species, *Rubrivivax gelatinosus* might play an essential role in conditioning the sediment surface facilitating subsequent diatom settlement and development as described for other heterotrophic bacteria (Roeselers *et al.*, 2007).

Moreover, the fast growth and the potential for high EPS production of *Rhodobacter capsulatus* and *Paracoccus aminophilus* (Onder *et al.*, 2010; Brimacombe *et al.*, 2013; Dziewit *et al.*, 2014) may lead to a solid biofilm fundament tightly attached to the sediment grains - especially in crucial early development stages. This could be of major structural importance for the overall biofilm system and lead to higher biofilm stability. Considering these structural aspects, the two detected dominant cyanobacteria might also be of high relevance as they form long filaments which are up to 5mm long (Kanellopoulos *et al.*, 2016). On one hand, these extended chains of

single cells constitute an option to increase micro-turbulence and availability of nutrients. On the other hand, these fibers can act as anchor points for settling cells and can be linked and tangled up to further increase the stability of the overall biofilm network.

In contrast to biofilm displaying very high stability, biofilm with low biostabilization capacity were dominated by bacteria of the genus *Caulobacter* or *Pseudomonas,* both exhibiting high motility. This feature is essential for fast colonization of favorable substrates and new nutrient resources (de Weert *et al.*, 2002). However, the lifestyle of the *Caulobacter vibrioides* might decrease overall biofilm stability as the anisomorph reproduction cycle with staked and swarmer cells (Henrici & Johnson, 1935) can be assumed to lead to a steadily shifting, comparably unstable cover with bacterial cells as opposed to a colonization by immotile bacteria such as *Paracoccus aminophilus* which forms stable clusters of cells (Urakami *et al.*, 1990). The swimming behaviour of the two dominant monotrichous *Pseudomonas fluorescens* and *Pseudomonas taeanensis* was described as very similar to *Caulobacter* specimen (Ping *et al.*, 2013). However, in contrast to *Caulobacter*, the flagellum is of major importance for *Pseudomonas* in order to adhere to the surface as an initial step of biofilm formation (Mastropaolo *et al.*, 2012). Decoin et al. (2015) could demonstrate the link between the production of flagellum compounds such as flagellin and antimicrobial agents which suggests that both motility and antibiotics secretion enhances competitiveness. The well-described chemical warfare against competing bacteria by different members of the genus *Pseudomonas* (Raaijmakers *et al.*, 1997) may effectively delay the maturation of the biofilm as well as biostabilization. Subsequently, when the biofilm system gradually changes by the development of algae, *Pseudomonas* might be able to even increase their antibiotic production by the usage of the algal secondary metabolites such as sugar alcohols

(Duffy & Défago, 1999). It can be only speculated whether this further impacts bacteria living in symbiosis with algae (Amin *et al.*, 2012), but shifts in community composition and consequences for biofilm functionality are highly likely.

VI.6. CONCLUSIONS

This study demonstrated a significant impact of the investigated abiotic boundary conditions (light intensity and bed shear stress) on biofilm development. Besides having a clear effect on microbial biomass, produced EPS, and the microbial community composition, the environmental conditions significantly influenced biostabilization. At dark conditions, the biostabilization increased but was still negligible over the observed period of time which might be the result of slower development of heterotroph bacteria in the oligotrophic setting. It further emphasized the important role of autotrophic microalgae for stabilizing the substratum. The highest BSS caused a general delay in biofilm formation and biostabilization since the initial microbial settlement, especially of microalgae, was apparently hampered. However, bacteria could adapt faster to the highly dynamic habitat than microalgae.

The results allow first insights into the role of different microbial key players and their respective mode of life during the process of biostabilization. In biofilm with the highest stability, the dominant species among bacteria and diatoms were sessile and/or had the capacity to produce high amounts of EPS adhesives. This lifestyle directly correlates to fast reproduction and colonization of freshly exposed sediment surfaces and may have directly enhanced the stability of the biofilm as well as the underlying fine sediment. The least stable biofilm were dominated by opportunistic, very flexible microbes often associated with later successional stages. These microorganisms displayed a high mobility and/or the potential for elaborated forms of chemical warfare. Generally, these species may be able to profit from opportunistic

strategies in many different natural niches. However, their dominance apparently had adverse effects on other microbes as well as on the overall integrity and stability of the biofilm matrix. This observation may reflect the unstable, ever changing nature of a matured biofilm system which is characterized by a constantly high degree of attachment and detachment as well as biological, chemical and structural reorganization.

All of the observed shifts in microbial community composition and processes resulted in different mechanical structures and types of erosion that need to be better understood and studied in order to develop a suitable model for predicting the erodibility of biostabilized sediments.

VII. Magnetic Particle Induction - MagPI: A promising Tool to determine Adhesive Capacity of Biofilm on the Mesoscale

VII.1. Abstract

The MagPI system consists of an electromagnet that attracts ferromagnetic particles from a surface and the force needed to retrieve those particles is equivalent to the surface adhesiveness. Ubiquitously distributed biofilm have a highly adhesive surface and their stickiness is clearly linked to biofilm stability - an issue that is significant in many areas such as ecology, biotechnology or medicine. It is thus important to allow determinations on biofilm stability and their possible detachment at high temporal and spatial resolution, as provided by MagPI measurements. In this work several technical aspects were addressed that are relevant to further improve the performance of this powerful experimental approach.

Several electromagnets were built as the main element of a thorough MagPI investigation to demonstrate the influence of material and geometry. First, possible remanence of the magnetic core demanded a proper choice of the core material such as permalloy due to its absent residual magnetism and better reproducibility of the results. Second, the influence of number of turns of copper thread around the core (solenoid) has been addressed concerning magnetic field strength and saturation level to build electromagnets of different strengths for different stages of biofilm growth and adhesion. To ensure correct calibration and best comparability of quantitative data, another focus was on the driving force that lifts up the particles. In general, the magnetic force is proportional to the magnetic field gradient at the position of the particle and its magnetic dipole moment. For the particles that are applied for MagPI measurements, this magnetic moment depends on the applied

magnet field strength. Thus both the magnetic field strength and the magnetic field gradient are decisive in the physics of the MagPI approach, and we demonstrated the possibly intricate combination of these two quantities with separate experiments that add permanent magnets to the MagPI electromagnets.

In future, topics such as the automatisation of the measurements, data evaluation as well as the conversion of the uplifting force to conventional units (e.g. Nm^{-2}) should be addressed to further facilitate and enhance the range of MagPI applications.

VII.2. BACKGROUND

VII.2.1. BIOFILM, THEIR ADHESIVE CAPACITY AND HOW TO ADDRESS IT

Microorganisms attach to all kind of interfaces (e.g. water-air, sediment-water) to subsequently organize themselves socially, while flourishing in a self-secreted matrix of polymers ("city of microbes") (Stoodley *et al.*, 2002; Flemming & Wingender, 2010). Biofilm occur almost ubiquitously and fulfill important ecosystem services in the natural environment such as controlling nutrient fluxes, enhancing self-purification, providing carbon to higher trophic levels or stabilizing aquatic sediments (Gerbersdorf *et al.*, 2011). While the positive characteristics of biofilm are deliberately and willingly utilized, for instance in the waste-water treatment process, their negative consequences in biotechnology (e.g. biocorrosion, biofouling) or medicine (e.g. encrustation within catheters, dental plaque, cystic fibrosis) are not to be tolerated (Flemming & Wingender, 2001b; Liu & Fang, 2003; Parsek & Tolker-Nielsen, 2008). Yet, whether aiming at promoting or inhibiting biofilm growth, it is important to learn more about the attachment and development of biofilm.

The existing methods to monitor biofilm growth are mainly based on counting cells, visualizing biofilm components via staining (e.g. Confocal Microscopy), estimating

metabolic activity (e.g. enzyme expression) or more recently, addressing the microbial community composition with modern molecular tools by sequencing entire genomes and transcriptomes (e.g. next generation sequencing) (Wood *et al.*, 2013; Gutleben *et al.*, 2018). Microbial biomass, physiology, the architecture and assemblages are vital parameters to characterize biofilm development; however, there is little information about the adhesive capacity (corresponding to attractive force) and the mechanical properties of a biofilm (Böl *et al.*, 2013). Techniques such as the Atomic Force Microscopy (AFM) or microcantilever methods aim to close this gap by measuring adhesive or tension forces of single cells or biomolecules (Poppele & Hozalski, 2003; Dugdale *et al.*, 2005) and with some successful attempts to apply them on intact biofilm pieces (Aggarwal *et al.*, 2010). Nevertheless, like with rheology (Koza *et al.*, 2009) or centrifugation devices (Ohashi & Harada, 1996), the biofilm needs to be transferred to the testing site with unpredictable changes during transport, mounting and testing (Böl *et al.*, 2013). Furthermore, the extrapolation of these results from the nano- and microscale to predictions on the mechanical resistance or potential failure of the biofilm-mediated matrix at mesoscale remains difficult although in order to, e.g. overcome biofouling or predict biostabilization in sediments, it is this level that one should approach.

Few biofilm studies addressed mechanical failure and sloughing-off in laboratory experiments at the mesoscale: Grün et al. (2016) determined the remaining biofilm dry weight on microscopic slides that were fixed in tubes and exposed to a constant water jet for 30s. While this approach gave first insights, the transferability of the data to growth on natural substratum and *in situ* shear forces comprises some uncertainties. This applies as well to experiments in more natural-like flow-through channel, where the amount of eroded sand/biofilm mixtures was measured after varying water flow and water depth (Pique *et al.*, 2016). Other attempts to directly

address the long-neglected biofilm mechanics on the microscale include the BioFilm Ring Test RT where the mobility of magnetic microbeads within a bacterial suspension was monitored over time (Galy *et al.*, 2014; Olivares *et al.*, 2016). This relatively new technique gives a certain range of biofilm indices between total immobilization of magnetic beads and their free mobility (i.e. no biofilm formed). Yet there is no direct value for the mechanical resilience, and the mixed suspensions are not representative for natural biofilm. In contrast, flume experiments enable the comparison between the erosional resistance of biofilm-colonized and control sediments devoid of biofilm to give enhanced critical shear stress values due to biostabilization, but this approach requires bed failure to occur (Witt & Westrich, 2003; Thom *et al.*, 2015). Consequently, by these erosion tests, it is difficult to detect smallest changes in the adhesive capacity of young growing biofilm.

VII.2.2. MEASURING PROCEDURE BY MAGPI

To address the adhesive capacity of biofilm directly and in high sensitivity as well as in high temporal and spatial resolution, the MagPI system (Figure 43A) has been developed (Larson *et al.*, 2009). With this method, adhesive capacity can be quickly determined at the mesoscale (mm–cm range) leaving a small footprint but covering an area large enough to predict biofilm detachment under certain hydraulic scenarios. For the measurement, ferromagnetic particles are spread on the substratum-biofilm surface, then an electromagnet is positioned above in a well-defined distance (3–15mm, in our experiments mostly 4–5mm) and switched on with gradually increasing current through the coil of the electromagnet (Figure 43).

(A)

(B)

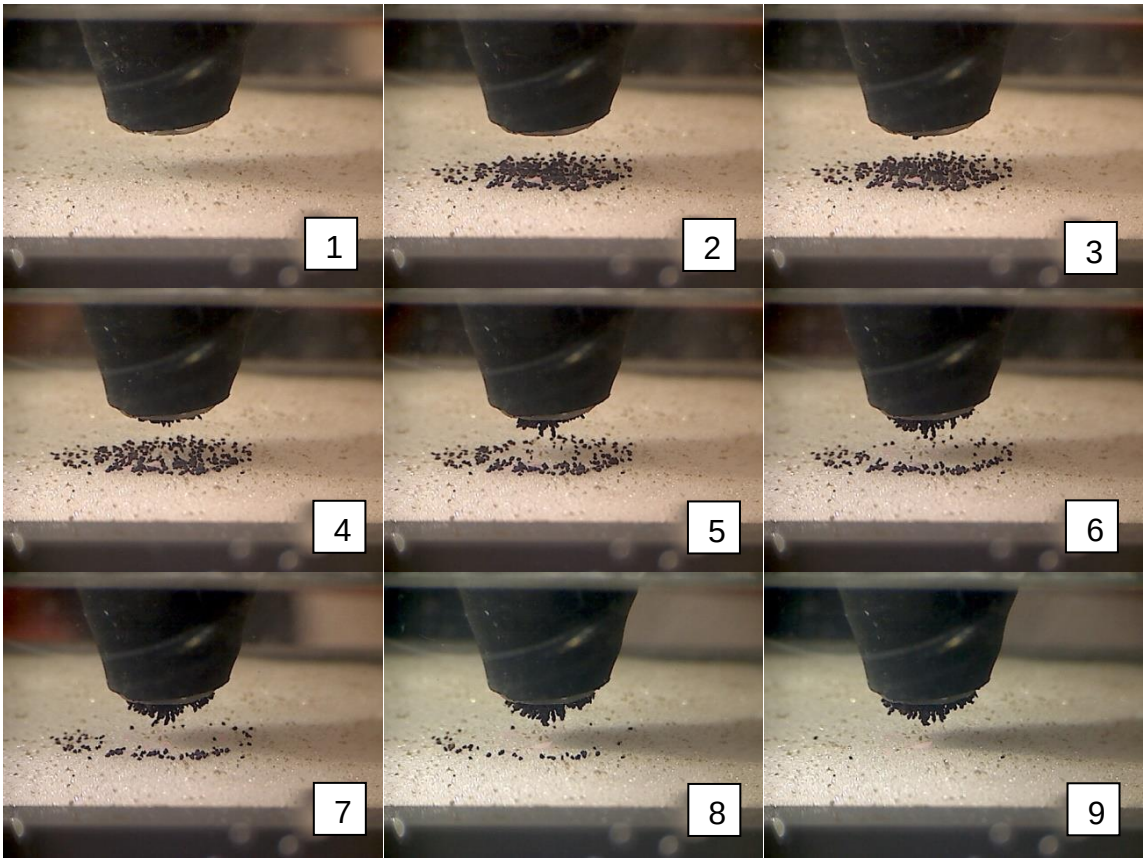

Figure 43: (A) *The setup of the MagPI (from left to right: electromagnet positioned by micromanipulator, multimeter, power supply) and* ***(B)*** *Stepwise attraction of the ferromagnetic particles by the overlying electromagnet (4mm distance from the surface) at increasing currents. Image 3 marks threshold 2 (first particle is attracted), image 4 resembles threshold 3 (few particles attracted) and image 9 indicates threshold 4 (total clearance).*

The force needed by the electromagnet to retrieve the ferromagnetic particles from the sticky biofilm surface is a direct measurement of the adhesive capacity of the biofilm (as described in Larson *et al.*, 2009). This adhesive capacity has been proven

to be significantly correlated to sediment stability or critical shear stress values as determined by CSM and SETEG flume (Lubarsky *et al.*, 2010; Thom *et al.*, 2015). The fundamental criteria that have been tested for the prototype of the MagPI in Larson et al. (2009) are described in the following.

VII.2.3. The Thresholds for Determination of Adhesion Levels

Originally, the MagPI has been constituted to quantify the decisive moment of particle attraction by the electromagnet using the following four thresholds that are already described in II.4.2. (Figure 43B):

Threshold 1–The particles align towards the overlaying electromagnet
Threshold 2–The first particle is attracted by the electromagnet
Threshold 3–Few particles (around 5) are retrieved by the electromagnet
Threshold 4–All particles are retrieved by the electromagnet–total clearance

All thresholds are determined by visual observation of the experimenter. Repeated measurements have shown that threshold T2 might be difficult to determine if particles are placed on top of each other and thus the consequent release of the top particle is not linked to biofilm adhesion. T3 can be highly subjective by the individual observation and varies demonstrably between different appliers. Hence, the focus of the first applications has been initially on T4 that indicates the maximum strength of the biofilm (Gerbersdorf *et al.*, 2009; Lubarsky *et al.*, 2010, 2012). However, also T4 may encounter potential overestimation due to physical trapping (see below). While we are always recording all four thresholds, the focus is currently on option T3. To avoid subjectivity related to threshold definitions in the future, we currently develop an automated image processing where particle surface coverage is monitored at each voltage increment (Thom et al., in prep.).

VII.2.4. Ferromagnetic Particles on Substratum

When measuring in initial stages of biofilm growth, some spots might be still devoid of biofilm and expose the bare substratum (e.g. inert glass beads or cohesive sediment particles). Hence, single ferromagnetic particles might sometimes be physically trapped within the substratum which in turn results in a significant overestimation of T4. Therefore, the ideal size of substratum as well as of ferromagnetic particles has been identified early on (Larson *et al.*, 2009). The ferromagnetic particles (ferrous material for magnetic response and fluorescent coating for visibility, Partrac, Glasgow, UK) were sieved to a size class between 180-250µm (smaller might be easily trapped and not easy to be seen). The glass beads (Müller, Germany) used as substratum were in a size range 100-200µm.

VII.2.5. Physics of magnetic Particles in a magnetic Field

For optimization of MagPI operation and in particular to obtain quantitative results that are comparable between different setups, certain aspects of physics should be considered. The MagPI approach relies on moving (ferro-) magnetic particles, and these movements are caused by an applied magnetic field. In this context, we can consider the particles as magnetic dipoles, and if the particle is elongated, (ferro-) magnets of the type discussed here will usually have their dipole oriented along the long axis of the particle. If such a dipole with a certain magnetic dipole moment is exposed to a magnetic field, then the dipole will tend to orient according to the magnetic field lines. The magnetic field thus causes a torque on the particle and the particle rotates. This process defines threshold T1: when deposited in the absence of the magnetic field, gravity will cause the particle to lie flat on the horizontal substrate, and then the predominantly vertical magnetic field (perpendicular to particle elongation) tends to rotate the particle, which in combination with the spatial

restrictions for the particle due to the substrate leads to erecting of the particles on the surface. This alignment of the particles occurs in any magnetic field that is predominantly vertical (along the z-axis, following our convention that the plane of the substratum is along x- and y-directions), regardless of whether the magnetic field is homogeneous or inhomogeneous.

Thresholds T2, T3 and T4, on the other hand, are related to genuine movements in space, and thus they only occur if an actual force acts on the particles. A homogeneous magnetic field (same field strength and field orientation everywhere) does not apply any force on a magnetic particle: in such a uniform field, all possible positions of the particle in space are energetically equal, and thus there is no force effect on the particle within. The situation is different in an inhomogeneous field. As the energy of the magnetic particle depends on the local magnetic field, an inhomogeneous magnetic field applies a force on a magnetic particle. The particles in our case are “high-field seekers”, and because the magnetic field generated by the electromagnetic is strongest at its poles, the particles feel a pulling force towards the nearby pole. This force is proportional to the gradient of the magnetic field, i.e. the direction of this force follows the direction of the steepest increasing slope in space of the magnetic field, and the strength of the force is proportional to the slope. Thus if we just consider a given magnetic dipole in a magnetic field, then threshold T1 is genuinely related to the magnetic field strength, and thresholds T2, T3 and T4 to the gradient of the magnetic field.

In our actual case, the situation is more complicated because the material properties of the magnetic particles depend on magnetic field. The magnetic dipole moment of each particle is proportional to the magnetization *M* of its material. Therefore, we recall the hysteresis cycle of ferromagnets: if an originally unmagnetized particle (magnetization zero) is exposed to a magnetic field, then its magnetization first rises

linearly, with slope proportional to the magnetic susceptibility χ. For ferromagnets like here, this (low-field) susceptibility is many orders of magnitudes larger than for paramagnets, and thus the magnetization increases strongly with increasing field. But this steep increase saturates at a certain field strength, and the magnetization increases more weakly at higher field, eventually saturating. This means that the susceptibility χ depends on field strength, χ (B), and that M depends on B in a non-linear fashion. If the external field is reduced again, *M(B)* decreases, but weaker than according to the virgin curve. Correspondingly, M does not vanish at zero B, but instead exhibits remanence M_r, and only becomes zero at the coercitive field B_c. The shape of *M(B)*, the hysteresis loop, characterizes the magnetic response of the material.

As discussed above, the magnetic force acting on a particle depends on its magnetization M and the magnetic field gradient grad(B)=∇B at the location of the particle: $F \propto M$ grad(B) = $M \nabla B$, but now M also explicitly depends on B, possibly in a non-linear fashion: $F \propto M(B)$ grad(B) = $M(B) \nabla B$. Therefore, not only the gradient of B, but also the absolute value of B is decisive for the force that acts on the magnetic particle. In the simple geometry of an ideal MagPI electromagnet, both B and grad(B) at a given particle position will have the same dependence on the electric current flowing through the solenoid, but this can be different for a more generic case that includes remanence or additional magnetic fields that are not caused by the MagPI solenoid and core.

VII.2.6. Open Questions and Objectives

Since the first documentation of MagPI by Larson et al. (2009), this technique has been applied successfully by several research groups working on aquatic biofilm

(Passarelli *et al.*, 2012; Thom *et al.*, 2015; Schmidt *et al.*, 2016, 2017). Thereby, the high sensitivity and suitability to determine biofilm adhesive capacity and how it is e.g. affected by pollutants could be clearly shown; however, due to the complexity of the underlying physics, the thresholds were mostly quantified in units of Ampere (Schmidt *et al.*, 2018a;b). While the scientific conclusions based on MagPI experiments are robust on a qualitative scale, the unit Ampere is related to adhesion in a setup-dependent fashion. It is high time to establish a procedure to quantitatively compare data obtained by different setups (different electromagnet material or geometry, varying positions of particles with respect to the magnet, or diverse magnetic particles) but that needs a full understanding of the physics behind. The range of application and the significance of the data obtained by MagPI measurements could be enhanced further by optimization of its individual components such as the features of the electromagnet. Ideally, this should include a conversion of MagPI data to the uplifting force in conventional units (e.g. Nm^{-2}). For future applications, the optimisation of the measuring principle along with the automatization of the measurements and data evaluation should be addressed to enhance the objectivity of the method further. Moreover, in ecological research, it would be highly attractive to develop a field device, but to this point the setup is not suitable for *in-situ* measurements because of the issues water depth and hydrodynamics in aquatic habitats. While all these MagPI aspects are still under development, this chapter focus on the key steps towards the understanding of (1) the impact of various features of the inner core and solenoid on the performance, addresses (2) the role of magnetic field and magnetic field gradient for MagPI operation and unravels (3) the influence of the field-dependent magnetisation of the particles. The long-term perspective of this work is to achieve more quantitatively

valid data and a better comparability of the results between laboratories using different MagPIs.

VII.3. Material and Methods

VII.3.1. Configuration of MagPI Electromagnets

For the inner core, first iron then permalloy was used with soft magnetic properties and low coercivity (0.015 Acm^{-1}), consisting of Ni (76.6%), Fe (14.7%), Cu (4.5%), Mo (3.3%) as well as others (Mn, Si) (Mu-metal, VAC Vakuumschmelze GmbH & Co.KG, Germany). The permalloy rod was cut to the appropriate length before final heat treatment (5h at 1000°C) to achieve full relative magnetic permeability $\mu_r = \chi+1$ (with magnetic susceptibility χ). For the solenoid, a coated copper wire has been used in two diameters: 0.375mm (MagPI Original and 0.52mm (new MagPIs). In Table 22, the features of the applied MagPIs are listed.

VII.3.2. Electrical Equipment

As a power supply, the following two devices were used: KA 3005P with a range of 0-30V and 0-5A, allowing fine adjustment of increments of 10 mV/1mA (Reichelt-Elektronik, Germany) as well as EA-PS 3016-10B with a range of 0-16V and 0-10A, allowing coarse and fine adjustment of increasing power (Conrad, EA Elektro-Automatik, Germany). A multimeter (M-4660M, Voltcraft, Conrad, Germany) has been applied to double-check the output values of both power supplies.

VII.3.3. Positioning of MagPI

The closer the electromagnet comes to the sample surface, the higher are magnetic field strength and gradient at the position of the particles. A wider distance offers a better visual observability of the surface, but the often strong adhesive biofilm require

a closer set-up. Here, the tip of the MagPIs was deployed in a working distance of 4mm above the biofilm surface, which has been tested to be ideal over a wider range of adhesive forces and in terms of particles observability. Positioning was done in high precision with the help of micromanipulators (MM33 and DC-3K-right, Märzhäuser Wetzler, Germany).

Table 22: *Overview of the tested MagPIs and their main features. Note 1: MagPI "1000_3a" has a flat end while MagPI "1000_3b" possesses a conically shaped end, but with little variations as to the magnetic field beneath the core. Note 2: the solenoids length refers to the part of the core where the copper wire is coiled around.*

Electromagnets	Core, Ø	Number of turns	Lengths of the solenoid [mm]
MagPI "Original"	Iron, 10mm	500	100
MagPI "200_1"	Permalloy, 7mm	200	135
MagPI "1000_1"	Permalloy, 7mm	1000	85
MagPI "1000_2"	Permalloy, 8mm	1000	85
MagPI "1000_3a"	Permalloy, 8mm	1000	62
MagPI "1000_3b"	Permalloy, 8mm	1000	62
MagPI "1500"	Permalloy, 8mm	1500	85

VII.3.4. MAGNETIC FIELD GENERATED BY A SOLENOID WITH MAGNETIC CORE

The MagPI electromagnets are solenoids with ferromagnetic core. Theoretically calculating the magnetic field of an empty solenoid (without core) of finite length using the Biot-Savart law is a traditional task of magnetostatics, and the formula for

the component of the magnetic field along the solenoid axis (here: z-axis) as a function of distance *z* from the end of the solenoid is documented in textbooks (Jiles, 1998):

$B_z = \frac{1}{2} \mu_0 I n [(z+L)/((z+L)^2+R^2)^{1/2} - z/(z^2+R^2)^{1/2}]$

with μ_0 vacuum permeability, *I* current through the solenoid, *n* number of turns of the solenoid, *L* length of the solenoid, and *R* radius of the solenoid.

The corresponding formula for the gradient then reads:
$\mathrm{grad}B_z = \mathrm{d}B_z/\mathrm{d}z = \frac{1}{2} \mu_0 I n [R^2/((z+L)^2+R^2)^{3/2} - R^2/(z^2+R^2)^{3/2}]$

Unfortunately, the situation in our case is substantially more complicated: the magnetic core of the magnet introduces an additional factor μ_r, which depends in a non-linear, material-dependent fashion on *B* (and thus on *I*). Furthermore, it is not clear *a priori* whether the length of our magnet core directly replaces *L* in the above equations (only a segment of the core is surrounded by the wiring whereas the end section near the particles is not surrounded), but probably will for our dimensions and Mu-metal. Finally, not all of the particles are located on the magnet axis, but “off-center” with a distance comparable to *z* and *R*, thus the analytical formulae above cannot be considered valid approximations any more. The pitfalls of all these considerations are avoided by experimentally determining the magnetic field for the relevant MagPI configurations and settings.

VII.3.5. QUANTIFICATION OF MAGNETIC FIELD

The magnetic field *B* was determined with a high-precision (4,5 digits for Tesla, Gauss, A/m, Oersted) teslameter FM 302 connected to the transversal probe 2000mT AS-NTP 0.6 (both Projekt Elektronik, GmbH, Germany), which in our measurement geometry is sensitive to the vertical component (along *z*-axis) of the

magnetic field. The magnetic gradient [grad(*B*)] was then calculated (approximating the spatial derivative by using two measurements at small but finite distance) by taking the difference between two measured values of the magnetic field *B* at a distance of 1mm, and division by this distance. To measure the magnetic field and the magnetic field gradient, the probe has been positioned with the micromanipulator at various vertical (height *z*) and horizontal (right *x*, left *y*) distances with respect to the electromagnet mounted above. At these different positions, the magnetic field was measured at a range of increasing current [*I*]. This procedure established the relation between values of current [*I*], magnetic field [*B*] and magnetic gradient [grad(*B*)], and thus these quantities can then be easily converted into each other.

VII.3.6. FERROMAGNETIC PARTICLES

The ferromagnetic particles consist of a maghaematite core and a fluorescent coating for better visibility (Partrac, Glasgow, UK). To measure biofilm adhesive capacity in experiments, the particles were usually sieved to a size class between 180–250µm. However, to determine their magnetic features with the SQUID (see below), the particles were additionally sieved into the following size classes: (A) 200–250µm, (B) 250–315µm, (C) >315µm. From each of these fractions, 10 particles of similar form (divided in “round” and “angular”) were selected under the light microscope, weighted with a high-precision balance (Sartorius Supermicro S4 D=0,0001mg) and their area, volume and density was calculated.

VII.3.7. SUPERCONDUCTING QUANTUM INTERFERENCE DEVICE (SQUID)

A SQUID can detect small magnetic fields in highest sensitivity. Here a SQUID-based Magnetic Property Measurement System (7T MPMS XL by Quantum Design) was used to determine the magnetic moment of individual ferromagnetic particles. The

weighted ferromagnetic particles of known size and form were fixed to a straw by using grease and inserted into the MPMS. Within the MPMS, the magnetic field was first increased up to a maximum value of +500mT, then decreased and inverted to–500mT and then increased again up to +500mT. This way, the full hysteresis curve could be plotted to evaluate the saturation of the particles and to check possible deviations in magnetic moment before and after switching on the external magnetic field.

VII.3.8. SUBSTRATUM USED

MagPIs of different geometric features were tested with four substrata 1-4 of increasing stickiness: 1=petridish (without adhesion), 2=5g/l Agar Agar, 3=3g/l Xanthan Gum, 4=7.5g/l Xanthan Gum (2-4 solved in deionized water).

VII.4. RESULTS AND DISCUSSION

VII.4.1. DESIGN OF THE ELECTROMAGNET

1. Core material

As a first step, the magnetic field intensity [*B*] of the original MagPI (as described in Larson *et al.*, 2009) was determined at *z*=4,5mm distance below the central point of the electromagnet tip (“pole”) and in dependence of the increasing current [*I*] (Figure 44). The data gave clear evidence of remanence. Thus, the metal core of ferrous alloy exhibits a macroscopic magnetic moment and thus a magnetic field at the position of the particles, with the current being turned off (“magnetic remanence”), a relevant feature that in this context has not been considered before. Consequently, an alternative core material has been chosen to fabricate a new MagPI: Permalloy (or Mu-metal) which has soft magnetic properties and mainly consists of nickel and iron

(VAC Vakuumschmelze GmbH & Co.KG, Germany). Its low coercivity (0.015 [A/cm]) goes hand in hand with low remanence (Figure 44). The permalloy is delivered semi-finished and needs a heat treatment (5h at 1000°C) to achieve its final characteristics of high magnetic permeability.

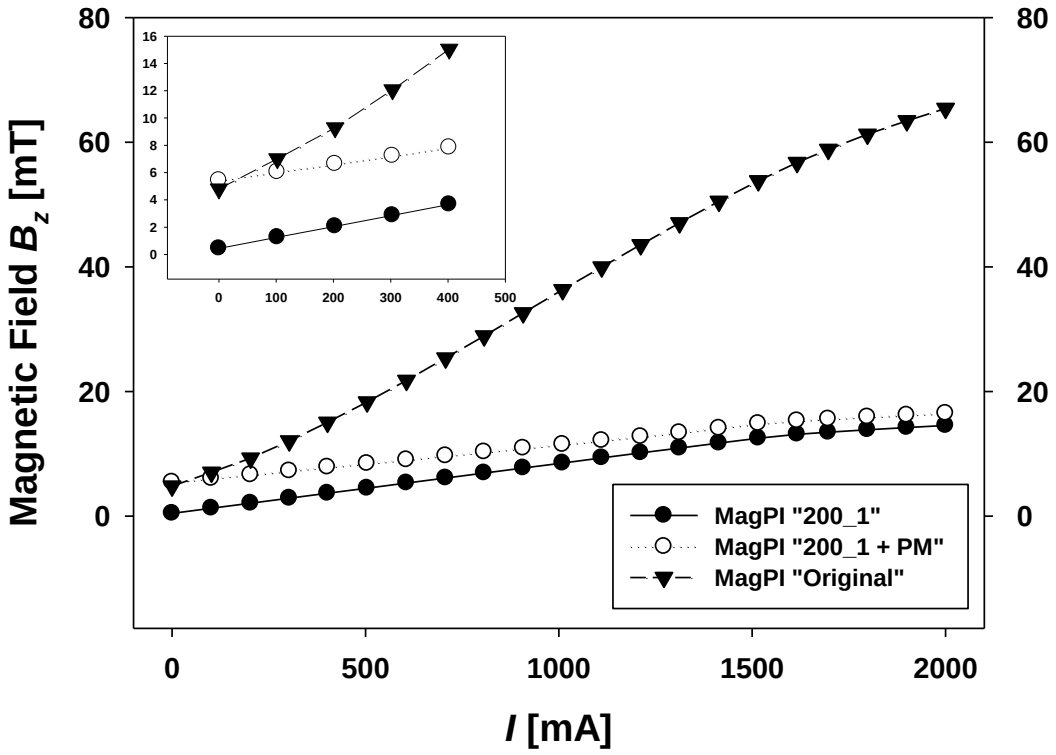

Figure 44: *The magnetic field B_z [mT] in dependence of the current I [mA] for MagPIs with different core material: "MagPI_Original" with iron core and "MagPI_200_1" as well as "MagPI_200_1 + PM" (permanent magnet) with permalloy as core material. Due to the permanent magnet, the "MagPI_200_1 + PM" causes a finite magnetic field strength at zero current; the same is true for the "MagPI_Original" after repeated measurements, indicating its remanence in contrast to "MagPI_200_1". The remanence can be clearly seen in the inset.*

2. The solenoid (a helical coil wrapped around the core)

A copper wire (diameter of 0.52mm) was coiled around the permalloy core (two types of diameters 7 and 8mm used), with various solenoid lengths (62–135mm) and turns (200 to 1500, see Table 22) of the wire. For a certain core and a given applied current, the magnetic field generated will strongly depend on the number of turns;

with a linear relation in the low-field regime. This is confirmed in Figure 45, where the influence of the number of turns can be clearly seen.

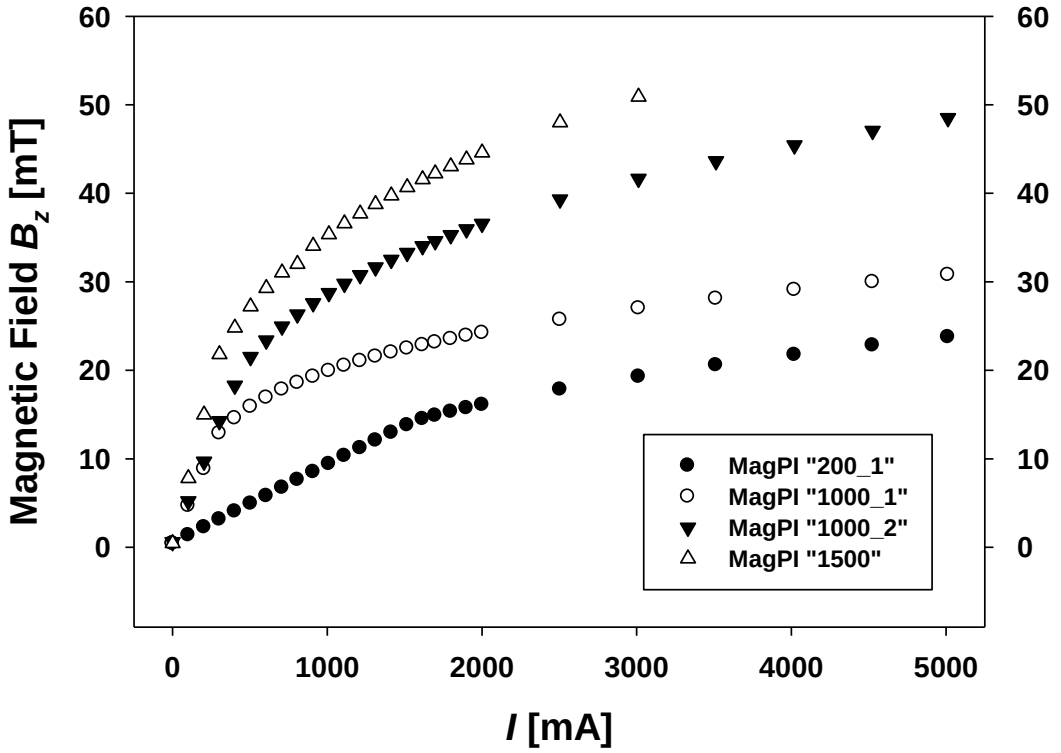

Figure 45: *The magnetic field B_z [mT] versus I [mA] for various MagPIs with different number of turns (from 200 up to 1500 turns), measured at a fixed position (z=4mm, x=y=0mm) with respect to the pole of the MagPI core. With increasing number of turns, the slope of the initial linear relation becomes steeper, and the saturation level (where the linear relation finishes) is achieved already at lower currents.*

Increasing the number of turns induces a higher field strength at a given current and thus, the initially linear relation between current and magnetic field shows a steeper slope as compared to MagPIs with fewer turns. Consequently, the slope increases from MagPI “200_1” to MagPI “1500” (Figure 45). Secondly, with further increasing current, the magnetic field strength shows saturation. This is due to the cumulative characteristics of the inner core which first contributes to the overall field strength in a linear response to the increasing current but eventually becomes saturated; an effect that is known to be material-specific and impacted by the heat treatment. With higher

number of turns, this saturation level is achieved at lower currents compared to MagPIs with lower numbers of coils wrapped around the core.

Incipient saturation can be seen where the linear relation between field intensity and current finishes and this was the case at approximately 300mA (MagPI “1500”), 400mA (MagPIs “1000_1” and “1000_2”) as well as 1600mA (MagPI “200_1”) (Figure 45). The magnetic field at which incipient saturation sets in was roughly similar for the four MagPIs in this figure (~15–22mT), and this matched expectation as the cores of these four MagPIs were fabricated from the same material.

3. Spatial distribution of magnetic field and magnetic field gradient

To characterize the spatial dependence of the magnetic field generated by the electromagnet, measurement profiles were conducted along different directions. Figure 46 illustrates the magnetic field strength as a function of (vertical) distance from the pole of the electromagnet. The derivative (slope) of this curve is the magnetic field gradient. Clearly, both the magnetic field and its gradient strongly decreased with increasing distance. Therefore, at smaller operating distances one can generate stronger forces for a given current, but at the expense of accessibility/visibility of the particle position. The lateral dependence of the magnetic field is shown in Figure 47. Here, the vertical distance from the magnet was constantly 4mm, and the horizontal position was varied. The lateral range around the centre where the magnetic field differs by less than 10% from the maximum value amounted to approximately 4mm radius, in coincidence with the diameter of the magnet core.

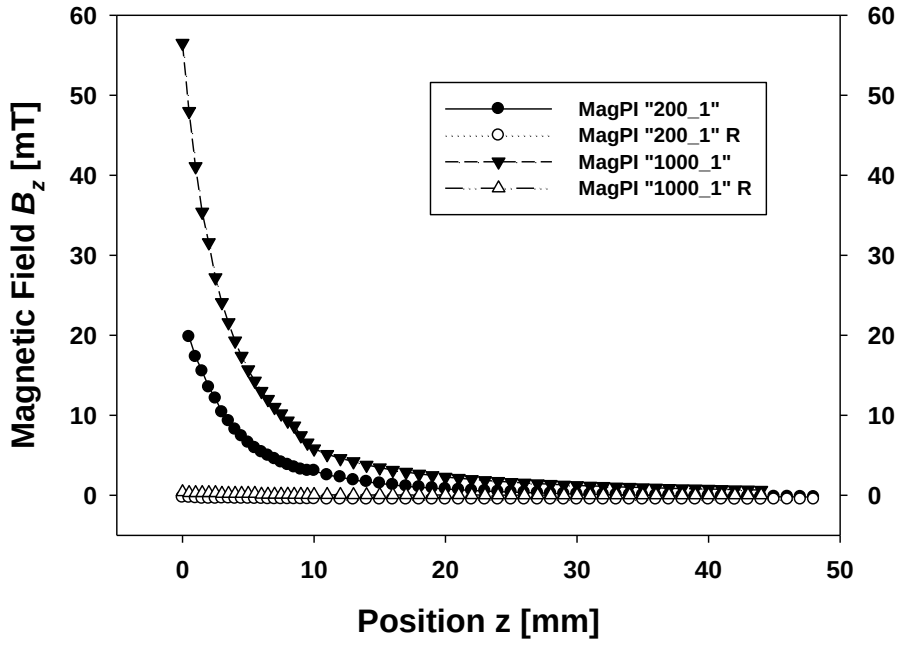

Figure 46: *The magnetic field B_z [mT] at a fixed current of 1000mA and varying heights z while x=y=0mm using two MagPIs with varying numbers of turns, with and without (remanence=R) current.*

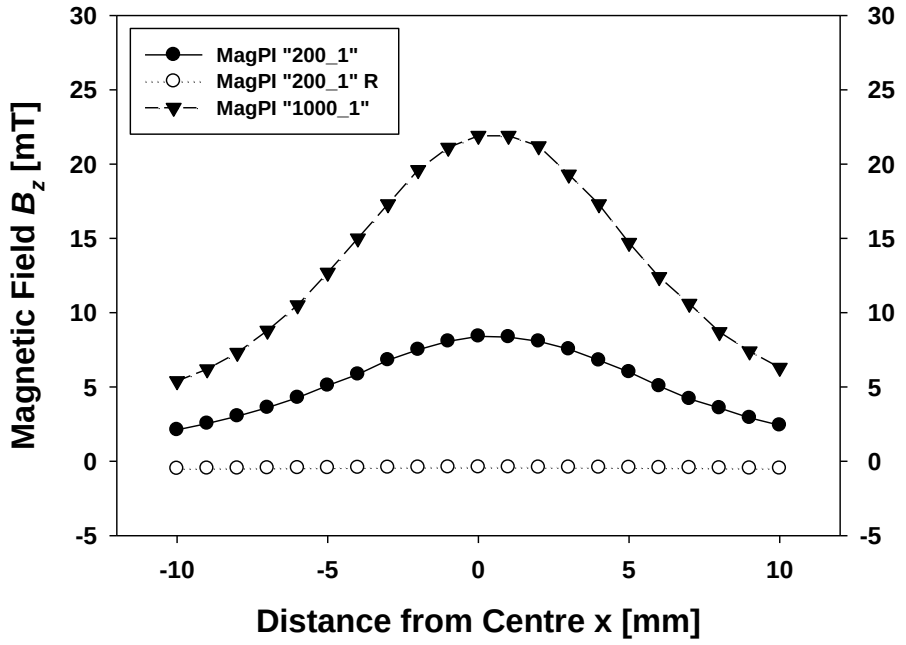

Figure 47: *The magnetic field B_z [mT] at a fixed current of 1000mA and varying horizontal positions x (up to 10mm away from the centre) while z=4mm and y=0mm using two MagPIs with varying numbers of turns, with and without (remanence=R) current.*

VII.4.2. Roles of magnetic Field and Gradient of magnetic Field

As mentioned above, the uplifting magnetic force acting on a particle depends on both *B* and grad(*B*), and these two quantities thus play crucial roles for the threshold determination. Changes in the MagPIs construction (e.g. length, diameter, core material, solenoid, tip form) as well as in its positioning and distribution of ferromagnetic particles cause variations in the relevant magnetic field and its gradient. To demonstrate that both the magnetic field and the gradient are relevant, the following experiment was conducted: Five different MagPIs with varying geometric features were used to measure the adhesion of four reproducible substrates with different stickiness (see VII.3.7). First, the T3 values were determined for each MagPI and each substratum and plotted as magnetic field strength *B* (Figure 48A) as well as the magnetic gradient [grad(*B*)] (Figure 48B). The used electromagnets differed not only in geometry. One setup combined the MagPI “200_1” with additional permanent magnets (PM) where the magnetic field is constantly higher as compared to the “solitary” electromagnets.

First, the increasing adhesion from substratum 1 (petridish) to 4 (7,5g/l xanthan gum) could be clearly detected (Figure 48). Second, the T3 values expressed as magnetic field were varying between all MagPIs for each of the substratum (Figure 48A). In contrast, the T3 values of the magnetic gradient were fairly close to each other for all solitary MagPIs (Figure 48B). However, the MagPI + PM combination behaved differently: expressed as magnetic field and magnetic gradient, the values were clearly higher and lower, respectively, as compared to the solitary electromagnets.

(A)

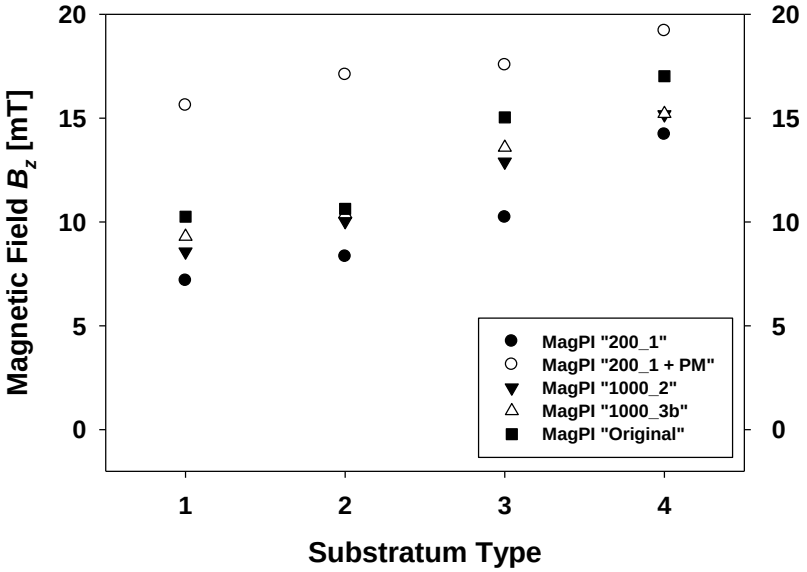

(B)

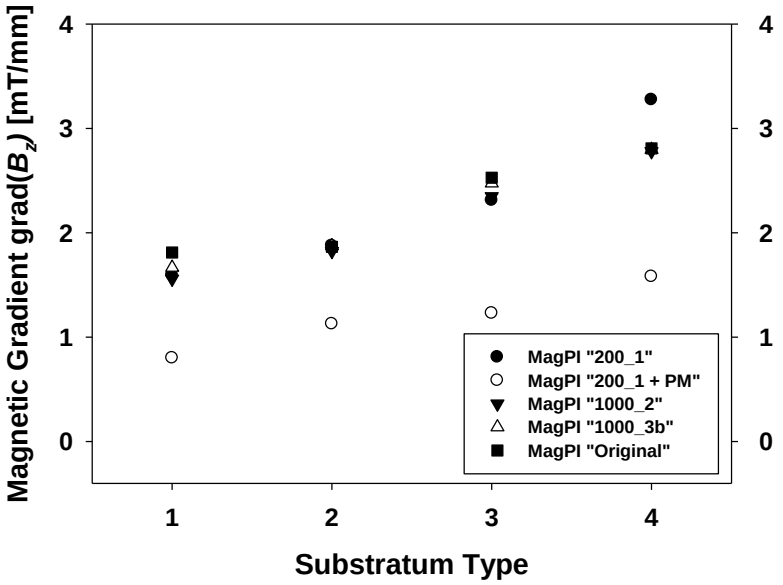

Figure 48: *Threshold T3 (retrieval of few particles) is determined for four different substrates with increasing adhesion from 1-4 (1=petridish, 2=5g/l Agar Agar, 3=3g/l Xanthan Gum, 4=7,5g/l Xanthan Gum) with an electromagnet at a fixed height (4mm). Image A (above) shows the relation between T3 values and the corresponding magnetic field; image B (below) indicates the relation between T3 values and the corresponding magnetic gradient.*

This applied especially for the direct comparison between the MagPI “200_1” with and without permanent magnets. While the MagPI “200_1” attracted the particles at already ~7mT from the petridish (substratum 1), the constant magnetic field of ~ 11mT with the permanent magnets was not sufficient here (it needs ~ 16mT for

particles retrieval, Figure 48A). This is a clear hint that the magnetic field alone is not decisive for particle retrieval. Nevertheless, if the magnetic gradient would be the only relevant quantity, the MagPI “200_1 + PM” should retrieve the particles at the same T3 values of the magnetic gradient as compared to the other solitary magnets - instead these were much lower. The explanation for this behaviour lies in the magnetic properties of the particles which themselves depend on magnetic field (see below). But the experiments with additional permanent magnets clearly showed that both magnetic field and magnetic field gradient have to be considered for a thorough understanding of the physical mechanism underlying MagPI.

VII.4.3. CHARACTERISTICS OF THE MAGNETIC PARTICLES

As explained above, the relevant magnetic force depends on two quantities: the magnetic gradient and the magnetic or dipole moment of the particles. The latter is not constant but increases with exposure to an external magnetic field by the accumulative alignment of elementary dipoles within the particles. This magnetisation process of the ferromagnetic particles was not considered before in this context and implies that the necessary magnetic gradient threshold for particle retrieval is lowered with increasing dipole moment. Indeed, the magnetisation of the particles was higher in presence of the permanent magnets (at low currents through the solenoid) compared to the case of the solitary electromagnets; consequently, the required magnetic gradient for particle lifting from the surface was lowest (Figure 48B).

To demonstrate the role of the particle magnetization and to characterize the magnetic particles as reference for future studies, a SQUID magnetometer was used to investigate the magnetic behaviour of the ferromagnetic particles depending on their form and size as function of external magnetic field in very high sensitivity. The

hysteresis curve in Figure 49 illustrates the magnetisation of one defined particle after first application of a magnetic field. Starting the measurement, the magnetic moment of the particle was zero without external magnetic field (0mT). After applying an external magnetic field up to 500mT, the elemental dipoles aligned themselves with it and when the field is removed, this alignment of the particle was partially retained (Figure 49). When the magnetic field was reduced again, the non-vanishing magnetisation that remained present at zero magnetic field is called remanence. Reversing the field to -500mT led to vanishing magnetization at the coercitive field and eventually to reversed, i.e. negative magnetization. Increasing the external magnetic field to 500mT again resulted in the hysteresis loop where the width of the middle section along the *B* axis was twice the coercivity of the material (Figure 49). Thus, this curve gives evidence of the magnetic moment of the particle that remained without external magnetic field. This clearly demonstrated that the magnetization of the particles drastically changes between the initial and further magnetic field sweeps. The present MagPI operation procedure thus demands that the particles are employed only once, during the initial magnetization procedure caused by the increasing magnetic field.

(A)

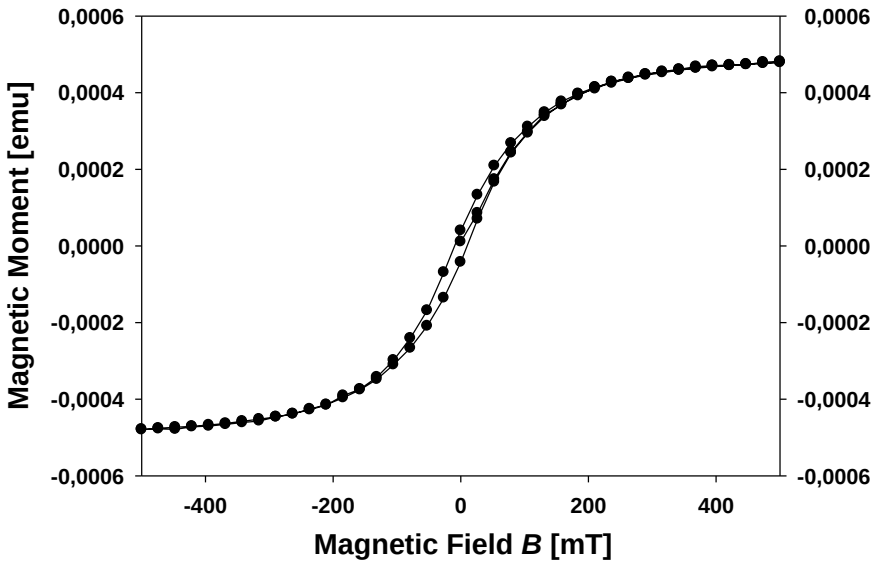

(B)

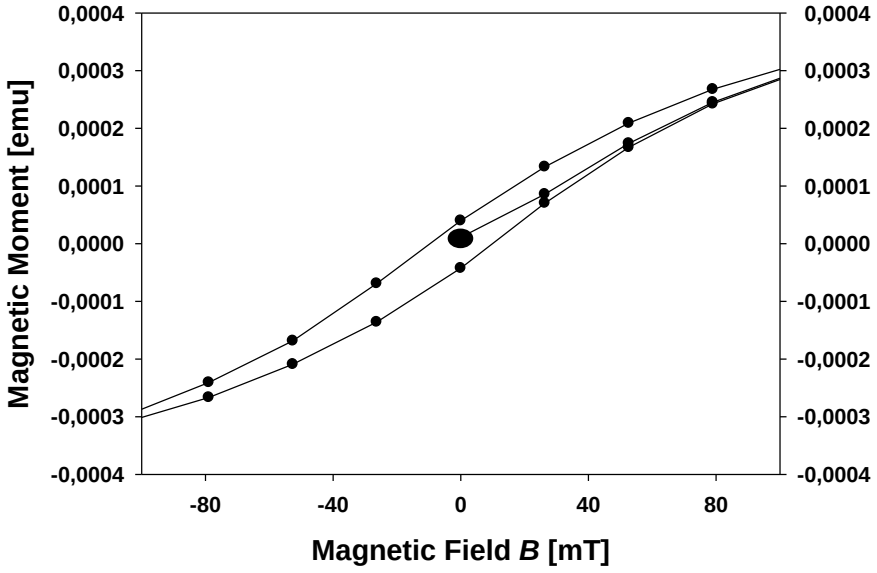

Figure 49: *Hysteresis curves for one ferromagnetic particle ("A1") from the size class 200–250µm with 15,5µg weight. (A) is showing the full hysteresis loop, while (B) presents a detailed view on the magnetic momentum which is zero before applying an external magnetic field (ellipse at starting point) and differs from zero after the field is reduced from finite values to zero again, thus indicating remanence after magnetisation (above and below ellipse).*

The hysteresis curves vary for the single particles tested since they showed considerable differences in size and form. For instance, the magnetic momentum was higher for particles of bigger size as indicated by Figure 50A where three

particles from different size classes were tested. Thus, in the next step of evaluation, the particles were standardized, first for their volume and second for their mass.

(A)

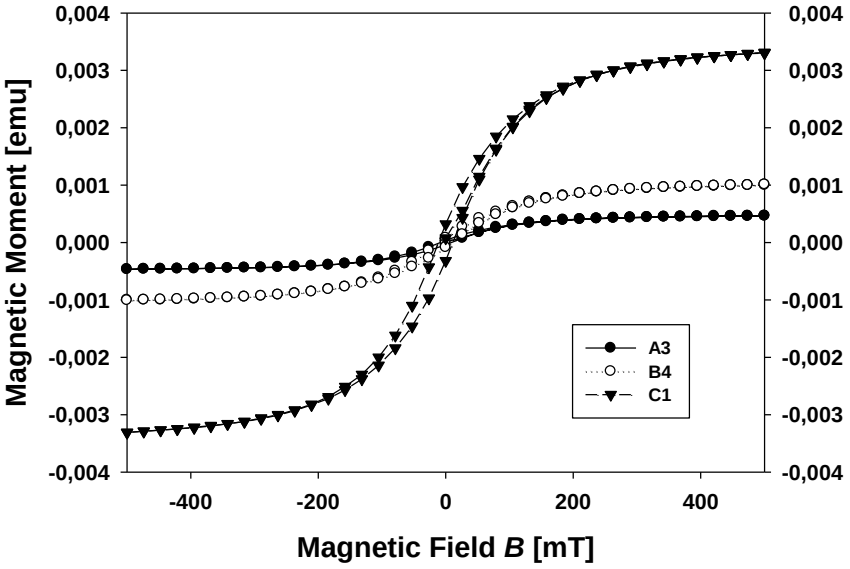

(B)

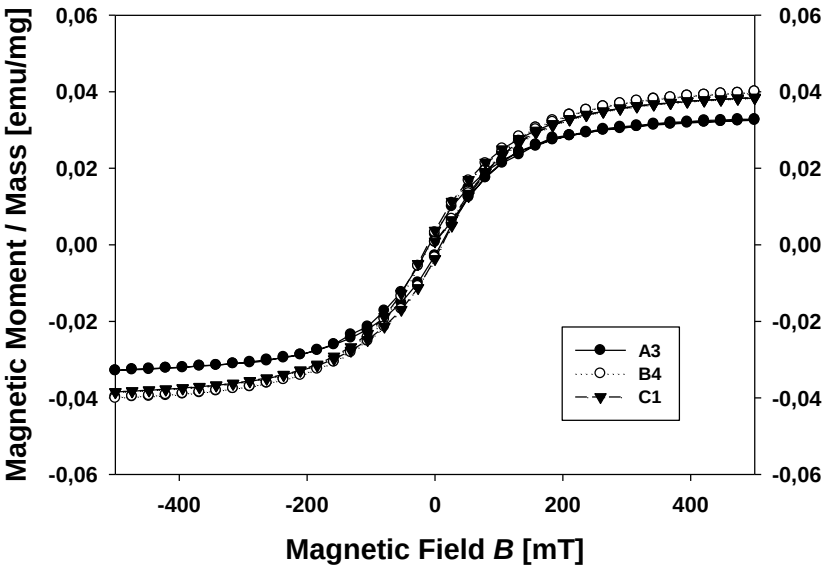

Figure 50: *Hysteresis curves for three ferromagnetic particle ("A3", "B4", "C1") from three different sizes classes (200–250µm, 250–315µm,>315µm), respectively, before (A) and after (B) correction for their individual mass [mg].*

With the correction for the volume, the hysteresis curves were still showing deviations up to 50% (data not shown) while this was significantly less (< 30%) for the mass

(Figure 50B). This might be due to the fact that “volume” relates to total volume that includes both the core material as well as to the outer coating (which does not contribute to magnetisation) while “mass” is linked more strongly to the maghaematite core and thus to magnetic behaviour, because the organic coating is expected to have a much smaller density than the maghaemetite.

VII.5.CONCLUSIONS

The MagPI system is a promising *in situ* tool that can give reproducible values of biofilm adhesive capacity at mesoscale to then allow predictions on biofilm and substratum stability and their possible detachment. The measurements can be done repeatedly in natural biofilm at high temporal as well as spatial resolution, and small changes in adhesion are detected. Since the MagPI is a relatively new device, there is still room for further development on (a) the physical setup itself, (b) the calibration in terms of magnetic field strength and gradient, (c) the measurement procedure, (d) automatization of measurements and data evaluation as well as (e) conversion of the uplifting force to common units.

In this chapter, the focus was on (a) and (b). The new inner core material permalloy has been introduced due to its absent residual magnetism in comparison to the iron core used before. Avoiding remanence is of high importance for the reproducibility of the results gained. The number of turns with copper thread around the core (solenoid) is decisive for the performance of the electromagnet. With more turns, a higher field strength is achieved for a given current, and with increasing current, the magnetic saturation of the core is reached earlier compared to electromagnets with lower turn density; all of which has direct implications for the MagPI operation. Tuning these parameters allows building electromagnets of different strengths for different stages of biofilm growth and adhesive capacity.

Since differently built MagPIs (e.g. inner core material, length, tip, solenoid) vary in their magnetic characteristics, it is important to calibrate them thoroughly in order to obtain reliable quantitative data. For this calibration, it is essential to know the driving force, but magnetic field strength and field gradient occur simultaneously and cannot be applied independently. With the help of the here presented experiment, the crucial role of the magnetic field gradient could be shown, but it also became evident that the absolute value of the magnetic field affects the experimental outcome via the field-dependent magnetization and thus the field-dependent magnetic moment of the particles.

Future work should concern optimisation of the MagPI application, for instance by controlling automatically the stepwise increase in the current increments and in parallel taking images with subsequent data evaluation. Research on this automated measuring approach is under way and is currently prepared as publication along with a pioneer idea on the conversion of the uplifting force to critical shear stress values (Thom et al., in prep.). Altogether, better knowledge on the working principle, the performance as well as efficiency of this MagPI device is of high value for its potential application in many disciplines that goes well beyond research on aquatic biofilm and ecology to address for instance medical questions or biotechnology issues.

BIBLIOGRAPH

Ackermann B., Esser M., Scherwass A. & Arndt H. (2011) Long-term dynamics of microbial biofilm communities of the river Rhine with special references to ciliates. *International Review of Hydrobiology* **96**, 1–19.

Aggarwal S., Poppele E.H. & Hozalski R.M. (2010) Development and testing of a novel microcantilever technique for measuring the cohesive strength of intact biofilms. *Biotechnology and Bioengineering* **105**, 924–934.

Agogué H., Mallet C., Orvain F., De Crignis M., Mornet F. & Dupuy C. (2014) Bacterial dynamics in a microphytobenthic biofilm: a tidal mesocosm approach. *Journal of Sea Research* **92**, 36–45.

Allesen-Holm M., Barken K.B., Yang L., Klausen M., Webb J.S., Kjelleberg S., Molin S., Givskov M. & Tolker-Nielsen T. (2006) A characterization of DNA release in pseudomonas aeruginosa cultures and biofilms. *Molecular Microbiology* **59**, 1114–1128.

Amann R.I., Binder B.J., Olson R.J., Chisholm S.W., Devereux R. & Stahl D.A. (1990) Combination of 16s rRNA-targeted oligonucleotide probes with flow cytometry for analyzing mixed microbial populations. *Applied and Environmental Microbiology* **56**, 1919–1925.

Amin S.A., Parker M.S. & Armbrust E.V. (2012) Interactions between diatoms and bacteria. *Microbiology and Molecular Biology Reviews* **76**, 667–684.

Amos C.L., Bergamasco A., Umgiesser G., Cappucci S., Cloutier D., DeNat L., Flindt M., Bonardi M. & Cristante S. (2004) The stability of tidal flats in venice lagoon - the results of in-situ measurements using two benthic, annular flumes. *Journal of Marine Systems* **51**, 211–241.

Amos C.L., Droppo I.G., Gomez E.A. & Murphy T.P. (2003) The stability of a remediated bed in Hamilton Harbour, Lake Ontario, Canada. *Sedimentology* **50**, 149–168.

Anderson A.M., Spears B.M., Lubarsky H.V., Davidson I., Gerbersdorf S.U. & Paterson D.M. (2011) Magnetic particle induction and its importance in biofilm research. In: *Biomedical Engineering-Frontiers and Challenges* (Ed. R. Fazei-Rezai), pp. 189–216. InTech, Rijeka.

Apoya-Horton M.D., Yin L., Underwood G.J.C. & Gretz M.R. (2006) Movement modalities and responses to environmental changes of the mudflat diatom Cylindrotheca closterium (Bacillariophyceae). *Journal of Phycology* **42**, 379–390.

Aslam S.N., Cresswell-Maynard T., Thomas D.N. & Underwood G.J.C. (2012) Production and characterization of the intra- and extracellular carbohydrates and polymeric substances (EPS) of three sea-ice diatom species, and evidence for a cryoprotective role for EPS. *Journal of Phycology* **48**, 1494–1509.

Baas J.H., Davies A.G. & Malarkey J. (2013) Bedform development in mixed sand-mud: The contrasting role of cohesive forces in flow and bed. *Geomorphology* **182**, 19–32.

Bahulikar R.A. & Kroth P.G. (2008) The complex extracellular polysaccharides of mainly chain-forming freshwater diatom species from epilithic biofilms. *Journal of Phycology* **44**, 1465–1475.

Battarbee R. (1986) Diatom Analysis. In: *Handbook of Holocene Palaeoecology and Palaeohydology* (Ed. B.E. Berglund), pp. 527–570. John Wiley & Sons Ltd, Chichester.

Battin E.E. & Brumaghim J.L. (2008) Metal specificity in DNA damage prevention by sulfur antioxidants. *Journal of Inorganic Biochemistry* **102**, 2036–42.
Battin T.J., Kaplan L.A., Newbold J.D., Cheng X.H. & Hansen C. (2003a) Effects of current velocity on the nascent architecture of stream microbial biofilms. *Applied and Environmental Microbiology* **69**, 5443–5452.
Battin T.J., Kaplan L.A., Newbold J.D. & Hansen C.M.E. (2003b) Contributions of microbial biofilms to ecosystem processes in stream mesocosms. *Nature* **426**, 439–442.
Battin T.J., Sloan W.T., Kjelleberg S., Daims H., Head I.M., Curtis T.P. & Eberl L. (2007) Opinion: Microbial landscapes: new paths to biofilm research. *Nature Reviews Microbiology* **5**, 76–81.
Becker K. (1996) Exopolysaccharide production and attachment strength of bacteria and diatoms on substrates with different surface tensions. *Microbial Ecology* **32**, 23–33.
Bender J., Rodriguezeaton S., Ekanemesang U.M. & Phillips P. (1994) Characterization of metal-binding bioflocculants produced by the cyanobacterial component of mixed microbial mats. *Applied and Environmental Microbiology* **60**, 2311–2315.
Besemer K., Singer G., Limberger R., Chlup A.-K., Hochedlinger G., Hoedl I., Baranyi C. & Battin T.J. (2007) Biophysical controls on community succession in stream biofilms. *Applied and Environmental Microbiology* **73**, 4966–4974.
Black K.S., Tolhurst T.J., Paterson D.M. & Hagerthey S.E. (2002) Working with natural cohesive sediments. *Journal of Hydraulic Engineering-ASCE* **128**, 2–8.
Blenkinsopp S.A. & Lock M.A. (1994) The impact of storm-flow on river biofilm architecture. *Journal of Phycology* **30**, 807–818.
Böckelmann U., Janke A., Kuhn R., Neu T.R., Wecke J., Lawrence J.R. & Szewzyk U. (2006) Bacterial extracellular DNA forming a defined network-like structure. *FEMS Microbiology Letters* **262**, 31–38.
Böckelmann U., Manz W., Neu T.R. & Szewzyk U. (2000) Characterization of the microbial community of lotic organic aggregates ('river snow') in the Elbe River of Germany by cultivation and molecular methods. *FEMS Microbiology Ecology* **33**, 157–170.
Boivin M.E.Y., Greve G.D., Garcia-Meza J.V., Massieux B., Sprenger W., Kraak M.H.S., Breure A.M., Rutgers M. & Admiraal W. (2007) Algal-bacterial interactions in metal contaminated floodplain sediments. *Environmental Pollution* **145**, 884–894.
Böl M., Ehret A.E., Albero A.B., Hellriegel J. & Krull R. (2013) Recent advances in mechanical characterisation of biofilm and their significance for material modelling. *Critical Reviews in Biotechnology* **33**, 145–171.
Boogert N.J., Paterson D.M. & Laland K.N. (2006) The implications of niche construction and ecosystem engineering for conservation biology. *Bioscience* **56**, 570–578.
Bowen J.L., Crump B.C., Deegan L.A. & Hobbie J.E. (2009) Increased supply of ambient nitrogen has minimal effect on salt marsh bacterial production. *Limnology and Oceanography* **54**, 713–722.
Bowes M.J., Ings N.L., McCall S.J., Warwick A., Barrett C., Wickham H.D., Harman S.A., Armstrong L.K., Scarlett P.M., Roberts C., Lehmann K. & Singer A.C. (2012) Nutrient and light limitation of periphyton in the River Thames: Implications for catchment management. *Science of The Total Environment* **434**, 201–212.

Brading M.G., Boyle J. & Lappinscott H.M. (1995) Biofilm formation in laminar-flow using pseudomonas-florescens EX101. *Journal of Industrial Microbiology* **15**, 297–304.
Brimacombe C.A., Stevens A., Jun D., Mercer R., Lang A.S. & Beatty J.T. (2013) Quorum-sensing regulation of a capsular polysaccharide receptor for the Rhodobacter capsulatus gene transfer agent (RcGTA). *Molecular Microbiology* **87**, 802–817.
de Brouwer J.F.C., Bjelic S., de Deckere E. & Stal L.J. (2000) Interplay between biology and sedimentology in a mudflat (Biezelingse Ham, Westerschelde, The Netherlands). *Continental Shelf Research* **20**, 1159–1177.
de Brouwer J.F.C., Ruddy G.K., Jones T.E.R. & Stal L.J. (2002) Sorption of EPS to sediment particles and the effect on the rheology of sediment slurries. *Biogeochemistry* **61**, 57–71.
de Brouwer J.F.C. & Stal L.J. (2002) Daily fluctuations of exopolymers in cultures of the benthic diatoms Cylindrotheca closterium and Nitzschia sp (Bacillariophyceae). *Journal of Phycology* **38**, 464–472.
de Brouwer J.F.C. & Stal L.J. (2001) Short-term dynamics in microphytobenthos distribution and associated extracellular carbohydrates in surface sediments of an intertidal mudflat. *Marine Ecology Progress Series* **218**, 33–44.
de Brouwer J.F.C., Wolfstein K., Ruddy G.K., Jones T.E.R. & Stal L.J. (2005) Biogenic stabilization of intertidal sediments: The importance of extracellular polymeric substances produced by benthic diatoms. *Microbial Ecology* **49**, 501–512.
Bruckner C.G., Bahulikar R., Rahalkar M., Schink B. & Kroth P.G. (2008) Bacteria associated with benthic diatoms from Lake Constance: phylogeny and influences on diatom growth and secretion of extracellular polymeric substances. *Applied and Environmental Microbiology* **74**, 7740–7749.
Bruckner C.G., Rehm C., Grossart H.-P. & Kroth P.G. (2011) Growth and release of extracellular organic compounds by benthic diatoms depend on interactions with bacteria. *Environmental Microbiology* **13**, 1052–1063.
Brümmer I.H.M., Fehr W. & Wagner-Döbler I. (2000) Biofilm community structure in polluted rivers: abundance of dominant phylogenetic groups over a complete annual cycle. *Applied and Environmental Microbiology* **66**, 3078–3082.
Brümmer I.H.M., Felske A. & Wagner-Döbler I. (2003) Diversity and seasonal variability of beta-proteobacteria in biofilms of polluted rivers: analysis by temperature gradient gel electrophoresis and cloning. *Applied and Environmental Microbiology* **69**, 4463–4473.
Bryers J. & Characklis W. (1981) Early fouling biofilm formation in a turbulent flow system: overall kinetics. *Water Research* **15**, 483–491.
Burggraf S., Mayer T., Amann R., Schadhauser S., Woese C.R. & Stetter K.O. (1994) Identifying members of the domain Archaea with rRNA-targeted oligonucleotide probes. *Applied and Environmental Microbiology* **60**, 3112–3119.
Burkholder J.M., Wetzel R.G. & Klomparens K.L. (1990) Direct comparison of phosphate uptake by adnate and loosely attached microalgae within an intact biofilm matrix. *Applied and Environmental Microbiology* **56**, 2882–2890.
Campa-Córdova A.I., Luna-González A., Ascencio F., Cortés-Jacinto E. & Cáceres-Martínez C.J. (2006) Effects of chloramphenicol, erythromycin, and furazolidone on growth of Isochrysis galbana and Chaetoceros gracilis. *Aquaculture* **260**, 145–150.

Characklis W.G. & Cooksey K.E. (1983) Biofilms and microbial fouling. *Advances in Applied Microbiology* **29**, 93–138.
Chiovitti A., Bacic A., Burke J. & Wetherbee R. (2003) Heterogeneous xylose-rich glycans are associated with extracellular glycoproteins from the biofouling diatom Craspedostauros australis (Bacillariophyceae). *European Journal of Phycology* **38**, 351–360.
Chiovitti A., Dugdale T.M. & Wetherbee R. (2006) Diatom adhesives: molecular and mechanical properties. In: *Biological Adhesives* (Eds A.M. Smith & J.A. Callow), pp. 79–103. Springer-Verlag, Berlin Heidelberg.
Chiovitti A., Heraud P., Dugdale T.M., Hodson O.M., Curtain R.C.A., Dagastine R.R., Wood B.R. & Wetherbee R. (2008) Divalent cations stabilize the aggregation of sulfated glycoproteins in the adhesive nanofibers of the biofouling diatom Toxarium undulatum. *Soft Matter* **4**, 811–820.
Cho B.C. & Azam F. (1990) Biogeochemical significance of bacterial biomass in the ocean's euphotic zone. *Marine Ecology Progress Series* **63**, 253–259.
Choi Y.C. & Morgenroth E. (2003) Monitoring biofilm detachment under dynamic changes in shear stress using laser-based particle size analysis and mass fractionation. *Water Science and Technology* **47**, 69–76.
Coma R., Ribes M., Gili J.-M. & Zabala M. (2000) Seasonality in coastal benthic ecosystems. *Trends in Ecology & Evolution* **15**, 448–453.
Costerton J.W., Geesey G.G. & Cheng K.J. (1978) How bacteria stick. *Scientific American* **238**, 86–95.
Costerton J.W., Lewandowski Z., Caldwell D.E., Korber D.R. & Lappinscott H.M. (1995) Microbial biofilms. *Annual Review of Microbiology* **49**, 711–745.
Coundoul F., Bonometti T., Graba M., Sauvage S., Sanchez Pérez J.-M. & Moulin F.Y. (2015) Role of local flow conditions in river biofilm colonization and early growth. *River Research and Applications* **31**, 350–367.
Cowan M.M., Warren T.M. & Fletcher M. (1991) Mixed species colonization of solid surfaces in laboratory biofilms. *Biofouling* **3**, 23–34.
Cyr H. & Morton K.E. (2006) Distribution of biofilm exopolymeric substances in littoral sediments of Canadian Shield lakes: the effects of light and substrate. *Canadian Journal of Fisheries and Aquatic Sciences* **63**, 1763–1776.
Czaczyk K. & Myszka K. (2007) Biosynthesis of extracellular polymeric substances (EPS) and its role in microbial biofilm formation. *Polish Journal of Environmental Studies* **16**, 799–806.
Dade W.B., Davis J.D., Nichols P.D., Nowell A.R.M., Thistle D., Trexler M.B. & White D.C. (1990) Effects of bacterial exopolymer adhesion on the entrainment of sand. *Geomicrobiology Journal* **8**, 1–16.
Dade W.B. & Nowell A.R.M. (1991) Moving muds in the marine enviroment.
Dade W.B., Self R.L., Pellerin N.B., Moffet A., Jumars P.A. & Nowell A.R.M. (1996) The effects of bacteria on the flow behavior of clay seawater suspensions. *Journal of Sedimentary Research* **66**, 39–42.
Daims H., Bruhl A., Amann R., Schleifer K.H. & Wagner M. (1999) The domain-specific probe EUB338 is insufficient for the detection of all Bacteria: development and evaluation of a more comprehensive probe set. *Systematic and Applied Microbiology* **22**, 434–444.
Davis D. (1999) Regulation of matrix polymer in biofilm formation and dispersion. In: *Microbial Extracellular Polymeric Substances: Characterization, Structure and Function* (Eds J. Wingender, T.R. Neu & H.-C. Flemming), pp. 99–112. Springer, Berlin.

Decho A.W. (1990) Microbial exopolymer secretions in Ocean Environments - their role(s) in food webs and marine processes. *Oceanography and Marine Biology* **28**, 73–153.
Decho A.W., Norman R.S. & Visscher P.T. (2010) Quorum sensing in natural environments: emerging views from microbial mats. *Trends in Microbiology* **18**, 73–80.
de Deckere E., Tolhurst T.J. & de Brouwer J.F.C. (2001) Destabilization of cohesive intertidal sediments by infauna. *Estuarine Coastal and Shelf Science* **53**, 665–669.
Decoin V., Gallique M., Barbey C., Le Mauff F., Poc C.D., Feuilloley M.G., Orange N. & Merieau A. (2015) A Pseudomonas fluorescens type 6 secretion system is related to mucoidy, motility and bacterial competition. *BMC Microbiology* **15**, 72.
Defew E.C., Tolhurst T.J. & Paterson D.M. (2002) Site-specific features influence sediment stability of intertidal flats. *Hydrology and Earth System Sciences* **6**, 971–981.
Delattre C., Pierre G., Laroche C. & Michaud P. (2016) Production, extraction and characterization of microalgal and cyanobacterial exopolysaccharides. *Biotechnology Advances* **34**, 1159–1179.
Delgado M., De Jonge V.N. & Peletier H. (1991) Effect of sand movement on the growth of benthic diatoms. *Journal of Experimental Marine Biology and Ecology* **145**, 221–231.
Dickhudt P.J., Friedrichs C.T., Schaffner L.C. & Sanford L.P. (2009) Spatial and temporal variation in cohesive sediment erodibility in the York River estuary, eastern USA: A biologically influenced equilibrium modified by seasonal deposition. *Marine Geology* **267**, 128–140.
Dignac M.F., Urbain V., Rybacki D., Bruchet A., Snidaro D. & Scribe P. (1998) Chemical description of extracellular polymers: implication on activated sludge floc structure. *Water Science and Technology* **38**, 45–53.
Dominiak D.M., Nielsen J.L. & Nielsen P.H. (2011) Extracellular DNA is abundant and important for microcolony strength in mixed microbial biofilms. *Environmental Microbiology* **13**, 710–721.
Donlan R.M. (2002) Biofilms: microbial life on surfaces. *Emerging Infectious Diseases* **8**, 881–890.
Droppo I.G. (2001) Rethinking what constitutes suspended sediment. *Hydrological Processes* **15**, 1551–1564.
Droppo I.G. (2004) Structural controls on floc strength and transport. *Canadian Journal of Civil Engineering* **31**, 569–578.
Droppo I.G., Ross N., Skafel M. & Liss S.N. (2007) Biostabilization of cohesive sediment beds in a freshwater wave-dominated environment. *Limnology and Oceanography* **52**, 577–589.
Dubois M., Gilles K.A., Hamilton J.K., Rebers P.A. & Smith F. (1956) Colorimetric method for determination of sugars and related substances. *Analytical Chemistry* **28**, 350–356.
Dueholm M.S., Otzen D. & Nielsen P.H. (2013a) Evolutionary insight into the functional amyloids of the pseudomonads. *PLoS One* **8**, e76630.
Dueholm M.S., Søndergaard M.T., Nilsson M., Christiansen G., Stensballe A., Overgaard M.T., Givskov M., Tolker-Nielsen T., Otzen D.E. & Nielsen P.H. (2013b) Expression of Fap amyloids in Pseudomonas aeruginosa, P. fluorescens, and P. putida results in aggregation and increased biofilm formation. *MicrobiologyOpen* **2**, 365–382.

Duffy B.K. & Défago G. (1999) Environmental factors modulating antibiotic and siderophore biosynthesis by Pseudomonas fluorescensbiocontrol strains. *Applied and Environmental Microbiology* **65**, 2429–2438.
Dugdale T.M., Dagastine R., Chiovitti A., Mulvaney P. & Wetherbee R. (2005) Single adhesive nanofibers from a live diatom have the signature fingerprint of modular proteins. *Biophysical Journal* **89**, 4252–4260.
Dugdale T.M., Dagastine R., Chiovitti A. & Wetherbee R. (2006a) Diatom adhesive mucilage contains distinct supramolecular assemblies of a single modular protein. *Biophysical Journal* **90**, 2987–2993.
Dugdale T.M., Willis A. & Wetherbee R. (2006b) Adhesive modular proteins occur in the extracellular mucilage of the motile, pennate diatom Phaeodactylum tricornutum. *Biophysical Journal* **90**, L58–L60.
Dumitriu S. (2004) *Polysaccharides: Structural Diversity and Functional Versatility*, 2nd edn (Ed. D. Severian). CRC Press, Boca Raton.
Durmaz B. & Sanin F.D. (2001) Effect of carbon to nitrogen ratio on the composition of microbial extracellular polymers in activated sludge. *Water Science and Technology* **44**, 221–229.
van Duyl F.C., de Winder B., Kop A.J. & Wollenzien U. (1999) Tidal coupling between carbohydrate concentrations and bacterial activities in diatom-inhabited intertidal mudflats. *Marine Ecology Progress Series* **191**, 19–32.
Dvorak P., Hindak F., Hasler P., Hindakova A. & Poulickova A. (2014) Morphological and molecular studies of Neosynechococcus sphagnicola, gen. et sp. nov. (Cyanobacteria, Synechococcales). *Phytotaxa* **170**, 024.
Dyhrman S.T., Jenkins B.D., Rynearson T.A., Saito M.A., Mercier M.L., Alexander H., Whitney L.P., Drzewianowski A., Bulygin V.V., Bertrand E.M., Wu Z., Benitez-Nelson C. & Heithoff A. (2012) The transcriptome and proteome of the diatom Thalassiosira pseudonana reveal a diverse phosphorus stress response. *PLoS One* **7**, e33768.
Dziewit L., Czarnecki J., Wibberg D., Radlinska M., Mrozek P., Szymczak M., Schlüter A., Pühler A. & Bartosik D. (2014) Architecture and functions of a multipartite genome of the methylotrophic bacterium Paracoccus aminophilus JCM 7686, containing primary and secondary chromids. *BMC Genomics* **15**, 124.
Edgar L.A. & Pickett-Heaps J.D. (1983) The mechanism of diatom locomotion. I. An ultrastructural study of the motility apparatus. *Proceedings of the Royal Society B: Biological Sciences* **218**, 331–343.
Elias S. & Banin E. (2012) Multi-species biofilms: living with friendly neighbors. *FEMS Microbiology Reviews* **36**, 990–1004.
Elifantz H., Malmstrom R.R., Cottrell M.T. & Kirchman D.L. (2005) Assimilation of polysaccharides and glucose by major bacterial groups in the Delaware Estuary. *Applied and Environmental Microbiology* **71**, 7799–7805.
Emtiazi F., Schwartz T., Marten S.M., Krolla-Sidenstein P. & Obst U. (2004) Investigation of natural biofilms formed during the production of drinking water from surface water embankment filtration. *Water Research* **38**, 1197–1206.
Fang H.W., Shang Q.Q., Chen M.H. & He G.J. (2014) Changes in the critical erosion velocity for sediment colonized by biofilm. *Sedimentology* **61**, 648–659.
Fink R., Oder M., Rangus D., Raspor P. & Bohinc K. (2015) Microbial adhesion capacity. Influence of shear and temperature stress. *International Journal of Environmental Health Research* **25**, 656–669.
Flemming H.C. (2011) The perfect slime. *Colloids and Surfaces B-Biointerfaces* **86**, 251–259.

Flemming H.C. & Wingender J. (2001a) Relevance of microbial extracellular polymeric substances (EPSs) - Part I: Structural and ecological aspects. *Water Science and Technology* **43**, 1–8.
Flemming H.C. & Wingender J. (2001b) Relevance of microbial extracellular polymeric substances (EPSs) - Part II: Technical aspects. *Water Science and Technology* **43**, 9–16.
Flemming H.C. & Wingender J. (2010) The biofilm matrix. *Nature Reviews Microbiology* **8**, 623–633.
Flemming H.C. & Wingender J. (2002) What biofilms contain - proteins, polysaccharides, etc. *Chemie in Unserer Zeit* **36**, 30–42.
Flemming H.C., Wingender J., Mayer C., Korstgens V. & Borchard W. (2000) Cohesiveness in biofilm matrix polymers. (Eds D. Allison, P. Gilbert, H. Lappin-Scott & M. Wilson), pp. 87–105. Cambridge University Press, Cambridge.
Fogg G.E. (1983) The ecological significance of extracellular products of phytoplankton photosynthesis. *Botanica Marina* **26**, 3–14.
Foley I. & Gilbert P. (1996) Antibiotic resistance of biofilms. *Biofouling* **10**, 331–346.
Franks J. & Stolz J.F. (2009) Flat laminated microbial mat communities. *Earth-Science Reviews* **96**, 163–172.
Friend P.L., Ciavola P., Cappucci S. & Santos R. (2003) Bio-dependent bed parameters as a proxy tool for sediment stability in mixed habitat intertidal areas. *Continental Shelf Research* **23**, 1899–1917.
Frolund B., Palmgren R., Keiding K. & Nielsen P.H. (1996) Extraction of extracellular polymers from activated sludge using a cation exchange resin. *Water Research* **30**, 1749–1758.
Fuhrman J.A. & Azam F. (1982) Thymidine incorporation as a measure of heterotrophic bacterioplankton production in marine surface waters: evaluation and field results. *Marine Biology* **66**, 109–120.
Fukami K., Nishijima T. & Ishida Y. (1997) Stimulative and inhibitory effects of bacteria on the growth of microalgae. *Hydrobiologia* **358**, 185–191.
Galy O., Zrelli K., Latour-Lambert P., Kirwan L. & Henry N. (2014) Remote magnetic actuation of micrometric probes for in situ 3D mapping of bacterial biofilm physical properties. *Journal of Visualized Experiments* **87**, e50857.
Gamier J., Billen G. & Coste M. (1995) Seasonal succession of diatoms and Chlorophyceae in the drainage network of the Seine River: Observation and modeling. *Limnology and Oceanography* **40**, 750–765.
Gärdes A., Iversen M.H., Grossart H.P., Passow U. & Ullrich M.S. (2011) Diatom-associated bacteria are required for aggregation of Thalassiosira weissflogii. *The ISME Journal* **5**, 436.
Garet M.J. & Moriarty D.J.W. (1996) Acid extraction of tritium label from bacterial DNA in clay sediment. *Journal of Microbiological Methods* **25**, 1–4.
Gashti M.P., Bellavance J., Kroukamp O., Wolfaardt G., Taghavi S.M. & Greener J. (2015) Live-streaming: Time-lapse video evidence of novel streamer formation mechanism and varying viscosity. *Biomicrofluidics* **9**, **9**, 041101–041101.
Gawne B., Wang Y., Hoagland K.D. & Gretz M.R. (1998) Role of bacteria and bacterial exopolymer in the attachment of Achnanthes longipes (Bacillariophyceae). *Biofouling* **13**, 137–156.
Gerbersdorf S.U., Bittner R., Lubarsky H., Manz W. & Paterson D.M. (2009) Microbial assemblages as ecosystem engineers of sediment stability. *Journal of Soils and Sediments* **9**, 640–652.

Gerbersdorf S.U., Cimatoribus C., Class H., Engesser K.-H., Helbich S., Hollert H., Lange C., Kranert M., Metzger J., Nowak W., Seiler T.-B., Steger K., Steinmetz H. & Wieprecht S. (2015) Anthropogenic Trace Compounds (ATCs) in aquatic habitats - Research needs on sources, fate, detection and toxicity to ensure timely elimination strategies and risk management. *Environment International* **79**, 85–105.

Gerbersdorf S.U., Hollert H., Brinkmann M., Wieprecht S., Schüttrumpf H. & Manz W. (2011) Anthropogenic pollutants affect ecosystem services of freshwater sediments: the need for a “triad plus x” approach. *Journal of Soils and Sediments* **11**, 1099–1114.

Gerbersdorf S.U., Jancke T. & Westrich B. (2005a) Physico-chemical and biological sediment properties determining erosion resistance of contaminated riverine sediments–Temporal and vertical pattern at the Lauffen reservoir/River Neckar, Germany. *Limnologica-Ecology and Management of Inland Waters* **35**, 132–144.

Gerbersdorf S.U., Jancke T. & Westrich B. (2007) Sediment properties for assessing the erosion risk of contaminated riverine sites. *Journal of Soils and Sediments* **7**, 25–35.

Gerbersdorf S.U., Jancke T., Westrich B. & Paterson D.M. (2008a) Microbial stabilization of riverine sediments by extracellular polymeric substances. *Geobiology* **6**, 57–69.

Gerbersdorf S.U., Manz W. & Paterson D.M. (2008b) The engineering potential of natural benthic bacterial assemblages in terms of the erosion resistance of sediments. *FEMS Microbiology Ecology* **66**, 282–294.

Gerbersdorf S.U., Meyercordt J. & Meyer-Reil L.-A. (2005b) Microphytobenthic primary production in the Bodden estuaries, southern Baltic Sea, at two study sites differing in trophic status. *Aquatic Microbial Ecology* **41**, 181–198.

Gerbersdorf S.U. & Schubert H. (2011) Vertical migration of phytoplankton in coastal waters with different UVR transparency. *Environmental Sciences Europe* **23**, 36.

Gerbersdorf S.U. & Wieprecht S. (2015) Biostabilization of cohesive sediments: revisiting the role of abiotic conditions, physiology and diversity of microbes, polymeric secretion, and biofilm architecture. *Geobiology* **13**, 68–97.

Goto N., Mitamura O. & Terai H. (2001) Biodegradation of photosynthetically produced extracellular organic carbon from intertidal benthic algae. *Journal of Experimental Marine Biology and Ecology* **257**, 73–86.

Graba M., Moulin F.Y., Bouletreau S., Garabetian F., Kettab A., Eiff O., Sanchez-Perez J.M. & Sauvage S. (2010) Effect of near-bed turbulence on chronic detachment of epilithic biofilm: Experimental and modeling approaches. *Water Resources Research* **46**.

Graba M., Sauvage S., Moulin F.Y., Urrea G., Sabater S. & Sanchez-Perez J.M. (2013) Interaction between local hydrodynamics and algal community in epilithic biofilm. *Water Research* **47**, 2153–2163.

Grabowski R.C., Droppo I.G. & Wharton G. (2011) Erodibility of cohesive sediment: the importance of sediment properties. *Earth-Science Reviews* **105**, 101–120.

Grant J. & Gust G. (1987) Prediction of coastal sediment stability from photopigment content of mats of purple sulfur bacteria. *Nature* **330**, 244–246.

Grossart H.P. & Simon M. (2007) Interactions of planktonic algae and bacteria: effects on algal growth and organic matter dynamics. *Aquatic Microbial Ecology* **47**, 163–176.

Grün A.Y., Meier J., Metreveli G., Schaumann G.E. & Manz W. (2016) Sublethal concentrations of silver nanoparticles affect the mechanical stability of biofilms. *Environmental Science and Pollution Research* **23**, 24277–24288.
Guerrini F., Mazzotti A., Boni L. & Pistocchi R. (1998) Bacterial-algal interactions in polysaccharide production. *Aquatic Microbial Ecology* **15**, 247–253.
Guo H., Yi W., Song J.K. & Wang P.G. (2008) Current understanding on biosynthesis of microbial polysaccharides. *Current Topics in Medicinal Chemistry* **8**, 141–151.
Gutleben J., De Mares M.C., van Elsas J.D., Smidt H., Overmann J. & Sipkema D. (2018) The multi-omics promise in context: from sequence to microbial isolate. *Critical Reviews in Microbiology* **44**, 212–229.
Haag I., Kern U. & Westrich B. (2001) Erosion investigation and sediment quality measurements for a comprehensive risk assessment of contaminated aquatic sediments. *Science of the Total Environment* **266**, 249–257.
Hagn F. (2012) A structural view on spider silk proteins and their role in fiber assembly. *Journal of Peptide Science: An Official Publication of the European Peptide Society* **18**, 357–365.
Hanlon A.R.M., Bellinger B., Haynes K., Xiao G., Hofmann T.A., Gretz M.R., Ball A.S., Osborn A.M. & Underwood G.J.C. (2006) Dynamics of extracellular polymeric substance (EPS) production and loss in an estuarine, diatom-dominated, microalgal biofilm over a tidal emersion-immersion period. *Limnology and Oceanography* **51**, 79–93.
Hannah D.M., Wood P.J. & Sadler J.P. (2004) Ecohydrology and hydroecology: A 'new paradigm'?. *Hydrological Processes* **18**, 3439–3445.
Haralampides K., McCorquodale J.A. & Krishnappan B.G. (2003) Deposition properties of fine sediment. *Journal of Hydraulic Engineering-ASCE* **129**, 230–234.
Havens K.E., East T.L., Meeker R.H., Davis W.P. & Steinman A.D. (1996) Phytoplankton and periphyton responses to in situ experimental nutrient enrichment in a shallow subtropical lake. *Journal of Plankton Research* **18**, 551–566.
Havskum H., Thingstad T.F., Scharek R., Peters F., Berdalet E., Sala M.M., Alcaraz M., Bangsholt J.C., Zweifel U.L., Hagström Å., Perez M. & Dolan J.R. (2003) Silicate and labile DOC interfere in structuring the microbial food web via algal—bacterial competition for mineral nutrients: Results of a mesocosm experiment. *Limnology and Oceanography* **48**, 129–140.
Haynes K., Hofmann T.A., Smith C.J., Ball A.S., Underwood G.J.C. & Osborn A.M. (2007) Diatom-derived carbohydrates as factors affecting bacterial community composition in estuarine sediments. *Applied and Environmental Microbiology* **73**, 6112–6124.
Henrici A.T. & Johnson D.E. (1935) Studies of freshwater bacteria. *Journal of Bacteriology* **30**, 61–93.
Hense B.A., Kuttler C., Mueller J., Rothballer M., Hartmann A. & Kreft J.U. (2007) Does efficiency sensing unify diffusion and quorum sensing?. *Nature Reviews Microbiology* **5**, 230–239.
Hibbing M.E., Fuqua C., Parsek M.R. & Peterson S.B. (2010) Bacterial competition: surviving and thriving in the microbial jungle. *Nature Reviews Microbiology* **8**, 15–25.
Higgins M.J., Crawford S.A., Mulvaney P. & Wetherbee R. (2002) Characterization of the Adhesive Mucilages Secreted by Live Diatom Cells using Atomic Force Microscopy. *Protist* **153**, 25–38.

Higgins M.J., Sader J.E., Mulvaney P. & Wetherbee R. (2003) Probing the surface of living diatoms with atomic force microscopy: the nanostructure and nanomechanical properties of the mucilage layer. *Journal of Phycology* **39**, 722–734.

Hillebrand H., Dürselen C.D., Kirschtel D., Pollingher U. & Zohary T. (1999) Biovolume calculation for pelagic and benthic microalgae. *Journal of Phycology* **35**, 403–424.

Hirst C.N., Cyr H. & Jordan I.A. (2003) Distribution of exopolymeric substances in the littoral sediments of an oligotrophic lake. *Microbial Ecology* **46**, 22–32.

Hoagland K.D., Rosowski J.R., Gretz M.R. & Roemer S.C. (1993) Diatom extracellular polymeric substances - function, fine-structure, chemistry and physiology. *Journal of Phycology* **29**, 537–566.

Hochbaum A.I., Kolodkin-Gal I., Foulston L., Kolter R., Aizenberg J. & Losick R. (2011) Inhibitory effects of D-amino acids on Staphylococcus aureus biofilm development. *Journal of Bacteriology* **193**, 5616–5622.

Hodl I., Mari L., Bertuzzo E., Suweis S., Besemer K., Rinaldo A. & Battin T.J. (2014) Biophysical controls on cluster dynamics and architectural differentiation of microbial biofilms in contrasting flow environments. *Environmental Microbiology* **16**, 802–812.

Hoffman M.D., Zucker L.I., Brown P.J.B., Kysela D.T., Brun Y.V. & Jacobson S.C. (2015) Timescales and frequencies of reversible and irreversible adhesion events of single bacterial cells. *Analytical Chemistry* **87**, 12032–12039.

Hofmann G., Werum M. & Lange-Bertalot H. (2011) *Diatomeen im Süßwasser-Benthos von Mitteleuropa* (Ed. H. Lange-Bertalot). A.R.G. Gantner Verlag K.G., Ruggell.

Hofmann T., Hanlon A.R.M., Taylor J.D., Ball A.S., Osborn A.M. & Underwood G.J.C. (2009) Dynamics and compositional changes in extracellular carbohydrates in estuarine sediments during degradation. *Marine Ecology Progress Series* **379**, 45–58.

Holtappels M. & Lorke A. (2011) Estimating turbulent diffusion in a benthic boundary layer. *Limnology and Oceanography: Methods* **9**, 29–41.

Horn H. & Hempel D.C. (1998) Modeling mass transfer and substrate utilization in the boundary layer of biofilm systems. *Water Science and Technology* **37**, 139–147.

Hu C.X., Liu Y.D., Paulsen B.S., Petersen D. & Klaveness B. (2003) Extracellular carbohydrate polymers from five desert soil algae with different cohesion in the stabilization of fine sand grain. *Carbohydrate Polymers* **54**, 33–42.

Hubas C., Artigas L.F. & Davoult D. (2007a) Role of the bacterial community in the annual benthic metabolism of two contrasted temperate intertidal sites (Roscoff Aber Bay, France). *Marine Ecology Progress Series* **344**, 39–48.

Hubas C., Lamy D., Artigas L.F. & Davoult D. (2007b) Seasonal variability of intertidal bacterial metabolism and growth efficiency in an exposed sandy beach during low tide. *Marine Biology* **151**, 41–52.

Jackson C.R., Churchill P.F. & Roden E.E. (2001) Successional changes in bacterial assemblage structure during epilithic biofilm development. *Ecology* **82**, 555–566.

Jain A., Gupta Y., Agrawal R., Khare P. & Jain S.K. (2007) Biofilms - a microbial life perspective: a critical review. *Critical Reviews™ in Therapeutic Drug Carrier Systems* **24**, 393–443.

Jesus B., Brotas V., Ribeiro L., Mendes C.R., Cartaxana P. & Paterson D.M. (2009) Adaptations of microphytobenthos assemblages to sediment type and tidal position. *Continental Shelf Research* **29**, 1624–1634.
Jiles D.C. (1998) *Introduction to Magnetism and Magnetic Materials*, 2nd edn. Chapman & Hall, London.
Jorand F., Boue-Bigne F., Block J.C. & Urbain V. (1998) Hydrophobic/hydrophilic properties of activated sludge exopolymeric substances. *Water Science and Technology* **37**, 307–315.
Jorand F., Guicherd P., Urbain V., Manem J. & Block J.C. (1994) Hydrophobicity of activated sludge flocs and laboratory-grown bacteria. *Water Science and Technology* **30**, 211–218.
Jung S.W., Kim B.H., Katano T., Kong D.S. & Han M.S. (2008) Pseudomonas fluorescens HYK0210-SK09 offers species-specific biological control of winter algal blooms caused by freshwater diatom Stephanodiscus hantzschii. *Journal of Applied Microbiology* **105**, 186–195.
Kaden R., Spröer C., Beyer D. & Krolla-Sidenstein P. (2014) Rhodoferax saidenbachensis sp. nov., a psychrotolerant, very slowly growing bacterium within the family Comamonadaceae, proposal of appropriate taxonomic position of Albidiferax ferrireducens strain T118T in the genus Rhodoferax and emended description of the genus Rhodoferax. *International Journal of Systematic and Evolutionary Microbiology* **64**, 1186–1193.
Kalmbach S., Manz W., Wecke J. & Szewzyk U. (1999) Aquabacterium gen. nov., with description of Aquabacterium citratiphilum sp. nov., Aquabacterium parvum sp. nov. and Aquabacterium commune sp. nov., three in situ dominant bacterial species from the Berlin drinking water system. *International Journal of Systematic and Evolutionary Microbiology* **49**, 769–777.
Kanellopoulos C., Lamprinou V., Mitropoulos P. & Voudouris P. (2016) Thermogenic travertine deposits in Thermopylae hot springs (Greece) in association with cyanobacterial microflora. *Carbonates and Evaporites* **31**, 239–248.
Karrasch B., Mehrens M., Rosenlöcher Y. & Peters K. (2001) The dynamics of phytoplankton, bacteria and heterotrophic flagellates at two Banks near Magdeburg in the River Elbe (Germany). *Limnologica - Ecology and Management of Inland Waters* **31**, 93–107.
Kendrick M.R. & Huryn A.D. (2015) Discharge, legacy effects and nutrient availability as determinants of temporal patterns in biofilm metabolism and accrual in an arctic river. *Freshwater Biology* **60**, 2323–2336.
Khandeparker R.D. & Bhosle N.B. (2001) Extracellular polymeric substances of the marine fouling diatom amphora rostrata Wm.Sm. *Biofouling* **17**, 117–127.
Klug J.L. (2005) Bacterial response to dissolved organic matter affects resource availability for algae. *Canadian Journal of Fisheries and Aquatic Sciences* **62**, 472–481.
Kolodkin-Gal I., Romero D., Cao S., Clardy J., Kolter R. & Losick R. (2010) D-amino acids trigger biofilm disassembly. *Science* **328**, 627–629.
Kondolf G.M. (1997) PROFILE: hungry water: effects of dams and gravel mining on river channels. *Environmental Management* **21**, 533–551.
Koza A., Hallett P.D., Moon C.D. & Spiers A.J. (2009) Characterization of a novel air-liquid interface biofilm of Pseudomonas fluorescens SBW25. *Microbiology-Sgm* **155**, 1397–1406.
Krammer K. & Lange-Bertalot H. (1986) Sueßwasserflora von Mitteleuropa. In: *Bacillariophyceae*, Teil 1-4 (Eds H. Ettl, H. Gerloff, H. Heynig & D. Mollenhauer). Gustav Fischer Verlag, Stuttgart.

Kudo I., Miyamoto M., Noiri Y. & Maita Y. (2000) Combined effects of temperature and iron on the growth and physiology of the marine diatom Phaeodactylum tricornutum (Bacillariophyceae). *Journal of Phycology* **36**, 1096–1102.
Lai H.T., Hou J.H., Su C.I. & Chen C.L. (2009) Effects of chloramphenicol, florfenicol, and thiamphenicol on growth of algae Chlorella pyrenoidosa, Isochrysis galbana, and Tetraselmis chui. *Ecotoxicology and Environmental Safety* **72**, 329–334.
Lane D. (1991) 16S/23S rRNA sequencing. In: *Nucleic Acid Techniques in Bacterial Systematics* (Eds M. Stackebrandt & M. Goodfellow), pp. 115–175. John Wiley & Sons, Chichester.
Lange K., Liess A., Piggott J.J., Townsend C.R. & Matthaei C.D. (2011) Light, nutrients and grazing interact to determine stream diatom community composition and functional group structure. *Freshwater Biology* **56**, 264–278.
Larned S.T., Packman A.I., Plew D.R. & Vopel K. (2011) Interactions between the mat-forming alga Didymosphenia geminata and its hydrodynamic environment. *Limnology and Oceanography: Fluids and Environments* **1**, 4–22.
Larson F., Lubarsky H., Gerbersdorf S.U. & Paterson D.M. (2009) Surface adhesion measurements in aquatic biofilms using magnetic particle induction: MagPI. *Limnology and Oceanography: Methods* **7**, 490–497.
Laspidou C.S. & Rittmann B.E. (2002) A unified theory for extracellular polymeric substances, soluble microbial products, and active and inert biomass. *Water Research* **36**, 2711–2720.
Law R.J., Elliott J.A., Jones I.D. & Page T. (2014) The influence of different environmental conditions upon the initial development and ecological dynamics of phytobenthic communities. *Fundamental and Applied Limnology/Archiv für Hydrobiologie* **185**, 139–153.
LAWA (1998) *Beurteilung der Wasserbeschaffenheit von Fließgewässern in der Bundesrepublik Deutschland - Chemische Gewässergüteklassifikation.* LAWA (Länderarbeitsgemeinschaft Wasser), Berlin.
Lawrence J.R., Chenier M.R., Roy R., Beaumier D., Fortin N., Swerhone G.D.W., Neu T.R. & Greer C.W. (2004) Microscale and molecular assessment of impacts of nickel, nutrients, and oxygen level on structure and function of river biofilm communities. *Applied and Environmental Microbiology* **70**, 4326–4339.
Le Hir P., Monbet Y. & Orvain F. (2007) Sediment erodability in sediment transport modelling: can we account for biota effects?. *Continental Shelf Research* **27**, 1116–1142.
Lee S. & Fuhrman J.A. (1987) Relationships between biovolume and biomass of naturally derived marine bacterioplankton. *Applied and Environmental Microbiology* **53**, 1298–1303.
Lemos M., Mergulhão F., Melo L. & Simões M. (2015) The effect of shear stress on the formation and removal of Bacillus cereus biofilms. *Food and Bioproducts Processing* **93**, 242–248.
Leon-Morales C.F., Leis A.P., Strathmann M. & Flemming H.C. (2004) Interactions between laponite and microbial biofilms in porous media: implications for colloid transport and biofilm stability. *Water Research* **38**, 3614–3626.
Leon-Morales C.F., Strathmann M. & Flemming H.-C. (2007) Role of biofilms on sediment transport- investigations with artificial sediment columns. In: *Sediment Dynamics and Pollutant Mobility in Rivers* (Eds W. Bernhard & F. Ulrich), pp. 358–368. Springer, Berlin Heidelberg.

Levy J.L., Stauber J.L., Wakelin S.A. & Jolley D.F. (2009) The effect of bacteria on the sensitivity of microalgae to copper in laboratory bioassays. *Chemosphere* **74**, 1266–1274.
Liao B.Q., Allen D.G., Droppo I.G., Leppard G.G. & Liss S.N. (2001) Surface properties of sludge and their role in bioflocculation and settleability. *Water Research* **35**, 339–350.
Lind J.L., Heimann K., Miller E.A., vanVliet C., Hoogenraad N.J. & Wetherbee R. (1997) Substratum adhesion and gliding in a diatom are mediated by extracellular proteoglycans. *Planta* **203**, 213–221.
Liu Y. & Fang H.H.P. (2003) Influences of extracellular polymeric substances (EPS) on flocculation, settling, and dewatering of activated sludge. *Critical Reviews in Environmental Science and Technology* **33**, 237–273.
Liu Y. & Tay J.H. (2002) The essential role of hydrodynamic shear force in the formation of biofilm and granular sludge. *Water research* **36**, 1653–1665.
Long R.A. & Azam F. (1996) Abundant protein-containing particles in the sea. *Aquatic Microbial Ecology* **10**, 213–221.
Lorenz M.O. (1905) Methods of measuring the concentration of wealth. *Publications of the American Statistical Association* **9**, 209–219.
Lubarsky H.V., Gerbersdorf S.U., Hubas C., Behrens S., Ricciardi F. & Paterson D.M. (2012) Impairment of the bacterial biofilm stability by triclosan. *PLoS One* **7**, e31183.
Lubarsky H.V., Hubas C., Chocholek M., Larson F., Manz W., Paterson D.M. & Gerbersdorf S.U. (2010) The Stabilisation Potential of Individual and Mixed Assemblages of Natural Bacteria and Microalgae. *PLoS One* **5**, e13794.
Lundkvist M., Gangelhof U., Lunding J. & Flindt M.R. (2007a) Production and fate of extracellular polymeric substances produced by benthic diatoms and bacteria: a laboratory study. *Estuarine, Coastal and Shelf Science* **75**, 337–346.
Lundkvist M., Grue M., Friend P.L. & Flindt M.R. (2007b) The relative contributions of physical and microbiological factors to cohesive sediment stability. *Continental Shelf Research* **27**, 1143–1152.
Lyautey E., Jackson C.R., Cayrou J., Rols J.-L. & Garabétian F. (2005) Bacterial community succession in natural river biofilm assemblages. *Microbial Ecology* **50**, 589–601.
Lynch D.J., Fountain T.L., Mazurkiewicz J.E. & Banas J.A. (2007) Glucan-binding proteins are essential for shaping Streptococcus mutans biofilm architecture. *FEMS Microbiology Letters* **268**, 158–165.
Magaletti E., Urbani R., Sist P., Ferrari C.R. & Cicero A.M. (2004) Abundance and chemical characterization of extracellular carbohydrates released by the marine diatom Cylindrotheca fusiformis under N- and P-limitation. *European Journal of Phycology* **39**, 133–142.
Manz B., Volke F., Goll D. & Horn H. (2005) Investigation of biofilm structure, flow patterns and detachment with magnetic resonance imaging. *Water Science and Technology* **52**, 1–6.
Manz W. (1999) In situ analysis of microbial biofilms by rRNA-targeted oligonucleotide probing. *Biofilms* **310**, 79–91.
Manz W., Amann R., Ludwig W., Vancanneyt M. & Schleifer K.H. (1996) Application of a suite of 16S rRNA-specific oligonucleotide probes designed to investigate bacteria of the phylum cytophaga-flavobacter-bacteroides in the natural environment. *Microbiology* **142**, 1097–1106.

Manz W., Amann R., Ludwig W., Wagner M. & Schleifer K.H. (1992) Phylogenetic oligodeoxynucleotide probes for the major subclasses of proteobacteria: problems and solutions. *Systematic and Applied Microbiology* **15**, 593–600.
Manzenrieder H. (1985) Retardation of initial erosion under biological effects in sandy tidal flats. *Australasian Conference on Coastal and Ocean Engineering*, 455.
Marcarelli A.M., Bechtold H.A., Rugenski A.T. & Inouye R.S. (2009) Nutrient limitation of biofilm biomass and metabolism in the Upper Snake River basin, southeast Idaho, USA. *Hydrobiologia* **620**, 63–76.
Marques A.M., Estanol I., Alsina J.M., Fuste C., Simonpujol D., Guinea J. & Congregado F. (1986) Production and rheological properties of the extracellular polysaccharide synthesized by Pseudomonas sp. strain EPS-5028. *Applied and Environmental Microbiology* **52**, 1221–1223.
Marshall K.C. (1985) Mechanisms of bacterial adhesion at solid-water interfaces. In: *Bacterial Adhesion: Mechanisms and Physiological Significance* (Eds D.C. Savage & M. Fletcher), pp. 133–161. Plenum Press, New York.
Marzorati M., Wittebolle L., Boon N., Daffonchio D. & Verstraete W. (2008) How to get more out of molecular fingerprints: practical tools for microbial ecology. *Environmental Microbiology* **10**, 1571–1581.
Mastropaolo M.D., Silby M.W., Nicoll J.S. & Levy S.B. (2012) Novel genes involved in Pseudomonas fluorescens Pf0-1 motility and biofilm formation. *Applied and Environmental Microbiology* **78**, 4318–4329.
Matz C. & Kjelleberg S. (2005) Off the hook - how bacteria survive protozoan grazing. *Trends in Microbiology* **13**, 302–307.
McDougald D., Rice S.A., Barraud N., Steinberg P.D. & Kjelleberg S. (2012) Should we stay or should we go: mechanisms and ecological consequences for biofilm dispersal. *Nature Reviews Microbiology* **10**, 39–50.
McKay R.M.L., Geider R.J. & LaRoche J. (1997) Physiological and biochemical response of the photosynthetic apparatus of two marine diatoms to Fe stress. *Plant Physiology* **114**, 615–622.
McKew B.A., Dumbrell A.J., Taylor J.D., McGenity T.J. & Underwood G.J.C. (2013) Differences between aerobic and anaerobic degradation of microphytobenthic biofilm-derived organic matter within intertidal sediments. *FEMS Microbiology Ecology* **84**, 495–509.
Meyer-Reil L.-A. (2005) *Mikrobiologie des Meeres*. WUV Fakultas, Wien.
Mieszkin S., Callow M.E. & Callow J.A. (2013) Interactions between microbial biofilms and marine fouling algae: a mini review. *Biofouling* **29**, 1097–1113.
Molino P.J., Hodson O.M., Quinn J.F. & Wetherbee R. (2006) Utilizing QCM-D to characterize the adhesive mucilage secreted by two marine diatom species in-situ and in real-time. *Biomacromolecules* **7**, 3276–3282.
Molino P.J. & Wetherbee R. (2008) The biology of biofouling diatoms and their role in the development of microbial slimes. *Biofouling* **24**, 365–379.
Moreira J.M.R., Simões M., Melo L.F. & Mergulhão F.J. (2015) The combined effects of shear stress and mass transfer on the balance between biofilm and suspended cell dynamics. *Desalination and Water Treatment* **53**, 3348–3354.
Morton L.H.G., Greenway D.L.A., Gaylarde C.C. & Surman S.B. (1998) Consideration of some implications of the resistance of biofilms to biocides. *International Biodeterioration & Biodegradation* **41**, 247–259.
Moss J.A., Nocker A., Lepo J.E. & Snyder R.A. (2006) Stability and change in estuarine biofilm bacterial community diversity. *Applied and Environmental Microbiology* **72**, 5679–5688.

Mu R.M., Fan Z.Q., Pei H.Y., Yuan X.L., Liu S.X. & Wang X.R. (2007) Isolation and algae-lysing characteristics of the algicidal bacterium B5. *Journal of Environmental Sciences* **19**, 1336–1340.
Mulholland P.J., Steinman A.D., Marzolf E.R., Hart D.R. & DeAngelis D.L. (1994) Effect of periphyton biomass on hydraulic characteristics and nutrient cycling in streams. *Oecologia* **98**, 40–47.
Muyzer G., Dewaal E.C. & Uitterlinden A.G. (1993) Profiling of complex microbial populations by denaturing gradient gel electrophoresis analysis of polymerase chain reaction-amplified genes coding for 16S rRNA. *Applied and Environmental Microbiology* **59**, 695–700.
Nadell C.D., Xavier J.B., Levin S.A. & Foster K.R. (2008) The evolution of quorum sensing in bacterial biofilms. *PLoS Biology* **6**, 171–179.
Neef A. (1997) *Anwendung der in situ Einzelzell-Identifizierung von Bakterien zur Populationsanalyse in komplexen mikrobiellen Biozönosen*. Technische Universität München, Germany.
Netzband A., Reincke H. & Bergemann M. (2002) The river Elbe: a case study for the ecological and economical chain of sediments. *Journal of Soils and Sediments* **2**, 112–116.
Nichols P.D. & Nichols C.A.M. (2008) Microbial signature lipid profiling and exopolysaccharides: experiences initiated with Professor David C White and transported to Tasmania, Australia. *Journal of Microbiological Methods* **74**, 33–46.
Niederdorfer R., Peter H. & Battin T.J. (2016) Attached biofilms and suspended aggregates are distinct microbial lifestyles emanating from differing hydraulics. *Nature Microbiology* **1**.
Nielsen K.M., Calamai L. & Pietramellara G. (2006) Stabilization of extracellular DNA and proteins by trans ent binding to various soil components. *Soil Biology* **8**, 141–157.
Nielsen P.H., Jahn A. & Palmgren R. (1997) Conceptual model for production and composition of exopolymers in biofilms. *Water Science and Technology* **36**, 11–19.
Nikora V. (2010) Hydrodynamics of aquatic ecosystems: an interface between ecology, biomechanics and environmental fluid mechanics. *River Research and Applications* **26**, 367–384.
Nikora V.I., Goring D.G. & Biggs B.J.F. (1998) A simple model of stream periphyton-flow interactions. *Oikos* **81**, 607–611.
Nikora V.I., Goring D.G. & Biggs B.J.F. (2002) Some observations of the effects of micro-organisms growing on the bed of an open channel on the turbulence properties. *Journal of Fluid Mechanics* **450**, 317–341.
Noffke N., Gerdes G. & Klenke T. (2003) Benthic cyanobacteria and their influence on the sedimentary dynamics of peritidal depositional systems (siliciclastic, evaporitic salty, and evaporitic carbonatic). *Earth-Science Reviews* **62**, 163–176.
Noffke N. & Paterson D. (2008) Microbial interactions with physical sediment dynamics, and their significance for the interpretation of Earth's biological history. *Geobiology* **6**, 1–4.
Nold S.C. & Zwart G. (1998) Patterns and governing forces in aquatic microbial communities. *Aquatic Ecology* **32**, 17–35.
Ohashi A. & Harada H. (1996) A novel concept for evaluation of biofilm adhesion strength by applying tensile force and shear force. *Water Science and Technology* **34**, 201–211.

Olapade O.A. & Leff L.G. (2004) Seasonal dynamics of bacterial assemblages in epilithic biofilms in a northeastern Ohio stream. *Journal of the North American Benthological Society* **23**, 686–700.
Olivares E., Badel-Berchoux S., Provot C., Jaulhac B., Prevost G., Bernardi T. & Jehl F. (2016) The BioFilm Ring Test: a rapid method for routine analysis of Pseudomonas aeruginosa biofilm formation kinetics. *Journal of Clinical Microbiology* **54**, 657–661.
Onder O., Aygun-Sunar S., Selamoglu N. & Daldal F. (2010) A glimpse into the proteome of phototrophic bacterium Rhodobacter capsulatus. In: *Recent Advances in Phototrophic Prokaryotes* (Ed. C.H. Patrick), pp. 179–209. Springer, New York.
Orvain F., Galois R., Barnard C., Sylvestre A., Blanchard G. & Sauriau P.G. (2003) Carbohydrate production in relation to microphytobenthic biofilm development: An integrated approach in a tidal mesocosm. *Microbial Ecology* **45**, 237–251.
Park C. & Novak J.T. (2009) Characterization of lectins and bacterial adhesins in activated sludge flocs. *Water Environment Research* **81**, 755–764.
Parry J.D. (2004) Protozoan grazing of freshwater biofilms. *Advances in Applied Microbiology, Vol 54* **54**, 167–196.
Parsek M.R. & Tolker-Nielsen T. (2008) Pattern formation in Pseudomonas aeruginosa biofilms. *Current Opinion in Microbiology* **11**, 560–566.
Pasmore M. & Costerton J.W. (2003) Biofilms, bacterial signaling, and their ties to marine biology. *Journal of Industrial Microbiology & Biotechnology* **30**, 407–413.
Passarelli C., Hubas C., Segui A.N., Grange J. & Meziane T. (2012) Surface adhesion of microphytobenthic biofilms is enhanced under Hediste diversicolor (OF Müller) trophic pressure. *Journal of Experimental Marine Biology and Ecology* **438**, 52–60.
Passarelli C., Olivier F., Paterson D.M., Tarik M. & Cédric H. (2014) Organisms as cooperative ecosystem engineers in intertidal flats. *Journal of Sea Research* **92**, 92–101.
Paterson D.M. (1989) Short-term changes in the erodibility of intertidal cohesive sediments related to the migratory behavior of epipelic diatoms. *Limnology and Oceanography* **34**, 223–234.
Paterson D.M. (1990) The influence of epipelic diatoms on the erodibility of an artificial sediment. In: *Proceedings of the 10th International Symposium on Living and Fossil Diatoms, 1988* (Ed. H. Simola), pp. 345–355. Koeltz Scientific Books, Joensuu.
Paterson D.M., Aspden R.J., Visscher P.T., Consalvey M., Andres M.S., Decho A.W., Stolz J. & Reid R.P. (2008) Light-dependant biostabilisation of sediments by stromatolite assemblages. *PLoS One* **3**.
Paterson D.M. & Black K.S. (1999) Water flow, sediment dynamics and benthic biology. *Advances in Ecological Research, Vol 29* **29**, 155–193.
Paterson D.M., Tolhurst T.J., Kelly J.A., Honeywill C., de Deckere E., Huet V., Shayler S.A., Black K.S., de Brouwer J. & Davidson I. (2000) Variations in sediment properties, Skeffling mudflat, Humber Estuary, UK. *Continental Shelf Research* **20**, 1373–1396.
Paul B.J. & Duthie H.C. (1989) Nutrient cycling in the epilithon of running waters. *Canadian Journal of Botany* **67**, 2302–2309.
Pennisi E. (2002) Biology reveals new ways to hold on tight. *Science* **296**, 250–251.

Pereira M.O., Kuehn M., Wuertz S., Neu T. & Melo L.F. (2002) Effect of flow regime on the architecture of a Pseudomonas fluorescens biofilm. *Biotechnology and Bioengineering* **78**, 164–171.
Perkins R.G., Honeywill C., Consalvey M., Austin H.A., Tolhurst T.J. & Paterson D.M. (2003) Changes in microphytobenthic chlorophyll a and EPS resulting from sediment compaction due to de-watering: opposing patterns in concentration and content. *Continental Shelf Research* **23**, 575–586.
Perkins R.G., Underwood G.J.C., Brotas V., Snow G.C., Jesus B. & Ribeiro L. (2001) Responses of microphytobenthos to light: primary production and carbohydrate allocation over an emersion period. *Marine Ecology Progress Series* **223**, 101–112.
Peterson C. (1996) Response of benthic algal communities to natural physical disturbance. *Algal Ecology*, 375–402.
Peyton B.M. & Characklis W.G. (1993) A statistical analysis of the effect of substrate utilization and shear stress on the kinetics of biofilm detachment. *Biotechnology and Bioengineering* **41**, 728–735.
Phoenix V.R., Bennett P.C., Engel A.S., Tyler S.W. & Ferris F.G. (2006) Chilean high-altitude hot-spring sinters: a model system for UV screening mechanisms by early Precambrian cyanobacteria. *Geobiology* **4**, 15–28.
Phoenix V.R. & Konhauser K.O. (2008) Benefits of bacterial biomineralization. *Geobiology* **6**, 303–308.
Pierre G., Graber M., Orvain F., Dupuy C. & Maugard T. (2010) Biochemical characterization of extracellular polymeric substances extracted from an intertidal mudflat using a cation exchange resin. *Biochemical Systematics and Ecology* **38**, 917–923.
Ping L., Birkenbeil J. & Monajembashi S. (2013) Swimming behavior of the monotrichous bacterium Pseudomonas fluorescens SBW25. *FEMS Microbiology Ecology* **86**, 36–44.
Pique G., Vericat D., Sabater S. & Batalla R.J. (2016) Effects of biofilm on river-bed scour. *Science of the Total Environment* **572**, 1033–1046.
Poff N.L. & Ward J.V. (1995) Herbivory under different flow regimes: a field experiment and test of a model with a benthic stream insect. *Oikos* **72**, 179–188.
Poindexter J.S. (1981) The caulobacters - ubiquitous unusual bacteria. *Microbiological Reviews* **45**, 123–179.
Pomeroy L.R., Williams P.J.I., Azam F. & Hobbie J.E. (2007) The microbial loop. *Oceanography* **20**, 28–33.
Poppele E.H. & Hozalski R.M. (2003) Micro-cantilever method for measuring the tensile strength of biofilms and microbial flocs. *Journal of Microbiological Methods* **55**, 607–615.
Potapova M. & Hamilton P.B. (2007) Morphological and ecological variation within the Achnanthidium minutissimum (Bacillariophyceae) species complex. *Journal of Phycology* **43**, 561–575.
Power M.E., Parker M.S. & Dietrich W.E. (2008) Seasonal reassembly of a river food web: floods, droughts, and impacts of fish. *Ecological Monographs* **78**, 263–282.
Prieto D.M., Devesa-Rey R., Rubinos D.A., Díaz-Fierros F. & Barral M.T. (2016) Biofilm formation on river sediments under different light intensities and nutrient inputs: a Flume Mesocosm Study. *Environmental Engineering Science* **33**, 250–260.

Pruesse E., Quast C., Knittel K., Fuchs B.M., Ludwig W., Peplies J. & Glöckner F.O. (2007) SILVA: a comprehensive online resource for quality checked and aligned ribosomal RNA sequence data compatible with ARB. *Nucleic Acids Research* **35**, 7188–96.

Raaijmakers J.M., Weller D.M. & Thomashow L.S. (1997) Frequency of antibiotic-producing Pseudomonas spp. in natural environments. *Applied and Environmental Microbiology* **63**, 881–887.

Rabus R., Fukui M., Wilkes H. & Widdel F. (1996) Degradative capacities and 16S rRNA-targeted whole-cell hybridization of sulfate-reducing bacteria in an anaerobic enrichment culture utilizing alkylbenzenes from crude oil. *Applied and Environmental Microbiology* **62**, 3605–3613.

Rasmussen K. & Lewandowski Z. (1998) Microelectrode measurements of local mass transport rates in heterogeneous biofilms. *Biotechnology and Bioengineering* **59**, 302–309.

Raunkjaer K., Hvitvedjacobsen T. & Nielsen P.H. (1994) Measurement of pools of protein, carbohydrate and lipid in domestic waste-water. *Water Research* **28**, 251–262.

Reisinger A.J., Tank J.L. & Dee M.M. (2016) Regional and seasonal variation in nutrient limitation of river biofilms. *Freshwater Science* **35**, 474–489.

Ribalet F., Intertaglia L., Lebaron P. & Casotti R. (2008) Differential effect of three polyunsaturated aldehydes on marine bacterial isolates. *Aquatic Toxicology* **86**, 249–255.

Riber H.H. & Wetzel R.G. (1987) Boundary-layer and internal diffusion effects on phosphorus fluxes in lake periphyton. *Limnology and Oceanography* **32**, 1181–1194.

Rice S.P., Lancaster J. & Kemp P. (2010) Experimentation at the interface of fluvial geomorphology, stream ecology and hydraulic engineering and the development of an effective, interdisciplinary river science. *Earth Surface Processes and Landforms* **35**, 64–77.

Riethmüller R., Heineke M., Kühl H. & Keuker-Rüdiger R. (2000) Chlorophyll a concentration as an index of sediment surface stabilisation by microphytobenthos?. *Continental Shelf Research* **20**, 1351–1372.

Righetti M. & Lucarelli C. (2007) May the Shields theory be extended to cohesive and adhesive benthic sediments?. *Journal of Geophysical Research: Oceans* **112**, C05039.

Roeselers G., Loosdrecht M.C.M. van & Muyzer G. (2007) Heterotrophic pioneers facilitate phototrophic biofilm development. *Microbial Ecology* **54**, 578–585.

Roller C., Wagner M., Amann R., Ludwig W. & Schleifer K.H. (1994) In situ probing of Gram-positive bacteria with high DNA G1C content using 23S rRNA-targeted oligonucleotides. *Microbiology* **140**, 2849–2858.

Romani A.M., Giorgi A., Acuna V. & Sabater S. (2004) The influence of substratum type and nutrient supply on biofilm organic matter utilization in streams. *Limnology and Oceanography* **49**, 1713–1721.

Rusconi R., Guasto J.S. & Stocker R. (2014) Bacterial transport suppressed by fluid shear. *Nature Physics* **10**, 212–217.

Sack E.L.W., Wielen P.W.J.J. van der & Kooij D. van der (2014) Polysaccharides and proteins added to flowing drinking water at microgram-per-liter levels promote the formation of biofilms predominated by Bacteroidetes and Proteobacteria. *Applied and Environmental Microbiology* **80**, 2360–2371.

Sanin S.L., Sanin F.D. & Bryers J.D. (2003) Effect of starvation on the adhesive properties of xenobiotic degrading bacteria. *Process Biochemistry* **38**, 909–914.
Schäfer H., Abbas B., Witte H. & Muyzer G. (2002) Genetic diversity of 'satellite' bacteria present in cultures of marine diatoms. *FEMS Microbiology Ecology* **42**, 25–35.
Schmidt H. (2017) *Microbial Stabilization of Lotic Fine Sediments*. University of Stuttgart, Germany.
Schmidt H., Gerbersdorf S.U., Ullrich X., Thom M. & Manz W. (2018a) Biofilm adhesiveness is a reliable proxy for the effect assessment of silver nanoparticles on the functionality of freshwater biofilms. *Austin Journal of Environmental Toxicology* **4**, 1022.
Schmidt H., Thom M., King L., Wieprecht S. & Gerbersdorf S.U. (2016) The effect of seasonality upon the development of lotic biofilms and microbial biostabilisation. *Freshwater Biology* **61**, 963–978.
Schmidt H., Thom M., Madzgalla M., Gerbersdorf S.U., Metreveli G. & Manz W. (2017) Exposure to silver nanoparticles affects biofilm structure and adhesiveness. *Journal of Aquatic Pollution and Toxicology* **1**.
Schmidt H., Thom M., Matthies K., Behrens S., Obst U., Wieprecht S. & Gerbersdorf S.U. (2015) A multi-disciplinarily designed mesocosm to address the complex flow-sediment-ecology tripartite relationship on the microscale. *Environmental Sciences Europe* **27**, 1–11.
Schmidt H., Thom M., Wieprecht S., Manz W. & Gerbersdorf S.U. (2018b) The effect of light intensity and shear stress on microbial biostabilization and the community composition of natural bioflms. *Research and Reports in Biology* **8**, 1–16.
Sekar R., Venugopalan V.P., Nandakumar K., Nair K.V.K. & Rao V.N.R. (2004) Early stages of biofilm succession in a lentic freshwater environment. In: *Asian Pacific Phycology in the 21st Century: Prospects and Challenges* (Ed. P.O. Ang), pp. 97–108. Springer, Dordrecht.
Seviour T., Hansen S.H., Yang L., Yau Y.H., Wang V.B., Stenvang M.R., Christiansen G., Marsili E., Givskov M., Chen Y., Otzen D.E., Nielsen P.H., Shochat S.G., Kjelleberg S. & Dueholm M.S. (2015) Functional amyloids keep quorum sensing molecules in check. *Journal of Biological Chemistry* **290**, 6457–6469.
Shannon C.E. & Weaver W. (1963) *The Mathematical Theory of Communication*. University of Illinois Press, Champaign.
Shields A. (1936) Anwendungen der Ähnlichkeitsmechanik und der Turbulenzforschung auf die Geschiebebewegung. *Mitteilungen der preußischen Versuchsanstalt für Wasserbau und Schiffbau, Berlin* **26**.
Singer G., Besemer K., Hoedl I., Chlup A., Hochedlinger G., Stadler P. & Battin T.J. (2006) Microcosm design and evaluation to study stream microbial biofilms. *Limnology and Oceanography: Methods* **4**, 436–447.
Smith D.J. & Underwood G.J.C. (1998) Exopolymer production by intertidal epipelic diatoms. *Limnology and Oceanography* **43**, 1578–1591.
Smith D.J. & Underwood G.J.C. (2000) The production of extracellular carbohydrates by estuarine benthic diatoms: the effects of growth phase and light and dark treatment. *Journal of Phycology* **36**, 321–333.
Somerfield P.J. (2008) Identification of the Bray-Curtis similarity index: Comment on Yoshioka (2008). *Marine Ecology Progress Series* **372**, 303–306.

Spears B.M., Saunders J.E., Davidson I. & Paterson D.M. (2008) Microalgal sediment biostabilisation along a salinity gradient in the Eden Estuary, Scotland: unravelling a paradox. *Marine and Freshwater Research* **59**, 313–321.

Staats N., De Winder B., Stal L.J. & Mur L.R. (1999) Isolation and characterization of extracellular polysaccharides from the epipelic diatoms Cylindrotheca closterium and Navicula salinarum. *European Journal of Phycology* **34**, 161–169.

Staats N., Stal L.J. & Mur L.R. (2000) Exopolysaccharide production by the epipelic diatom Cylindrotheca closterium: effects of nutrient conditions. *Journal of Experimental Marine Biology and Ecology* **249**, 13–27.

Stal L.J. (2010) Microphytobenthos as a biogeomorphological force in intertidal sediment stabilization. *Ecological Engineering* **36**, 236–245.

Stal L.J. (2003) Microphytobenthos, their extracellular polymeric substances, and the morphogenesis of intertidal sediments. *Geomicrobiology Journal* **20**, 463–478.

Stewart P.S. (2012) Mini-review: convection around biofilms. *Biofouling* **28**, 187–198.

Stoodley P., Dodds I., Boyle J.D. & Lappin-Scott H.M. (1999a) Influence of hydrodynamics and nutrients on biofilm structure. *Journal of Applied Microbiology* **85**, 19S-28S.

Stoodley P., Lewandowski Z., Boyle J.D. & Lappin-Scott H.M. (1999b) Structural deformation of bacterial biofilms caused by short-term fluctuations in fluid shear: an in situ investigation of biofilm rheology. *Biotechnology and Bioengineering* **65**, 83–92.

Stoodley P., Sauer K., Davies D.G. & Costerton J.W. (2002) Biofilms as complex differentiated communities. *Annual Review of Microbiology* **56**, 187–209.

Sun J. & Liu D. (2003) Geometric models for calculating cell biovolume and surface area for phytoplankton. *Journal of Plankton Research* **25**, 1331–1346.

Sutherland I. (1999) Biofilm polysaccharides. In: *Microbial Extracellular Polymeric Substances: Characterization Structure and Function* (Eds J. Wingender, T.R. Neu & H.-C. Flemming), pp. 73–89. Springer-Verlag, Berlin.

Sutherland I.W. (2001) Biofilm exopolysaccharides: a strong and sticky framework. *Microbiology* **147**, 3–9.

Sutherland I.W. (1998) Novel and established applications of microbial polysaccharides. *Trends in Biotechnology* **16**, 41–46.

Sutherland T.F., Amos C.L. & Grant J. (1998a) The effect of buoyant biofilms on the erodibility microtidal estuary of sublittoral sediments of a temperate Lunenburg Bay. *Limnology and Oceanography* **43**, 225–235.

Sutherland T.F., Grant J. & Amos C.L. (1998b) The effect of carbohydrate production by the diatom Nitzschia curvilineata on the erodibility of sediment. *Limnology and Oceanography* **43**, 65–72.

Svensater G., Welin J., Wilkins J.C., Beighton D. & Hamilton I.R. (2001) Protein expression by planktonic and biofilm cells of Streptococcus mutans. *FEMS Microbiology Letters* **205**, 139–146.

Svetličić V., Žutić V., Pletikapić G. & Radić T.M. (2013) Marine polysaccharide networks and diatoms at the nanometric scale. *International Journal of Molecular Sciences* **14**, 20064–20078.

Taylor I.S., Paterson D.M. & Mehlert A. (1999) The quantitative variability and monosaccharide composition of sediment carbohydrates associated with intertidal diatom assemblages. *Biogeochemistry* **45**, 303–327.

Tena A., Vericat D. & Batalla R.J. (2014) Suspended sediment dynamics during flushing flows in a large impounded river (the lower River Ebro). *Journal of Soils and Sediments* **14**, 2057–2069.
Thom M., Schmidt H., Gerbersdorf S.U. & Wieprecht S. (2015) Seasonal biostabilization and erosion behavior of fluvial biofilms under different hydrodynamic and light conditions. *International Journal of Sediment Research* **30**, 273–284.
Thom M., Schmidt H., Wieprecht S. & Gerbersdorf S.U. (2012) Investigations with physical model tests on the influence of biofilm on bed stability. *Wasserwirtschaft* **102**, 32–36.
Tichi M.A. & Tabita F.R. (2001) Interactive control of Rhodobacter capsulatus redox-balancing systems during phototrophic metabolism. *Journal of Bacteriology* **183**, 6344–6354.
Tolhurst T.J., Black K.S., Shayler S.A., Mather S., Black I., Baker K. & Paterson D.M. (1999) Measuring the in situ erosion shear stress of intertidal sediments with the Cohesive Strength Meter (CSM). *Estuarine Coastal and Shelf Science* **49**, 281–294.
Tolhurst T.J., Defew E.C., de Brouwer J.F.C., Wolfstein K., Stal L.J. & Paterson D.M. (2006) Small-scale temporal and spatial variability in the erosion threshold and properties of cohesive intertidal sediments. *Continental Shelf Research* **26**, 351–362.
Tuson H.H. & Weibel D.B. (2013) Bacteria-surface interactions. *Soft Matter* **9**, 4368–4380.
Underwood G.J.C. (2002) Adaptations of tropical marine microphytobenthic assemblages along a gradient of light and nutrient availability in Suva Lagoon, Fiji. *European Journal of Phycology* **37**, 449–462.
Underwood G.J.C., Boulcott M., Raines C.A. & Waldron K. (2004) Environmental effects on exopolymer production by marine benthic diatoms: Dynamics, changes in composition, and pathways of production. *Journal of Phycology* **40**, 293–304.
Underwood G.J.C. & Paterson D.M. (2003) The importance of extracellular carbohydrate production by marine epipelic diatoms. *Advances in Botanical Research, Vol 40* **40**, 183–240.
Underwood G.J.C. & Smith D.J. (1998) Predicting epipelic diatom exopolymer concentrations in intertidal sediments from sediment chlorophyll a. *Microbial Ecology* **35**, 116–125.
Urakami T., Araki H., Oyanagi H., Suzuki K.-I. & Komagata K. (1990) Paracoccus aminophilus sp. nov. and Paracoccus aminovorans sp. nov., which utilize N, N-dimethylformamide. *International Journal of Systematic and Evolutionary Microbiology* **40**, 287–291.
Valle J., Da Re S., Schmid S., Skurnik D., D'Ari R. & Ghigo J.-M. (2008) The amino acid valine is secreted in continuous-flow bacterial biofilms. *Journal of Bacteriology* **190**, 264–274.
Vancanneyt M., Segers P., Abraham W. & De Vos P. (2009) Brevundimonas. In: *Bergey's Manual of Systematic Bacteriology* (Ed. G. Garrity), pp. 308–316. Springer, New York.
Vardy S., Saunders J.E., Tolhurst T.J., Davies P.A. & Paterson D.M. (2007) Calibration of the high-pressure cohesive strength meter (CSM). *Continental Shelf Research* **27**, 1190–1199.

Vignaga E., Haynes H. & Sloan W.T. (2012) Quantifying the tensile strength of microbial mats grown over noncohesive sediments. *Biotechnology and Bioengineering* **109**, 1155–1164.
Vignaga E., Sloan D.M., Luo X., Haynes H., Phoenix V.R. & Sloan W.T. (2013) Erosion of biofilm-bound fluvial sediments. *Nature Geoscience* **6**, 770.
Vogt M., Flemming H.C. & Veeman W.S. (2000) Diffusion in Pseudomonas aeruginosa biofilms: a pulsed field gradient NMR study. *Journal of Biotechnology* **77**, 137–146.
Vu B., Chen M., Crawford R.J. & Ivanova E.P. (2009) Bacterial extracellular polysaccharides involved in biofilm formation. *Molecules* **14**, 2535–2554.
Wagner K., Besemer K., Burns N.R., Battin T.J. & Bengtsson M.M. (2015) Light availability affects stream biofilm bacterial community composition and function, but not diversity. *Environmental Microbiology* **17**, 5036–5047.
Wagner M., Amann R., Lemmer H. & Schleifer K.H. (1993) Probing activated sludge with oligonucleotides specific for proteobacteria: inadequacy of culture-dependent methods for describing microbial community structure. *Applied and Environmental Microbiology* **59**, 1520–1525.
Wang J., Cao S., Du C. & Chen D. (2013) Underwater locomotion strategy by a benthic pennate diatom. *Protoplasma* **250**, 1203–1212.
Wang Y., Chen Y., Lavin C. & Gretz M.R. (2000) Extracellular matrix assembly in diatoms (Bacillariophyceae). iv. ultrastructure of Achnanthes longipes and Cymbella cistula as revealed by high-pressure freezing/freeze substituton and cryo-field emission scanning electron microscopy. *Journal of Phycology* **36**, 367–378.
Waters C.M. & Bassler B.L. (2005) Quorum sensing: cell-to-cell communication in bacteria. *Annual Review of Cell and Developmental Biology* **21**, 319–346.
Wawrousek K., Noble S., Korlach J., Chen J., Eckert C., Yu J. & Maness P.-C. (2014) Genome annotation provides insight into carbon monoxide and hydrogen metabolism in Rubrivivax gelatinosus. *PLoS One* **9**, e114551.
de Weert S., Vermeiren H., Mulders I.H.M., Kuiper I., Hendrickx N., Bloemberg G.V., Vanderleyden J., De Mot R. & Lugtenberg B.J.J. (2002) Flagella-driven chemotaxis towards exudate components is an important trait for tomato root colonization by Pseudomonas fluorescens. *Molecular Plant-Microbe Interactions* **15**, 1173–1180.
Weitere M., Bergfeld T., Rice S.A., Matz C. & Kjelleberg S. (2005) Grazing resistance of Pseudomonas aeruginosa biofilms depends on type of protective mechanism, developmental stage and protozoan feeding mode. *Environmental Microbiology* **7**, 1593–1601.
Wey J.K., Scherwass A., Norf H., Arndt H. & Weitere M. (2008) Effects of protozoan grazing within river biofilms under semi-natural conditions. *Aquatic Microbial Ecology* **52**, 283–296.
Whitchurch C.B., Tolker-Nielsen T., Ragas P.C. & Mattick J.S. (2002) Extracellular DNA required for bacterial biofilm formation. *Science* **295**, 1487–1487.
Wichard T., Poulet S.A. & Pohnert G. (2005) Determination and quantification of alpha,beta,gamma,delta-unsaturated aldehydes as pentafluorobenzyl-oxime derivates in diatom cultures and natural phytoplankton populations: application in marine field studies. *Journal of Chromatography* **814**, 155–161.
Widdows J., Brinsley M.D., Salkeld P.N. & Lucas C.H. (2000) Influence of biota on spatial and temporal variation in sediment erodability and material flux on a tidal flat (Westerschelde, The Netherlands). *Marine Ecology Progress Series* **194**, 23–37.

Wigglesworth-Cooksey B., Berglund D. & Cooksey K.E. (2001) Cell-cell and cell-surface interactions in an illuminated biofilm: Implications for marine sediment stabilization. *Geochemical Transactions* **10**.
Willis A., Chiovitti A., Dugdale T.M. & Wetherbee R. (2013) Characterization of the extracellular matrix of Phaeodactylum tricornutum (Bacillariophyceae): structure, composition, and adhesive characteristics. *Journal of Phycology* **49**, 937–949.
Wimpenny J., Manz W. & Szewzyk U. (2000) Heterogeneity in biofilms. *FEMS Microbiology Reviews* **24**, 661–671.
de Winder B., Staats N., Stal L.J. & Paterson D.M. (1999) Carbohydrate secretion by phototrophic communities in tidal sediments. *Journal of Sea Research* **42**, 131–146.
Witt O. & Westrich B. (2003) Quantification of erosion rates for undisturbed contaminated cohesive sediment cores by image analysis. *Hydrobiologia* **494**, 271–276.
Wolfaardt G.M., Lawrence J.R., Robarts R.D. & Caldwell D.E. (1998) In situ characterization of biofilm exopolymers involved in the accumulation of chlorinated organics. *Microbial Ecology* **35**, 213–223.
Wolfstein K. & Stal L.J. (2002) Production of extracellular polymeric substances (EPS) by benthic diatoms: effect of irradiance and temperature. *Marine Ecology Progress Series* **236**, 13–22.
Wommack K.E. & Colwell R.R. (2000) Virioplankton: viruses in aquatic ecosystems. *Microbiology and Molecular Biology Reviews* **64**, 69–114.
Wood S.A., Smith K.F., Banks J.C., Tremblay L.A., Rhodes L., Mountfort D., Cary S.C. & Pochon X. (2013) Molecular genetic tools for environmental monitoring of New Zealand's aquatic habitats, past, present and the future. *New Zealand Journal of Marine and Freshwater Research* **47**, 90–119.
Wotton R.S. (2004) The ubiquity and many roles of exopolymers (EPS) in aquatic systems. *Scientia marina* **68**, 13–21.
Wustman B.A., Gretz M.R. & Hoagland K.D. (1997) Extracellular matrix assembly in diatoms (Bacillariophyceae)(I. A model of adhesives based on chemical characterization and localization of polysaccharides from the marine diatom Achnanthes longipes and other diatoms). *Plant Physiology* **113**, 1059–1069.
Wustman B.A., Lind J., Wetherbee R. & Gretz M.R. (1998) Extracellular Matrix Assembly in Diatoms (Bacillariophyceae): III. Organization of Fucoglucuronogalactans within the Adhesive Stalks of Achnanthes longipes. *Plant Physiology* **116**, 1431–1441.
Xin L., Hong-ying H., Ke G. & Ying-xue S. (2010) Effects of different nitrogen and phosphorus concentrations on the growth, nutrient uptake, and lipid accumulation of a freshwater microalga Scenedesmus sp.. *Bioresource Technology* **101**, 5494–5500.
Yallop M.L., Paterson D.M. & Wellsbury P. (2000) Interrelationships between rates of microbial production, exopolymer production, microbial biomass, and sediment stability in biofilms of intertidal sediments. *Microbial Ecology* **39**, 116–127.
Yannarell A.C. & Triplett E.W. (2005) Geographic and environmental sources of variation in lake bacterial community composition. *Applied and Environmental Microbiology* **71**, 227–239.
Yoshioka T., Wada E. & Hayashi H. (1994) A stable isotope study on seasonal food web dynamics in a eutrophic lake. *Ecology* **75**, 835–846.
Zeng G., Vad B.S., Dueholm M.S., Christiansen G., Nilsson M., Tolker-Nielsen T., Nielsen P.H., Meyer R.L. & Otzen D.E. (2015a) Functional bacterial amyloid

increases Pseudomonas biofilm hydrophobicity and stiffness. *Frontiers in Microbiology* **6**.

Zeng Y., Baumbach J., Barbosa E.G.V., Azevedo V., Zhang C. & Koblížek M. (2016) Metagenomic evidence for the presence of phototrophic Gemmatimonadetes bacteria in diverse environments. *Environmental Microbiology Reports* **8**, 139–149.

Zeng Y., Selyanin V., Lukeš M., Dean J., Kaftan D., Feng F. & Koblížek M. (2015b) Characterization of the microaerophilic, bacteriochlorophyll a-containing bacterium Gemmatimonas phototrophica sp. nov., and emended descriptions of the genus Gemmatimonas and Gemmatimonas aurantiaca. *International Journal of Systematic and Evolutionary Microbiology* **65**, 2410–2419.